Resistance to Airflow and Moisture Loss of Table Grapes Inside Multi-scale Packaging

By

Mduduzi Elijah Khulekani Ngcobo

Dissertation presented for the degree of Doctor of Philosophy in the Faculty of AgriSciences at Stellenbosch University

Promoter: Prof. Umezuruike Linus Opara

Postharvest Technology Research Laboratory, South African Research Chair in Postharvest Technology, Department of Horticultural Science, Faculty of AgriSciences

Co-promoter: Prof. Chris J. Meyer

Department of Mechanical and Mechatronics Engineering, Faculty of Engineering

March, 2013

DECLARATION

By submitting this dissertation electronically, I declare that the entirety of the work contained therein is my own, original work, and that I have not previously in its entirety or in part submitted it for obtaining any qualification.

March 2013

SUMMARY

Postharvest quality of fresh table grapes is usually preserved through cooling using cold air. However, cooling efficiencies are affected by the multi-scale packaging that is commercially used for handling grapes after harvest. There is usually spatial temperature variability of grapes that often results in undesirable quality variations during postharvest handling and marketing. This heterogeneity of grape berry temperature inside multi-packages is largely due to uneven cold airflow patterns that are caused by airflow resistance through multi-package components. The aims of this study were therefore to conduct an in-depth experimental investigation of the contribution of grape multi-packaging components to total airflow resistance, cooling rates and patterns of grapes inside the different commercially used multi-packages, and to assess the effects of these multi-packages on table grape postharvest quality attributes. A comprehensive study of moisture loss from grapes during postharvest storage and handling, as well as a preliminary investigation of the applicability of computational fluid dynamics (CFD) modeling in predicting the transport phenomena of heat and mass transfer of grapes during cooling and cold storage in multi-packages were included in this study.

Total pressure drop through different table grapes packages were measured and the percentage contribution of each package component and the fruit bulk were determined. The liner films contributed significantly to total pressure drop for all the package combinations studied, ranging from 40.33±1.15% for micro-perforated liner film to 83.34±2.13 % for non-perforated liner film. The total pressure drop through the grape bulk (1.40±0.01 % to 9.41±1.23 %) was the least compared to the different packaging combinations with different levels of liner perforation.

The cooling rates of grapes in the 4.5 kg multi-packaging were significantly ($P<0.05$) slower than that of grapes in 5 kg punnet multi-packaging, where the 4.5 kg box resulted in a seven-eighths cooling time of 30.30-46.14% and 12.69-25.00% more than that of open-top and clamshell punnet multi-packages, respectively. After 35 days in cold storage at -0.5°C, grape bunches in the 5 kg punnet box combination (open-top and clamshell) had weight loss of 2.01 – 3.12%, while the bunches in the 4.5 kg box combination had only 1.08% weight loss.

During the investigation of the effect of different carton liners on the cooling rate and quality attributes of 'Regal seedless' table grapes in cold storage, the non-perforated liner films maintained relative humidity (RH) close to 100 %. This high humidity inside non-perforated liner films resulted in delayed loss of stem quality but significantly ($P \leq 0.05$) increased the incidence of SO_2 injury and berry drop during storage compared to perforated liners. The perforated liners improved fruit cooling rates but significantly ($P \leq 0.05$) reduced RH. The low RH in perforated liners also resulted in an increase in stem dehydration and browning compared to non-perforated liners.

The moisture loss rate from grapes packed in non-perforated liner films was significantly ($P<0.05$) lower compared to the moisture loss rate from grapes packed in perforated liner films (120 x 2 mm and 36 x 4 mm). The effective moisture diffusivity values for stem parts packed in non-perforated liner films were lower than the values obtained for stem parts stored without packaging liners, and varied from 5.06×10^{-14} to 1.05×10^{-13} m^2s^{-1}. The dehydration rate of stem parts was inversely proportional to the size (diameter) of the stem parts. Dehydration rate of stems exposed (without liners) to circulating cold air was significantly ($P<0.05$) higher than the dehydration rates of stems packed in non-perforated liner film. Empirical models were successfully applied to describe the dehydration kinetics of the different parts of the stem.

The potential of cold storage humidification in reducing grape stem dehydration was investigated. Humidification delayed and reduced the rate of stem dehydration and browning; however, it increased SO_2 injury incidence on table grape bunches and caused wetting of the packages.

The flow phenomenon during cooling and handling of packed table grapes was also studied using a computational fluid dynamic (CFD) model and validated using experimental results. There was good agreement between measured and predicted results. The result demonstrated clearly the applicability of CFD models to determine optimum table grape packaging and cooling procedures.

OPSOMMING

Naoes kwaliteit van vars tafeldruiwe word gewoonlik behou deur middel van verkoeling van die produk met koue lug. Ongelukkig word die effektiwiteit van dié verkoeling beïnvloed deur die multivlakverpakking wat kommersieel gebruik word vir die naoes hantering van druiwe. Daar is gewoonlik ruimtelike variasie in die temperatuur van die druiwe wat ongewenste variasie in die kwaliteit van die druiwe veroorsaak tydens naoes hantering en bemarking. Die heterogene druiwetemperature binne die multivlakverpakkings word grootliks veroorsaak deur onegalige lugvloeipatrone van die koue lug as gevolg van die weerstand wat die verskillende komponente van die multivlakverpakkings teen lugvloei bied. Die doel van hierdie studie was dus om ‘n indiepte eksperimentele ondersoek te doen om die bydrae van multivlakverpakking op totale lugvloeiweerstand, verkoelingstempo’s en –patrone van druiwe binne kommersieël gebruikte multivlakverpakkings te ondersoek, asook die effek van die multivalkverpakking op die naoes kwaliteit van druiwe te bepaal. ‘n Omvattende studie van vogverlies van druiwe tydens naoes opberging en hantering, asook ‘n voorlopige ondersoek na die bruikbaarheid van ‘n berekende vloei dinamika (BVD) model om die bewegingsfenomeen van hitte en massa oordrag van druiwe tydens verkoeling en koelopberging in multivlakverpakkings te voorspel, was ook by die studie ingesluit.

Die totale drukverskil deur verskillende tafeldruif verpakkingssisteme is gemeet en die persentasie wat deur elke verpakkingskomponent en die vruglading bygedra is, is bereken. Van al die verpakkingskombinasies wat gemeet is, het die voeringfilms betekenisvol tot die totale drukverskil bygedra, en het gewissel van 40.33±1.15% vir die mikro geperforeerde voeringfilm tot 83.34±2.13 % vir die nie-geperforeerde voeringfilm. Die totale drukverskil oor die druiflading (1.40±0.01 % to 9.41±1.23 %) was die minste in vergelyking met die verskillende verpakkingskombinasies met die verskillende vlakke van voeringperforasies.

Die verkoelingstempos van die druiwe in die 4.5 kg multiverpakking was betekenisvol ($P<0.05$) stadiger as vir die druiwe in die 5 kg handmandjie (‘punnet’) multiverpakking. Die 4.5 kg karton het ‘n seweagstes verkoelingstyd van 30.30-46.14% en 12.69-25.00% langer, respektiewelik, as oop-vertoon en toeslaan-‘punnet’ multiverpakkings gehad. Na 35 dae van koelopberging by -0.5°C het druiwetrosse in die 5 kg ‘punnet’-kartonkombinasies (oop-

vertoon en toeslaan-'punnet') 'n massaverlies van 2.01 – 3.12% gehad, terwyl die trosse in die 4.5 kg kartonkombinasie slegs 'n 1.08% massaverlies gehad het.

In die ondersoek na die effek van verskillende kartonvoerings op die verkoelingstempo en kwaliteitseienskappe van 'Regal seedless' tafeldruiwe tydens koelopbering, het die nie-geperforeerde kartonvoerings 'n relatiewe humiditeit (RH) van byna 100 % gehandhaaf. Hierdie hoë humiditeit in die nie-geperforeerde voeringfilms het 'n verlies in stingelkwaliteit vertraag, maar het die voorkoms van SO_2-skade en loskorrels betekenisvol ($P < 0.05$) verhoog in vergelyking met geperforeerde voerings. Die geperforeerde voerings het vrugverkoelingstempos verbeter, maar het die RH betekenisvol ($P \leq 0.05$) verlaag. Die lae RH in die geperforeerde voerings het gelei tot 'n verhoging in stingeluitdroging en –verbruining in vergelyking met die nie-geperforeerde voerings.

Die vogverliestempo uit druiwe verpak in nie-geperforeerde voeringfilms was betekenisvol ($P<0.05$) stadiger in vergelyking met druiwe verpak in geperforeerde voeringfilms (120 x 2 mm and 36 x 4 mm). Die effektiewe vogdiffusiewaardes vir stingelgedeeltes verpak in nie-geperforeerde voeringfilms was stadiger as vir stingelgedeeltes wat verpak is sonder verpakkingsvoerings, en het gevarieer van $5.06x10^{-14}$ – $1.05x10^{-13}$ m^2s^{-1}. Die uitdrogingstempo van stingelgedeeltes was omgekeerd eweredig aan die grootte (deursnit) van die stingelgedeeltes. Die uitdrogingstempo van stingels wat blootgestel was (sonder voerings) aan sirkulerende koue lug was betekenisvol ($P<0.05$) hoër as die uitdrogingstempos van stingels wat verpak was in nie-geperforeerde voeringfilms. Empiriese modelle is gebruik om die uitdrogingskinetika van die verskillende stingelgedeeltes te beskryf.

Die potensiaal van koelkamer humidifisering in die vermindering van die uitdroging van druifstingels is ondersoek. Humidifisering het stingeluitdroging vertraag en het die tempo van stingeluitdroging en -verbruining verminder, maar dit het die voorkoms van SO_2-skade op die tafeldruiftrosse verhoog en het die verpakkings laat nat word.

Die bewegingsfenomeen tydens verkoeling en hantering van verpakte tafeldruiwe is ook ondersoek deur gebruik te maak van 'n BVD model en is bevestig met eksperimentele

resultate. Daar was goeie ooreenstemming tussen gemete en voorspelde resultate. Die resultaat demonstreer duidelik die toepaslikheid van BVD-modelle om die optimum tafeldruifverpakkings- en verkoelingsprosedures te bepaal.

ACKNOWLEDGEMENT

The author would like to thank and acknowledge the following people and organisations for their great contributions:

Prof. Umezuruike Linus Opara, South African Research Chair in Postharvest Technology (SARChI), for his guidance, mentorship, and support through this entire research study

Dr. Mulugeta Delele, Postharvest Technology Research Lab, I am indebted, this study would not been easily accomplished without your great expertise, support, friendship and guidance.

Dr. Pankaj Pathare, Postharvest Technology Research Lab, for your assistance during dehydration section of this study.

PPECB for their financial support and allowing me to be further developed through acquisition of new skills.

Postharvest Innovation Programme (PHI-2), for financially supporting the project, 'Packaging for the Future', of which this study was part of.

Ms Rebogile Mphahlele and Mr Goodman Sibiya, PPECB, for your tireless assistance in data collection during this entire study, you ensured that all my trials were running smoothly.

Ms. Nazneen Ebrahim, Postharvest Technology Research Lab, for assistance in ensuring smooth running of projects, from purchasing project consumables to booking vehicles for collecting fruits.

Dr. Mariana Jooste, Department of Horticultural Science, for all the assistance, guidance and encouragement.

My lovely wife, Phumzile Ngcobo, your support, encouragement and love has enabled me to successfully complete this study.

My beautiful daughter, Ms Mafuzamahle Ngcobo, when the going got tough, your pretty smile gave me a reason to soldier on. May this be symbolic for you as you grow up, that you can accomplish anything in life, as long as you put your heart and mind to it.

Finally I would like to give thanks to the Almighty for it was His will that this study be successfully completed, and for giving me strength and wisdom from day to day.

TABLE OF CONTENTS

LIST OF PUBLICATIONS

1. Papers published on international journals:

1.1 Paper 1, published as:

Ngcobo M.E.K., Delele M.A., Opara U.L., Zietsman C.J., Meyer C.J. 2012. Resistance to airflow and cooling patterns through multi-scale packaging of table grapes. Int. J. Refrig. 35 (2), 445-452.

1.2 Paper 2, published as:

Ngcobo M.E.K., Opara U.L., Thiart G.D. 2012. Effects of packaging liners on cooling rate and quality attributes of table grape (cv. Regal Seedless). Packaging Technol. Sci. 25(2), 73-84.

1.3 Paper 3, published as:

Ngcobo M.E.K., Delele M.A., Opara U.L., Meyer C.J. 2013. Performance of multi-packaging for table grapes based on airflow, cooling rates and fruit quality. J Food Eng. 116, 613-621.

1.4 Paper 4, published as:

Ngcobo M.E.K., Delele M.A., Pathare P.J., Chen L., Opara U.L., Meyer C.J. 2012. Moisture loss characteristics of fresh table grapes packed in different film liners during cold storage. Biosystems Eng. 113 (4), 363-370.

1.5 Paper 7, published as:

Delele M.A., Ngcobo M.E.K., Opara U.L., Meyer C.J. 2012. Investigating the Effects of Table Grape Package Components and Stacking on Airflow, Heat and Mass Transfer Using 3-D CFD Modelling. Food Bioprocess Technol. DOI 10.1007/s11947-012-0895-5.

2 Manuscript under review:

2.1 Paper 5, submitted as:

Ngcobo M.E.K., Pathare P.B., Delele M.A., Opara U.L., Meyer C.J. Moisture diffusivity of table grape stems during low temperature storage conditions. Submitted to Biosystems Engineering.

2.2 Paper 6, submitted as:

Ngcobo M.E.K., Delele M.A., Opara U.L., Meyer C.J. Investigating the Potential of Humidification System to Control Moisture Loss and Quality of Table Grapes during Cold Storage. Submitted to *Postharvest Biology and Technology*.

3. Conference presentations

3.1 Ngcobo M.E.K., Opara U.L., Thiart Thiart G.D. 2011. Effects of multi-packaging on heat and mass transfer of table grapes during cold storage (Poster). 6th International CIGR Technical Symposium: Towards a sustainable food chain. Nantes, France (18 – 20th April 2011).

3.2 Ngcobo M.E.K., Delele M.A., Opara U.L. Heat transfer and external attributes of 'Regal seedless' table grapes inside multi-layered packaging during postharvest cooling and storage. **All African Horticultural Congress (AAHC): Horticulture for Humanity. Skukuza, South Africa (15-20 January 2012)**

3.3 Ngcobo M.E.K., Delele M.A., Opara U.L. Comparative performance of multi-scale packages with punnets on heat and mass transfer of table grapes. **7th International CIGR Technical Symposium: Innovating the food value chain. Stellenbosch, South Africa (25-29 November 2012)**

NOTE

This dissertation presents a compilation of manuscripts where each chapter is an individual entity and some repetition between chapters, therefore, has been unavoidable.

1. General Introduction

1.1 Introduction

Table grapes and other fruits destined for export are usually consumed in the distant markets at least three weeks after they have been harvested. This brings about the need for postharvest technologies such as cooling to be employed in order to maintain harvest quality. The efficiency and success of cooling and perhaps other postharvest technologies is usually affected by other necessary practices and applications within the value chain. Factors affecting the effectiveness of cooling include the lag time which is the time taken between packing and the start of pre-cooling, package designs (Thompson et al., 1998), and human error.

Table grapes are packed in multi-scale packages and cooled down to -0.5 °C and should be maintained at this temperature for the duration of the value chain. However, grape berries deteriorate during postharvest handling in the cold chain (Nelson, 1978) and this is often ascribed to inefficient cooling, poor temperature management and improper packaging (Thompson et al., 1998). Deterioration of table grapes is characterized by stem dehydration and browning due to moisture loss, decay, berry drop and SO_2 injury (Nelson, 1978; Valero et al., 2006). These quality defects could be alleviated through improvements in cooling efficiencies and packaging systems.

1.2 Refrigeration

Cooling is one of the main techniques used to preserve the postharvest quality of horticultural products. This is due to the widely reported ability of low temperatures to reduce biochemical reactions (such as respiration), retard the growth of microbial organisms (Brosnan and Sun, 2001; Arin and Akdemir, 2004) and minimize moisture loss. The relationship between product temperature and biochemical reaction follows van't Hoff's rule, which states that the rate of most chemical and biochemical reactions increases two to three times with every 10 degrees rise in product temperature (Hardenburg et al, 1986; Brosnan and Sun, 2001; Kays

and Paull, 2004). Hence, cooling plays an important role in reducing these biochemical reactions.

In many postharvest produce refrigeration systems, cooling is achieved using cold air. This means that during produce cooling heat is transferred primarily by convection and therefore, produce temperature and its homogeneity is largely governed by the patterns of airflow (Smale et al., 2006; Moureh and Flick, 2004; Moureh et al., 2009; Zou et al., 2006). Previous studies have shown significant spatial temperature variability in some food refrigerated systems, with non-uniform airflow implicated as a major cause of this variability (Brosnan and Sun, 2001; Smale et al., 2006). Temperature variability causes quality variation among fruit in the same consignment and promotes postharvest losses and waste.

1.3 Packaging

Packaging has been practiced for as long as fresh produce has been traded (Wills et al., 2007). Its importance in the fresh produce industry has involved two main functions, which are to assemble the produce into convenient units for handling (unitization), and to protect the produce during distribution, storage and marketing. However, modern packages and packaging for horticultural produce are now expected to meet a range of basic requirements such as sufficient mechanical strength and facilitatation of easy disposal, reuse or recycling (Wills et al., 2007). Apart from protecting contents against damage during transportation and distribution of fruit and vegetables, package containers are often used during precooling (Vigneault and Goyette, 2002). To ensure efficient cooling during postharvest handling, the packaging should allow for sufficient airflow (Thompson et al., 1998). However, the combination of packaging and the fruit usually induce some airflow resistance and thus negatively affecting cooling efficiency (Delele et al. 2008). The non-homogeneous flow of the cooling air inside the stack could also cause uneven cooling and product quality (Alvarez and Flick, 1999a, Alvarez and Flick, 1999b, Alvarez and Flick, 2007; Verboven et al., 2006). Many studies have reported on vent-hole ratio, fruit physical properties, and fruit stacking pattern as important components to be considered for improving airflow through fruit packages (Chau et al., 1985; Vingeault and Goyette, 2002). The more vent area there is on packages, the better the airflow through fruit packaging. Depending on the packaging material used to make fruit packages, there is usually a tradeoff between the number of

ventilation holes and package mechanical strength requirements. Vingeault and Goyette (2002) recommended a vent-hole ratio of 25–27% for good airflow through plastic boxes and de Castro et al. (2005) recommended a vent-hole ratio of 8-16% of the surface of the container to optimise the use of energy. There is therefore a need for science based packaging designs (Pathare et al., 2012 see Food and Bioprocess Technology) to ensure efficient airflow and cooling of fruits while fulfilling other packaging requirements for the different postharvest applications.

1.4 Postharvest quality of horticultural produce

The importance of temperature management in maintaining the quality of fresh fruit and vegetables is well documented (Kader, 1992). Apart from the reduction of biochemical reactions associated with fruit senescence, proper cooling reduces the rate of quality and moisture losses of fruit. Poor cooling and cold chain breakages tend to promote produce moisture loss and reduce marketability of fruits and vegetables (Thompson et al., 1998). Previous studies have shown significant loss of firmness and weight from strawberries due to delayed cooling (Nunes et al., 1994; Nunes et al., 1995; Thompson et al., 1998). Table grapes suffer rapid moisture loss if temperatures are not well managed. Moisture loss of grapes manifests as dry and brittle stems which appear just under 2 % of weight loss and berries show signs only after 5% of moisture loss (Thompson et al., 1998). Moisture loss symptoms such as loss of firmness and dull colour in strawberries, as well as stem dehydration and browning in table grapes seriously detract the consumers' interest of buying affected produce.

Good cold chain management is therefore of utmost importance to ensure the marketability and competitiveness of produce in the distant markets.

1.5 Postharvest handling systems performance evaluation methodologies

The performance of postharvest packaging is usually evaluated using experimental methods such as measuring product cooling rates (Chonhenchob and Singh, 2005) and airflow using probes. The commonly used experimental method for the improvement of airflow through postharvest packages is the pressure drop method. Many researchers have used Darcy–

Forchheimer and Ramsin equations to develop correlations to estimate pressure drop through bulk produce and packages containing horticultural produce (Chau et al., 1985; Smale, 2004; van der Sman, 2002; Verboven et al., 2004; Vingeault and Goyette, 2002; Vingeault et al., 2004).

These experimental methods are fairly easy to use; however, they tend to be intrusive and destructive in nature (Ferrua and Singh, 2009). To date, the South African perishable industries utilize such experimental methods for testing postharvest packaging performance and improvements. Although the experimental methods work, they also have limited scope for sustainable packaging design due to high cost of instrumentation and the time required to gather appropriate data for meaningful results (Ferrua et al., 2009). Another limitation is based on the fact that the packaging has to be manufactured before its performance can be tested, thereby increasing costs especially in cases where the manufactured package performs poorly.

Numerical modelling has gained popularity in the past decade within the agricultural and food industry research (Xia and Sun, 2002 and Norton and Sun, 2006). Many researchers have used mathematical modelling methodologies for the design and improvements of horticultural packages (Tanner et al., 2002a; Tanner et al., 2002b) and others have used numerical tools such as computational fluid dynamics (CFD) (Verboven et al. 2006; Zou et al., 2006; Opara and Zou, 2007; Delele et al., 2008; Tutar et al., 2009). However, any numerically developed model would still require experimental validation to ensure its relevance and applicability to a wide range of conditions.

In this study, table grapes are the fruit of interest due to its complex multi-layered packaging system. There are many different multi-package combinations that are used commercially to pack and handle grapes after harvest. Cooling is usually commenced after the grapes have been packed in these multi-packages. However, there are postharvest quality problems such as moisture loss which manifests as stem (rachis) drying and browning, SO_2 damage and decay that are reported to be associated with poor postharvest cold chain management (Valero et al., 2006) and these quality defects reduce the marketability of grapes. To mitigate

the problem of poor quality that is mainly ascribed to an inadequate cold chain (Nelson 1978), it is important to improve the cooling airflow through the table grape packaging.

1.6 Objectives and outline of the dissertation

This dissertation aims to investigate the performance of the different grape multi-packages in terms of cooling and fruit quality attributes during postharvest storage and handling for improvement of packaging designs and cold chain performance.

The specific objectives are to:

- Investigate the airflow resistance through the different components of table grape multi-scale packages
- Compare the cooling performance and quality of table grapes in different multi-packages;
- Conduct a comprehensive study of table grape moisture loss in different packages and test the application of drying models in moisture loss from grape stems;
- Investigate the application of postharvest cold storage humidification on the quality of grapes; and
- Investigate the heat and mass transfer processes of packed table grapes using computational fluid dynamics (CFD)

To address the set out objectives, the dissertation is arranged into three parts. The first part covers an in-depth comparative study of performance of different grapes multi-packages in terms of cooling rates and their effects on grapes quality attributes (Papers 1; 2 and 3). In Paper 1, the resistance to airflow by the different table grape multi-package combinations was studied. This is achieved determining the percentage contribution of each grape packaging component and grape bunches to total resistance to airflow of multi-packaging. The pressure drop as a function of incoming airflow is characterized for each packaging component and for the grapes bunches. The different components of the grape multi-packaging included the carton boxes; liner films and bunch carry-bags. Such work has never been reported before for the multi-scale packaging.

Based on the results obtained in Paper 1, the effect of six different liner films on the cooling rates and quality attributes of table grapes is studied in Paper 2. The cooling rates and patterns of grapes inside the different liner films were compared in conjunction with resulting effects on different postharvest quality attributes of grapes namely: grape stem condition; bunch weight loss and berry drop; colour changes; SO_2 injury and decay development under both cold storage and shelf-life storage. No study has been reported, that characterizes the postharvest quality defects of grapes to the different multi-packages. Therefore the results from this study give a deeper understanding on the performance of multi-scale packaging of table grapes taking into consideration the postharvest quality of grapes.

Part of Paper 3 is an extension of work done in Papers 1 and 2, where the contribution of grape punnet multi-packaging components to total airflow resistance was investigated (Paper 3). Another part of Paper 3 looks at the cooling rates and patterns of grapes in different multi-packages stacked on pallets. The cooling rates and patterns were also studied in conjunction with changes in grape quality attribute changes.

The second part of the dissertaion covers a comprehensive study of grapes moisture loss (Papers 4; 5 and 6). In Paper 4 the total moisture loss of grape bunches is characterized into individual parts that make up the bunch. The different parts of the bunch include grape berries and stems. However, the stems are further divided into spheres (i.e. cap like structure connecting stems to berries); small; intermediate and large cylinder parts of the stem. No work has been reported in literature on grape moisture loss which considered the different parts that make up the grape bunch individually under cold storage conditions. In Paper 5, the application of drying models is investigated in predicting the dehydration of grape stems during cold storage in multi-packages. In literature no work has been reported on the application of drying models on the moisture loss studies.

In Paper 6, the potential of humidification for controlling postharvest moisture loss is investigated. Previous studies (Lichter et al., 2011), have shown some potential improvements in the control of stem quality and weight loss of some grapes cultivars as associated with an increase in humidity. However, these studies were conducted under high

temperature conditions that prevail during marketing of the grapes in some markets (Lichter et al., 2011). In this study, a humidification system was applied during cold storage conditions.

The third part of the dissertation involves a preliminary investigation of heat and moisture transfer using computational fluid dynamics (CFD) modelling (Paper 7). Table grape multi-packaging is very complex and therefore numerical modelling would be a bit difficult due to the different geometries and boundary conditions that need to be considered to study the flow. However, attempts were made to develop CFD models for heat and mass transfer from grapes in multi-packages during cooling. These models were validated using experimental results obtained from earlier work reported in Papers 1, 2 and 3, and there was a good agreement between the models and the experimental data.

In the last chapter of the dissertation, a general discussion and conclusion of the work is reported.

References

Arin S., and Akdemir S. 2004. Quality properties changing of grapes during storage period. J. Biol. Sci. 4(2), 253-257.

Alvarez, G., and Flick, D. 1999a. Analysis of heterogeneous cooling of agricultural products inside bins. Part I: Aerodynamic study. J. Food Eng. 39, 227–237.

Alvarez, G., and Flick, D. 1999b. Analysis of heterogeneous cooling of agricultural products inside bins. Part II: Thermal study. J. Food Eng. 39, 239–245.

Alvarez, G., and Flick, D. 2007. Modelling turbulent flow and heat transfer using macro-porous media approach used to predict cooling kinetics of stacks of food products. J. Food Eng. 80, 391–401.

Brosnan T., and Da-Wen S. 2001. Precooling techniques and applications for horticultural products. Int. J. Refrig. 24, 154-170.

Chau K.V., Gaffney J.J., Baird C.D., Church G.A. 1985. Resistance to Air Flow of Oranges In Bulk and in Cartons. ASAE. 28 (6), 2083-2088.

Chonhenchob V, and Singh SP. 2005. Packaging performance comparison for distribution and export of Papaya fruit. Packag. Technol. Sci. 18, 125–131.

de Castro L.R., Vigneault C., Cortez L.A.B., 2005. Cooling performance of horticultural produce in containers with peripheral openings. Postharvest Biol. Technol. 38 (3), 254-261.

Delele M.A., Tijskens E., Atalay Y.T., Ho Q.T., Ramon H., Nicolaï B.M., Verboven P. 2008. Combined discrete element and CFD modelling of airflow through random stacking of horticultural products in vented boxes. J. Food Eng. 89, 33-41.

Ferrua M.J. and Singh R.P. 2009. Modeling the forced-air cooling process of fresh strawberry packages, Part I: Numerical model. Int. J. Refrig. 32, 335 – 348.

Hardenburg R, E., Watada A,E., Yi Wang, C. 1986. The Commercial Storage of Fruits, Vegetables, and Florist and Nursery Stocks. U.S. Department of Agriculture.

Kader, A.A., 1992. Postharvest biology and technology: an overview. In: A.A. Kader (Editor), Postharvest Technology of Horticultural Crops. University of California., Division of Agriculture and Natural Resources, Publ., 3311: 1520.

Kays S.J., and Paull R.E, 2004. Postharvest Biology. Exon Press, USA.

Lichter A., Kaplunov T., Zutahy Y., Daus A., Alchanatis V., Ostrovsky V., Lurie S. 2011. Physical and visual properties of grape rachis as affected by water vapour pressure deficit. Postharvest Biol. Technol. 59, 25-33.

Moureh J., and Flick D. 2004. Airflow pattern and temperature distribution in a typical refrigerated truck configuration loaded with pallets. Int. J. Refrig. 27, 464-474.

Moureh J., Tapsoba S., Derens E., Flick D. 2009. Air velocity characteristics within vented pallets loaded in a refrigerated vehicle with and without air ducts. Int. J. Refrig. 32 (2), 220-234

Nelson K.E. 1978. Pre-cooling – its significance to the market quality of table grapes. Int. J. Refrig. 1, 207 – 215.

Norton T. and Sun Da-Wen. 2006. Computational fluid dynamics (CFD) – an effective and efficient design and analysis tool for food industry: A review. Trends Food Sci. Technol. 17, 600 – 620.

Nunes M.C.N., Brecht J.K., Sargent S.A., Morais A.M.M.B. 1994. Physical and chemical quality characteristics of strawberries after storage are reduced by a short delay to cooling. Postharvest Biol. and Technol. 6, 17-28.

Nunes M.C.N., Brecht J.K., Sargent S.A., Morais A.M.M.B. 1995. Effects of delays to cooling and wrapping on strawberry quality (cv. Sweet Charlie). Food Control. 6 (6), 323-328.

Opara L.U. and Zou Q. 2007. Sensitivity Analysis of a CFD Modelling System for Airflow and Heat Transfer of Fresh Food Packaging: Inlet Air Flow Velocity and Inside-Package Configurations. J. Food Eng. 3(5), Article 16.

Smale, N.J. 2004. Mathematical modelling of airflow in the shipping systems: model development and testing. Ph.D. thesis, Massey University, Palmerston North, New Zealand.

Smale N.J., Moureh J., and Cortella G., 2006. A review of numerical models of airflow in refrigerated food applications. Int. J. Refrig. 29, 911 – 930.

Tanner D.J., Cleland A.C., and Opara L.U. (2002a). A generalized mathematical modelling methodology for design of horticultural food packages exposed to refrigerated conditions: Part 2: Heat transfer modelling and testing. Int. J. Refrig. 25, 54 – 65.

Tanner D.J., Cleland A.C., and Robertson T.R. (2002b). A generalized mathematical modelling methodology for design of horticultural food packages exposed to refrigerated conditions: Part 3: mass transfer modelling and testing. Int. J. Refrig. 25, 43 – 53.

Thompson J.F., Mitchell F.G., Rumsey T.R., Kasmire R.F., Crisosto C.H. 1998. Commercial cooling of fruits, vegetables, and flowers. Regents of the University of California. USA

Tutar M., Erdogdu F., Toka B. 2009. Computational modeling of airflow patterns and heat transfer prediction through stacked layers' products in a vented box during cooling. Int. J. Refrig. 32, 295 – 306.

van der Sman, R.G.M., 2002. Prediction of airflow through a vented box by the Darcy-Forchheimer equation. J. Food Eng. 55, 49-57.

Vigneault C., and Goyette B. 2002. Design of plastic container opening to optimize forced–air cooling of fruits and vegetables. ASAE. 18(1), 73–76.

Vigneault, C., Markarian, N.R., da Silva, A., Goyette, B., 2004. Pressure drop during forced-air ventilation of various horticultural produce in containers with different opening configurations. Trans. ASAE. 47 (3), 807-814.

Verboven, P., Hoang, M.L., Baelmans, M., Nicolai, B.M., 2004. Airflow through beds of apples and chicory roots. Biosystems Eng. 88 (1), 117-125.

Verboven, P., Flick, D., Nicolaï, B.M., Alvarez, G., 2006. Modelling transport phenomena in refrigerated food bulks, packages and stacks: basics and advances. Int. J. Refrig. 29, 985–997.

Valero D., Valverde J.M., Martínez-Romero D., Guillén F., Castillo S., and Serrano M. 2006. The combination of modified atmosphere packaging with eugenol or thymol to maintain quality, safety and functional properties of table grapes. Postharvest Biol. Technol. 41, 317 – 327.

Wills R., McGlasson B., Graham D., and Joyce D. 2007. Postharvest: An introduction to the physiology and handling of fruit, vegetables and ornamentals. University of New South Wales Press Ltd. Australia.

Xia B. and Sun Da-Wen. (2002). Application of computational fluid dynamics (CFD) in the food industry: A review. Comput. Electron. Agric. 34, 5 – 24.

Zou, Q., Opara, L.U., McKibbin, R., 2006. A CFD modelling system for airflow and heat transfer in ventilated packaging for fresh foods: I. Initial analysis and development of mathematical models. J. Food Eng. 77, 1037-1047.

2. Literature Review

Postharvest handling systems of table grapes and measurement of resistance to airflow inside horticultural packages

Nomenclature

A_{box}	box face area, m^2
A_{hole}	vent hole area, m^2
a	resistance coefficient, kg $s^{(b-2)}m^{-(b+2)}$
b	resistance exponent
d_{eff}	effective product diameter, m
D_h	package hydraulic diameter, m
κ	Darcy permeability, m^2
p	pressure, Pa
O	vent hole ratio, %
u	velocity vector, m s^{-1}
β	Forchheimer drag coefficient, m^{-1}
ε	porosity
μ	dynamic viscosity
ρ	density, kg m^{-3}

2.1. Introduction

Table grapes is the second largest export crop from South Africa consisting of about 45 million cartons exported (PPECB, 2012), and therefore contributes a significant percentage to the South African economy. The fruit is a cluster consisting of stems and berries (Winkler et al., 1974). The stems (rachis, branches, and pedicels), on which berries are borne, constitute 2 to 6 percent of the total weight at maturity, differing with variety. The skin of the berries accounts for 5% to 12% of the total weight and consists of an epidermis which is composed of 6-10 layers of small, thick-walled cells. The skin is covered with a thin waxlike layer know

as cutin which consistitutes about 1-2 % of the total weight of the skin. The cutin consists mainly of oleanolic acid, and long chain alcohols with traces of ester, fatty acids, aldehydes, and paraffins. The cutin protects the berries against water loss and the attack of organisms. The thickness and toughness of the skin differ among varieties and are factors in the degree of resistance of table grapes to handling injury in packaging, transport, and storage (Winkler et al., 1974).

Table grapes are non-climacteric fruit, which means they do not continue to ripen after harvest and for this reason they should be harvested when they reach optimum maturity (Ginsburg et al., 1978; Hardenburg et al., 1986). However, fruit quality tends to deteriorate rapidly during postharvest handling and storage, thus reducing shelf-life during marketing. Deterioration of table grape quality is mainly characterized by weight loss, stem (rachis) dehydration and browning, colour changes, accelerated berry softening, berry drop and high incidence of berry decay due mainly *to Botrytis cinerea* (Nelson, 1978; Valero et al., 2006). Sulphur dioxide gas (released by SO_2 pad) is used to control decay caused by fungi such as *Botrytis cinerea*, which grows well in the optimum storage condition [−0.5°C to 0°C, 95% relative humidity (RH)] for table grape (Ginsburg et al., 1978). However, the presence of SO_2 gas may also cause various degrees of injury to the grapes (Zoffoli et al., 2008; Harvey and Uota, 1978).

Cooling is the main technique that is widely employed to reduce postharvest related defects of fresh horticultural produce (Hardenburg et al., 1986). However, cooling efficiencies of produce such as fruit in different packages has been reported as a challenge, which often results in spatial variability of fruit temperature inside packages (Smale et al., 2006; Zou et al., 2006a). This variability of fruit temperature has been reported to cause fruit quality variability (Smale et al., 2006). Cooling of horticultural produce is achieved mainly through forced air cooling (FAC), which means that fruit temperature and its homogeneity is largely governed by the patterns of airflow (Smale et al., 2006; Zou et al., 2006a). It is therefore important that fruit packaging allows sufficient airflow in order to achieve good cooling efficiencies. Table grapes are packed in multi-scale packages to ensure good protection of fruit; however, they still suffer postharvest quality losses during cold storage and handling in the cold chain due in part to effects of packaging and packaging components on airflow patterns and produce cooling rates.

Airflow can be described as the resulting motion of air molecules when subjected to unbalanced forces and pressure differences (Tutar et al., 2009; van der Sman, 2002). During pre-cooling of table grapes, air is forced through the fruit package in response to a pressure gradient between the two sides of pallets. In the subsequent stages of the cold chain, post pre-cooling (FAC) stage, the air is not actively forced through fruit packages due to the aerodynamics of facilities and equipment used, as well as the airflow resistance caused by packaging. Since the target temperature of produce is reached during pre-cooling, the subsequent cold chain stages are required to supply sufficient airflow to maintain low product temperatures and remove respiratory heat. In these latter stages of the cold chain, cooling of packed produce could therefore be achieved primarily through conduction as the cold air circulates around fruit packages rather than being forced through packages (Nelson, 1978).

The cold chain can be segmented into four main refrigerated systems namely: cooling and storage facilities; refrigerated transport which is subdivided into road, sea and air transport; distribution centres and refrigerated displays in super-markets. Once pre-cooled the horticultural products should be handled from one segment of the chain to the next with minimal to no breakages of the cold chain. This requires good temperature management throughout the chain. However, this cold chain requirement is not always adhered to in practice, either due to human error or to poor designs of the refrigeration infrastructure being used. Since temperature homogeneity of products is governed by the patterns of air flow in refrigerated systems (Smale et al., 2006), the knowledge air flow patterns in the different refrigeration systems is imperative for proper packaging designs, cooling efficiencies and good temperature management within the cold chain.

Air flow improvement in different cold chain applications is a well-established research field in postharvest. A lot of work has been reported on the improvement of packaging design, fruit stacking inside packages and stacking patterns of fruit packages on pallets for efficient air flow and cooling (Chau et al., 1985; Haas et al., 1976; Neale and Messer 1976; Neale and Messer, 1978; Verboven et al., 2004; Vigneault and Goyette, 2002; Vigneault et al., 2004; de Castro et al., 2005; Zou et al., 2006a;b ; Ferrua and Singh, 2009b; Tutar et al., 2009). Many

researchers have reported on airflow distribution inside refrigerated storage rooms (Foster et al., 2002; 2003); refrigerated transport (Moureh et al., 2002; Moureh et al., 2004; Moureh et al., 2009c; James et al., 2006) and refrigerated display cabinets (Field et al., 2006; Amin et al., 2009; Amin et al., 2011).

In literature different techniques were used to measure and quantify airflow in the different applications within the cold chain. These techniques are either experimental or predictive. The experimental techniques could be divided into intrusive and non-intrusive techniques (Childs et al., 2000). The main differences between intrusive and non-intrusive techniques lie on the degree of contact between the measuring instrument and the medium being measured. During the intrusive measurement, the measuring device is in direct contact with the medium of interest, e.g. probes and air velocity meters in an air stream; while for the non-intrusive measurement, the medium of interest is observed remotely (Childs et al., 2000). The intrusive methods can be further divided into direct-intrusive and indirect intrusive measuring techniques. Prediction methods include different numerical modelling and simulation.

The objective of this chapter is to review table grape postharvest cold chain handling systems, including techniques used to assess the performance in cold chain systems and table grape postharvest quality defects.

2.2 Table grapes refrigeration systems

Table grape refrigeration systems could be divided into pre-cooling and cold storage; refrigerated transport and display cabinets. The commonality between all these refrigeration systems is that they use cold air as a cooling medium.

2.2.1 Pre-cooling system

Pre-cooling has been defined as the rapid removal of field heat from freshly harvested produce in order to slow down metabolism and reduce deterioration prior to transport or storage (Brosnan and Sun, 2001). During table grape pre-cooling, FAC is used to rapidly remove field heat and this technique has also been referred to as forced convection (Nelson, 1978). The term FAC has been used to describe the cooling of fruits or similar contents of packages by cold air forced through containers by a static head (Guillou, 1960). Storage of grapes for periods from a week to one month requires pre-cooling to the storage temperature of -0.5°C at a relative humidity of 95% and higher if possible (Ginsburg et al., 1978). The pre-cooling is a separate operation from the normal storage in refrigerated room, as most storage rooms designed for holding the produce have neither the capacity nor the air movement needed for rapid cooling (Hardenburg et al., 1986).

During FAC of table grapes inside refrigerated rooms, fruit pallets are placed in two parallel lanes forming a channel and then a tarpaulin is placed over the top of pallets covering the open channel (Fig. 1b), (Thompson et al., 1998; Ferrua and Singh, 2009a). Following the placement of a tarpaulin over pallets, a fan is sealed against the channel and then switched on to remove air from the channel and thus creating a pressure difference between two sides of the pallets (Fig. 1). Cold air circulating inside the cold room is then forced through the packed products in response to the created pressure gradient and thus convectively cooling the fruit (Thompson et al., 1998). Other pre-cooling facilities are equipped with a racking system, where grape pallets are placed in parallel lanes and with two layers of pallets on top of each other in racks (Fig. 2). In this system the suction fans are situated on top of the tunnel near the roof and the tarpaulin is suspended down from roof to seal off the channel between the two lanes (rows of pallets) (Fig. 2).

Some of the table grape cold store facilities have a number of small sized rooms (Winkler et al., 1974), holding a few grape pallets at a time (Figure 2). These smaller rooms are often referred to as pre-cooling rooms or tunnels. Other cooling facilities have bigger warehouse-type refrigerated room, where pallets are arranged in a pre-cooling tunnel setup and a number of these pre-cooling tunnels are built in the same refrigerated room. Each tunnel is made up of 18 to 20 pallets on average and they each have individual fans forcing cold air through packages.

2.2.2 Table grape storage system

Although not ideal for table grapes quality, sometimes grapes are stored for some period until either a shipping opportunity becomes available (especially in the production countries) or the buying power of consumers increases (mostly in importing countries and supermarkets). During grape storage, air must be circulated sufficiently to keep a cold storage room at even temperature throughout the room (Hardenburg et al., 1986). Since table grapes are pre-cooled to the desired pulp temperatures prior to cold storage, a high air velocity is unnecessary and usually undesirable. Only enough air movement should be provided to remove respiratory heat and heat entering the room (Hardenburg et al., 1986). A simplified arrangement of a typical cold room is such that cold air is discharged from the evaporator coils into the room with the aid of fans. The evaporators are usually situated near the ceiling of the room, and so the cold air sweeps the ceiling (Fig. 1) and circulates past the produce and is then returned to the evaporator with absorbed heat from the produce (Thompson et al., 1998). Amos (2005), characterised airflow in a commercial cold store and he found that there was an uneven distribution of airflow within the cold store. He reported that the top layers and side columns of bins tended to receive sufficient airflow, while the central positions received lower airflow. The temperature results indicated that the hot spots coincided with the area of lowest airflow (Amos, 2005). Chourasia and Goswami (2007), also found some temperature and airflow variability inside a potato cold store, with some areas showing possible hot and cold spots. Xie et al. (2006), used CFD modelling to study the effect of design parameters (such as corner baffle, the stack mode of foodstuffs, etc.) on the flow and temperature fields of a cold store and they found that all these design parameters, especially the stack mode of foodstuffs, greatly influenced the flow and temperature fields inside the cold store (Xie et al., 2006).

2.2.3 Refrigerated trucks, reefer containers and reefer vessels (ships)

Refrigerated truck trailers do not have enough air flow or refrigeration capacity to cool perishable commodities rapidly (Thompson et al., 1998; Moureh and Flick, 2004). For this

reason table grapes and other horticultural products should always be properly cooled to desired product temperature (-0.5°C for grapes) before loading in refrigerated trucks (Thompson et al., 1998).

Smale et al. (2006) stated that from an aerodynamic perspective, the key characteristic of transport equipment is the placement of both the air delivery and return on the same face. This configuration is almost universally used, as it is practical to place all the refrigerating equipment at one end of the transport unit (Smale et al., 2006). The drawback of this asymmetrical design is the presence of a strong pathway between the two sections, implying high velocities in the front of the refrigerated enclosure (Fig. 3) (Smale et al., 2006; Moureh and Flick, 2004; Moureh et al., 2009c). In addition, the compactness of the cargo and high resistance to airflow due to narrow air spaces between pallets result in an uneven air distribution in the cargo where stagnant zones with poor ventilation can be observed in the rear part of the vehicle (Smale et al., 2006).

Moureh et al. (2009c) characterised air velocity within ventilated packages inside a refrigerated vehicle with or without an air duct. The authors reported that vehicles without air ducts tended to have poor air velocities at rear positions (near doors), while by comparison, the use of air ducts contributes significantly to a more even distribution throughout the container by improving air supply towards the rear, whilst reducing airflow intensity at the front (Moureh et al., 2009c).

Tanner and Amos (2003) reported significant spatial variability in temperature along the length and width of reefer containers during shipping of kiwifruits. Punt and Huysamer (2005) reported that plum pallets positioned near the doors responded poorly to changes in set-point temperature of the reefer container while those positioned near the cooling unit responded well during shipping of plums under dual temperature regimes of -0.5 °C (2 days); 7.5 °C (5 days) and -1 °C (for the remainder of the journey). These results could also be attributed to the aerodynamics of reefer containers where the rear positions (near doors) are associated with poor airflow velocities.

The aerodynamics in reefer vessels (ships) is also similar to that found in reefer containers and refrigerated trailers, where both the delivery and the return air ducts are on the same side. Tanner and Amos (2003) found significant variability in temperatures along the length of the vessel deck (Fig. 4), probably due to compactness of loaded pallets bringing about resistance to airflow. They attributed this temperature variability to a possibility of insufficient airflow in the deck. They also reported that the largest cause of variability in pallet temperature was related to slow rate of cooling after placement in the cargo hold. The results from their study indicated that it took up to 10 days for the kiwi fruit temperatures to reach steady state (Tanner and Amos, 2003).

The resistance to airflow through packed products in refrigerated transport systems could be related to the tight loading arrangement of pallets inside the transport confinement and possibly also the misalignment of the ventilation holes between fruit packages.

2.2.4 Refrigerated display cabinets

In supermarkets, open-type refrigerated display cabinets (RDCs) are used extensively to merchandise perishable food at suitable temperatures (Fig. 5) (Moureh et al., 2009a). A typical RDC consists of a limited container, insulating heat shell and a small refrigerating unit. The refrigeration system controls product storage temperatures by removing all of the heat gain from components of the display case. RDCs operate by circulating cold air around the displayed products (Moureh et al., 2009a). Two or more fans circulate the air through an evaporator heat exchanger from the inlet to the outlet section (Moureh et al., 2009a).

Display cabinets are known to be the weakest link from the cold chain point of view and, therefore, particular attention needs to be paid to their design (Cortella, 2002). The main challenge facing the efficiency of refrigerated display cabinets is to prevent warm ambient air in the supermarket from entering the open display cabinet system, thereby adding the heat load to the display's refrigeration system and causing inefficient cooling. Refrigerated air curtains (which are cold turbulent air jets) are usually used in open display cabinets of

supermarkets as a barrier between the warm ambient air and the cold refrigerated air (Field and Loth, 2006; Moureh et al., 2009a). Most studies regarding the improvement of efficiency in open refrigerated display cases focus on improving the performance of these air curtains through improvement of cabinet designs (Amin et al., 2011). Amin et al. (2011) studied the effect of variables (such as jet throw angle, height of the opening, airflow rate ratio, etc) on the entrainment and penetration of outside ambient air into the refrigerated cabinet system, and they also investigated the relationship between these variables and the infiltration. They found a strong and direct relationship between jet exit Reynolds number and offset angle. Reynolds number defines how turbulent or laminar the air flow is; the higher the Reynolds number is, the more turbulent the flow becomes. The increase in Reynolds number resulted in an increase in absolute infiltration rate. The offset angle resulted in similar effects on absolute infiltration rate as the Reynolds number. They also reported that although the relationship between infiltration and the tested variables (i.e. jet throw angle, height of the opening, and flow rate ratio), was significant, the effect of each variable was better pictured in combination with other variables (Amin et al., 2011). Amin et al. (2012) studied the effect of what they referred to as ‘secondary variables’ on the efficiency of the air curtain. These secondary variables included the turbulence intensity of the air curtain jet at its discharge nozzle, average percentage of the space between the shelves that was filled with food products, difference between the temperatures of ambient air and the jet at the discharge nozzle, as well as the relative humidity between the aforementioned locations. They found that the temperature and relative humidity changes were of little or no importance, while the turbulence intensity changes infiltration rate almost linearly and the food level (amount of food on shelf) varies it in a nonlinear manner (Amin et al., 2012).

Field and Loth (2006) measured air velocity and temperatures of the air curtains in a refrigerated display case in order to better understand the fluid dynamics which governs the entrainment. The results obtained from their study showed that the entrainment of the ambient air was governed by a variety of eddy engulfing structures. Eddy is defined as the swirling of a fluid (e.g. air) and the reverse current created when the fluid flows past an obstacle. They also reported that the flow measurement results indicated negatively-buoyant acceleration following the jet exhaust, followed by a more linear curtain growth characteristic of isothermal wall jets (Field and Loth, 2006).

Moureh et al. (2009a) studied the use of mist flow whereby fine water droplets are injected into the air curtain to improve the performance of refrigerated display cabinets. They found that the deposition and evaporation of droplets on the surface of products partially compensate the radiative heat gained by the products by removing from it the amount of latent heat of the evaporated droplets (Moureh et al., 2009a).

2.3 Table grape packaging

In order to maximise the cooling efficiency and maintain temperature homogeneity of packed products, the total ventilation areas of fruit packages should be large enough not to restrict the airflow (Pathare et al., 2012). The vent positions should cover most of the walls and the bottom (and the top if the container includes a cover) of the container and not affect the container structure (de Castro et al. 2004; Arifin and Chau 1987; Vigneault and Goyette 2002). Several experimental studies have been reported in the literature to elucidate the influence of different package vent designs on the efficiency of the forced-air precooling process. The importance of these design criteria does not change with the size of the container since vent openings of individual consumer package, reusable box or standard pallet-size container play all the same major role in the efficiency of the cooling process (Émond et al., 1996).

Table grapes are packed in different multi-scale packages (Fig. 6). Most of the published work on table grape packaging has focussed on modified atmosphere packaging (MAP) as an alternative to controlling decay and postharvest quality of grapes (Artés-Hernández et al., 2006; Candir et al., 2012; Costa et al., 2011; Ustun et al., 2012; Valero et al., 2006; Zoffoli et al., 1999). There is, therefore, a very limited knowledge on the effects of table grape multi-packages on resistance to airflow and cooling performance. In literature, the resistance to airflow through fruit packages has largely been related to the amount of vent-hole area of packages, product porosity, and fluid properties (Chau et al., 1985; Haas et al., 1976; Vigneault and Goyette, 2002; Vigneault et al., 2004; Neale and Messer, 1976; Neale and Messer, 1978; Zou et al., 2006a). Based on extensive experimental research, de Castro et al.

(2005) recommended a vent-hole ratio of 8-16% of the surface of the container to optimise the use of energy.

Resistance to airflow may even be higher during table grape cooling due to the fact that grape bunches are packed inside multi-scale packages. These multi-scale packages include the carton boxes with multiple inner packaging materials which include carton liner films, SO_2 pad, moisture absorption sheets and bunch carry bags.

2.4 Assessment of pre-cooling, storage and packaging

The assessment of airflow, cooling and moisture loss characteristics within the cold chain systems could be done using experimental and mathematical techniques. This section reviews the principles and application of these techniques.

2.4.1 Experimental techniques for measuring and quantifying airflow within cold chain

The experimental techniques can be subdivided into direct intrusive; indirect intrusive and non-intrusive methods.

Direct intrusive methods

The direct intrusive methods include all techniques that measure airflow directly; however, they are intrusive in nature in that the instruments used for measuring are in direct contact with the air flow fields. These include hot-wire and vane anemometers.

Hotwire anemometer

The “hotwire anemometer” is a well-known transducer and has been used for many years in measuring mean and fluctuating flow velocities (Al khalfioui et al., 2003; Sanyal et al.,

2006). It usually refers to the use of a small (2–5 μm in diameter) electrically heated element placed in a fluid with the aim of measuring the flow velocity of that fluid (Al khalfioui et al., 2003). The commonly used wire materials include the platinum, platinum– iridium and tungsten (Sanyal et al., 2006). The hotwire meter may be operated either in constant current or in constant temperature mode (Sanyal et al., 2006). In the first method, an electric circuit is adjusted to feed a constant current to the hotwire. The current and the wire resistance define the power being fed to the wire, which is a function of the flow velocity. The second mode of hotwire operation is known as constant-temperature mode. In a constant-temperature anemometer (CTA), resistance and temperature are maintained at constant values; so when fluid velocity increases the system also increases the current through the sensor to restore equilibrium. Consequently, voltage drop across the element increases, thus giving a voltage signal dependent on fluid velocity (Sanyal et al., 2006).

The principle of constant-temperature anemometry was discovered experimentally in 1909. A thin uniform wire, kept at constant resistance and temperature (by an adjusted continuous electric current) and immersed in a uniform transverse wind, dissipates heat convectively in proportion to the temperature elevation of the wire above that of the passing air, and also in proportion to the square-root of the wind velocity (Anon, 1917).

Hot wire anemometry has a number of qualities, which includes an easy implementation and low cost. However, its main drawback is its high operating temperature as well as its high sensitivity to variations in the fluid temperature (Al khalfioui et al., 2003). Other disadvantages include the intrusive nature of the instrument during measurement, which often disrupt the parameter being measured. This happens either because they induce singular main loss in the air network or they generate some natural convection as a result of their operating temperature (Al khalfioui et al., 2003). In addition, the hotwire anemometer is a local measurement which has to be reproduced many times in order to get a profile of velocity allowing the determination of a volumetric flow (Al khalfioui et al., 2003; Glaniger et al., 2000).

The hot-wire anemometer has been widely used by many researchers to measure airflow during cooling and other applications in the cold chain (Alvarez and Flick, 1999; Irving and Shepherd, 1982; Foster et al., 2002; Hammond et al., 2011; Laguerre et al., 2012; Moureh et al., 2009a; Xie et al., 2006).

Xie et al. (2006) and Foster et al. (2007) used hotwire anemometers to measure the fan outlet velocity and air jet velocity across the width of the air curtain at the door of cold rooms, respectively. Moureh et al. (2009b) used an original experimental technique which consisted of indirect velocity measurement by means of heat transfer analogy for hot wire anemometry. They measured internal macroscopic velocities within porous fruit boxes. Alvarez and Flick, (1999) measured air velocity and turbulence intensity inside fruit bins containing spheres and upstream of the pallets using a constant temperature hot-wire anemometer. However, they found that the use of a single hot wire made it impossible to separate the two components (x and y) of the velocity vector, and another challenge they encountered was that the velocity and turbulence between the spheres could not be measured without removing some spheres, which meant that two rows of spheres had to be removed each time to accommodate the hot wire. This removal of the spheres may have modified the velocity field to some extent (Alvarez and Flick, 1999).

Irving and Shepherd (1982) used hot wire anemometers to measure air circulation rate inside integral refrigerated shipping containers. They found that the hot wire anemometers tended to overestimate the flow rate by 5 to 40% during their experiments (Irving and Shepherd, 1982).

Some researchers used hotwire anemometers to measure the discharge velocity and turbulence across the air discharge grille (ADG) of refrigerated display cabinets (Hammond et al., 2011; Laguerre et al., 2012). Moureh et al. (2009a) also used a constant temperature hot wire anemometer to measure air velocity in a refrigerated display cabinet (RDC). They reported that the hotwire probe could be used to measure the time-averaged velocities, but did not give any information on flow turbulence due to the long response time (2 s).

Vane anemometers

Vane anemometers have been used for many years to measure velocities in ducts (Ower and Pankhurst; 1966), weather stations and ventilation systems. The mechanical instruments are made of rotating blades (vane) which are orientated at an angle to the incoming air stream and pointers moving over a graduated dial marked with scales of feet or metres (Ower and Pankhurst; 1966). The instrument is based on the principle that air forces acting on the vane cause the spindle to rotate at a rate depending mainly on the air speed. However, to determine air speed using the mechanical vane anemometer, a stop watch is required in order to measure time taken for a number of 'feet or metres of air', as shown by the indicating mechanism, to pass the instrument's ducts (Ower and Pankhurst; 1966). Modern digital vane anemometers indicate velocity readings (m/s) directly on an odometer counter, an illuminated screen, or feed an electric signal to a data logging system.

Foster et al. (2002) used mini vane anemometers based on the impeller unit of Krestrel K1001 anemometer (diameter 25 mm) to measure air movement through the doorway of a refrigerated room. Irving and Shepherd (1982) also used vane anemometers to measure air circulation rate inside integral refrigerated shipping containers. They found that the vane anemometers overestimated the flow rate by 10 to 55% during their experiments (Irving and Shepherd, 1982).

Indirect intrusive

The indirect intrusive methods include those techniques that measure the parameters in the flow field that could be correlated to the airflow patterns. They are also intrusive in that the instrumentation used is inside the flow field. The indirect intrusive techniques discussed in this review include the tracer gas methods and thermal tracing methods e.g. thermocouples and compact sensors.

Tracer gases

The tracer gas technique is one of the flow visualisation methods, where the movement of a tracer gas is monitored using instruments rather than by visual observation (Tanner et al., 2000; Smale 2004). The tracer techniques generally involve injecting a tracer gas into a flow path and monitoring concentration changes at numerous sample points. Analysis can involve either calculation of a 'time of gas arrival' at each of the sample points or concentrations at the sample points to determine the level of mixing (Smale, 2004). Figure 7 shows a typical tracer method setup. In literature, the choice of tracer gas used in each application has largely been associated with the price, availability, accuracy and response time of the measuring sensors (Sherman, 1990; Smale, 2004). Smale (2004) made a cost comparison and response times of different tracer gas instrumentations.

A good tracer gas should comply with certain requirements in order to successfully study flow systems. According to Sherman (1990), an ideal tracer gas must have some of the following properties:

Safety: the presence of the tracer should not pose a hazard to people, materials, or activities in and around the test area. The tracer therefore should be non-flammable, non-toxic, non-allergenic, etc.

Non-reactivity: because conservation of tracer will be used to infer airflow, the tracer gas should not react chemically or physically with any part of the system under study.

Insensibility: the presence of the tracer should in no way affect the processes that are being studied. Thus, an ideal tracer gas should not affect the airflow or air density of the system.

Uniqueness: an ideal tracer should be able to be recognized from all other constituents of air. In general it should not be a normal constituent of air in which it is being placed, but a tracer with non-zero back-ground may be used provided that the background is stable and additional tracer concentration is significantly larger than the (steady) background.

Measurability: the (true) concentration and all injected tracer gas must be quantifiable through some sort of instrumentation.

Table 1 summarises the different applications of tracer gas techniques in the cold chain. Details of different gases used, measuring method (i.e. time of tracer arrival or concentration at point of measurement) and instrumentation used are reported.

Thermal tracing

Ways of indirect airflow measurement involving measuring the product's (or thermal spheres) cooling patterns have been reported by few researchers (de Castro et al., 2005; Vigneault and de Castro, 2005; Vigneault et al., 2007). This method involves placing instrumented balls or thermal sensors in different positions inside fruit packages and then correlating their cooling rates to air-flow rates. In most forced-air cooling studies thermo-electronic sensors such as thermocouples and probes are used to monitor cooling rates and temperature patterns of packed produce in response to the approach cold air velocity (Gaffney and Baird 1977; Dincer, 1995a; b; c; Foster et al., 2002). This involves systematic suspension of probes in air spaces or inside fruit-core to monitor spatial temperature changes in the flow direction.

Thermocouples

In its simplest form thermocouples are made up of two dissimilar metals (Metal A and Metal B) fused together by soldering at the hot junction (measuring point) and the cold junction is the loose end of the two metals, which connect to the voltmeters or data loggers to read or log the temperature data (Kasap, 1997-2001; Herwaarden and Sarro, 1986; Genix et al., 2009). The principle of thermocouples is based on the Seebeck effect (Kasap 1997-2001; Drebushchak, 2009; Genix et al., 2009) which was discovered by Seebeck in 1821. Seebeck discovered that that when dissimilar two metals having different Seebeck coefficients are joined together at one end, a voltage called Electromotive Force (EMF) could be detected using a voltmeter at the other end (Genix et al., 2009). This measured electromotive force was proportional to the thermal gradient between the hot and cold junction materials (Kasap,

1997-2001; Drebushchak, 2009; Genix et al., 2009). The Seebeck effect is defined as the potential voltage difference (ΔV) across a piece of metal due to a temperature difference (ΔT) between the hot and cold junctions. There are different types of thermocouples that are commercially available and these are presented in the review by Childs et al. (2000).

Many researchers have used thermocouples to measure spatial temperature changes inside ventilated fruit packages and fruit in bulk during forced air cooling (Acevedo et al., 2007; Amara et al., 2004; Barbin et al., 2010; 2012; Ferrua and Singh, 2009c; 2011; Gordon and Thorne, 1990; Hu and Sun, 2001; Laguerre et al., 2006; Martínez-Romero et al., 2003; Moureh et al., 2009c; van der Sman et al., 1996; 2000). Others (Foster et al., 2002; Xie et al., 2006) have used thermocouples to monitor air temperature changes inside cold rooms with or without products. Some researchers (Punt and Huysamer, 2005; Tanner and Amos, 2003; Tso et al., 2002) studied the cooling patterns of fruits inside refrigerated trucks; reefer containers and reefer vessel holds. Thermocouples have also been used to measure air and product cooling in refrigerated display cabinets (Field and Loth., 2006; Hammond et al., 2011; Laguerre et al., 2012; Moureh et al., 2009a). In these studies thermocouples were suspended in different positions inside fruit packages; cold stores; refrigerated transport and display cabinets, mainly in the direction of the airflow in order to monitor spatial air and fruit temperatures distribution inside confined spaces. Thermocouples were also inserted in fruits or spheres or aluminium bodies in order to monitor fruit cooling in different positions.

One of the main advantages of thermocouples is that they are relatively cheap (Childs et al., 2000) and they are compatible with a wide range of data loggers (Table 3). However, Hu and Sun (2002) showed that there could be an error in temperature readings obtained using thermocouples if care is not taken during installation. They found inaccuracies in temperature readings associated with thermocouples inserted too shallow (near sample surface) into the sample (Hu and Sun, 2002). Too long thermocouple wires hanging out side the sample (exposed to cold air-blasts) also adds to error readings (Hu and Sun, 2002). This suggests that care should be taken when installing thermocouple wires into fruits in order to avoid error readings.

Infrared sensors

Temperature measurement systems based on monitoring thermal radiation in the infrared spectrum are useful for monitoring temperatures in the ranges from 50 to 6000 K (Childs et al., 2000). An infrared measuring system comprises of the source or target, the environment, the medium through which the radiant energy is transmitted, usually a gas, and the measurement device. The measuring device may include an optical system, a detector, and a control and analysis system. Radiation detectors can be broadly grouped into three categories: disappearing filament optical pyrometers, thermal detectors, and photon or quantum detectors.

Thermal detectors convert the absorbed electromagnetic radiation into heat energy, causing the detector temperature to rise (Childs et al., 2000). This can be sensed by effects on certain physical properties, such as electrical resistance used by bolometers, thermoelectric emf used by thermocouple and thermopile detectors, and electrical polarization used by pyro-electric detectors. The principal application of thermal detectors is for measurement of low temperatures where there is limited radiant flux and the peak of the Planck curve is well into the infrared. Thermal detectors offer wide spectral response by detecting the emitted radiation across the whole spectrum at the expense of sensitivity and response speed. For higher temperatures, devices with narrower spectral bandwidth are more suitable (Childs et al., 2000). Bolometers are thermal detectors in which the incident thermal radiation produces a change in temperature of a resistance temperature device, which may be a RTD or a thermistor. Bolometers can however be comparatively slow with time constants of 10-100 ms. A thermopile is an alternative to the use of thermal resistance temperature device. A thermopile consists of a number of series-connected thermocouples arranged such that the local heat flux generates a temperature difference between each pair of thermocouple junctions. In an infrared thermal detector, the thermopile is arranged so that half of the junctions are maintained at a constant temperature by being in contact with a component with relatively large thermal inertia. The radiant energy heats the other junctions, generating a thermoelectric emf (Childs et al., 2000).

Resistance Thermometers

The temperature dependence of electrical resistance is fundamental to the operation of these sensors (Childs et al., 2000). The resistance of a conductor is related to its temperature because the motion of free electrons and of atomic lattice vibrations is also temperature dependant. Any conductor could in theory be used for a resistance temperature device (RTD), however, considerations of cost, temperature coefficient of resistance (a large coefficient value leads to a more sensitive instrument), ability to resist oxidation, and manufacturing constraints limit the choice. The most widely used conductors include copper, gold, nickel, platinum, and silver. Resistance temperature devices can be highly accurate. They are also widely used in industrial applications. The particular design of the sensing element depends on the application, the required accuracy, sensitivity, and robustness (Childs et al., 2000).

Dincer (1995a) used such probes to measure the center temperatures of individual figs (thermal spheres) at the air flow velocities of 1.1, 1.5, 1.75, and 2.5 m/s. He found that the cooling coefficient and lag factor varied linearly, the half cooling time and seven-eighths cooling time decreased by 21.5% and 20.9% and the heat transfer coefficient increased by 27.3% with increasing air-flow velocity from 1.1 to 2.5 m/s.

Tso et al. (2002) used resistance temperature detectors (RTD-100) to measure the air temperature inside the body of a refrigerated truck, and a compact transducer to measure the relative humidity in order to characterise the heat and mass transfer in a refrigerated truck with or without air and plastic strip curtains. They reported that an average air temperature inside the truck increased to 14°, 7° and 8 °C from an initial temperature of – 10 °C, for cases without an air curtain, with a fan air curtain and with a plastic strip curtain, respectively, within 2 min after the door was opened.

Vigneault et al. (2007) developed an airflow rate (AFR) measuring method without modifying the airflow pattern inside horticultural crop packages. The method involved the use of instrumented balls to determine the correlations among their cooling rates (CR),

cooling indexes (CI), air approach velocities, and AFRs. With this method they successfully determined the relationships between the AFRs and the CRs as a function of the position of the instrumented balls in reference to the air entrance through packages with different vent-hole ratio. De Castro et al. (2005) used similar instrumented balls to investigate the air pathways for peripheral and central opening configurations of packages during horticultural produce forced-air cooling process.

Moureh et al. (2009a) used a black painted thermal sensor (type not specified) to measure locally the surface temperature along the refrigerated display cabinet. The black paint served to increase the emissivity of the sensor and thus to increase the proportion of absorbed heat flux emitted by the external walls. This sensor was set precisely on the top plane representing the food surface in order to avoid a flow disturbance.

As part of the review by Ruiz-Garcia and Lunadei (2011), the application of RFID tags with embedded temperature sensors in the cold chain is reported. The cost the RFID technology was reported to be a major hurdle in the widespread use of this technology in agricultural industries (Ruiz-Garcia and Lunadei, 2011).

Non-intrusive experimental methods

The non-intrusive measurement techniques do not cause any disturbances to the flow fields under study, and therefore are capable of measuring difficult conditions (Kumara et al., 2010). Advances in optical diagnostics as well as in computers have led to rapid progress in the development of non-invasive measurements and flow visualization techniques for multiphase flows. The Particle Image Velocimerty (PIV) and Laser Doppler Velocimetry (LDV) are the two widely used optical measurement techniques for gas-liquid two-phased flow applications (Kumara et al., 2010).

Laser Doppler Velocimetry (LDV)

In its simplest form, LDV crosses two beams of collimated, monochromatic and coherent laser light in the flow of the fluid being measured (Kumara et al., 2010). The two beams are usually obtained by splitting a single beam, thus ensuring coherency between the two. The two beams are made to intersect at their waists (the focal point of the laser beam) (Kumara et al., 2010). The velocity measurement is made in the region where the beams intersect. It is called the measurement volume. The interference of the light beams in the measurement volume creates a set of equally spaced fringes (light and dark bands) that are parallel to the bisector of the beams. A measurement is made when a tiny particle being carried by the flow passes through these fringes. The frequency of the light scattered (and/or refracted) from the particles is different from that of the incident beam. This difference in frequency, called the Doppler shift, is linearly proportional to the particle velocity. The seeded particles must be big enough to scatter sufficient light for signal detection but small enough to follow the flow faithfully (Kumara et al., 2010). The light scattered by the particle is collected by the receiving lens and focussed into a photodetector which converts the fluctuations in light intensity into fluctuations in a voltage signal. An electronic device known as a signal processor is then used to determine the frequency of the signal and therefore the flow velocity (Kumara et al., 2010).

The LDV technique has the advantages of (Wang, 1988; Kumara et al., 2010):

- fast dynamic response and wide measuring range;
- no need for calibration, because the speed of light and laser wavelength are known;
- no interference to the flow field, because there is no physical probe inside the flow field;
- independence of density and temperature variations, because the particle velocity and light frequency are not influenced by density and temperature fluctuations;
- small spatial resolution--the wavelength of light is very short and can easily be focused to a very small spot;
- remote sensing, because the laser beam can propagate a long distance without spreading too much;

- high quality of operation in a hostile environment, because the laser and detectors can be isolated from the environment by the use of optical windows.

Its disadvantages are (Wang, 1988):

- a usually low signal-to-noise ratio, because the scattered light intensity is very weak;
- critical optical alignment--to obtain spatial coherence, alignment accuracy should be of the order of light wavelength;
- possible need for seed particles to increase the signal-to-noise ratio;
- high cost, because both laser and signal processing equipment are very expensive;
- LDV has a major drawback due to the fact that in order to obtain a full-field profile of a given flow regime, multiple measurements must be made at various points throughout the flow and simultaneously as well if the flow is unsteady (Kumara et al., 2010).

Particle Image Velocimetry (PIV)

Adrian (1991) reported a comprehensive review on the origin and principles of the particle image velocimetry (PIV) technique. PIV differs from LDV in that the output of a pulsed high energy laser is directed through a cylindrical lens system which shapes the resulting beam into a thin planer sheet of high-intensity laser light (Kumara et al., 2010; Adrian, 1991). This sheet of light is subsequently aligned and directed through the flow where it is scattered by seed particles (Adrian 1991; Kumara et al., 2010). A camera positioned at 90° to the light sheet captures the images of illuminated particles. The laser light is pulsed and the camera captures particle images at that instant. Individual photographic film would be exposed for two or more pulses of laser light with a known time separation between pulses, thus capturing the sequential locations of the particles as they are convicted by the flow (Forliti et al., 2000). Images are formed on a photographic film or on a video array detector, and the images are subsequently transferred to a computer for automatic analysis (Adrian 1991).

The analysis or “interrogation” of the recorded images field is one of the most important steps in the entire process, as it couples with the image-acquisition process to determine the

accuracy, reliability, and spatial resolution of the measurements; it is also the most time-consuming part of the process (Adrian, 1991). There are four main interrogation techniques, namely, Direct Autocorrelation; Direct cross correlation; Young's Fringes and Optical correlation and the principles of these techniques are detailed in the review by Adrian (1991). In a case where the recorded image contains a small amount of information, as for a typical video camera that consists of an array of approximately 500 x 500 pixels, the entire image field (e.g. 2.5 x 105 pixels) can be digitized and passed to the computer in one file (Adrian, 1991). However, if the image field is very rich in information, as for a 100 mm x 125 piece of 300 lines mm^{-1} resolution photographic film containing over 1.1 x 109 pixels, the local velocity in a small region of the image field is found by digitizing an interrogation spot and analysing the images within the spots, one spot at a time. The velocity field is then obtained by repeating this process on a grid of such interrogation spots (Adrian 1991).

The LDV and PIV have been used to measure and quantify airflow in the different segments of the cold chain. Some researchers have used PIV and LDV to study airflow through ventilated fruit packages (Ferrua and Singh, 2008; Moureh et al., 2009b; 2009c; Tapsoba et al., 2007), others have studies airflow through cold rooms (Foster et al., 2002; Nahor et al., 2005), while others have used PIV and LDV to study airflow in refrigerated trucks (Moureh et al., 2002; Moureh and Flick, 2004; Tapsoba et al., 2006) and display cabinets (Field and Loth, 2006; Laguerre et al., 2012b)

The primary advantages associated with PIV lie in the non-invasive nature of the measurements and in the full-field velocity profile generated from a single measurement (Kumara et al., 2010). One of the disadvantages of PIV is that air cannot be used as the working fluid in an enclosed transparent structure due to the large differences between the refractive indices of air and the transparent solids such as acrylic. This difference in refractive indices tends to distort the laser sheet and the light scattered from the seeded particles as they pass through the system (Ferrua and Singh, 2008; Hopkins et al., 2000; Kelly et al., 2000). An appropriate transparent solid/liquid model, compatible with PIV measurements, must be selected (Ferrua and Singh, 2008).

2.4.2 Mathematical methods used to quantify and predict airflow

In the past decade, there has been a number of review articles reporting on the different applications of numerical models in the food refrigerated systems (Xia and Sun, 2002; Wang and Sun, 2003; Smale et al., 2006; Verboven et al., 2006; Norton and Sun, 2006; Delele et al., 2010; Ambaw et al., 2012; Laguerre et al., 2012a). The increasing number of these review papers indicates the rapid rate of uptake and interest in the application of numerical modelling by researchers within the food and postharvest refrigeration industries. There are a number of mathematical models that are being employed to predict and quantify airflow within the postharvest cold chain and some of these are presented in the subsequent sections.

Computational Fluid Dynamic models (CFD)

The principles of computational fluid dynamics (CFD) are well covered in the reviews by Norton and Sun (2006), Smale et al. (2006) and Xia and Sun (2002). CFD has become a widely used tool in the food industry in recent years and is defined as a numerical solution for the governing equations (i.e. the Navier-Stokes equations) in a geometrical domain (Smale et al., 2006; Xia and Sun, 2002). As discussed by Smale et al. (2006) and Xia and Sun (2002), the CFD simulation process can be subdivided into three main stages or phases, namely; the pre-processing; processing or solving and post-processing phases. Pre-processing includes problem thinking, meshing and generation of computational domain; defining thermo-physical properties, the transfer processes and simulation type (Xia and Sun, 2002). These mathematical equations are discretised and solved to obtain an approximation of the values for each variable at specific points in the domain (Smale et al., 2006). During post-processing the analysis of the results of all the variables throughout the domain is performed. The result must be processed so that it can be easily reported, visualised and analysed. The application of CFD and other numerical models in the different systems of the cold chain have recently been reviewed by Ambaw et al. (2012) and Laguerre et al. (2012).

Lattice Boltzmann Method

The Lattice Boltzmann method (LBM) has been reported as a good alternative numerical solution method of the convection-diffusion problem, requiring little advanced mathematics (van der Sman et al., 2002). Unlike conventional numerical schemes based on discretization of macroscopic continuum equations, the lattice Boltzmann method is based on microscopic models and mesoscopic kinetics (Chen and Doolen, 1998). Chen and Doolen (1998), did a comprehensive review of LBM including the origin of the scheme and the fundamental equations involved. The kinetic nature of the LBM introduces three important features that distinguish it from other numerical methods (Chen and Doolen, 1998). First, the convection operator (or streaming process) of the LBM in phase space (or velocity space) is linear. Second, the incompressible Navier-Stokes (NS) equations can be obtained in the nearly incompressible limit of the LBM. Third, the LBM utilizes a minimal set of velocities in phase space (Chen and Doolen, 1998).

The application of LBM in food refrigerated systems was last reviewed by Smale et al. (2006) and there have been no recent reports found in literature on the application of LBM in the cold chain after their review.

2.4.3 Assessment of airflow resistance

The relationship between the pressure drop and air velocity is governed by Darcy's law, which states that for small airflows the air flow rate is proportional to the applied pressure drop (van der Sman, 2002). The Darcy's law which can be represented by, $-\nabla p = \mu/\kappa u$, where p is the pressure, μ is the dynamic viscosity of air, κ is the permeability of the porous medium, u is the airflow velocity, and holds where small airflow velocity ranges are concerned, and these small airflows are indicated by the particle Reynolds number $Re_p < 1$. However, at higher flow rates, i.e. at particle Reynolds number $Re_p > 1$, the airflow is described by the Darcy–Forchheimer equation, which includes a quadratic term (van der Sman, 2002). The Forchheimer term applies at higher velocities and it represents a form drag. For flow through a confined packed bed, such as a vented packaging, the Darcy–

Forchheimer equation is extended with the Brinkman term, which is required for the description of the boundary layer at the solid/porous-media interface (van der Sman, 2002);

$$-\nabla p = \frac{\mu}{\kappa}\vec{u} + \beta\rho|u|\vec{u} - \mu_{eff}\nabla^2\vec{u} \tag{1}$$

which is complemented with the continuity equation

$$\nabla.\vec{u} = 0 \tag{2}$$

Here p is the pressure, μ is the dynamic viscosity of air, κ is the permeability of the porous medium, u is the airflow velocity, ρ is the density of air, β is the Forchheimer constant, and μ_{eff} is the effective dynamic viscosity in the boundary layer at the solid/porous-media interface (van der Sman, 2002). It can be assumed that $\mu_{eff} \approx \mu$ (Vafai & Tien, 1980; van der Sman 2002). The Brinkman term is usually applied in highly porous media and its effect is that it will give rise to a small boundary layer, where the velocity reduces to zero exactly at the solid wall. On the scale of the vented box, the velocity profile is nearly uniform (van der Sman, 2002). Omitting this term from Eq. (1) will result in numerical solution of the velocity profiles showing bumps near the wall, which is not physical, but a numerical artefact (Vafai & Tien, 1980; van der Sman 2002). On the global scale the Brinkman term does not have a significant influence on the pressure drop over the packed bed, and will follow the global Darcy–Forchheimer equation (van der Sman, 2002). Consequently, the coefficients in Eq. (1) can be computed for near spherical products, using the Ergun relations (Ergun, 1952), Eq. 3.

$$\frac{1}{\kappa} = \frac{K_1(1-\varepsilon)^2}{d_{eff}^2\varepsilon^3} \text{ and } \beta = \frac{K_2(1-\varepsilon)}{d_{eff}\varepsilon^3} \tag{3}$$

Here d_{eff} is the effective product diameter, and is calculated by $d_{eff} = 6V/A$, with V the volume of the product, and A the surface area. The porosity of the packed bed is denoted as ε. Ergun determined experimentally that K_1 = 150 and K_2 = 1.75 (Chau et al., 1985). Some researchers have reported that, for spherical products the constants have the following values $K_1 = 180$ and $K_2 = 1.8$ (MacDonald et al., 1979). However, Anderson (1963) found that K_1 is not a constant but is a function of porosity, and K_2 is a function of the tortuosity and the Reynolds number (Chau et al., 1985). The parameters $1/K$ (m^2) and β (m^{-1}) are the Darcy permeability of the porous matrix and the Forchheimer drag constant (van der Sman, 2002;

Verboven et al., 2004), respectively, and are dependent on stacked product diameter, porosity, stacking pattern, fluid property, product shape, roughness, confinement ratio $\left(D_h/d_{eff}\right)$ and vent hole ratio of the container $\left(O\right)$ (Delele et al., 2008; van der Sman, 2002; Smale, 2004). The vent hole ratio is defined as the area of the vent hole divided by the total surface area of the face of the package the vent is placed: $\left(O = A_{hole}/A_{box}\right)$, (Delele et al., 2008; van der Sman, 2002; Smale, 2004).

Some studies have questioned the validity of the Darcy–Forchheimer equation for the turbulent regime, indicated by $\mathrm{Re}_p > 300$ (Antohe & Lage, 1997; Lage et al., 1997; Tobis, 2001; Pakrash et al., 2001). The experimental study of Lage et al. (1997) suggests that in the turbulent (post-Forchheimer) regime the pressure drop correlates with a cubic polynomial in the fluid velocity. The nature of porous media flow in the turbulent post-Forchheimer regime is at this moment still a controversial issue as indicated by the studies of Pakrash et al. (2001) and Tobis (2001). The main difficulty for resolving this question is the almost inaccessibility of porous media for a detailed flow measurement (van der Sman, 2002).

Chau et al. (1985) used the power-law relationship of Ramsin equation to develop correlations that could estimate pressure drop through bulk fruits and packages with horticultural fruits (Chau et al., 1985)

$$\nabla p = -au^b \tag{4}$$

The coefficients a and b in Equation (4), are experimentally determined (Vigneault et al., 2004) and are dependent on stacking pattern, diameter and porosity (Delele et al., 2008).

Many researchers have carried experiments and developed correlations that could estimate pressure drop through bulk products and ventilated containers with horticultural products (Chau et al., 1985; Haas et al., 1976; Vigneault and Goyette, 2002; Vigneault et al., 2004; Neale and Messer, 1976; Neale and Messer, 1978). The product bulk properties include porosity, size, shape, roughness, stacking parameter and confinement. Based on extensive experimental research, de Castro et al. (2005) recommended a vent ratio of 8-16% of the surface of the container to optimise the use of energy. Haas et al. (1976) and Chau et al. (1985) reported that bed porosity had a much greater effect on pressure drop than the

diameter of oranges. Regardless of the fruit size, a stacking arrangement with a low porosity will produce a higher pressure drop than a stacking arrangement with a high porosity (Chau et al., 1985).

2.5 Table grape postharvest quality defects developing during cold storage and handling

2.5.1 Moisture loss

The moisture loss process in fresh produce involves diffusion of moisture from cells into the intercellular spaces until a level of saturation is reached in these intercellular spaces. Moisture then vaporises from the intercellular spaces to the atmosphere through lenticels, stomates, scars, injured areas, or directly through the cuticle (Thompson et al., 1998; Veraverbeke et al., 2003). The rate of loss of moisture from fresh fruits is largely dependent on the humidity and temperature of the surrounding air, as well as on the heat and mass transfer properties of the fruit such as thermal conductivity, thermal and moisture diffusivity, interface heat and mass transfer coefficients (Margaris & Ghiaus, 2007; Thompson et al., 1998; Nelson, 1978). The rate of moisture loss is also influenced by the product surface area to volume ratio (Thompson et al., 1998). Produce with high surface area to volume ratios such as leafy vegetables lose moisture more rapidly than fruit which has a lower ratio (Thompson et al., 1998).

There are at least three symptoms of moisture loss from grapes: (i) shrivelled stems (also known as dry stems) which usually become brittle and break easily; (ii) browning of stem which occurs as stem dehydration becomes more severe; and (iii) berry softening which is followed by wrinkle like formation that starts to appear radiating out from the pedicel (Nelson, 1978). Dry and brittle stems often give rise to the detachment of berries from stems (often referred to as berry shatter or loose berries). Both the dry and brown stems detract seriously from the appearance of the grapes (Nelson, 1978). Grape berries do not show symptoms of water loss until the damage is quite evident on the stems. At about 4-5% mass loss, berries feel soft and above 5% loss in mass the wrinkles start to appear (Nelson, 1978).

Lichter et al. (2011) studied the effects of water vapour pressure deficit (WVPD) and ambient temperatures that prevail during marketing on the quality of grape stems (rachis) and cluster moisture loss of 'Superior' and 'Thompson' varieties. The grape clusters were stored at 20 °C or at 10 °C with low (70%) or high (>95%) RH and thus creating 4 levels of WVPD. They reported a poor overall correlation between cluster weight loss and rachis dry weight to browning for 'Superior' grapes but a good correlation for 'Thompson'. The rachis of 'Superior' suffered extensive browning at 20 °C even at high RH while the rachis of 'Thompson' remained relatively green under similar conditions. 'Thompson' grape rachis remained green during the entire examination period (11 d) when held at high RH in either 10 °C or 20 °C.

Du Plessis (2003) studied the moisture loss and stem browning of table grapes (*c.v's*. 'Red Globe', 'Waltham Cross', 'Dauphine' and 'Barlinka') during cold storage at -0.5 °C for 28 days. He found that the stem condition worsened with storage period regardless of cultivar. Transections of stems showed no morphological differences between the cultivars. However, the study showed that accelerated stem dehydration could be associated to bunch straggly nature.

2.5.2 Berry drop

Some table grapes are susceptible to berry drop, which is characterised by the detachment of berries from grape stems (rachis). The berry drop is a quality problem that negatively affects the storability and marketability of grapes in markets. Berry drop can be divided into three categories as per Deng et al. (2007a): (1) berry shatter, which denotes a detachment of berries from the cap stem due to the fragile tissue structure of the stalk, (2) wet drop, where berries are sloughed from the stems and the short and thin berry brushes are still attached to the pedicel (Wu et al., 1992), (3) dry drop, or abscission, which is caused by the formation of an abscission zone in the grape (Deng et al., 2007a; Chen et al., 2000). In literature, the area between grape stalk and berries where abscission takes place is referred to as the abscission zone (AZ), and it is usually localized at the junction between the pedicel and berry or at the

junction between the stalk and pedicel or at the most fragile portion of the pedicel (Deng et al., 2007a; b; Wu et al., 1992).

The Abscission zone

Some researchers studied the morphology of the abscission zone (AZ) under electron microscope, and they found that AZ cells could be characterized by a small vacuole, a long karyon, invagination of the cell membrane and additional paramural body (Zhang and Zhang, 2009). The cells at the AZ are often morphologically distinguishable from their immediate neighbours and are generally differentiated as a band composed of isodiametric or non-isodiametric cells, 2–50 cells in thickness (Deng et al., 2007a). They are much smaller, closely packed cells that contain enlarged nuclei and mitochondria, dilated Golgi stacks and endoplasmic reticulum, and dense cytoplasm (Deng et al., 2007a).

The mechanism of berry drop

The major cause of abscission is the cell separation caused by the degradation of the cell wall in the AZ, (Zhang and Zhang, 2009), which often results in the lowering of the fruit detachment force (FDF). The FDF is defined as an index of berry adherence strength, which comprises the linking force (between berry brush and berry flesh) and tensile strength of the AZ. The dissolution of the middle lamella or shared cell wall in the abscission zone is a fundamental step in the abscission process which is attributed to the activity of catabolic enzymes such to pectinesterase (PE, EC 3.1.1.11), polygalacturonase (PG, EC 3.2.1.15) and cellulase (Cx, EC 3.2.1.4), (Deng et al., 2007a).

Some studies (Deng et al., 2006; Deng et al., 2007a; b), have investigated the effects of different O_2 and CO_2 concentrations in cold (0 °C and 95% RH) storage environment of grape, on the catabolic enzyme activities, FDF and berry drop. Deng et al. (2007a) found that, in contrast to normal air storage of ‘Kyoho’ grapes, high O_2 levels inhibited Cx, PG and PE activity and the reverse for peroxidase (POD), decreased the degree of swelling and distorting

of the abscission cell walls, and tended to keep berry adherence strength high and reduced berry drop (Deng et al., 2007a). The inhibitory mechanism of high O_2 on berry drop possibly could be explained by the fact that disassembly of the AZ cells was delayed by a synergistic impact on degradation enzymes whose activities were affected by high O_2 levels (Deng et al., 2007a).

Deng et al. (2007b) investigated the effects of low O_2 and high CO_2 atmospheres on the berry drop of 'Kyoho' grapes, changes of fruit detachment force (FDF) and berry abscission and enzyme activities in the abscission zone during 60 days of storage in air (control), 4% O_2 + 9% CO_2 or 4% O_2 + 30% CO_2 at 0°C and 95% RH. They reported that, in comparison to air storage, the combined effects of the lower level of O_2 and the higher level of CO_2 suppressed the activities of cellulase, PG and POD, maintained greater FDF, and reduced berry abscission during storage.

Zhang and Zhang (2009) investigated the relationship between the abscisic acid (ABA) concentrations and berry drop. They stated that ABA enhances the activities of cellulase and polygalacturonase, and accelerates the decomposition of cellulose and pectin, which determines the level of abscission zone development and berry falling. They found that when the ABA concentration was less than 20 ng g^{-1} of fresh weight (FW), the abscission zone was not developed, and the berry drop was effectively stopped. As part their study, they investigated the effects of treating grape bunches with growth regulators and chemicals and their results indicated that that 2,3,5-triiodobenzoic acid (TIBA) can (a) inhibit the generation of ABA significantly, (b) inactivate the activities of cellulase and PG, (c) delay the development of the abscission zone, and (d) stop berry falling. Indole acetic acid (IAA), gibberellic acid (GA_3), naphthalene acetic acid (NAA), 6-benzylaminopurine (6-BA), calcium chloride ($CaCl_2$), and potassium permanganate ($KMnO_4$) caused similar results as TIBA. Chlorocholine chloride (CCC), dimethyl amino succinamic acid (B9), chloroethylphosphonic acid (CEPA) and exogenous ABA showed opposite effects.

2.5.3 Decay

Gray mould, caused by *Botrytis cinerea*, is the main decay organism that causes rapid and extensive postharvest deterioration of table grapes (Romanazzi et al., 2012). It can develop in the vineyard and even more after harvest, during long-distance transport, cold storage, and shelf-life. Occasional infections by *Penicillium spp.*, *Aspergillus spp*. and *Alternaria* spp., that cause blue mold, *Aspergillu*s rot and *Alternaria* rot, respectively, can also occur. In conventional agriculture, bunches are sprayed with fungicides after flowering, at pre-bunch closure, at veraison, and later, depending on the time of harvest (Luvisi et al., 1992; Romanazzia et al., 2012). These decay organisms are latent and grow well when cold storage conditions are broken.

Conventional methods to control decay problems after harvest include SO_2 fumigation or release from generator pads containing a metabisulfite salt, and packaging of the fruit in polyethylene liners (Lichter et al., 2002; Lurie et al., 2006). Cold storage fumigation is usually done on a weekly basis especially when long term storage of grapes is employed. Since the late 1960s, dual release (DR; quick release plus a slow release phase) SO_2 generators inside boxes have been widely used for table grape storage and transport for periods of up to 2 months. The dual release of SO_2 is achieved by using small and large sodium metabisulfite particles and by proprietary formulations of the salt and the pad (Zutahy et al., 2008). SO_2 is usually effective in preventing decay as long as its level is sufficiently high. However, high levels can result in fruit damage, unpleasant aftertaste, and allergies (Lichter et al., 2002; Lurie et al., 2006).

Many researchers have investigated alternatives to SO_2 for the control of decay in table grapes during cold storage. Lichter et al. (2002) examined the effect of applying a postharvest ethanol dip on the decay of table grapes. They reported that immersion of detached berries in 70% ethanol eliminated most of the fungal and bacterial populations on the berry surface, but had little effect on survival of yeasts. They also found that the in vitro development of *Botrytis cinerea* spores was arrested by 40% ethanol. Dipping of grape bunches in 50%, 40%

or 33% of ethanol prior to packaging, resulted in inhibition of berry decay that was equivalent to, or better than that achieved with SO_2, released from generator pads (Lichter et al., 2002).

Candir et al. (2012) investigated the efficacy of several alternative postharvest treatments to sulphur dioxide (SO_2) in maintaining quality and reducing fungal decay during cold storage of 'Red Globe' table grapes. They packaged the grapes in perforated polyethylene (PPE) or modified atmosphere packaging (MAP) bags (ZOEpac or Antimicrobial) with or without different grades of ethanol vapor-generating sachets (Antimold®30, Antimold®60 or Antimold®80) or an SO_2-generating pad, and the grapes were kept at 0 ◦C and 90–95% relative humidity for 4 months. The results obtained from their study indicated that packaging of grapes with a SO_2 pad in PPE or ZOEpac bags provided better control of fungal decay and stem browning than PPE or ZOEpac bags alone, PPE or ZOEpac bags with Antimold sachets or Antimicrobial bags alone. The PPE bag containing the Antimold®80 sachet was as effective as the SO_2 treatments in reducing the incidence of fungal decay in naturally infected and artificially inoculated grapes for 1 month.

Karabulut et al. (2005) investigated the potential of ethanol and potassium sorbate treatments on the germination of Botrytis spores in vitro. They reported that the germination of *Botrytis cinerea* spores on potato dextrose agar after a 30 s immersion in 10 or 20% ethanol was 87 and 56%, respectively, compared to 99% among untreated controls. After similar immersion in 0.5 or 1.0% potassium sorbate, 84 and 68% of the spores germinated, respectively (Karabulut et al., 2005). Addition of 0.5 and 1.0% potassium sorbate to 10 and 20% ethanol solution significantly increased the inhibition of spore germination. The germination of spores after 30 s immersion in 20% ethanol plus 0.5% potassium sorbate was 9.7% (Karabulut et al., 2005). The incidence of gray mold, caused by on detached berries of 'Flame Seedless' grapes immersed for 30 s in water, 10 and 20% ethanol, and 0.5 or 1.0% potassium sorbate was 55.2, 42.1, 31.0, 37.7, or 24.4%, respectively (Karabulut et al., 2005). Addition of 0.5 and 1.0% potassium sorbate to 10 and 20% ethanol reduced decay to 10% or less and was more effective than either alone. After 30 days of storage at 1 ◦C, the combination of 20% ethanol either with 0.5 or 1.0% potassium sorbate was equal in efficacy to commercial SO_2 generator pads in reducing the incidence of gray mold on 'Thompson Seedless' grapes (Karabulut et al., 2005).

Karabulut et al. (2004) investigated the exposure times to heated ethanol and water on the mortality of *Botrytis cinerea*. They reported that a complete inhibition of the germination of spores occurred after a 10 s exposure to 30% ethanol or more at 24 °C. Mortality of spores in heated 10% ethanol was higher than in water at the same temperatures. They found that immersion of naturally infected, freshly harvested table grapes for 30 s in 30% ethanol at 24 °C, reduced decay by approximately 50% after 35 days of storage at 1 °C. They also found that the addition of ethanol significantly improved the efficacy of a hot water treatment applied to grapes that were inoculated with *B. cinerea* two hours prior to immersion in heated solutions. Immersion for 30 or 60 s at 50, 55, or 60 ◦C in water or 10% ethanol also significantly reduced the number of decayed berries that developed after storage for 30 days at 1 °C (Karabulut et al., 2004).

Lurie et al. (2006) tested the efficacy of three methods of applying ethanol to prevent storage decay on two cultivars of table grapes, ‘Superior’ and ‘Thompson Seedless’. The three application methods they tested included: (1) dipping grapes in 50% ethanol for 10 s followed by air drying before packaging; (2) placing a container with a wick and 4 or 8 ml ethanol/kg grapes inside the package; (3) applying 4 or 8 ml ethanol/kg grapes to paper and placing this paper above the grapes in the package. They found that all methods of application controlled decay as well as or better than a SO_2-releasing pad. The ethanol impregnated paper caused high levels of berry browning, perhaps because of high levels of acetaldehyde inside the package. They also found that the taste of ‘Thompson Seedless’ grapes stored for 8 weeks in modified atmosphere storage was affected by CO_2 levels above 7%. Some methods of applying ethanol used here show promise as alternatives to SO_2 to prevent decay of grapes during storage while maintaining fruit quality (Lurie et al., 2006).

Pretel et al. (2006) evaluated the quality of ‘Aledo’ table grapes, during storage at 2±1 °C followed by a period of 4 days at 20 °C in a slightly CO_2 enriched atmosphere in combination with generators of SO_2 in cardboard boxes. They found that a slightly CO_2 enriched atmosphere, SO_2 micro-generators and their combination extended the storage period of late-harvested ‘Aledo’ table grapes without relatively affecting their organoleptic characteristics.

Art'es-Herńandez et al. (2006) investigated the use of modified atmosphere packaging (MAP) made from polypropylene films (PP) and storage at 0 °C followed by 8 °C and then 20 °C for 7 days, 4 days and 2 days respectively, on the quality of 'Superior Seedless' table grapes. The two polypropylene films they used to generate MAP were the micro-perforated PP-30 and an oriented polypropylene (OPP). The OPP film was applied with and without fungicide (10 μL of *trans*-2-hexenal or 0.4 g $Na_2S_2O_5$ kg^{-1}). They found that the control clusters showed the highest weight losses and decay while almost no losses occurred under MAP treatments. They concluded that SO_2-free MAP kept the overall quality of clusters close to that at harvest, with few differences when SO_2 was added.

Xu et al. (2007) conducted an in vitro and in vivo experiment to test the antifungal activity of grapefruit seed extract (GSE) on deteriorating 'Redglobe' grapes with *Botrytis cinerea*. Their results of inhibition of spore germination and radial growth of *B. cinerea* in vitro indicated that GSE could efficiently inhibit the growth of the tested fungi. They also investigated the effectiveness of GSE and chitosan to control postharvest decay and quality of 'Redglobe' grape berries stored at 0–1 °C. They found that chitosan and GSE treatments, alone or combined, significantly reduced postharvest fungal rot of the fruit compared with controls infected with *B. cinerea*. They reported that GSE and chitosan might have a synergistic effect in reducing postharvest fungal rot and maintaining the keeping quality of 'Redglobe' grapes.

2.5.4 SO_2 injury

SO_2 injury of table grapes is a disorder that usually occurs in storage due to excessive levels of SO_2 gas that is in contact with grapes (Lichter et al., 2002; Lurie et al., 2006). Cases of poor or irregular control of fumigant dosage or high release of SO_2 gas from an SO_2 pad occur in table grape industry. The symptoms of SO_2 injury are bleached, sunken areas that develop wherever the gas can readily penetrate the skin through wounds or natural openings at the stem ends (Harvey and Uota, 1978; Smilanick and Henson, 1992). Hairline cracking is another expression of phytotoxicity due to overexposure of table grapes to SO_2 (Zoffoli et al., 2008). These cracks are characterized by small, fine, longitudinal cracking lines, almost undetectable with the naked eye (Zoffoli et al., 2008). Postharvest practices of table grapes,

packaged with a SO_2 generating pad, such as extended delay cooling periods and those practices that involve a raise in temperature, considerably enhance this disorder (Zoffoli et al., 2008).

Zoffoli et al. (2008) investigated the concentrations of SO_2 and time of exposure on the development of hairline cracking on table grapes. The authors found that conditions that favoured higher concentrations of SO_2 (in practice commercial conditions), such as the use of two SO_2 generating pads (one on top and one on the bottom of the packaged table grapes), promoted hairline cracking. Hairline incidence increased linearly when the concentration and time product (CT) of SO_2 exceeded 3 (mL L^{-1}) h, and no hairline cracking was observed with CT below 0.8 (mL L^{-1}) h. The authors noted that hairline symptoms were greatly induced on Thompson Seedless table grapes that were immersed in acidic solutions (citric acid and disodium phosphate) at pH 2 or 4. Based on these findings, Zoffoli et al. (2008) recommended that it is essential to use a minimal dose of SO_2 that allows adequate protection from decay without reducing the berry quality, in order to reduce incidence of hairline split.

2.6 Conclusion

Sufficient airflow through fruit packages is required to ensure efficient cooling and preservation of postharvest quality. However, the role of resistance to airflow has not been sufficiently studied in table grape packaging systems. Therefore, special attention needs to be given to this aspect in order to gain an in-depth understanding of airflow and cooling patterns of grapes in multi-packages. Knowledge of resistance to airflow through table grape multi-packages will assist in future improvement of packaging designs.

Different techniques of measuring and quantifying airflow within the cold chain have been used. These are divided into experimental and numerical techniques. The limitation of experimental techniques lies in the cost of instrumentations and time taken to get meaningful results. Other limitations are the fact that most of the experimental techniques are only capable to do point measurements of the flow and so repeated measurements are required in

order to study the whole flow field. Although the numerical approach seems promising, its major drawbacks are computational power and the fact that its success lies on the degree of agreement with the experimental results.

Despite the efforts given to cold chain improvement, table grapes still suffer quality deterioration during cold storage and postharvest handling in the cold chain. Few studies have reported on the mechanisms of moisture loss in table grapes; however, a more comprehensive study which considers the effects of different packaging components is warranted in order to gain a deeper understanding of this quality problem for better management within cold chain handling. Grape berry drop has been well investigated and possible solutions have been reported. However, the application of the new technologies proposed in literature is still limited and has not been tested on a commercial scale. The combination of efficient cooling and the SO_2 generator or fumigation, appear to be the only practical alternative at this stage. Many researchers have shown the potential of using alternatives to SO_2, but these have not been tested at a commercial scale. The challenge of using SO_2 lies in applying optimum dosage to avoid berry damage and/or inadequate control of decay.

References

Acevedo C., Sánchez E., Young M.E. 2007. Heat and mass transfer coefficients for natural convection in fruit packages. J. Food Eng. 80, 655-661.

Adrian R.J. 1991. Particle-imaging techniques for experimental fluid mechanics. Annu. Rev. Fluid Mech. 23, 261-304.

Al khalfioui M., Michez A., Giani A., Boyer A., Foucaran A. 2003. Anemometer based on Seebeck effect. Sensor. Actuator. A107, 36-41.

Alvarez G., Flick D. 1999. Analysis of heterogeneous cooling of agricultural products inside bins, Part I: aerodynamic study. J. Food Eng. 39, 227-237.

Amara S.B., Laguerre O., Flick D. 2004. Experimental study of convective heat during cooling with low air velocity in a stack of objects. Int. J. Therm. Sci. 43, 1213-1221.

Ambaw, A., Delele M.A., Defraeye T., Ho Q.T., Opara U.L., Nicolaï B.M., Verboven P. 2012. The use of CFD to characterize and design post-harvest storage facilities: Past, present and future. Comput. Electron. Agric. http://dx.doi.org/10.1016/j.compag.2012.05.009

Amin M., Dabiri D., Navaz H.K. 2009. Tracer gas technique: A new approach for steady state infiltration rate measurement of open refrigerated display cases. J. Food Eng. 92, 172-181.

Amin M., Dabiri D., Navaz H.K. 2011. Comprehensive study on the effects of fluid dynamics of air curtain and geometry, on infiltration rate of open refrigerated cavities. Appl. Therm. Eng. 31, 3055-3065.

Amin M., Dabiri D., Navaz H.K. 2012. Effects of secondary variables on infiltration rate of open refrigerated vertical display cases with single-band air curtain. Appl. Therm. Eng. 35: 120-126.

Amos N.D. 2005. Characterisation of air flow in a commercial cool store using a carbon monoxide gas tracer. Acta Hort. 687, 305-311.

Anderson, K. E. B. 1963. Pressure drop through packed beds. Transactions Royal Institute Technology, Stockholm, No. 201.

ANON. 1917. Improvement in hot wire anemometers. J. Franklin Inst. 183 (6), 783-785.

Antohe, B. V., & Lage, J. L. 1997. A general two-equation macroscopic turbulence model for incompressible flow in porous media. International Journal of Heat and Mass Transfer, 20(13), 3013–3024.

Arifin, B., Chau, K. 1987. Forced-air cooling of strawberries. ASAE, (USA).

Art'es-Herńandez F., Toḿas-Barbeŕan F.A., Art'es F. 2006. Modified atmosphere packaging preserves quality of SO2-free 'Superior seedless' table grapes. Postharvest Biol. Techn. 39, 146–154.

Barbin D.F., Filho L.C.N., Júnior V.S. 2010. Convective heat transfer coefficients evaluation for a portable forced air tunnel. Appl. Therm. Eng. 30, 229-233.

Barbin D.F., Filho L.C.N., Júnior V.S. 2012. Portable forced-air tunnel evaluation for cooling products inside cold storage rooms. Int. J. Refrig. 35, 202-208.

Brosnan T., Sun D. –W. 2001. Precooling techniques and applications for horticultural products - a review. Int. J. Refrig. 24, 154-170.

Candir E., Ozdemir A.E., Kamiloglu O., Soylu E.M., Dilbaz R., Ustun D. 2012. Modified atmosphere packaging and ethanol vapor to control decay of 'Red Globe' table grapes during storage. Postharvest Biol. Techn. 63, 98–106.

Chau K.V., Gaffney J.J., Baird C.D., Church G.A. 1985. Resistance to air flow of oranges in bulk and in cartons. ASAE. 28(6), 2083-2088.

Chen, F.H., Yu, X., Zhang, W.Y., Tan, D.Y., 2000. Study on relationship between pedicel structure and berry abscission of 'Xinjiang Wuhebai' grape cultivars. J. Xinjiang Agric. Univ. 23, 44–48 (in Chinese).

Childs P.R.N., Greenwood J.R., Long C.A. 2000. Review of temperature measurement. Rev. Sci. Instr. 71 (8), 2959-2978.

Chourasai M.K., Goswami T.K. 2007. Steady state CFD modelling of airflow, heat transfer and moisture loss in a commercial potato cold store. Int. J. Refrig. 30, 672-689.

Cortella G. 2002. CFD-aided retail cabinet design, Comput. Electron. Agric. 34, 43-66.

Costa C., Lucera A., Conte A., Mastromatteo M., Speranza B., Antonacci A., Del Nobile M.A. 2011. Effects of passive and active modified atmosphere packaging conditions on ready-to-eat table grape. J. Food Eng. 102 (2), 115-121.

Cromatry A.S. 1968. A gas tracer technique for predicting chilling pattern in stored barley. J. Agric. Eng. Res. 13 (1), 1-11.

de Castro, L. R., Vigneault, C., Cortez, L. A. B. 2004. Container opening design for horticultural produce cooling efficiency. J. Food Agric. Environ. 2(1), 135–140.

de Castro L.R., Vigneault C., Cortez L.A.B., 2005. Cooling performance of horticultural produce in containers with peripheral openings. Postharvest Biol. Technol. 38 (3), 254-261.

Delele M.A., Verboven P., Ho Q.T., Nicolaï B.M. 2010. Advances in mathematical modelling of postharvest refrigeration processes. Stewart Postharvest Review, doi:10.2212/spr.2010.2.1

Delele, M.A., Tijskens, E., Atalay, Y.T., Ho, Q.T., Ramon, H., Nicolaı¨, B.M., Verboven, P., 2008. Combined discrete element and CFD modelling of airflow through random stacking of horticultural products in vented boxes. J. Food Eng. 89, 33-41.

Deng Y., Wu Y., Li Y. 2006. Physiological responses and quality attributes of ‘Kyoho’ grapes to controlled atmosphere storage, LWT. 39, 584–590.

Deng Y., Wu Y., Li Y., Yang M., Shi C., Zheng C. 2007a. Studies of postharvest berry abscission of ‘Kyoho’ table grapes during cold storage and high oxygen atmospheres. Postharvest Biol. Technol. 43, 95–101.

Deng Y., Wu Y., Li Y. 2007b. Effects of high CO_2 and low O_2 atmospheres on the berry drop of ‘Kyoho’ grapes. Food Chem. 100, 768–773.

Dincer I. 1995a. Thermal cooling data for figs exposed to air cooling. Int. Commun. Heat Mass Transfer. 22 (4), 559-566.

Dincer I. 1995b. Cooling parameters and film conductances of spherical products cooled in an air flow. Appl. Energy. 50, 269-280.

Dincer I. 1995c. Air flow precooling of individual grapes. J. Food Eng. 26, 243-249.

Drebushchak V.A. 2009. Universality of the emf of thermocouples. Thermochim. Acta. 496, 50-53.

Du Plessis S.F. 2003. Effects of packaging and postharvest cooling on quality of table grapes (Vitis vinifera L.). MScAgric. Thesis. University of Stellenbosch. South Africa. Pp. 101-119.

Émond, J. P., Mercier, F., Sadfa, S., Bourré, M., Gakwaya, A. 1996. Study of parameters affecting cooling rate and temperature distribution in forced-air precooling of strawberry. Trans. of ASAE, 39(6), 2185–2191.

Ergun, S., 1952. Fluid flow through packed columns. Chemical Engineering Progress 48, 89–94.

Ferrua M.J., Singh R.P. 2008. A nonintrusive flow measurement technique to validate the simulated laminar fluid flow in a packed container with vented walls. Int. J. Refrig. 31, 242-255.

Ferrua M.J., Singh R.P. 2009a. Design guidelines for the forced-air cooling process of strawberries. Int. J. Refrig. 32, 1932-1943.

Ferrua M.J., Singh R.P. 2009b. Modeling the forced-air cooling process of fresh strawberry packages, Part II: Experimental validation of the flow model. Int. J. Refrig. 32, 349-358.

Ferrua M.J., Singh R.P. 2009c. Modeling the forced-air cooling process of fresh strawberry packages, Part III: Experimental validation of the energy model. Int. J. Refrig. 32, 359-368.

Ferrua M.J., Singh R.P. 2011. Improved airflow method and packaging system for forced-air cooling of strawberries. Int. J. Refrig. 34, 1162-1173.

Field B.S. and Loth E. 2006. Entrainment of refrigerated air curtains down a wall. Exp. Therm. Fluid Sci. 30, 175-184.

Forliti D.J., Strkowski P.J., Debatin K. 2000. Bias and precision errors of digital particles image velocimetry. Exp. Fluids. 28, 436-447.

Foster A.M., Barrett R., James S.J., Swain M.J. 2002. Measurement and prediction of air movement through doorways in refrigerated rooms. Int. J. Refrig. 25, 1102–1109.

Foster A.M., Swain M.J., Barrett R., James S.J. 2003. Experimental verification of analytical and CFD predictions of infiltration through cold store entrances Int. J. Refrig. 25, 1102–1109.

Foster A.M., Swain M.J., Barrett R., D'Agaro P., Ketteringham L.P., James S.J. 2007. Three-dimensional effects of an air curtain used to restrict cold room infiltration. Appl. Math. Modell. 31, 1109-1123.

Gaffney J.J., Baird C.D. 1977. Forced-air cooling of bell peppers in bulk. Trans. ASAE, 1174-1179.

Genix M., Vairac P., Cretin B. 2009. Local temperature surface measurement with intrinsic thermocouple. Int. J. Therm. Sci. 48, 1679-1682.

Ginsburg, L., Combrink, J.C., Truter, A.B., 1978. Long and short term storage of table grapes. Int. J. Refrig. 1, 137-142.

Glaniger A., Jachimovicz A., Kohl F., Chabicovsky R., Urbain G.. 2000. Wide range semiconductor flow sensors. Sens. Actuators AA. 85, 139-146.

Gordon C., Thorne S. 1990. Determination of the thermal diffusivity of foods from temperature measurements during cooling. J. Food Eng. 11, 133-145.

Guillou R. 1960. Forced-air fruit cooling. Trans. ASAE, 16-18.

Haas, E., Felsenstein, G., Shitzer, A., & Manor, G. (1976). Factors affecting resistance to airflow through packed fresh fruit. ASHRAE Trans. 82(2), 548–554.

Hammond E., Quarini J., Foster A. 2011. Development of a stability model for a vertical single band recirculated air curtain sealing a refrigerated cavity Int. J. Refrig. 34, 1455-1461.

Hardenburg R.E., Watada A.E., Wang C.Y. 1986. The Commercial Storage of Fruits, Vegetables, and Florist and Nursery Stocks. USDA Handbook. Government Printing Office: Washington, D.C.

Harvey J.M., Uota M. 1978. Table grapes and refrigeration: fumigation with sulphur dioxide. Int. J. Refrig. 1, 167–172.

Hellickson M.L., Baskins R.A. 2003. Visual documentation of air flow patterns in a controlled atmosphere storage. Acta Hort. 600, 173-179.

Herwaarden A.W., Sarro P.M. 1986. Thermal sensors based on the seebeck effect. Sens. Actuators. 10, 321-346.

Hopkins L.M., Kelly J.T., Wexler A.S. Prasad A.K. 2000. Particle image velocimetry measurements in complex geometries. Exp. Fluids. 29, 91-95.

Hu Z., Sun D. –W. 2001. Effect of fluctuation in inlet airflow temperature on CFD simulation of air-blast chilling process. J. Food Eng. 48, 311-316.

Hu Z., Sun D.-W. 2002. CFD evaluating the influence of airflow on the thermocouple-measured temperature data during air-blasting chilling. Int. J. Refrig. 25, 546-551.

Irving A.R., Shepherd I.C. 1982. Measurement of air circulation rate in integral refrigerated shipping containers. Int. J. Refrig. 5(4), 231-234.

Kasap S.O. Thermoelectric effects in metals: Thermocouples, An e-booklet, 1997-2001.

Karabulut O.A., Gabler F.M., Mansour M., Smilanick J.L.. 2004. Postharvest ethanol and hot water treatments of table grapes to control gray mold. Postharvest Biol. Technol. 34, 169–177.

Karabulut O.A., Romanazzi G., Smilanick J.L., Lichter A. 2005. Postharvest ethanol and potassium sorbate treatments of table grapes to control gray mold. Postharvest Biol. Technol. 37, 129–134.

Kelly J.T., Prasad A.D., Wexler A.S. 2000. Detailed flow patterns in the nasal cavity. J. Appl. Physiol. 89, 323-327.

Kumara W.A.S., Elseth G., Halvorsen B.M., Melaaen M.C. 2010. Comparison of particle image velocimetry and laser Doppler anemometry measurement methods applied to the oil-water flow in horizontal pipe. Flow Meas. Instrum. 21, 105-117.

Lage, J. L., Antohe, B. V., & Nield, D. A. 1997. Two types of nonlinear pressure-drop versus flow-rate relation observed for saturated porous media. J. Food Eng. 199, 700–706.

Laguerre O., Amara S.B., Flick D. 2006. Heat transfer between wall and packed bed crossed by low velocity airflow. Appl. Therm. Eng. 26, 1951-1960.

Laguerre O., Hoang H.M., Flick D. 2012a. Experimental investigation and modelling in the food cold chain: Thermal and quality evolution. Trends in Food Sci. Technol. http://dx.doi.org/10.1016/j.tifs.2012.08.001

Laguerre O., Hoang M.H., Ossswald V., Flick D. 2012b. Experimental study of heat and air flow in a refrigerated display cabinet. J. Food Eng. 113, 310-321.

Lichter A., Kaplunov T., Zutahy Y., Daus A., Alchanatis V., Ostrovsky V., Lurie S. 2011. Physical and visual properties of grape rachis as affected by water vapour pressure deficit. Postharvest Biol. Technol. 59(1), 25-33.

Lichter A., Zutkhy Y., Sonego L., Dvir O., Kaplunov T., Sarig P., Ben-Arie R. 2002. Ethanol controls postharvest decay of table grapes. Postharvest Biol. Technol. 24, 301–308.

Lurie S, Pesis E., Gadiyeva O., Feygenberg O., Ben-Arie R., Kaplunov T., Zutahy Y., Lichter A. 2006. Modified ethanol atmosphere to control decay of table grapes during storage. Postharvest Biol. Technol. 42, 222–227.

Luvisi, D., Shorey, H., Smilanick, J. L., Thompson, J., Gump, B. H., Knutson, J., 1992. Sulfur dioxide fumigation of table grapes. Bulletin 1932, University of California, Division of Agriculture and Natural Resources, Oakland, CA, USA, 21 pp.

MacDonald, I. F. et al. (1979). Flow through porous media-Ergun equation revisited. Industrial Engineering Chemistry and Fundamentals, 18, 199–208.

Margaris D.P. and Ghiaus A-G. 2007. Experimental study of hot air dehydration of Sultana grapes. J. Food Eng. 79 (4), 1115-1121.

Martínez-Romero D., Castollo S., Valero D. 2003. Forced-air cooling applied before fruit handling to prevent mechanical damage of plums *(Prunus salicina Lindl.)*. Postharvest Biol. Technol. 28, 135-142.

Moureh J., Menia N., Flick D. 2002. Numerical and experimental study of airflow in a typical refrigerated truck configuration loaded with pallets. Comput. Electron. Agric. 34, 25-42.

Moureh J., Flick D. 2004. Airflow patterns and temperature distribution in a typical refrigerated truck configuration loaded with pallets. Int. J. Refrig. 27, 464-474.

Moureh J., Letanga G., Palvadeaua B., Boissonb H. 2009a. Numerical and experimental investigations on the use of mist flow process in refrigerated display cabinets. Int. J. Refrig. 32, 203-219.

Moureh J., Tapsoba M., Flick D. 2009b. Airflow in a slot-ventilated enclosure partially filled with porous boxes: Part II – Measurements and simulations within porous boxes. Comput. Fluids. 38, 206-220.

Moureh J., Tapsoba S., Derens E., Flick D. 2009c. Air velocity characteristics within vented pallets loaded in a refrigerated vehicle with and without air ducts. Int. J. Refrig. 32, 220-234.

Nahor H.B., Hoang M.L., Verboven P., Baelmans M., Nicolaï B.M. 2005. CFD model of the airflow, heat and mass transfer in cool stores. Int. J. Refrig. 28, 368-380.

Neale M.A., Messer H.J.M. 1976. Resistance of root and bulb vegetables to airflow. J. Agric. Eng. Res. 21, 221-231.

Neale M.A., Messer H.J.M. 1978. Resistance of leafy vegetables and inflorescences to airflow. J. Agric. Eng. Res. 23, 67-75.

Nelson K.E. 1978. Pre-cooling – its significance to the market quality of table grapes. Int. J. Refrig. 1(4), 207-215.

Norton T., Sun D.-W. 2006. Computational fluid dynamics (CFD) – an effective and efficient design and analysis tool for the food industry: A review. Trends in Food Sci. Technol. 17, 600-620.

Ower E., Pankhurst R.C.1966. The measurement of air flow. Chapma and Hall, Britain.

Pakrash, M., Turan, O. F., Li, Y., Mahoney, J., & Thorpe, G. R. 2001. Impinging round jet studies in a cylindrical enclosure with and without a porous layer: Part I – Flow visualisations and simulations. Chem. Eng. Sci. 56, 3855–3878.

Pathare P.B., Opara U.L., Vigneault C., Delele M.A., Al-Said F.A. 2012. Design of packaging vents for cooling fresh horticultural produce. Food Bioprocess Technol. DOI 10.1007/s11947-012-0883-9.

PPECB (www.ppecb.com).

Pretel M.T., Martínez-Madrid M.C., Martínez J.R., Carreño J.C., Romojaro F. 2006. Prolonged storage of 'Aledo' table grapes in a slightly CO_2 enriched atmosphere in combination with generators of SO_2. LWT. 39, 1109–1116.

Punt H., Huysamer M. 2005. Temperature variability in a 12 m integral reefer container carrying plums under a dual temperature shipping regime. ACTA Hort., 687, 289-295.

Romanazzi G., Lichter A., Gabler F.M., Smilanick J.L. 2012. Recent advances on the use of natural and safe alternatives to conventional methods to control postharvest gray mold of table grapes. Postharvest Biol. and Technol. 63, 141–147.

Ruiz-Garcia L., Lunadei L. 2011. The role of RFID in agriculture: Applications, limitations and challenges. Comput. Electron. Agric. 79, 42-50.

Sanyal N., Bhattacharyya B., Munshi S. 2006. An analog non-linear signal conditioning circuit for constant temperature anemometer. Measurement, 39, 308-311.

Sherman M.H. 1990. Tracer-gas techniques for measuring ventilation in a single zone. Build. Environ. 25(4), 365-374.

Smale N.J. 2004. Mathematical modelling of airflow in shipping systems: Model development and testing. PhD thesis. Massey University. New Zealand.

Smale N.J., Moureh J., Cortella G. 2006. A review of numerical models of airflow in refrigerated food applications. Int. J. Refrig. 29, 911-930.

Smilanick J.L., Henson D.J. 1992. Minimum gaseous sulphur dioxide concentrations and exposure periods to control Botrytis cinerea. Crop Prot. 11, 535-540.

Tanner D.J., Amos N.D. 2003. Temperature variability during shipping of fresh produce. ACTA Hort. 599, 193-203.

Tanner D.J., Cleland A.C., Robertson T.R., Opara U.L. 2000. Use of Carbon Dioxide as a tracer gas for determining in-package airflow distribution. J. Agric. Eng. Res. 77 (4), 409-417.

Tapsoba M., Moureh J., Flick D. 2006. Airflow patterns in an enclosure loaded with slotted pallets. Int. J. Refrig. 29, 899-910.

Tapsoba M., Moureh J., Flick D. 2007. Airflow patterns inside slotted obstacles in a ventilated enclosure. Comput. Fluids. 36, 935-948.

Thompson J.F., Mitchell F.G., Rumsey T.R., Kasmire R.F., Crisosto C.H. 1998. Commercial cooling of fruits, vegetables, and flowers. Regents of the University of California. USA.

Tobis, J. 2001. Turbulent resistance of complex bed structures. Chem. Eng. Comm. 184, 71–88.

Tutar M., Erdogdu F., Toka B. 2009. Computational modelling of airflow patterns and heat transfer prediction through stacked layers' products in a vented box during cooling. Int. J. Refrig. 32, 295-306.

Tso C.P., Yu S.C.M., Poh H.J., Jolly P.G. 2002. Experimental study on the heat and mass transfer characteristics in a refrigerated truck. Int. J. Refrig. 25, 340–350.

Ustun D., Candir E., Ozdemir A.E., Kamiloglu O., Soylu E.M., Dilbaz R. 2012. Effects of modified atmosphere packaging and ethanol vapor treatment on the chemical composition of 'Red Globe' table grapes during storage. Postharvest Biol. Technol. 68: 8-15.

Vafai, K., & Tien, C. 1980. Boundary and intertial effects of convective mass transfer in porous media. Int. J. Heat Mass Transfer. 25(8), 1183–1190.

Valero D, Valverde JM, Martínez-Romero D. et al. 2006. The combination of modified atmosphere packaging with eugenol or thymol to maintain quality, safety and functional properties of table grapes. Postharvest Biol. Technol. 41, 317–327.

Van der Sman R.G.M., Evelo R.G., Wilkinson E.C. van Doorn W.G. 1996. Quality loss in packed rose flowers due to Botrytis cinerea infection as related to temperature regimes and packaging design. Postharvest Biol. .Technol. 7, 341-350.

Van der Sman R.G.M., Ernst M.H., Berkenbosch A.C. 2000. Lattice Boltzmann scheme for cooling of packed cut flowers. Int. J. .Heat .Mass Transfer. 43, 577-587.

Van der Sman R.G.M. 2002. Prediction of airflow through a vented box by the Darcy–Forchheimer equation. J. Food Eng. 55, 49–57.

Veraverbeke, E. A., Verboven, P., Scheerlinck, N., Hoang, M. L., Nicolai¨, B. M. 2003. Determination of the diffusion coefficient of tissue, cuticle, cutin and wax of apple. J. Food Eng. 58, 285-294.

Verboven P., Hoang M.L., Baelmans M., Nicolai B.M. 2004. Airflow through beds of apples and chicory roots. Biosystems Eng. 88 (1), 117-125.

Verboven P., Flick D., Nicolaï B.M., Alvarez G. 2006. Modelling transport phenomena in refrigerated food bulks, packages and stacks: basics and advances. Int. J. Refrig. 29, 985-997.

Vigneault C., de Castro L.R. 2005. Produce-simulator property evaluation for indirect airflow distribution measurement through horticultural crop package. J. .Food Agric. Environ. 3(2), 93 – 98.

Vigneault C. and Goyette B. 2002. Design of plastic container opening to optimize forced-air precooling of fruits and vegetables. Appl. Eng. Agric. 18(1), 73-76.

Vigneault C., Markarian N.R., da Silva A., Goyette B. 2004. Pressure drop during forced-air ventilation of various horticultural produce in containers with different opening configurations. Trans. ASAE. 47 (3), 807-814.

Vigneault C., de Castro L.R., Goyette B., Markarian N.R., Charles M.T., Bourgeois G., Tang Line Foot E., Cortez L.A.B. 2007. Indirect airflow distribution measurement method for horticultural crop package design. Canadian Biosystems Eng. 49, 3.13-3.22.

Wang C.P. 1988. Laser Doppler velocimetry. J. Quant. Spectrosc. Radiat. Transfer. 40 (3), 309-319.

Wang L., Sun D.-W. 2003. Recent developments in numerical modelling of heating and cooling processes in the food industry – a review. Trends in Food Sci. Technol. 14, 408-423.

Winkler A.J., Cook J.A., Kliewer W.M., Lider L.A. 1974. General viticulture. The Regents of the University of California. USA.

Wu, Y.M., Ren, J.C., Hua, X.Z., Liu, Y., 1992. Postharvest berry abscission and storage of grape fruit. Acta Phytophysiol. Sin. 18, 267–272 (in Chinese).

Xia B., Sun D.-W. 2002. Application of computational fluid dynamics (CFD) in the food industry: a review. Comput. Electron. Agric. 34, 5-24.

Xie J., Qu X-H., Shi J-Y., Sun D.-W. 2006. Effects of design parameters on flow and temperature fields of a cold store by CFD simulation. J. Food Eng. 77, 355-363.

Xu W.-T., Huang K.-L., Guo F., Qu W., Yang J.-J., Liang Z.-H., Luo Y.-B. 2007. Postharvest grapefruit seed extract and chitosan treatments of table grapes to control Botrytis cinerea. Postharvest Biol. Technol. 46, 86–94.

Zhang Y.-L., Zhang R.-G. 2009. Effects of ABA Content on the Development of Abscission Zone and Berry Falling After Harvesting of Grapes. Agric. Sci. China. 8(1), 59-67.

Zoffoli J.P., Latorre B.A., Naranjo P. 2008. Hairline, a postharvest cracking disorder in table grapes induced by sulfur dioxide. Postharvest Biol. Technol. 47, 90–97.

Zou, Q., Opara, L.U., McKibbin, R., 2006a. A CFD modeling system for airflow and heat transfer in ventilated packaging for fresh foods: I. Initial analysis and development of mathematical models. J. Food Eng. 77, 1037–1047.

Zou, Q., Opara, L.U., McKibbin, R., 2006b. A CFD modeling system for airflow and heat transfer in ventilated packaging for fresh foods: II. Computational solution, software development and model testing. J. Food Eng. 77, 1048–1058.

Zutahy Y., Lichter A, Kaplunov T., Lurie S. 2008. Extended storage of ‘Red Globe’ grapes in modified SO_2 generating pads. Postharvest Biol. Technol. 50, 12–17.

Table 1: Reported applications of tracer techniques in food cold chain

Reference	Tracer gas/material used	Application	Data measured/calculated	Instrument used
Amin et al. (2009); Amin et al. (2011)	Carbon Dioxide	Refrigerated display cases	Concentration of tracer gas	Horiba gas analyser (VA-3000)
Amos (2005)	Carbon Monoxide	Commercial cool store	Time of arrival at sample point from injection point	CO sensors (Figaro TGS2440, with detection range of 30-1000 ppm)
Cromarty (1968)	Halogen compound refrigerant (Dichlorodifluoromethane)	Duct ventilated bins of barley	Time of arrival at sample point from injection point	Milliampere and an audible alarm
Hellickson and Baskins (2003)	Neutrally bouyant helium-filled soup bubbles	Commercial cool room filled with bins	Bubble movement video taped	Bubble movement was analysed with either multiple frame capture software or slow motion movement at various locations

Foster et al. (2003)	Carbon Dioxide	Infiltration through cold store entrances	Concentration of tracer gas	Infra-red CO_2 analyser (accuracy 5 % of full scale)
Foster et al. (2007)	Carbon Dioxide	Restriction of cold room infiltration	Decay of an elevated CO_2 concentration	Infra-red CO_2 analyser (Model ABPA-210, Horiba Ltd., Japan)
Smale (2004)	Fog	Ventilated packages	Arrival of fog at sample point	Fog sensor made up of a light emitting diode (LED) and a phototransistor
Tanner et al. (2000); Smale (2004)	Carbon Dioxide	Ventilated packages	Concentration of tracer gas	Gas analyser (Model LI- 6262, LI-COR Inc. Lincoln, Nebraska, USA)

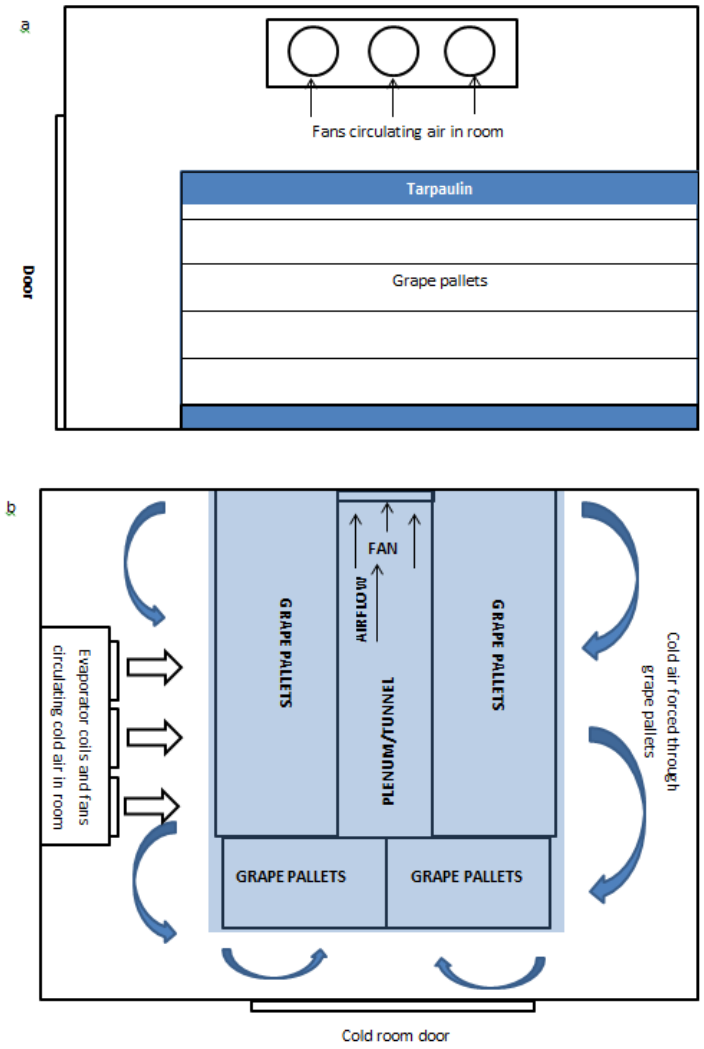

Figure 1: Schematic representation of a typical forced-air cooling room with pallets arranged in a pre-cooling tunnel, a) side view of the pre-cooling room and b) top view of the pre-cooling room setup.

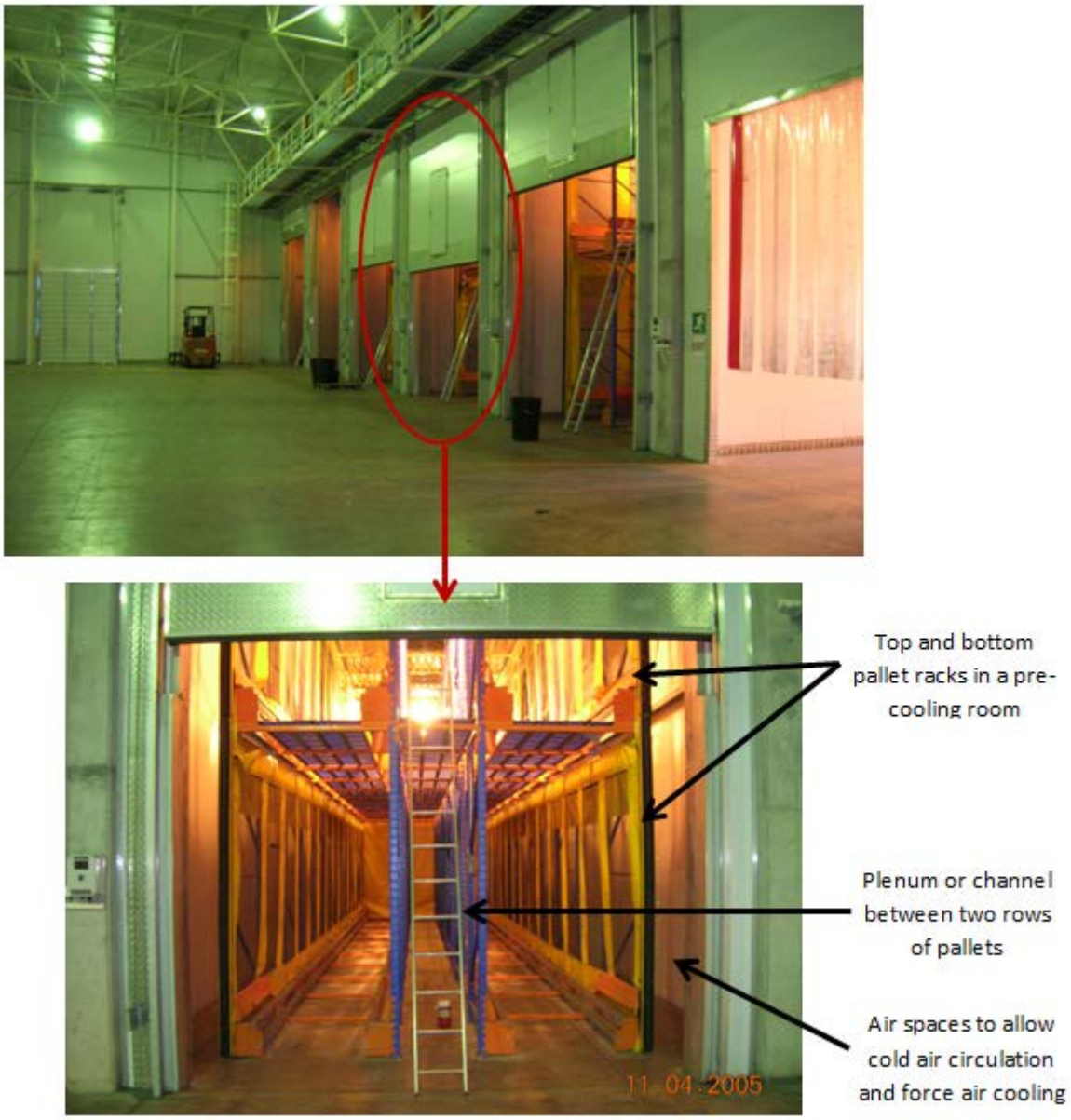

Figure 2: Pre-cooling rooms with racking system

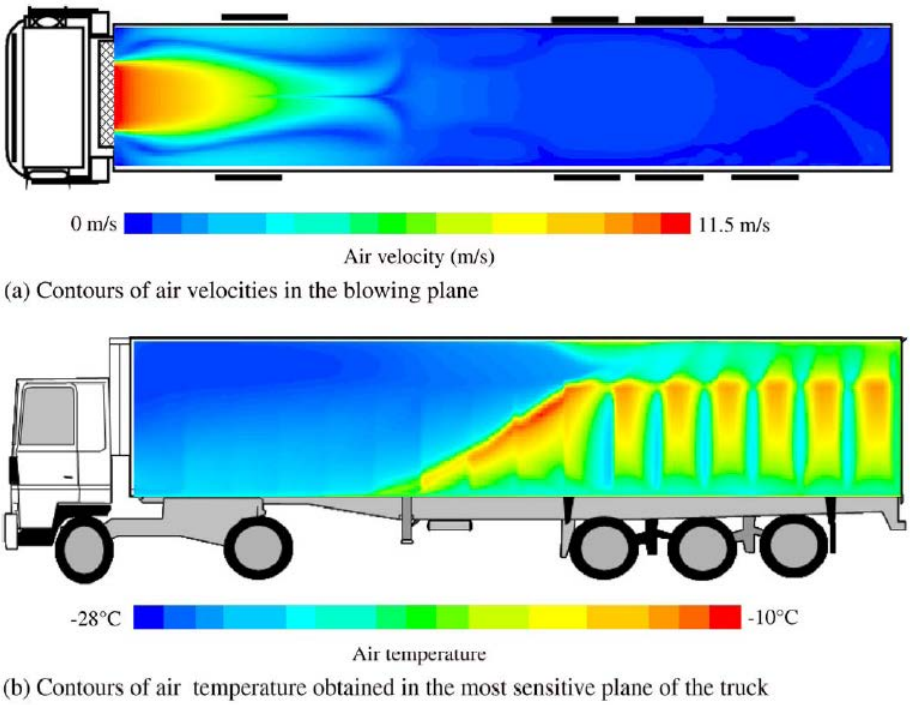

(a) Contours of air velocities in the blowing plane

(b) Contours of air temperature obtained in the most sensitive plane of the truck

Figure 3: Contour maps showing the (a) predicted air velocities in the blowing plane and (b) temperatures inside a refrigerated trailer (Moureh and Flick, 2004)

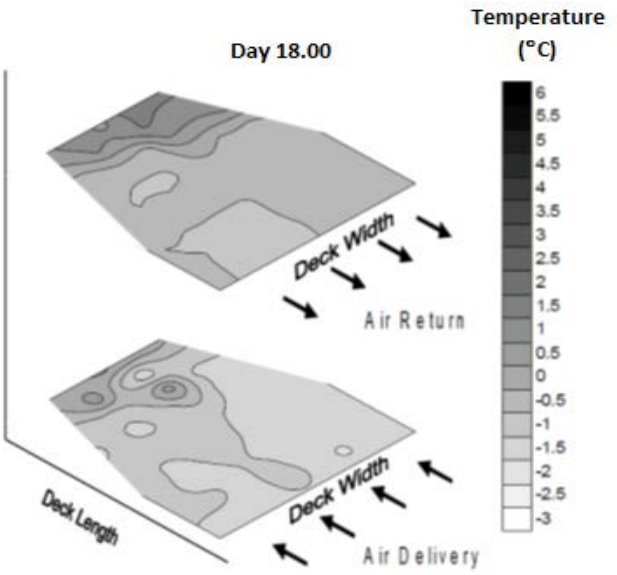

Figure 4: Typical air delivery and return contour plots for a deck in a reefer vessel, (Tanner and Amos 2003).

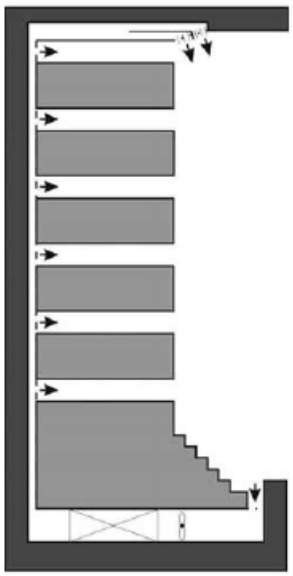

Figure 5: Schematic presentation of a vertical multi-deck display cabinet (Cortella, 2002).

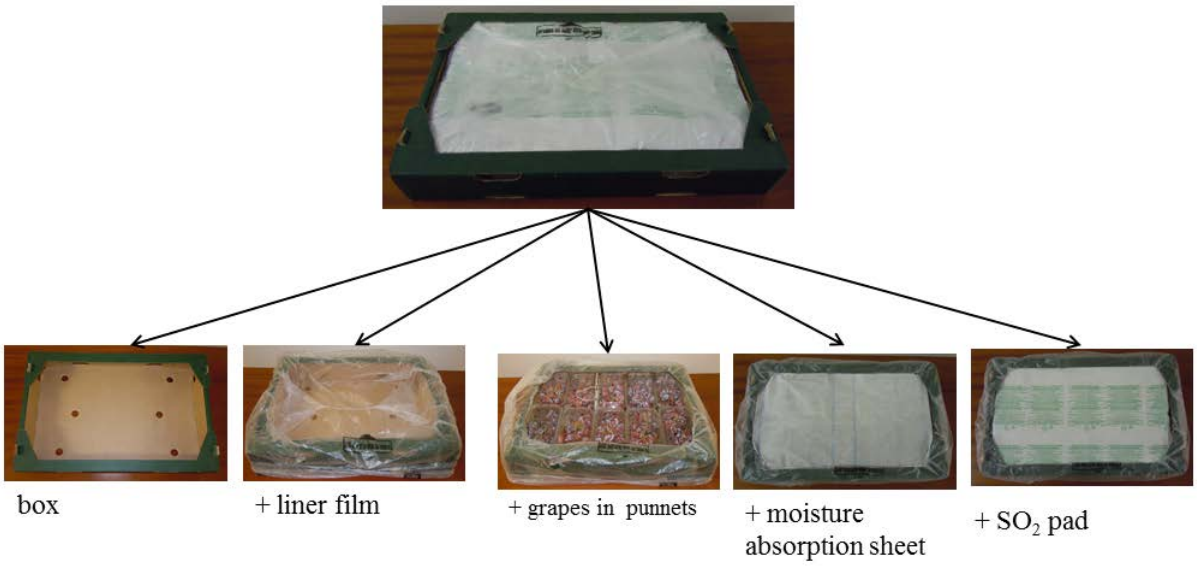

Figure 6: A typical table grape multi-scale setup.

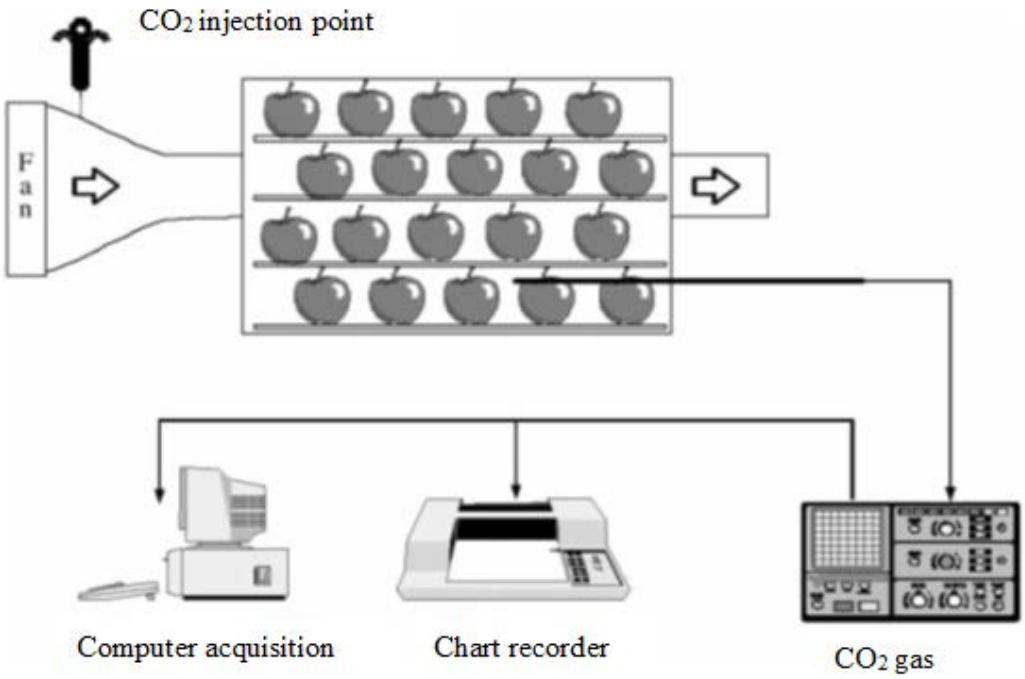

Figure 7: CO_2 tracer gas measurement system (Tanner et al., 2000)

PAPER 1

Resistance to airflow through 4.5 kg multi-scale packaging of table grapes

Abstract

Postharvest handling of table grape is commonly carried out using multi-scale packages comprised of the main container, inner liner film and pouches holding individual bunches of berries. Total pressure drop through different table grapes packages systems was measured and the percentage contribution of each package component and the fruit bulk were determined. The liner films contributed significantly to total pressure drop for all package combinations, ranging from 40.33±1.15% for micro-perforated liner film to 83.34±2.13 % for non-perforated liner film. The total pressure drop through the grape bulk (1.40±0.01 % to 9.41±1.23 %) was the least compared to the different packaging combinations with different levels of liner perforation.

Keywords: Packaging; Pressure drop; Air distribution; Cold chain; Table Grape

Nomenclature

A_{box}	box face area, m^2
A_{hole}	vent hole area, m^2
a	resistance coefficient, kg $s^{(b-2)}m^{-(b+2)}$
B	resistance exponent
c	vent resistance coefficient
d_p	effective product diameter, m
D_h	package hydraulic diameter, m
κ	Darcy permeability, m^2
N	vent resistance exponent
P	pressure, Pa
O	vent hole ratio, %

r^2	coefficient of determination
U	velocity vector, m s^{-1}
β	Forchheimer drag coefficient, m^{-1}
ε	Porosity
μ	dynamic viscosity
ρ	density, kg m^{-3}
θ	dimensionless temperature

1. Introduction

Cooling and proper cold chain management are commonly used methods to control postharvest ripening and senescence of fruit and vegetables (Arin and Akdemir, 2004). In most fresh food refrigeration systems, heat is transferred primarily by forced convection, where cold air is forced through food packages, therefore, the temperature and its homogeneity is largely governed by the patterns of the airflow (Smale et al., 2006; Zou et al., 2006).

Table grapes are non-climacteric fruit, which means they do not continue to ripen after harvest and for this reason they should be harvested when they reach optimum maturity (Ginsburg et al., 1978; Hardenburg et al., 1986) However, fruit quality tends to deteriorate rapidly during postharvest handling and storage, thus reducing shelf-life during marketing. There are three compelling reasons why table grapes should be cooled promptly and thoroughly after harvest to maintain quality: to minimize water loss from fruit; to retard developments of decay by fungi; and to reduce the rate of respiration. Minimizing water loss is probably the most urgent reason for cooling (Nelson, 1978). Like many other fruit cooling systems, table grape cooling is achieved by forcing cold air through the ventilated package. The forced air cooling technique has been discussed by many researchers (Guillou, 1960; Nelson, 1978; Thompson et al., 1998; Brosnan and Sun, 2001), but its application is often not efficiently achieved, mainly due to the resistance to airflow imposed by the packaging container and the contents (Vigneault et al., 2004; Delele et al., 2008). Resistance to airflow may even be higher during table grape cooling due to the fact that berry bunches are packed inside multi-scale packages. Table grape multi-scale packages include the carton boxes with

multiple inner packaging materials which include carton liner films, SO_2 pad, moisture absorption sheets and bunch carry bags (Ngcobo et al., 2011). It is therefore important to understand the effects of the packaging materials and the produce on airflow in order to fully understand cooling patterns and moisture transfer properties for the design of efficient cooling systems.

Many researchers have studied the resistance to airflow as a function of bulk product properties, fluid properties and container (carton) ventilation (Chau et al., 1985; Hass et al., 1976; Vigneault and Goyette, 2002; Vigneault et al., 2004, Neale and Messer 1976; Neale and Messer, 1978). The product bulk properties include porosity, size, shape, roughness, stacking parameter and confinement. Based on extensive experimental research, de Castro et al. *(*2005) recommended a vent ratio of 8 to 16% of the surface of the container to optimise the use of energy. Hass et al. (1976) and Chau et al. (1985) reported that bed porosity had a much greater effect on pressure drop than the diameter of oranges. Regardless of the fruit size, a stacking arrangement with a low porosity will produce a higher pressure drop than a stacking arrangement with a high porosity (Chau et al., 1985).

The correlation between the resistance to airflow through fruit packages and the pressure drop has been described by many researchers (Chau et. al., 1985; Vigneault et al., 2002; Vigneault et al., 2004) and is mainly expressed by either Ramsin, $\left(\nabla p = -au^b\right)$ or Darcy-Forchheimer $\left(\nabla p = -\frac{\mu}{\kappa}u - \beta\rho|u|u\right)$ equations 1 and 2 (Table 1). These equations have been used to estimate airflow resistance through bulk fruit, vegetables and vented packages (Chau et al., 1985; Haas et al., 1976; Neale and Messer 1976; Neale and Messer, 1978; Vigneault and Goyette, 2002; Vigneault et al., 2004). The coefficients a and b in equation (1), are experimentally determined (Vigneault et al., 2004) and are dependent on stacking pattern, diameter and porosity (Delele et al., 2008). In equation (2) the parameters $\frac{1}{\kappa}$ (m^2) and β (m^{-1}) are the Darcy permeability of the porous matrix and the Forchheimer drag constant (van der Sman, 2002; Verboven et al., 2004), respectively, and are dependent on stacked product diameter, porosity, stacking pattern, fluid property, product shape, roughness, confinement

ratio $\left(D_h / d_p \right)$ and vent hole ratio of the container (O) which is defined as the area of the vent hole area divided by the total surface area of the face of the package in which the vent is placed: $\left(O = A_{hole} / A_{box} \right)$, (Delele et al., 2008; van der Sman, 2002; Smale, 2004). Power law expression has been used to determine the effect of container vent-hole ratio on total pressure drop.

Although empirical equations have been derived for estimating pressure loss through vented packages (Vigneault and Goyette, 2002) and produce porosity (Chau et al., 1985; Haas et al., 1976; Vigneault et al., 2004), no work has been reported on the effects of multi-scale packages of table grapes on airflow resistance and cooling dynamics. Despite a widely held view among industry practitioners that table grape cooling is best achieved through efficient forced air cooling, detailed knowledge on the airflow, heat and mass transfer processes occurring during cooling is still lacking.

The objectives of this work were, therefore, to study the contribution of the different components of multi-scale packaging to airflow resistance and cooling rate during table grapes cooling. Special attention was given to quantify the contributions of liner films, the carry bag, the grape and the container (carton) to the total airflow resistance. The airflow and cooling performance of commonly used liner films were also evaluated.

2. Materials and Methods

2.1. Fruit supply

Regal Seedless grapes were obtained from the HexRiver area of the Western Cape, South Africa. The size of the grapes used was extra-large (diameter of 21.15±0.13mm). The airflow resistance experiments were carried out in the wind tunnel at the Mechanical and Mechatronics laboratory at Stellenbosch University, South Africa.

2.2. Experimental setup

2.2.1. Pressure loss

Figure 1 shows the wind tunnel setup. The dimensions of the test section were 600 mm (perpendicular to airflow) x 399 mm high x 400 mm (in the airflow direction). The test-section was built in such a way that it could be adjusted to fit different carton box configuration. The desired approach airflow was achieved by means of suction fans built in the wind tunnel and the approach air velocities used ranged from 0.7 to 3.2 ms^{-1}, which corresponded to fan frequencies of 10 to 50 Hz. The air velocities were measured in an empty wind tunnel and in a loaded wind tunnel during the experiment in order to determine the corresponding velocity to each fan frequency (Table 2). The pressure loss of the flow through the bulk grapes and packages was measured by a pressure transducer device (PMD70-AAA7D22AAU, ENDRESS+HAUSER, Weil am Rhein, Germany)**.**

Table 3 shows the venting information of the different grape packages studied. The airflow resistance experiments were carried out in a stepwise manner as follows:

(i) Empty packages:

The carton boxes were arranged into two configurations in the test-section of the wind tunnel during the experiment, (1) boxes arranged with the 300 mm side perpendicular to the airflow and the 400 mm side in the direction of airflow and (2) boxes arranged with the 400 mm side perpendicular to the airflow and 300 mm side in the direction of airflow. This was done due to the differences in vent area on these box sides and the difference in bed depths (Table 3). Six carton boxes were tested at a time (two stacks of three adjacent to each other). The dimension of single carton box was 300 mm x 400 mm x 133 mm.

(ii) Grape bulk:

The pressure drop through grapes in bulk were tested by placing grape bunches in a highly porous wire-mesh box. A thin wire-mesh was built for testing the airflow through bulk grapes. The wire mesh box dimensions used for bulk experiment were 600 mm x 399 mm and its length in the direction of airflow was 400 mm and it had approximately zero

resistance to airflow. The porosity (ε) of the grapes was determined by using the displacement method (Chau et al., 1985). The grape bunches were put in a container of a known volume V. Water was then added to fill the container to the known volume V. The difference between the volume V and the volume of water added was occupied by the fruit (Chau et al. 1985). The porosity was taken as a ratio of the difference between the total bulk volume and the actual volume occupied by the fruit and the total bulk volume (Chau et al. 1985; Koc et al., 2008; Owolarafe and Shotonde, 2003; Verboven et al., 2004).

(iii) Grape bunch carry bag:

The resistance to airflow due to bunch carry-bags was tested by packing grapes in carry-bags and placing the carry bags containing grape bunches inside the wire mesh boxes in the test-section similar to step (ii).

(iv) The final test investigated the resistance to airflow of complete multi-scale packaging, comprised of six types of liner films and thus six different packaging combinations (Table 3).

3. Results and discussion

3.1. Airflow through empty grape box

Figure 2 shows the effect of empty carton orientation on pressure drop. The resulting pressure drop was expressed in the form of Ramsin (eqn. 1) and Darcy-Forchheimer (eqn. 2) equations. The main difference between the carton orientations was the vent-hole ratios. The values of coefficients a and b, and $\frac{1}{\kappa}$ and β were determined by fitting the experimental data to the relevant equations (Table 4 and 5). Both equations expressed the relationship between the pressure drop through vent-holes and the approach air velocity well as indicated by the coefficient of determination (r^2) values greater than 99%.

The carton boxes orientated with the short (300 mm) side wall perpendicular to the inflow direction resulted in higher pressure drop compared to long (400 mm) side wall orientation. Higher values of all the parameters (a, b, $\frac{1}{\kappa}$ and β) were observed for the 300 mm side

than the 400 mm side. These results could be attributed to the higher percentage ventilation (opening) on the 400 mm side compared to the 300 mm side. The vent hole ratios (O) were 2.8 % and 6.7 % for the 300 mm and 400 mm sides, respectively (Table 3). Such an increase of vent hole ratio by 139.3 % resulted in 31.2 %, 28.5 %, 32.1 % and 88.0 % reduction in values of $a, b, \frac{1}{\kappa}$ and β, respectively. The effect of vent hole ratio on β was higher than the other coefficients. Similar reduction of the coefficients with an increase in vent hole ratio was also reported by previous studies (Smale, 2004; van der Sman, 2002; Delele et al., 2008). van der Sman (2002) and Delele et al. (2008) expressed the coefficient β as a function of the vent hole ratio ($\beta = CO^n$) and reported values of -1.5 and -0.89 for the exponent *n*, respectively. In our case, the value of *n* was -2.43. These results indicated that the value of this exponent varies from case to case and recommending a single value would not be correct.

3.2. Air flow resistance of bulk fruit and bunch carry bag

Figure 3 shows the pressure drop through the bulk grape bunches and through grapes packed in carry bags. The values of the Ramsin and Darcy-Forchheimer equation constants are shown in Tables 4 and 5, respectively. The vent hole ratio (O) for the bulk grape can be considered as 100% as the grapes packed in a wire mesh box and the Δp_{hole} of the wire mesh can be regarded as 0 (van der Sman, 2002). Thus in the case of the bulk grapes, $\Delta p_{tot} = \Delta p_{bulk}$, which was influenced by the porosity.

Due to high grape bunch porosity (56.45±0.04%), the pressure drop remained relatively low (just below 100 Pa m^{-1} for 2.06 m s^{-1} air superficial velocity). However, the introduction of the bunch carry bag into the bulk setup significantly increased the total pressure drop (Δp_{tot}) (Fig 3.). This result of increase in pressure drop with the introduction of the bunch carry bag is supported by the resistance coefficients $a, b, \frac{1}{\kappa}$ and Forchheimer coefficient β that all showed a similar increase (Table 4 and 5). The corresponding increase of $a, b, \frac{1}{\kappa}$

and β was 25.8 %, 39.1 %, 74.2 % and 830.2 %, respectively. The percentage increase of Forchheimer coefficient β due to the presence of the bunch carry bag was higher than the other coefficients. The carry bag has some slot like cuts that open when it is loaded with the grape. The extent to which they stretch and open depends on the bunch size and weight. The bigger and heavier the bunch was, the more elliptic openings were formed. Both the Ramsin and Darcy-Forchheimer constants (Tables 4 and 5) were higher for the bunch-carry bag combination than the grapes in bulk, indicating more resistance of airflow through carry bag than through the grapes in bulk.

3.3. Airflow resistance multi-packages

Figure 4 shows the total pressure drop through the different multi-scale packages of table grapes and the results of curve fitting using equations 1 and 2 are summarised in Tables 4 and 5. The total pressure drop for each multi-package combination was regarded as the sum of pressure drop contributed by each package $\left(\Delta p_{tot} = \Delta p_{box} + \Delta p_{film} + \Delta p_{CB} + \Delta p_{bulk}\right)$. Liner films were the only components that were uniquely different between the multi-scale package combinations, since the carton box and other inner packages were kept constant.

The results (Fig. 5) indicated that the liner films contributed more than 50 percent of the total pressure drop, with the exception of the micro-perforated liners (40.33±1.15%). The non-perforated liners contributed about 83.34±2.13%, while the perforated liners contribution was less than 69% but greater than 40%. The high resistance to airflow by the liner films could be ascribed to very low perforation percentage (Table 3). Although the liner film perforations generally reduced the resistance to airflow, compared to non-perforation liners, there was no clear correlation between the amount of perforation and the pressure drop. This poor correlation between pressure drop and the amount of perforation of the different liner films was also evident in the manner in which the resistance coefficients a, b, $\frac{1}{\kappa}$ and β responded to vent hole ratio of the liner films (Table 4 and 5). There was an unusual increase in these coefficients with an increase in vent hole ratio of the liner, while they were supposed to decrease with increase in vent hole ratio. This behaviour could be ascribed to the fact that the

2 mm perforation holes on the liner films are too small and they get easily blocked by fruit and inner packages. The holes of the highest perforated liner film (452.4 mm^2) are 4 mm in diameter, but there are a total of only 36 holes in the film which means that if their distribution is not aligned with vent holes of the other packages such as of the box and carry bag, then there is no airflow through them once the film has been wrapped. The values of the Ramsin and Darcy-Forchheimer coefficients suggest that the non-perforation liner multi-scale packaging combination resulted in highest resistance to airflow (Tables 4 and 5).

The carton boxes were the second largest contributor to the total pressure drop with contributions ranging from 9.89±2.43% to 37.68±1.51%. This resistance to airflow by the carton boxes can be ascribed to the low vent-hole ratio of 2.80%. de Castro et al. *(*2005) recommended a vent ratio of 8 to 16% of the surface of the container to optimise the use of energy. These results corresponded to those of Vigneault *et al*. (2004), who found from their experimental studies that large vent area (88 %) resulted in lower pressure drop compared to small (25%) opening. The authors, thus, concluded that percentage opening is more important than the opening configuration.

The bunch carry bag contributed between 2.43±0.41% and 12.58±0.88% to total pressure drop, while the grapes contribution was between 1.40±0.01% and 9.41±1.23%. The carry bags are well ventilated and are open at the top and hence have low resistance to airflow. The grape bunch porosity was calculated to be 56.45±0.04% and the low resistance to airflow by grapes was due to this high porosity of the grape bunches.

4. Conclusion

The effects of table grape packaging components on airflow and heat transfer characteristics were studied. Liner films contributed by far the greater resistance to airflow than the rest of the package components of the grapes' multi-packaging. Although the perforated liner films contributed less compared to non-perforated liner films, there were no clear trends that could be correlated to the amount of perforation area. It is, therefore, not easy to clearly predict the differences in airflow patterns through the liner films packed with grapes as resistance

coefficients did not respond normally to the vent-hole ratio of the liner films, largely due to the fact that some vent holes may be blocked by fruit and inner packages. The percentage ventilation on carton boxes side walls (2.80% and 6.70%) was found to be low compared to the 8 -16% recommended in literature. This problem of limited ventilation area (and the potential effect on slow cooling of table grapes) is further exacerbated because vents are often blocked by the inner packaging and the fruit.

References

Arin S., and Akdemir S., 2004. Quality properties changing of grapes during storage period. J. Biol. Sci. 4 (2), 253 – 257.

Brosnan T., Sun Da-Wen. 2001. Precooling techniques and applications for horticultural products. Int. J. Refrig. 24, 154-170.

Castro (de), L.R., C. Vigneault, L.A.B. Cortez. 2005. Cooling performance of horticultural produce in containers with peripheral openings. Postharvest Biol. and Technol. 38(3), 254-261

Chau K.V., Gaffney J.J., Baird C.D., Church G.A. 1985. Resistance to air flow of oranges in bulk and in cartons. Trans. ASAE. 28 (6), 2083 – 2088.

Delele M.A., Tijskens E., Atalay Y.T., Ho Q.T., Ramon H., Nicolaï B.M., Verboven P. 2008. Combined discrete element and CFD modelling of airflow through random stacking of horticultural products in vented boxes. J. Food Eng. 89, 33-41.

Forchheimer P. 1901. Wasserbewegung durch Boden. Z. Ver. Dtsch. Ing. 45, 1736-1741.

Ginsburg L., Combrink J.C., Truter AB. 1978. Long and short term storage of table grapes. Int. J. Refrig. 1, 137 – 142.

Guillou R. 1960. Forced air fruit cooling. Trans. ASAE. 3(2), 16-18.

Hardenburg RE, Watada AE, Wang CY. 1986. The commercial storage of fruits, vegetables, and florist and nursery stocks. USDA Handbook, Government Printing Office: Washington, DC.

Hass E., Felsenstein G., Shitzer A., Manor G. 1976. Factors affecting resistance to air flow through packed fresh fruit. ASHRAE Trans. 82(2), 548-554.

Koc B., Eren I., Ertekin F.K. 2008. Modelling bulk density, porosity and shrinkage of quince during drying: The effect of drying method. J. Food Eng. 85, 340 – 349.

Neale M.A., Messer H.J.M. 1976. Resistance of root and bulb vegetables to airflow. J. Agric. Eng. Res. 21, 221-231.

Neale M.A., Messer H.J.M. 1978. Resistance of leafy vegetables and inflorescences to airflow. J. Agric. Eng. Res. 23, 67-75.

Nelson K.E.1978. Pre-cooling-Its significance to the market quality of table grapes. Int. J. Refrig. 1, 207-215.

Ngcobo M.E.K, Opara U.L., Thiart G.D. 2011. Effects of packaging liners on cooling rate and quality attributes of table grape (cv. Regal Seedless*)*. Packag. Technol. Sci. DOI: 10.1002/pts.961

Owolarafe O.K., Shotonde H.O. 2003. Some physical properties of fresh okra fruit. J. Food Eng. 63, 299 – 302.

Smale, N.J. 2004. Mathematical modelling of airflow in the shipping systems: model development and testing. Ph.D. thesis, Massey University, Palmerston North, New Zealand.

Smale N.J., Moureh J., Cortella G. 2006. A review of numerical models of airflow in refrigerated food applications. Int. J. Refrig. 29, 911 – 930.

Thompson J.F., Mitchell F.G., Rumsey T.R., Kasmire R.F., Crisosto C.H. 1998. Commercial cooling of fruits, vegetables, and flowers. Regents of the University of California. USA.

van der Sman, R.G.M. 2002. Prediction of airflow through a vented box by the Darcy-Forchheimer equation. J. Food Eng. 55, 49 – 57.

Verboven P., Hoang M.L., Baelmans M., Nicolai B.M. 2004. Airflow through beds of apples and chicory roots. Biosystems Eng. 88 (1), 117 – 125.

Vigneault C., and Goyette B. 2002. Design of plastic container openings to optimize forced-air precooling of fruits and vegetables. Appl. Eng. Agric. 18(1), 73-76.

Vigneault C., Markarian N.R., da Silva A., Goyette B. 2004. Pressure drop during forced-air ventilation of various horticultural produce in containers with different opening configurations. Trans. ASAE. 47 (3), 807-814.

Zou Q., Opara L.U., McKibbin R. 2006. A CFD modelling system for airflow and heat transfer in ventilated packaging for fresh foods: I. Initial analysis and development of mathematical models. J. Food Eng. 77, 1037-1047.

Table 1: Key equations correlating resistance to airflow and pressure drop in fruit packages

	Equation	Source	
Ramsin	$\nabla p = -au^b$	Chau *et al.*, 1985	(1)
Darcy-Forchheimer	$\nabla p = -\frac{\mu}{\kappa}u - \beta\rho\|u\|u$	Forchheimer, 1901	(2)

Table 2: Wind tunnel's fan oscillation frequencies and the corresponding air velocity (m s^{-1})

	Empty wind tunnel	Empty box		Multi-packages				
Fan frequency (Hz)		300 mm side	400 mm side	Non perforated liner	Micro perforated liner	30 x 2 mm liner	54 x 2 mm liner	120 x 2 mm liner
0	0.00	0.00	0.00	0.00	0.00	0.00	0.00	0.00
10	0.70	0.58	0.65	0.28	0.49	0.41	0.40	0.37
15	1.06	0.87	0.99	0.41	0.74	0.61	0.61	0.55
20	1.42	1.17	1.33	0.56	0.99	0.83	0.80	0.74
25	1.76	1.45	1.67	0.66	1.17	1.03	0.97	0.90
30	2.08	1.76	1.98	0.78	1.24	1.19	1.12	1.06
35	2.38	2.03	2.28	1.25	1.92	1.94	1.73	1.73
40	2.68	2.29	2.58	1.39	1.98	2.13	1.90	1.94
45	2.95	2.56	2.85	1.50	2.03	2.26	2.70	2.10
50	3.21	2.79	3.09	1.63	2.13	2.34	2.97	2.21

Table 3: Ventilation details of grape multi-packages and porosity of table grapes

Package, product details	**Effective ventilation across test section (m^2)**	**Package surface area exposed across test section (m^2)**	**%ventilation or porosity across test section area**
6 x empty cartons (300 mm side)	0.01	0.48	2.80
6 x empty carton box (400 mm side)	0.02	0.32	6.70
non-perforation liner film	0.00	0.84	0.00
Micro-perforation liner film	-	0	-
94.2 mm^2 (30 x 2 mm) perforation liner film	9.42E-05	0.81	0.01
452.4 mm^2 (36 x 4 mm) perforation liner film	4.52E-04	0.86	0.05
169.6 mm^2 (54 x 2 mm) perforation liner film	1.70E-04	0.84	0.02
376.9 mm^2 (120 x 2 mm) perforation liner film	3.77E-04	0.81	0.05
Wire-mesh box	0.48	0.48	≈100

Table 4**:** The a and b coefficients derived from equation 1 for multi-scale packages and grapes with the maximum and minimum velocity.

	Coefficients of Equation 1 $\nabla p = -au^b$		
	a	b	r^2
Packaging format and produce			
Empty carton showing respective ventilation side			
300mm side perpendicular to airflow	4.46	1.86	0.9994
400mm side perpendicular to airflow	3.07	1.33	0.9902
Bulk produce			
Grapes in bulk bin	3.57	1.05	0.9877
Grapes packed in bunch carry bags in bulk bin	4.49	1.46	0.9992
Multi-scale packaging (carton, liner bag, and carry bags containing berries)			
Non perforation	7.87	2.16	0.9955
Micro-perforation	6.29	2.37	0.9544
0.012 % perforation	6.72	1.94	0.9926
0.053 % perforation	6.88	2.14	0.9938
0.046 % perforation	7.07	2.04	0.9969

Table 5: The κ and β coefficients derived from equation 2 for multi-scale packages and grapes with the maximum and minimum velocity.

Packaging and produce	Coefficients of Equation 2 $\nabla p = -\frac{\mu}{\kappa}u - \beta\rho\|u\|u$		
	$\frac{1}{\kappa}$	β	r^2
Empty carton showing respective ventilation side			
300mm side perpendicular to airflow	9.23E+05	56.26	0.9999
400mm side perpendicular to airflow	6.27E+05	6.74	0.9979
Bulk produce			
Grapes in bulk bin	1.51E+06	3.31	0.9969
Grapes packed in bunch carry bags in bulk bin	2.63E+06	30.79	0.9999
Multi-scale packaging (carton, liner bag, and carry bags containing berries)			
Non perforation	2.87E+06	1756.25	0.9998
Micro-perforation	8.45E+05	352.12	0.9995
0.012 % perforation	5.94E+06	528.95	1.0000
0.053 % perforation	4.62E+05	724.32	0.9996
0.046 % perforation	2.73E+06	865.46	1.0000

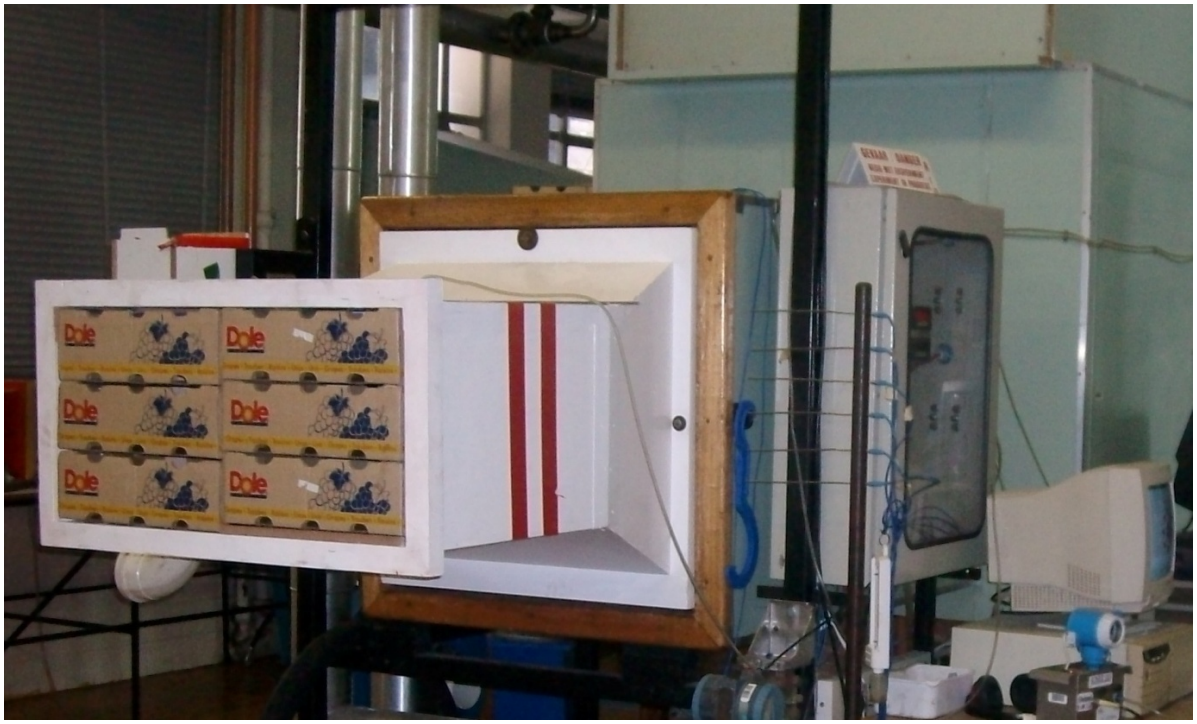

Figure 1: Picture of the wind tunnel with cartons/boxes of table grape

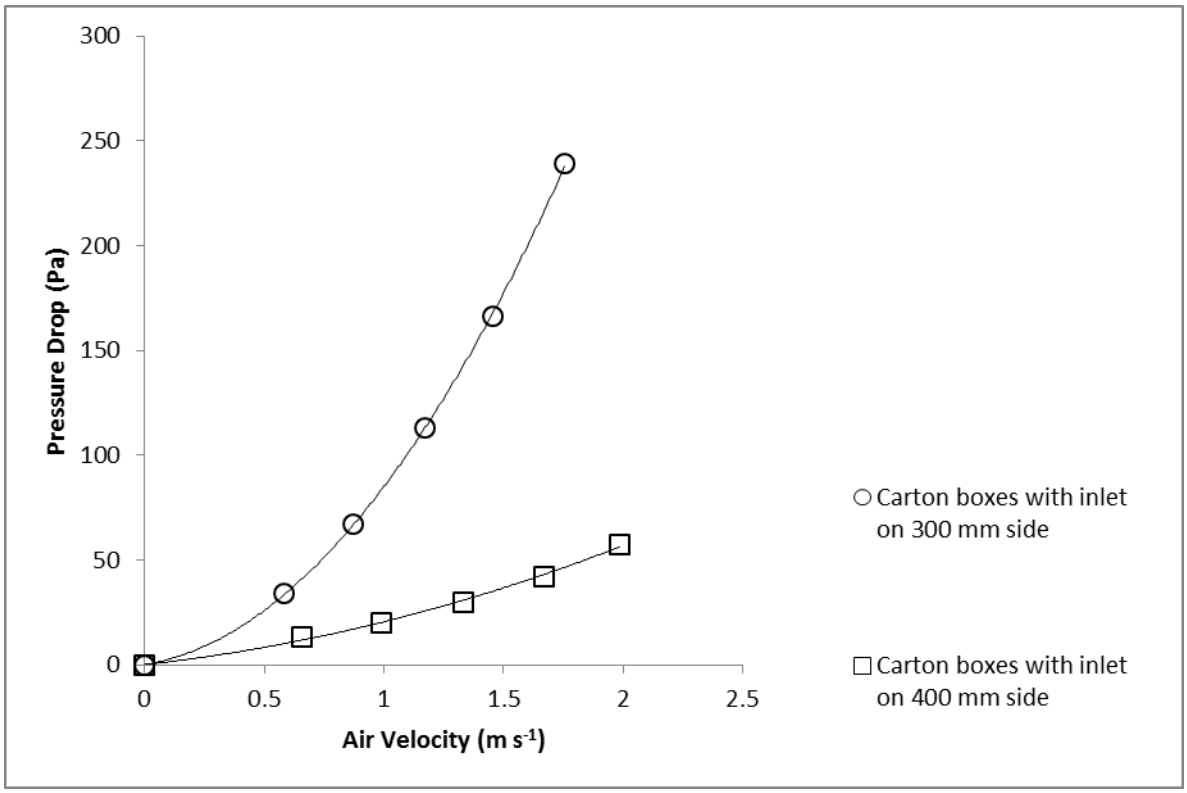

Figure 2: Pressure drop as a function of approach air velocity for the empty cartons

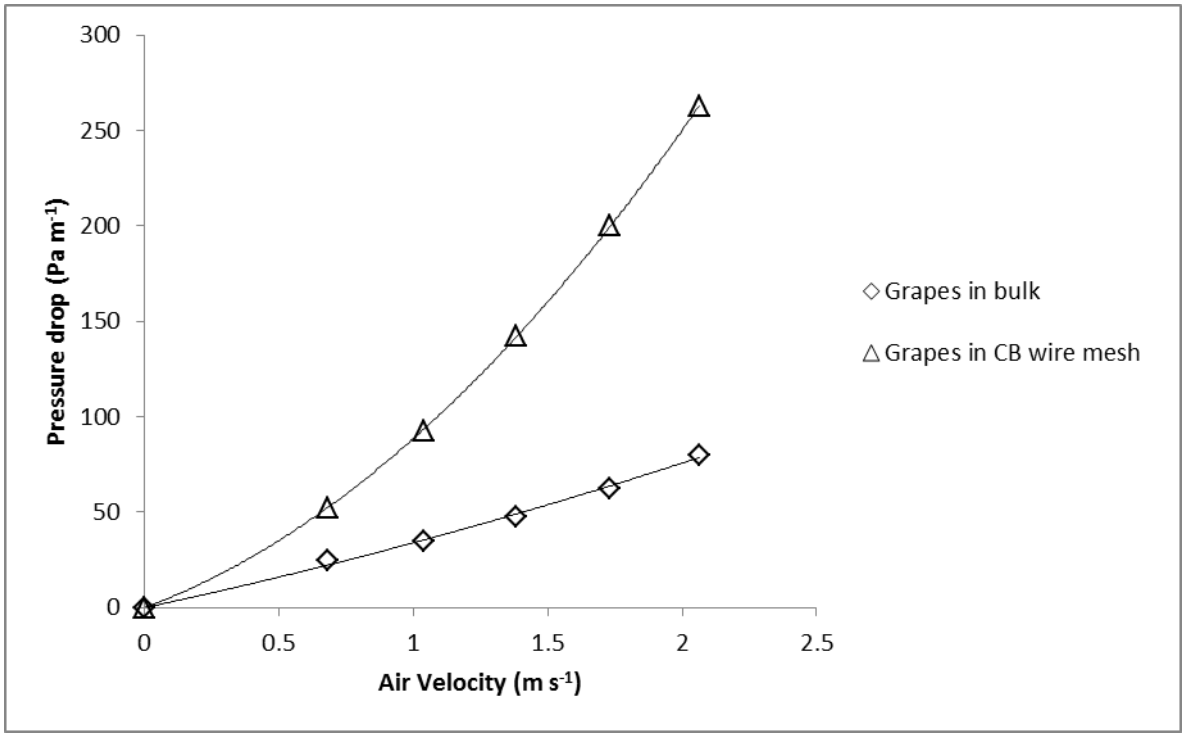

Figure 3: Pressure drop as a function of approach air velocity for the grapes in bulk and packed in carry bags in porous wire mesh box.

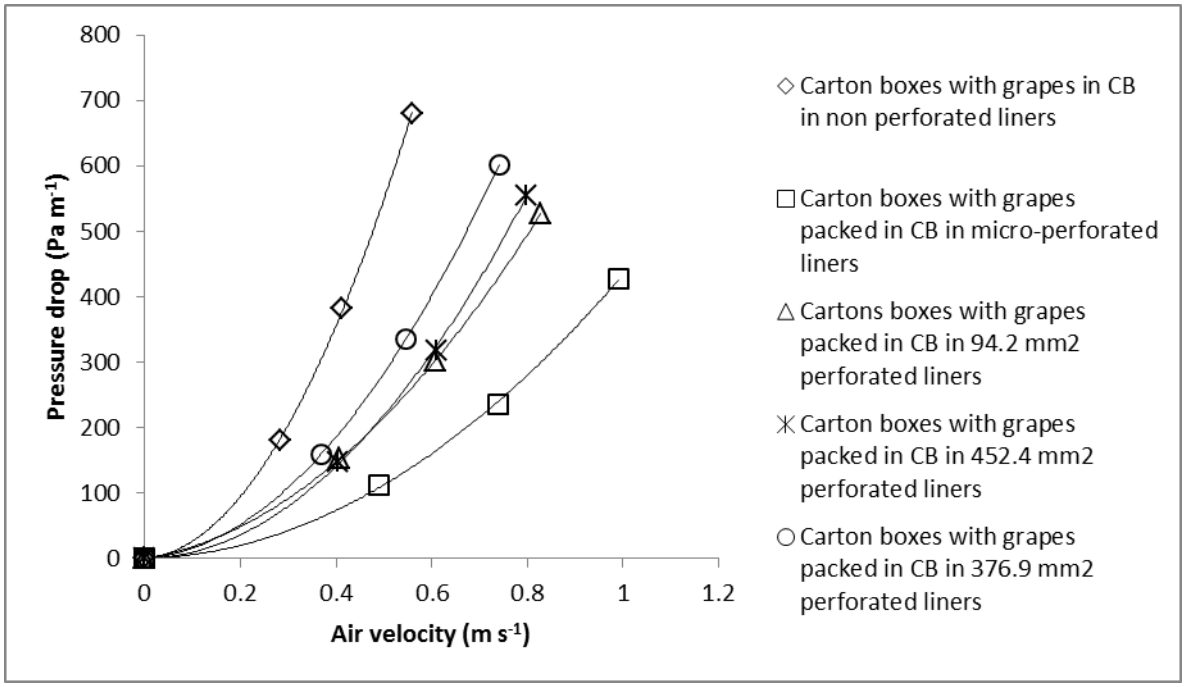

Figure 4: Total pressure drop as a function of approach air velocity for multi-packages with the different perforation liner films

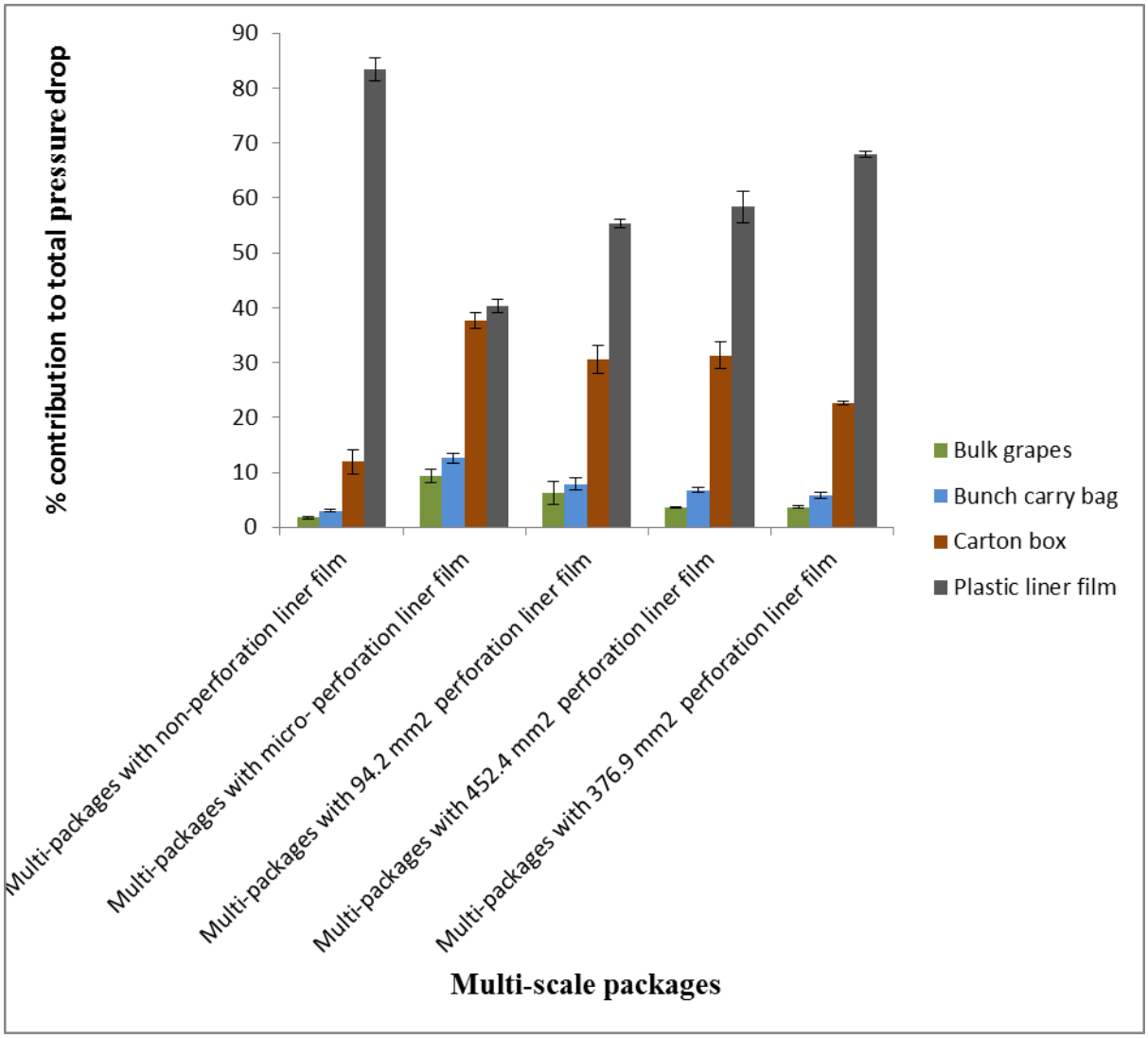

Figure 5: Percentage contribution of the different packages and fruit to the total pressure drop of grape multi-scale packaging.

PAPER 2

Effects of packaging liner films on cooling rate and quality attributes of table grapes (cv. Regal Seedless)

Abstract

Table grapes are commonly packed in multi-layered packages consisting of a cardboard carton, a plastic liner and bunch carry bags to maintain product quality along the cold chain. Each liner is characterized by the number and size of perforations which influence the environmental conditions around the produce inside the package. This study investigated the effects of different carton liners on the cooling rate and quality attributes of 'Regal Seedless' table grapes. Fruit quality attributes measured include weight loss, stem dehydration and browning, SO_2 injury, decay, berry firmness and colour. Non-perforated liners maintained relative humidity (RH) close to 100 % during cold storage and during a 7 day shelf life period, which resulted in delaying the loss of stem quality but significantly ($P \leq 0.05$) increased the incidence of SO_2 injury and berry drop during storage compared to perforated liners. Perforated liners improved fruit cooling rates but significantly ($P \leq 0.05$) reduced RH. Low RH in perforated liners resulted in a significant ($P \leq 0.05$) increase in stem dehydration and browning compared to non-perforated liners. Berry firmness decreased by 78 % after 42 days storage at -0.5°C. Significant ($P \leq 0.05$) differences in berry firmness between the different packages were observed only during the first 7 days of storage. Berry colour changed from greenish-yellow to yellowish-green in all types of plastic liners during the storage period. Fruit decay occurred in all packages after 7-day shelf-life, with the highest incidence of decay occurring in liners with less perforation.

Keywords: 'Regal Seedless' table grapes; Heat transfer; Packaging liners; Postharvest quality

1. Introduction

Table grapes are the second largest crop in the South African perishable product exports, making it one of the major contributors to the economy. About sixty one percent of the total table grape exports is destined for the European market (PPECB, 2010) and they are mainly packed in 4.5 kg boxes with multiple inner packaging materials. The inner packaging material includes carton liners, SO_2 pad, moisture absorption sheets and bunch carry bags (Figures 2a and b). The use of multi-packaging is primarily aimed at protecting the grapes from bruising and other postharvest handling related injuries. This multi packaging is also required to allow sufficient airflow to ensure good heat transfer from the grapes to maintain the cold chain.

Table grapes are non-climacteric fruit, which means they do not continue to ripen after harvest and for this reason they should be harvested when they reach optimum maturity (Ginsburg et al., 1978; Hardenburg et al., 1986). However, fruit quality tends to deteriorate rapidly during postharvest handling and storage, thus reducing shelf-life during marketing. Deterioration of table grape quality is mainly characterised by weight loss, stem (rachis) dehydration and browning, colour changes, accelerated berry softening, berry shatter and high incidence of berry decay due mainly to *Botrytis cinerea* (Valero et al., 2006). Sulphur dioxide gas (released by the SO_2 pad) is used to control decay caused by fungi such as *B. cinerea* which grows well in the optimum storage condition (-0.5 to 0°C, 95% RH) for table grapes. The presence of SO_2 gas may also cause various degrees of injury to the grapes (Zoffoli et al., 2008). The symptoms of SO_2 injury are bleached, sunken areas that develop wherever the gas can readily penetrate the skin through breaks, wounds, or natural openings at the stem ends (Harvey and Uota, 1978), which further reduces the quality of table grapes during postharvest storage and handling. Many researchers (Artés-Hernández et al., 2006; Lurie et al., 2006; Zoffoli et al., 1999) have investigated the application of modified atmosphere packaging (MAP) to mitigate the loss of table grape quality and other types of fruit (An et al., 2007). However, no work has been reported on the effects of multi packaging currently used in the industry under regular atmosphere (RA) on the environmental condition inside the package and produce quality.

The aim of this work was to investigate the performance of different package liners that are commercially used to pack export quality table grapes based on heat transfer properties and effects on the quality of grape berries and stems.

2. Materials and Methods

2.1. Fruit supply

'Regal Seedless' table grapes used in this study were grown in a commercial orchard in the Hex River area of South Africa. Size "large" bunches (average berry size of 17 mm diameter) were hand-harvested at a commercial maturity of 17 °Brix (DAFF, 2010) . The export quality grapes (free of quality defects) were cleaned, sorted and packed at a commercial pack-house and then transported by air-conditioned car for 2 hours to the Postharvest Technology Laboratory at the University of Stellenbosch.

2.2. Packaging materials

The majority of export table grapes are packed inside 4.5 kg cartons with dimensions of 400 mm x 300 mm x 118 mm which are lined inside with polyethylene liners. The physical characteristics of the six types of liner bags used are described in Table 1. Each carton of fruit was packed as follows: the carton was lined with a liner bag and corrugated paper sheets placed in the bottom of the liner bag to protect produce against bruising; grape bunches were then packed inside carry bags and each carry bag was placed carefully inside the liner; when the box was packed to full capacity, a moisture absorption paper sheet was placed on top of the packed bunches and finally an SO_2 pad (Proteku Grape Guard, INSUMOS FRUTICOLAS S.A., Chile) was placed on top of the absorption sheet to protect the grapes from a direct contact with the SO_2 pad (Zoffoli et al., 2008). Once, packing was complete, the liner was folded and taped with a plastic adhesive tape to enclose the grapes together with inner packaging.

2.3. Cooling system

The cooling method that was used to cool the grapes was room cooling, where cold air (-0.5°C) was forced to pass the grape packages through circulation by fans. The cooling system inside the room was mounted at the top on the side wall and consisted of four (500 mm diameter) fans (Recam International Fans, model RE623H/L), connected to evaporator coils in such a way that the air is chilled as it passes through the evaporator (heat exchanger). The cold room dimensions were 6.8 x 4.8 m^2. The chilled air was then circulated through the cold room at about 3.1 m s^{-1}. The cooling was therefore achieved by approaching natural convection, rather than forced convection cooling (Nelson, 1978).

2.4. Heat transfer and relative humidity measurement

Cooling rate of produce and relative humidity inside the package are commonly used to assess the performance of fresh produce packaging in the cold chain (Chonhenchob and Singh, 2005; Nelson, 1978; Smale et al., 2006). The grape packages were placed inside a cold room (set point -0.5 °C). Berry temperature was measured with probes (LogTag Trix-8 Remote probe, LogTag Recorder Limited, China) inserted into berries in three positions (P1, P2 and P3) inside each carton. P1 and P3 were outmost measuring position (near shortest side wall of each carton), and P2 was the middle position inside each carton. Air temperature was measured with a LogTag air temperature recorder (LogTag Trix-8 Temperature Recorder, LogTag Recorder Limited, China) inside each carton. Air relative humidity (%RH) inside each carton was measured with a SENSITECH TempTale 4 monitor (Temptale4 Humidity and Ambient Temperature 16000, SensiTech, USA). Fruit cooling rates were calculated according to Thompson et al. (1998), and expressed as the time required to cool produce to seven-eighths of the initial product-coolant temperature difference. The seven-eighths cooling time was calculated by multiplying the time taken to reach the half cool temperature by a factor of three (Thompson et al., 1998). Half cool temperature was determined as per the following equation (Thompson et al., 1998):

Half cool temperature = (initial product temperature – cooling air temperature) x 0.5 (1)

2.5. Fruit quality measurement

Fruit quality measurements were carried out on the day of harvest (day 0) and every consecutive week for six weeks in cold storage plus one week at ambient at 24.3°C. The initial (day 0) fruit quality was according to Table 2. Quality attributes measured included stem dehydration and browning, bunch weight loss, berry drop, firmness, SO_2 injury colour and decay incidence.

2.5.1. Stem dehydration and stem browning

Stem dehydration was assessed using the following scoring system: fresh stems =1; some drying of thinner stems=2; all thinner stems dry=3; all thinner and some thicker stems dry=4; and all stems dry=5. Stem browning development was measured using the following scoring system: (1) fresh and green; (2) some light browning; (3) significant browning; (4) severe browning.

2.5.2. Weight loss and berry drop

The weight of individual bunches was measured on day 0 and then weekly for six weeks in storage with a scale (EEW-5000, 5500g x 0.5g, UWE, SOUTH AFRICA). Bunch weight loss was expressed as percentage loss of the initial weight. Berry drop (%) was expressed as ratio of loose berry weight to the initial bunch weight.

2.4.1. Fruit firmness

Firmness of four berries per bunch in each replication was measured non-destructively using a digital firmness tester (DUROFEL DFT100, AGRO-TECHNOLOGIE®, France) fitted with a cylindrical probe with a plain tip of 5.64 mm diameter. Two opposite measurements

were made in the equatorial region of each grape berry with a maximum value 100 for a non-deformable surface (Pretel et al., 2006).

2.4.2. Colour measurement

Colour was determined using a Chroma Meter (CR-400, KONICA MINOLTA® (Japan), which expresses colour in dimensions L*, a*, b*, C and H, where L* is a measure of lightness, C* (chroma) is a measure of intensity or saturation and H (Hue angle) is derived from the two coordinates a* and b* (Wrolstad et al., 2005). The hue angle is expressed on a 360 ° grid where 0° = bluish-red, 90° = yellow, 180° = green, and 270° = blue. Two measurements were made in the equatorial region of opposite sides of the berries.

2.4.3. SO_2 injury and decay incidence

SO_2 injury was measured according to the following scoring system: (1) none (0%); (2) slight damage (<5%); (3) moderate damage (5-10%); (4) severe damage (> 10 %). Decay was scored as follows: (1) no decay; (2) slight (< 2 infected berries per carton); (3) severe (2 – 5 infected berries); (4) extreme (>5 infected berries per carton)

2.5. Statistical Analysis

The six different packaging liners studied using standard 4.5 kg carton boxes are described in Table 2. Each liner was replicated six (6) times, in order to compensate for any temperature difference inside the cold room, as well as to accommodate the natural and biological variability. In each liner replicate, there were two bunched (sub-replicates) that were marked and used for measuring quality attributes over the experimental period. This made a total of 36 experimental cartons/liners and 72 experimental bunches. For temperature and relative humidity measurements, inside each liner, the pulp temperatures were measured at three different positions (P1, P2 and P3), while for air temperature and RH there was one measuring instrument in each liner. The quality data were analysed using the SPSS program

to determine the analyses of variance (ANOVA), Duncan's Multiple Range Test and LSD values with a 5 % significance level. Daily mean temperature data were analysed using the repeated measures analyses of variance (ANOVA) of Statistica program, version 9.

3. Results and Discussion

3.1. Heat transfer rate

Table grapes should be cooled promptly and thoroughly after harvest to maintain quality and the main reasons for the cooling are to minimize water loss from fruit, retard development of decay caused by fungi and reduce the rate of respiration (Nelson, 1978; Zutahy et al., 2008). Therefore, a good packaging is required to allow for adequate and uniform cooling of the packed produce. The air temperature profiles inside all the liners (Fig 1) indicate that the grapes were all exposed to a similar cooling temperature, as no significant air temperature differences were observed between liner bags. According to the cooling results (Table 3), grapes packed in perforated liners cooled faster (743 min) than those in non-perforated liners (795 min) and micro perforated liners (795 min) with the exception of those packed in a 30 x 2mm perforated liner which cooled the slowest (840 min). The micro-perforation liners cooling rate was similar to that of non-perforated liners, and this may be due to the dimensions of the holes in the micro-perforated liners being very small (pin size), and are thus not adequately opened to allow good air flow through the bag. Although the use of perforated liners generally resulted in faster cooling rates, the cooling rate was not correlated with the perforated area of the liners. This may be due to non-uniform airflow patterns inside the package which may be ascribed to the possibility of the inner packaging blocking some of the perforation holes. Although the perforated liners contain a certain number of holes to allow airflow to pass through individual fruits, it is possible that the effective perforated area is limited to the liner holes that are in alignment with the carton ventilation holes, while the rest of perforated area remain less effective. The results also suggest that a spatial variation in terms of cooling rates exists between the different positions (P1, P2 and P3) within each carton (Table 3). The spatial temperature variability conforms to the work reviewed by Smale et al., 2006) where non-uniform airflow was implicated as a major cause of this variability.

3.2. Postharvest quality attributes

3.2.1 Weight loss, stem quality and berry drop

The industry quality protocol stipulates that table grapes must be stored and handled at – 0.5 °C and 95 % relative humidity (PPECB, 2010; Ginsburg et al., 1978). This is mainly to minimize water loss from the fruit. Stem dehydration and browning, weight loss and berry drop are the main symptoms of water loss in grape bunches (Nelson, 1978).

The results obtained from this study (Table 4) show that the non-perforated liners stabilised and maintained RH at 100 % during cold storage and after shelf life study, while the perforated liners resulted in significantly ($P < 0.05$) lower RH. This difference may be ascribed to the differences in liner materials and the perforations. Non-perforated liners are made up of low-density polyethylene (LDPE) and one of the characteristics of LDPE is being a good moisture barrier, with relatively high gas permeability (Fellows, 2000; Jacomino et al., 2005). This suggests that cooling of grapes packed in non-perforated liners may be due to conduction rather than convection mode of heat transfer, resulting in moisture condensation inside the liners and thus 100% RH inside these liners. The perforated liners are made up of high-density polyethylene (HDPE), which has a lower permeability to gases and moisture (Fellows, 2000). Although perforated liners did maintain the required level of RH, the formation of condensation was also observed (Fig. 3), suggesting that a combination of conductive and convective heat transfer may play a role in the cooling of grapes packed in these liners. The results also show that RH affects stem quality (Table 4). The 36 x 4 mm and 120 x 2 mm liners resulted in a higher loss of stem quality than the non-perforated liners. Percentage weight loss (Fig. 2) was significantly higher ($P<0.05$) in perforated liners than in the micro- and non-perforated liners, where the 36 x 4 mm resulted in the highest amount of average bunch weight loss (± 3%) after shelf life study. This corresponds with the inability of perforated liners to maintain high (≥ 95 %) RH. Nelson (1978) related water (weight) loss to the combination of temperature and relative humidity, and concluded that water loss is strictly a physical factor related to the evaporative potential of the surrounding air. The higher the evaporative potential of the air surrounding the fruit, the more water is lost from the fruit.

This relationship may be expressed directly as the vapour pressure deficit (Vpd), a term which indicates the combined influence of temperature and relative humidity (Nelson, 1978).

3.2.2. Berry drop

The non-perforated liner resulted in a significantly ($P < 0.05$) higher berry drop percentage (± 8 % per bunch) than the perforated liners during 42 days of cold storage (Table 5). Reduction in fruit detachment force has been widely associated with the natural abscission of fruits (Deng et al., 2005). Berry drop has also been associated with different gas compositions during storage, such low O_2 and high CO_2 compositions (Deng et al., 2007). It is therefore possible that the gas compositions inside the non-perforated liners changes during cold storage and thus resulting in an increase in berry drop. However, this hypothesis was not tested in this study.

3.2.3. SO_2 injury and decay incidence

The results obtained show that SO_2 injury incidence occurred within the first 7 days of cold storage on the table grapes packed in non-perforated liners, while the perforated liners showed no injury (Table 6). However, after 42 days of cold storage the grapes packed in perforated liners started to show symptoms of SO_2 injury as well. The SO_2 injury incidence remained significantly ($P<0.05$) higher on grapes packed in the non-perforated liner than those packed in perforated liners. No incident of SO_2 injury was observed on grapes packed in 36 x 4mm perforated liner. These data confirm the observations by Zoffoli et al. (2008), they suggested that hairline split development, which is a symptom of SO_2 injury could be partially explained by the acidic conditions developed on berry surfaces after the SO_2 contacts with water vapour. The combination of liquid vapour (100 % RH) and the SO_2 in the non-perforated liner may have resulted in a formation of acidic conditions (Kiss et al., 2010), that may have increased SO_2 injury observed in this study (Zoffoli et al., 2008).

No incidence of decay was observed prior to the shelf life study, (data not shown) indicating that table grapes require packages that allow good cooling and need to be handled under a good cold chain management environment to retard development of decay. However, after the shelf life, a high incidence of decay occurred (Table 7) and decay nests were observed in all fruit packages (Fig 4b). *Botrytis cinerea* spores germinate when free moisture and high relative humidity conditions prevail and low temperatures do not prevent spore germination but merely delay it. Free water at a relatively high temperature of approximately 20°C is conducive to the development of decay (Ginsburg et al., 1978).

3.2.4. Firmness

The firmness of the grape berries decreased from 69.63±0.55 (Table 2) to 54.28±0.48 Durofel units as the storage period increased for all the packaging types (Table 8). Since the berry firmness was varied prior to cooling trials, it was difficult to ascribe the differences observed in Table 8 to the different packages. Based on the results (Table 9) significant difference ($P<0.05$) was observed during the first seven days, and between 14 and 42 days of storage at – 0.5°C and there were no differences observed between 7 and 14 days of the storage period. A decrease in firmness of the grape berries may be caused by a drop in turgor pressure as the grapes lose water or by physiological changes in the tissue which weaken the structure (Bernstein and Lustig, 1985). According Deng et al. (2005), the decrease in firmness of grape in storage conditions was accompanied by a dramatic decrease in hemicelluloses and moderate decreases in cellulose and total pectin. This indicates that the softening of grape resulted from an increase in depolymerisation and degradation of cell wall polysaccharides (Brummell and Harpster, 2001; Deng et al., 2005).

3.2.5. Colour

The results (Table 10) show a decrease in Hue angle from an average of 118.1° at day 0 to 108.8° after 42 days in cold storage. This indicates a colour shift of grape berries from

greenish yellow (green =180°) toward yellowish green (yellow = 90°) during storage. The reduction of L* from 44.99±0.29 (Table 2) to 35.86±0.29, was observed (Table 10) as the berries turned yellowish brown due to SO_2 injury and incidence of decay. The decayed brown berries (data not shown) showed a further reduction in Hue angle to less than 89.00° and very low values of L*. The trends also showed a decrease in colour intensity C* from 16.59±0.22 (Table 2) to 12.32±0.21 (Table 10). These results are in agreement with those observed on 'Alido' table grapes by Pretel et al. (2006).

Because sensory analysis by trained panellists for colour and firmness measurements of table grapes was not carried out due to resource limitations and time constraints, it is not possible to ascertain if the differences observed instrumentally can be translated to a sensory perception by human subjects and vice-versa. However, anecdotal evidence by untrained laboratory personnel who tasted some grape berries indicated that when firmness was less than 55 Durofel units the berries were considered soft to the extent that they had lost their characteristic texture. Future studies should include detailed correlation between instrumental measurements and sensory analysis of berry quality attributes.

4. Conclusion

Grape berries are susceptible to quality defects during postharvest handling and marketing and the combination of cold chain management and packaging plays a crucial role in fresh produce quality. Grape berries packaged and stored in perforated liners performed better in terms of higher cooling rate, low SO_2 damage and low berry drop, while non-perforated liners performed better in terms of maintaining higher RH and stem quality. The SO_2 injury of berries observed in the non-perforated liners bag due to SO_2 toxicity may have been induced by generator pad releasing rate under saturated atmospheres and this highlights the need to adjust the perforation area of liner bags in consideration of the SO_2 pad release rate. The results indicate that the use of perforated liners offers a potential in maintaining the postharvest quality of table grape. Given the importance of stem quality in table grape marketing, the optimization of liner perforation (size and number) for both berry and stem quality is warranted.

References

An, Jianshen, Zhang M., Zhan Z. 2007. Effect of packaging film on the quality of 'Chaoyang' Honey peach fruit in modified atmosphere packages. Packag. Technol. Sci. 20, 71–76.

Artés-Hernández F., Tomás-Barberán F.A., Artés F. 2006. Modified atmosphere packaging preserves quality of SO_2-free 'Superior seedless' table grapes. Postharvest Biol. Technol. 39, 146-154.

Bernstein Z., Lustig I. 1985. Hydrostatic methods of measurement of firmness and turgor pressure of grape berries (Vitis Vinifera L.). Scientia Hort. 25, 129 – 136.

Brummell D.A., Harpster M.H. 2001. Cell wall metabolism in fruit softening and quality and its manipulation in transgenic plants. Plant Molecular Biol. 47, 311 – 340.

Chonhenchob V., Singh S.P. 2005. Packaging performance comparison for distribution and export of Papaya fruit. Packag. Technol. Sci. 18, 125-131.

Deng Y., Wu Y., Li Y. 2005. Changes in firmness, cell wall composition and cell wall hydrolases of grapes stored in high oxygen atmospheres. Food Research Int. 38**,** 769 – 776.

Deng Y., Wu Y., Li Y. 2007. Effects of high CO_2 and low O_2 atmospheres on the berry drop of 'Kyoho' grapes. Food Chem. 100, 768–773.

Department of Agriculture Forestry and Fisheries (DAFF)**. http://www.daff.gov.za/#** (link: Divisions/food safety and quality assurance/export standards/deciduous fruit/grapes).

Fellows P. 2000. Food processing technology, principles and practice. Woodhead publishing Ltd.: New York. p 483.

Ginsburg L., Combrink J.C., Truter A.B. 1978. Long and short term storage of table grapes. Int. J. Refrig. 1, 137 – 142.

Hardenburg R.E., Watada A.E., Wang C.Y. 1986. The Commercial Storage of Fruits, Vegetables, and Florist and Nursery Stocks. USDA Handbook, Government Printing Office: Washington, DC.

Harvey J.M., Uota M. 1978. Table grapes and refrigeration: fumigation with sulphur dioxide. Int. J. Refrig. 1, 167 – 172.

Jacomino A.P., Bron I.U., de Luca Sarantópoulos C.I.G., Sigrist J.M.M. 2005. Preservation of cold-stored guavas influenced by package materials. Packag. Technol. Sci. 18**,** 71–76.

Kiss A.A., Bildea C.S., Grievink J. 2010. Dynamic modelling and process optimization of an industrial sulfuric acid plant. Chem. Eng. J. 158, 241 – 249.

Lurie S., Pesis E., Gadiyeva O., Feygenberg O., Ben-Arie R., Kaplunov T., Zutahy Y., Lichter A. 2006. Modified ethanol atmosphere to control decay of table grapes during storage. Postharvest Biol. Technol. 42, 222 – 227.

Nelson KE. 1978. Pre-cooling – its significance to the market quality of table grapes. Int. J. Refrig. 1, 207 – 215.

PPECB. 2010. Export directory. Malachate Design and Publishing: Republic of South Africa. (www.ppecb.com).

Pretel M.T., Martínez-Madrid M.C., Martínez J.R., Carreño J.C., Romojaro F. 2006. Prolonged storage of 'Aledo' table grapes in a slightly CO_2 enriched atmosphere in combination with generators of SO_2. LWT. 39, 1109 – 1116.

Smale N.J., Moureh J., and Cortella G. 2006. A review of numerical models of airflow in refrigerated food applications. Int. J. Refrig. 29, 911 – 930.

Thompson J.F., Mitchell F.G., Rumsey T.R., Kasmire R.F., Crisosto C.H. 1998. Commercial Cooling of Fruits, Vegetables, and Flowers. Publication 21567, Regents of the University of California. USA.

Valero D., Valverde J.M., Martínez-Romero D., Guillén F., Castillo S., Serrano M. 2006. The combination of modified atmosphere packaging with eugenol or thymol to maintain quality, safety and functional properties of table grapes. Postharvest Biol. Technol. 41**,** 317 – 327.

Wrolstad R.E., Durst W., Lee J. 2005. Tracking color and pigment changes in anthocyanin products. Trends in Food Sci. Technol. 16, 423-428.

Zoffoli J.P., Latorre B.A., Naranjo P. 2008. Hairline, a postharvest cracking disorder in table grapes induced by sulfur dioxide. Posharvest Biol. Technol. 47, 90 – 97.

Zoffoli J.P., Latorre B.A., Rodriguez E.J., Aldunce P. 1999. Modified atmosphere packaging using chlorine gas generators to prevent Botrytis cinerea on table grapes. Postharvest Biol. Technol. 15, 135 – 142.

Zutahy Y., Lichter A., Kaplunov T., Lurie S. 2008. Extended storage of 'Red Globe' grapes in modified SO_2 generating pads. Postharvest Biol. Technol. 50, 12-17.

Table 1: Physical characteristics of the package materials

Item	Material type	Thickness (μm)	Number and size of perforations (mm)	Perforation area (mm^2)/Package area (mm^2)
Liner 1	LDPE	20.00	None	0/8.39 x 10^4
Liner 2	HDPE	16.00	Micro-perforated (9 pin holes per 1 x 10^4 mm^2 liner)	-
Liner 3	HDPE	16.00	30 x 2	377.14/8.08 x 10^4
Liner 4	HDPE	16.00	36 x 4	1810.29/8.56 x 10^4
Liner 5	HDPE	16.00	54 x 2	678.86/8.36 x10^4
Liner 6	HDPE	16.00	120 x 2	1508.57/8.14 x 10^4
Carry bag	(LDPE)	18.75	-	11055.11/10.23 x 10^4
Carton box	Corrugated fibreboard	4.00 mm	-	1.414x10^4/29.36 x 10^4

LDPE- Low density polyethylene; HDPE- High density polyethylene

Table 2: Initial quality characteristics of the grapes prior to cold storage

Baseline quality characteristic	**Value**
L*	
Hue (°)	44.99±0.21
C*	118.11±0.22
	16.59±0.22
Firmness (0-100)	69.63±0.55
Berry drop	None

Table 3**:** Rate of cooling (7/8 cooling time) of table grapes packed in different carton liners

Carton liner type	**Seven-eighths cooling time (min)**			
	Mean	**P1**	**P2**	**P3**
Non perforated	795	1134	534	687
Micro perforation	795	747	849	789
30 x2 mm perforation	840	708	900	939
36 x 4 mm perforation	747	807	777	645
54 X 2 mm perforation	672	567	663	831
120 x2 mm perforation	714	564	969	576
Means	760.5±25.08	754.5±85.72	782±65.59	744.5±54.43

P- Denotes the position of temperature measurement in each carton inside the liner where berries with pulp temperature recorders were placed. The numbers 1 and 3 were outermost measuring positions (near shortest side walls of each carton), and 2 is the middle position inside each box.

Table 4: Effect of different packaging liners on RH and stem quality of 'Regal Seedless' table grapes

Packaging	**% Relative humidity**	**Stem dehydration (1 – 5)***	**Stem browning (1 – 4)****
After 14 days at -0.5°C			
Non perforated	100.00c	3.70a	2.20a
Micro-perforation	91.10a	4.70b	2.80b
30x2mm perforation	91.90b	4.90b	2.80b
36x4mm perforation	92.30b	4.60b	2.90b
54x2mm perforation	91.90b	4.70b	2.90b
120x2mm perforation	92.20b	4.80b	3.20b
Means	92.9±0.22	4.56±0.11	2.82±0.09
After 42 days at -0.5°C			
Non perforations	100.00e	4.50a	2.70a
Micro-perforation	92.30b	5.00b	3.20b
30x2mm perforation	92.90cd	5.00b	3.30bc
36x4mm perforation	92.70c	5.00b	3.80c
54x2mm perforation	91.70a	5.00b	3.60bc
120x2mm perforation	93.00d	5.00b	3.70bc
Means	93.50±0.13	4.92±0.03	3.37±0.08
Shelf life study: 7 days			
24.3 °C			
Non perforations	100.00b	4.80a	2.80a
Micro-perforation	91.70a	5.00b	3.20ab
30x2mm perforation	91.20a	5.00b	3.60bc
36x4mm perforation	88.80a	5.00b	3.90c
54x2mm perforation	91.10a	5.00b	3.70bc
120 X 2mm perforation	89.90a	5.00b	3.80c
Means	91.8±0.53	4.97±0.02	3.51±0.08

*Score: 1= fresh stems; 2= some drying of thinner stems; 3 = all thinner stems dry; 4 = all thinner and some thicker stems dry; and 5 = all stems dry. **Score: 1 = fresh and green stems; 2 = some light browning of stems; 3 = significant browning of stems; and 4 = severe browning of stems. Values within a column and within a sampling period followed by a different letter are significantly different ($P \leq 0.05$) according to Duncan tests.

Table 5: Effect of different packaging liners on berry drop of 'Regal Seedless' table grapes after cold storage

Packaging	**Percentage Berry drop**		
	After 7 days at -0.5°C	**After 14 days at -0.5°C**	**After 42 days at -0.5°C**
Non perforated	0.60a	1.60ab	8.20b
Micro-perforation	0.30a	1.40ab	6.90ab
30x2mm perforation	0.60a	1.90b	5.00ab
36x4mm perforation	0.20a	0.90ab	2.90a
54x2mm perforation	0.00a	0.10a	5.70ab
120x2mm perforation	0.10a	0.40ab	4.30ab
Means	0.3±0.08	1.07±0.22	5.52±0.65

* Values within a column followed by a different letter are significantly different ($P \leq 0.05$) according to Duncan's Multiple Range Test.

Table 6: SO_2 injury index of 'Regal Seedless' table grapes during cold storage at -0.5°C

Packaging	SO_2 Injury Index*		
	After 7 days storage at -0.5°C**	After 14 days storage at -0.5°C**	After 42 days storage at -0.5°C**
Non perforated	1.08a	1.17b	2.17c
Micro-perforation	1.00a	1.00a	1.67b
30x2mm perforation	1.00a	1.00a	1.25ab
36x4mm perforation	1.00a	1.00a	1.00a
54x2mm perforation	1.00a	1.00a	1.25ab
120x2mm perforation	1.00a	1.00a	1.42ab
Means	1.01±0.01	1.03±0.02	1.46±0.07

*SO2 injury score (1-4): 1 = no injury; 2 = slight injury (< 5%); 3 = moderate injury (5 – 10%); and 4 = severe injury (> 10%). ** Values within a column followed by a different letter are significantly different ($P \leq 0.05$) according to Duncan's Multiple Range Test.

Table 7: Effect of packaging liners on the occurrence of decay incidence on 'Regal Seedless' table grapes after 42 days cold storage and shelf life

Packaging	Decay (1 – 4)*
Shelf life study: 7 days at 24.3 °C	
Non perforations	2.90b
Micro-perforation	3.30b
30x2mm perforation	3.20b
36x4mm mm^2 perforation	2.30ab
54x2mm perforation	1.70a
120x2mm perforation	2.50ab
Mean	2.68±0.15
Significance level	*P = 0.018**

*Score: 1 = no decay; 2= slight (<2 infected berries carton); 3 = severe (2-5 infected berries per carton); and 4 = extreme (> 5 infected berries per carton). * Values within a column followed by a different letter are significantly different ($P \leq 0.05$) according to Duncan's Multiple Range Test.

Table 8: Changes in 'Regal Seedless' grape berry firmness in cold storage

Packaging	Durofel units		
	After 7 days at -0.5°C	After 14 days at -0.5°C	After 42 days at -0.5°C
Non perforated	66.60ab	60.50ab	55.70a
Micro-perforation	62.10a	56.90a	52.90a
30x2mm perforation	66.40ab	61.50ab	55.20a
36x4mm perforation	67.80b	59.60ab	54.30a
54x2mm perforation	70.40b	62.20b	54.90a
120x2mm perforation	65.30ab	60.90ab	52.60a
Means	66.44±0.73	60.29±0.62	54.28±0.48

* Values within a column followed by a different letter are significantly different (P ≤ 0.05) according to Duncan tests.

Table 9: Differences in berry firmness measured at different intervals during storage at –0.5°C

Packaging	Difference in firmness (Durofel units)			
	Prior storage – Day 7 at -0.5°C	Day 7 – Day 14 at -0.5°C	Day 14 – Day 42 at -0.5°C	Prior storage – Day 42 at -0.5°C
Non perforated	4.80a	6.50a	6.00a	14.50a
Micro-perforation	9.80b	6.10a	6.60ab	16.70ab
30x2mm perforation	5.60a	7.60a	5.40a	14.10a
36x4mm perforation	7.10ab	9.20a	6.90ab	19.00ab
54x2mm perforation	9.30b	9.30a	10.30b	20.50b
120x2mm perforation	5.60a	6.40a	8.30ab	14.30a
Means	7.03±0.49	7.51±0.48	7.27±0.56	16.53±0.76

* Values within a column followed by a different letter are significantly different (P ≤ 0.05) according to Duncan's Multiple Range Test.

Table 10: Changes in colour parameters (L*, C* and Hue angle) of 'Regal Seedless' table grapes during cold storage

Packaging	L*	C*	Hue angle
After 7 days at – 0.5°C			
Non perforations	41.20a	16.90a	117.76b
Micro-perforation	40.90a	17.30a	117.13b
30x2mm perforation	42.20ab	18.50ab	116.63b
36x4mm perforation	41.90ab	17.90a	109.55a
54x2mm perforation	43.30b	19.50b	116.76b
120x2mm perforation	42.30ab	17.40a	117.67b
Means	41.90±0.22	17.90±0.22	115.92±0.69
After 14 days at – 0.5°C			
Non perforations	39.00a	16.20a	114.59a
Micro-perforation	39.40ab	16.70ab	115.50a
30x2mm perforation	39.70ab	16.60ab	116.54a
36x4mm perforation	40.40ab	17.50ab	116.16a
54x2mm perforation	41.20b	18.30b	114.41a
120x2mm perforation	39.90ab	16.80ab	114.33a
Means	39.93±0.28	17.02±0.25	115.26±0.67
After 42 days at - 0.5°C			
Non perforations	38.07c	12.70ab	112.67c
Micro-perforation	36.40bc	11.80a	109.28ab
30x4 mm perforation	35.20ab	11.60a	106.15ab
36x4mm perforation	33.70a	11.80a	105.37a
54x2mm perforation	36.30bc	13.80b	108.81ab
120x2mm perforation	35.50ab	12.10a	110.37bc
Means	35.86±0.29	12.32±0.21	108.78±0.68

*Values within a column at each interval followed by a different letter are significantly different ($P \leq 0.05$) according to Duncan tests.

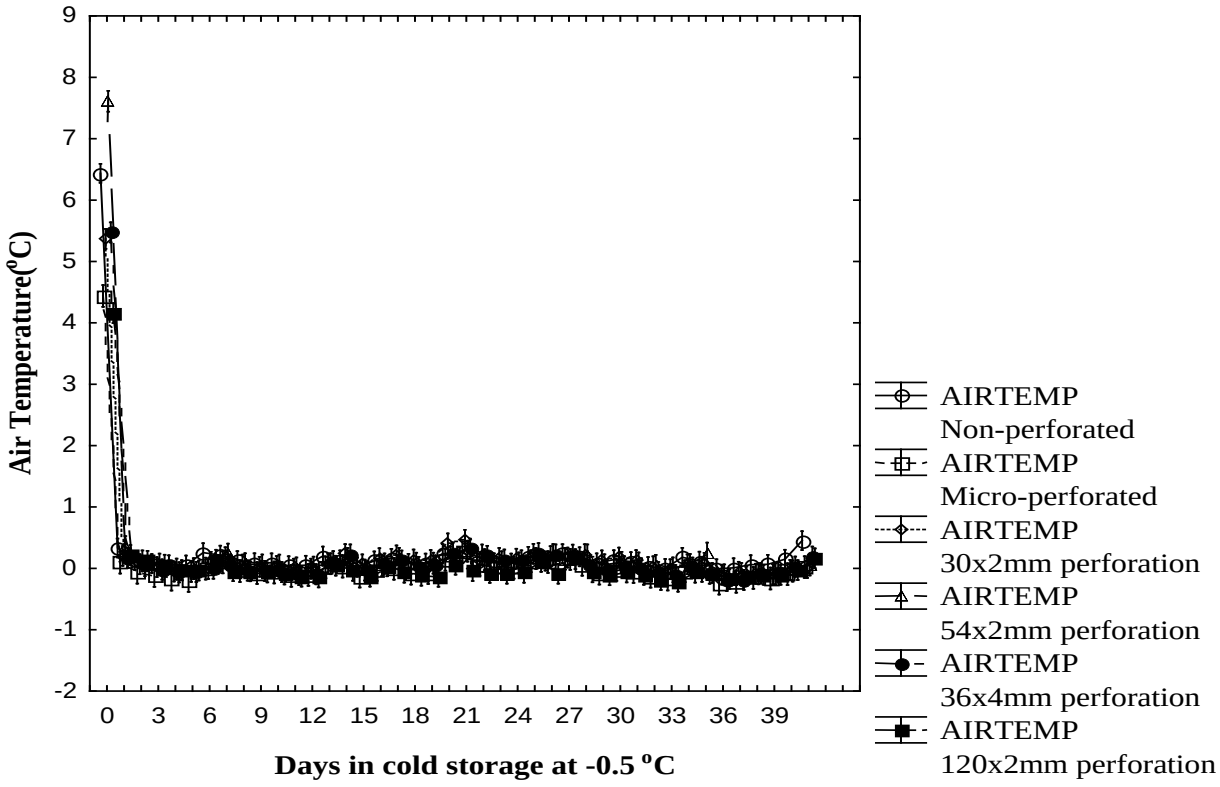

Figure 1: Air temperature profiles inside grape packages during the storage period

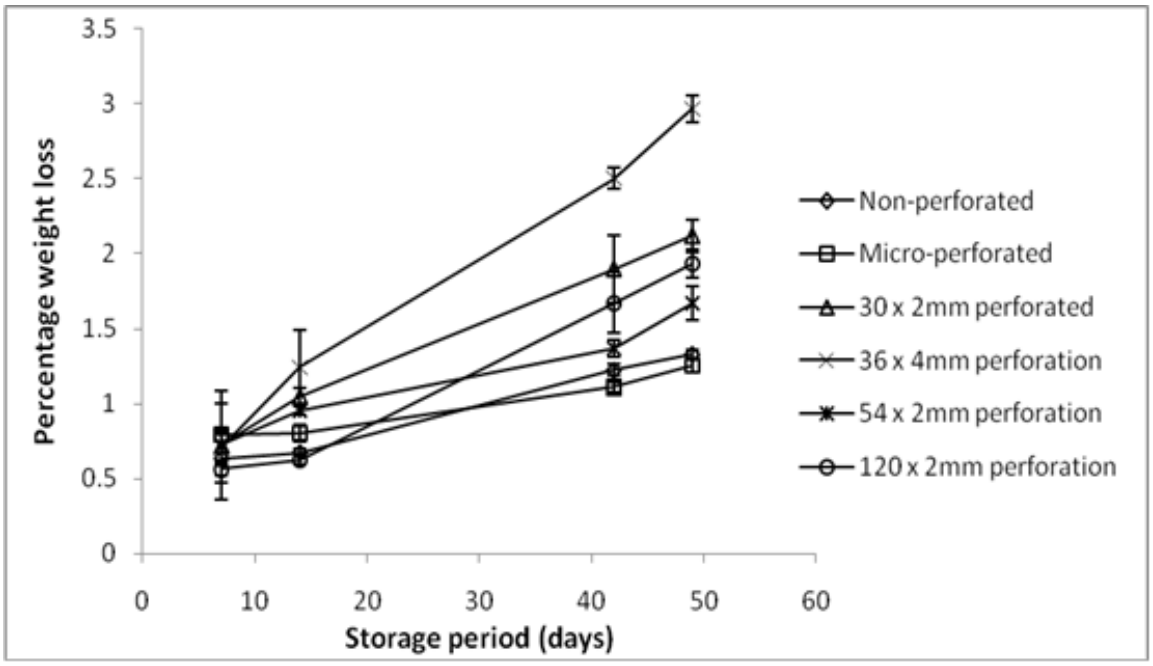

Figure 2: Percentage (±SE) weight loss of 'Regal Seedless' table grapes during cold storage at -0.5°C and after 7 days shelf life at 24.3 C.

Figure 3: Condensation in a 120 x 2 mm perforated liner in cold storage

(a) 

(b) 

Figure 4: (a) Fresh table grape bunch prior to storage and (b) complete decay of ‘Regal Seedless’ table grapes after seven days shelf life study at 24.33±0.04°C

(a)  (b) 

Figure 5: Packing pattern , multi-packages (a) and inner packages (b) (corrugated board; absorbtion and SO_2 pad) of table grapes

PAPER 3

Performance of punnet multi-packaging for table grapes based on airflow, cooling rates and fruit quality

Abstract

The performance of three table grape multi-scale designs, namely the 4.5 kg box, 5 kg open-top punnet and 5 kg clamshell punnet, was studied. Results showed that vent-hole ratio of empty grape boxes had a significant influence on the resistance to airflow, where the 5 kg punnet box with a vent-hole ratio of 6.13±0.04% had a lower pressure drop than the 4.5 kg boxes with a lower vent-hole ratio of 3.80±1.74%. The addition of liner films and inner packages changed the pressure patterns, indicating that inner packaging had a great influence on airflow resistance and airflow patterns through multi-scale packages of grapes. Cooling rates of grapes in the 4.5 kg multi-packaging was significantly ($P<0.05$) slower than that of grapes in 5 kg punnet multi-packaging, where the 4.5 kg box resulted in a seven-eighths cooling time of 30.30-46.14% and 12.69-25.00% more than that of open-top and clamshell punnet multi-packages, respectively. After 35 days in cold storage at -0.5°C, grape bunches in the 5 kg punnet box combination (open-top and clamshell) had weight loss of 2.01 – 3.12%, while the bunches in the 4.5 kg box combination had only 1.08% weight loss. The bunch stem dehydration rates were also higher in the 5 kg punnet multi-package. These results were attributed to differences in vapor pressure deficit (VPD) measured between the three multi-scale packages, where the VPD inside the 4.5 kg multi-packaging was 40.95 Pa, while the VPD inside the 5 kg open-top and clamshell punnet packaging were 92.97 Pa and 100.71 Pa, respectively.

Keywords: Table grape; multi-packaging; Forced air cooling; Pressure drop; vapour pressure; moisture loss

1. Introduction

Precooling and refrigerated storage have been widely reported as effective techniques to preserve fruit quality and freshness after harvest, as these techniques tend to reduce the rate of biochemical reactions and microbiological growth (Baird and Gaffney, 1976; Brosnan and Sun, 2001; Dincer, 1991, 1992; Dincer and Akaryildiz, 1993; Ginsburg et al., 1978; Thompson et al., 1998). Forced air cooling is one of the precooling techniques that is commonly used to remove the field heat from the freshly harvested fresh produce (de Castro et al., 2004; Hardenburg 1986; Thompson et al., 1998). In forced air cooling systems heat is primarily transferred by convection, and therefore temperature and its homogeneity is largely governed by patterns of airflow (Smale et al., 2006; Zou et al., 2006).

Forced air cooling is usually commenced after the fruits have been packaged in carton boxes and stacked on pallets and therefore, it is important that the packaging used allows for sufficient airflow in order to achieve homogenous airflow and thus uniform cooling of packed fruits. Many studies have been reported on the resistance to airflow of fruit packages as a function of vent hole ratio and shape (Chau et al., 1985; Vigneault and Goyette, 2002; Zou et al., 2006); bulk fruit stacking and porosity (Chau et al., 1985; Delele et al., 2008; Neale and Messer, 1976; Neale and Messer, 1978; Verboven et al., 2004; van der Sman, 2002; Smale et al., 2004) and carton boxes stacked on a pallet (Delele et al., 2012). Fruit packaging and box stacking patterns are likely to contribute much to airflow resistance, as the flow is strongly dependant on vent-area and alignment of vent-holes of stacked boxes (Ngcobo et al., 2012b; Delele et al., 2012). Poor ventilation of fruit packages may result in heterogeneous cooling of fruits within packages and between different packages in stacked pallets and this has been associated with poor fruit quality in previous studies (Smale et al., 2006).

Table grape packaging is characterised by different types of multi-scale package combinations (Ngcobo et al., 2012a). These multi-scale packages are aimed at protecting the grapes against mechanical damage during postharvest handling and contamination from foreign matter. However, these multi-packages are also required to allow for sufficient and homogenous cooling in order to prolong at-harvest grape quality after harvest. Previous studies (Delele et al., 2012; Ngcobo et al., 2012a; Ngcobo et al., 2012b) have focused on investigating the effects of liner films, and 4.5 kg boxes stacking on the resistance to airflow;

cooling rates and patterns respectively. The results obtained from these studies have shown that the plastic liner films component of the multi-scale packaging contributed the most (ranging from 40.33 ± 1.15% for micro-perforated liner film to 83.34 ± 2.13% for non-perforated liner film) to airflow resistance (Delele et al., 2012; Ngcobo et al., 2012b). The multi-scale packages may well cause heterogeneous grape cooling which results in postharvest quality variation observed in practice despite the great efforts put in to ensure efficient pre-cooling and good temperature management in the cool chain.

Poor quality in table grapes includes weight loss, stem (rachis) dehydration and browning, colour changes, accelerated berry softening, berry shatter and high incidence of berry decay due mainly to *Botrytis cinerea* and incidence of SO_2 injury (Ginsburg et al., 1978; Nelson, 1978; Ngcobo et al., 2012a; Zoffoli et al., 2008;). It is possible that grape postharvest quality problems may be associated with the type of multi-scale packaging combinations used and therefore an investigation focused on the performance of the different commercially available types of grape packaging combinations is warranted.

The aim of this study was to evaluate the performance of different table grape package systems based on airflow, cooling and quality characteristics. The effects of box design, bunch carrying bag and punnet (open and clamshell) were analysed.

2. Materials and Methods

2.1. Fruit supply

‘Regal Seedless’ grapes were sourced and packed at a commercial farm in the Worcester Area of Western Cape in South Africa. The fruit was then transported to the Postharvest Technology Lab at Stellenbosch University, where it was prepared for forced air cooling and cool storage trials.

2.2. Fruit packaging

The grapes were packed in three types of commercially used grape multi-packages (Fig. 1a and b) namely (i) the 4.5 kg boxes containing the following inner packaging material (120 x 2mm perforated liner film; corrugated paper sheet; bunch carry-bags; moisture absorption sheet and SO_2 pads); (ii) 5 kg boxes containing the following inner packaging material (112 x 4 mm perforated liner film; clamshell punnets; moisture absorption sheet and SO_2 pads); and (iii) 5 kg boxes containing inner packages (112 x 4 mm perforated liner film; open-top punnets; moisture absorption sheet and SO_2 pads).

2.3. Airflow studies

The resistance to airflow studies (measured as pressure loss across grape package) of individual grape packaging components were carried out in a wind tunnel as detailed by Ngcobo et al., (2012b), in a stepwise manner as follows: (i) pressure loss over empty boxes orientated either with its length (L) or breadth (B) perpendicular to inflow (Fig. 2a and b); (ii) pressure loss over boxes containing empty punnets; (iii) pressure loss over boxes containing punnets with grape bunches; and (iv) the pressure loss over complete grape multi-package combinations (boxes plus liner film plus punnets or carry bags containing fruits). The air velocities ranged from 0.70 – 3.21 ms^{-1}; 0.10 – 0.60 ms^{-1} and 0.02 – 0.20 ms^{-1} for the empty wind tunnel, empty packages and fully packed multi-packages, respectively.

2.4. Cooling System

Forced air cooling of grapes boxes was done using a moveable forced air cooler (Fig. 3) inside a refrigerated room. The air temperature inside the cool room was -0.5°C, and was circulated by means of three fans (Delele et al., 2012). The fruit boxes were stacked on a pallet base and tightly positioned in front of the forced air cooler (Fig. 3). The 5 kg punnet boxes were stacked up to 9 layers, with each layer containing 5 boxes as per Figure 4a. The 4.5 kg boxes were stacked up to 5 layers, with each layer containing 10 boxes laid out as per Figure 4b. A total mass of 225 kg was cooled at a time. Following the stacking of fruit boxes, strong plastic was used to seal the sides and top of the fruit stack to the cooler in order to

form a tunnel and to ensure that there was no air leakage when the cooler suction fan was switched on. After sealing with plastic, the cooler fan was switched on and sucked the cold room air through the stack and thus ensuring pre-cooling.

For the quality measurements, six grapes boxes were cooled and stored in a separate but identical cool room at -0.5°C and at 95 % humidity.

2.5. Temperature and humidity measurements

Berry temperature was measured with probes (LogTag Recorder Limited, Northcote, Auckland, New Zealand) inserted into berries positioned in the centre of each carton. Air temperature was measured with a LogTag air temperature recorder (LogTag Trix-8 temperature Recorder) at the central position inside each carton. Air relative humidity (%RH) inside each carton was measured with a SENSITECH TempTale 4 monitor (Temptale4 Humidity and Ambient Temperature 16000, SENSITECH, Beverly, MA, USA).

2.6. Quality measurements

Quality attributes measured included stem dehydration and browning, bunch weight loss, SO_2 injury, colour and decay incidence. The measurements were recorded at 7 days intervals under cold storage and for 35 days. The measuring procedure was done according to Ngcobo et al., 2012a and is detailed as follows:

Bunch weight loss. The weight of individual bunches was measured with a scale (Mettler, Toledo, Switzerland, with an accuracy of 0.01 g). Bunch weight loss data were normalised with respect to the initial bunch weight.

Stem drying and browning. Stem dehydration was assessed using the following scoring system: without drying (fresh stems) = 1, some drying of thinner stems = 2, all thinner stems dry = 3, all thinner and some thicker stems dry = 4 and all stems dry = 5. Stem browning

development was measured by using the following scoring system: (1) fresh and green, (2) some light browning, (3) significant browning and (4) severe browning.

SO_2 injury and decay incidence. SO2 injury was measured according to the following scoring system: (1) none (0%), (2) slight damage (<5%), (3) moderate damage (5–10%) and (4) severe damage (>10 %). Decay was scored as follows: (1) no decay, (2) slight (less than two infected berries per carton), (3) severe (two to five infected berries), and (4) extreme (more than five infected berries per carton).

2.7. Statistical Analysis

The forced air cooling experiments were replicated 4 times and the cooling rate (seven eights cooling times) data between boxes in a layer and between layers was subjected to a two-way analysis of variance (ANOVA) to evaluate the significance of differences. The analysis was done using a STATISTICA 10, software (StatSoft, Inc., Tulsa, USA). Comparison of cooling rate between boxes was done on the mean values using LSD (Least Significant Difference) test (p = 0.05 level).

The quality experiments were replicated 36 times (i.e. six boxes per multi-packaging type and from each box 6 bunches were evaluated) and the data (weight loss) were analysed in Microsoft Excel® and plotted as Mean ± SD.

2.7.1. Cooling data

The cooling data were normalised and presented as dimensionless temperature according to equation 1 (Dincer, 1995):

$$\theta = \left(T - T_a\right) \Big/ \left(T_i - T_a\right) \tag{1}$$

where θ, is the dimensionless temperature; T (°C) is the product temperature; T_a (°C) is the air temperature and T_i (°C) is the product's initial temperature .

The dimensionless temperature change with time is generally expressed in the form of an exponential equation, including the cooling parameters in terms of a cooling coefficient (C, degree per hour degree) and lag factor (J) as (Dincer, 1995; Thompson 1998):

$$\theta = J\exp(-Ct) \tag{2}$$

The cooling rates were then calculated as the half-cooling time (H), (hour) which by substituting $\theta = 0.5$ into equation (2);

$$H = \left[\ln(2J)\right] / C \tag{3}$$

and seven-eighths cooling time (S) in hours. By substituting $\theta = 0.125$ into equation (2), the seven eighths cooling time is calculated by the following equation:

$$S = \left[\ln(8J)\right] / C \tag{4}$$

2.7.2. Pressure loss

The equation used for calculating pressure drop over the packages is the Ramsin equation (Chau et al., 1985; Ngcobo et al., 2012b):

$$\nabla p = -aV^{b} \tag{5}$$

Where p is the pressure (Pa); V is the velocity vector (m/s) ; a is the resistance coefficient $\left(kgs^{(b-2)}m^{-(b+2)}\right)$ and b is the resistance exponent.

2.7.3. Determination of vapour pressure deficit (Vpd)

The vapour pressure deficit (Vpd = p_s - p_∞) was calculated from measured dry bulb temperature and relative humidity data. The corresponding vapour pressure (p_∞) of the

surrounding air inside the multi-packaging treatments was determined by using a psychrometric chart. The determination of vapour pressure over the product surface (p_s) took into account vapour pressure lowering effect of the solutes:

$$p_s = VPL * p_{sat} \quad (6)$$

Where p_{sat} is the saturated vapour pressure (Pa) at the produce surface temperature and VPL is the vapour pressure lowering effect of the produce. In the case of grapes, Becker *et al*., (1995) reported a value of 0.98, and was used in this research.

3. Results and Discussion

3.1. Resistance to airflow

Figure 5 shows the results of pressure drop through empty boxes (i.e. 4.5 kg and 5 kg boxes) indicating that the vent-hole ratio has a significant influence to pressure drop, where the 5 kg boxes with higher vent-hole ratios of 6.16 and 6.10 % (Table 1) resulted in a lower pressure drop than the 4.5 kg boxes with lower vent-hole ratios of 2.57 and 5.03 % (Table 1).

The addition of inner packaging containing fruit (i.e. bunch carry bags and punnets) into the 4.5 kg and 5 kg boxes respectively, resulted in increased pressure drop (Fig. 6), but similar trends as in Fig. 5, where the pressure drop in the 5 kg boxes and punnets with grapes combination resulted in lower pressure drop than in 4.5 kg boxes and bunch carry bag with fruit combination (Fig. 6). However, as soon as the plastic liner films were added the pressure drop results (Fig. 7) were reversed, where the pressure drop in the 4.5 kg box multi-package combination became lower than the pressure drop in the 5 kg punnet combination. This was despite the fact that the punnet box liner film had a slightly higher vent-hole ratio (perforation 114 x 4 mm) of 0.06 % than that of the 4.5 kg liner film 0.05% (120 x 2 mm perforation) (Table 1). This change in pressure drop results may be attributed to the structured (rigid) nature of punnet containers which makes more box structure on the plastic liner film and thus blocks the box vent-holes and thus more resistant to airflow. The bunch carry-bags have no structure other than that of the fruit they contain, and during cooling the pressure of the

incoming air results in deformed shapes that allow more air to pass through between the liner film and the box walls, thus bypassing the fruit.

The results obtained for the resistance coefficients a and b (Table 2), are in agreement with the pressure drop results, where the values of the a coefficient increased by averages of 31.36%; 32.35% and 27% (4.5 kg; 5kg clamshell and 5 kg open-top punnet multi-packages respectively) from empty boxes to fully packed multi-packages (Table 2). The b coefficient also increased slightly with increase in multi-packaging, however, it remained fairly constant. The Ramsin equation fitted well with the pressure drop data as indicated by the r^2 values greater than 0.9. These results suggest that the inner package components have more influence on airflow patterns inside boxes than the box itself. These results agree with those obtained by Ngcobo et al. (2012b), where they found that the plastic liner film contributed the highest to pressure loss than any of the other packaging components.

3.2. Cooling rates

The cooling rates and patterns of stacked grape boxes measured in the central box of the stack under forced air cooling conditions are shown in Table 3 and Figures 8 and 9. Figure 8 shows the cooling patterns of grape multi-packaging combinations stacked in layers on a pallet base and the pallet orientated with its 1 m in the direction of the airflow. Figure 9 shows the cooling results when the pallet was orientated with its 1.2 m side in the direction of the airflow. The two orientations of pallets come with differences in stacking patterns of boxes in a layer (Figures 4a and 4b). When the pallet (stack) was oriented with its 1 m in the airflow direction, the cooling results (Fig. 8) indicated that the 4.5 kg multi-packaging combination resulted in a significantly ($P<0.05$) slower cooling rate than the cooling rates of 5 kg punnet box combination. When pallet orientation was 1.2 m in the airflow direction, the 4.5 kg multi-packaging combination still cooled the slowest, however, its cooling pattern was not significantly different from the 5 kg clamshell punnets box combination, while the 5 kg open-top punnets combinations cooled significantly ($P<0.05$) faster than the two multi-package combinations. The seven-eighths cooling time shown in Table 3, was in agreement with the results observed in the Figures 8 and 9, as the 7/8 cooling time for the open-top punnets combination were significantly ($P<0.05$) lower than that of 4.5 kg packaging and the 5 kg

punnets combination. These results may be attributed to the fact that the 4.5 kg boxes had a smaller vent-hole ratio than the 5 kg punnet boxes. Another possible reason for such results may have been due to the rigid structure of the punnets forcing a good contact between the cold air and fruit by properly sealing the plastic liner film to the inner box walls, while the deformed structure of bunch carry-bags and liner film in a 4.5 kg box may have allowed cold air to bypass the fruit through the formation of channels between liner films and the inner walls of the boxes and thus reducing cooling rate of the grapes. Based on the results, it was also evident that the table grape package design and box stacking patterns had an influence on the airflow patterns and thus the cooling rates.

The results also indicated that the cooling pattern of boxes in a layer of the stack is such that the boxes upstream (incident to incoming airflow) tended to cool at a faster rate than the boxes positioned downstream (near the FAC) (Table 4). There were significant ($P<0.05$) differences in cooling rates of individual boxes in a layer, suggesting some uneven spatial variability within each layer of a stacked pallet. This may have been due to non-uniform airflow patterns within a stack as a result of misalignment of vent holes adjacent to each other and the inner packaging may have exacerbated heterogeneous flow.

3.3. Quality attributes

3.3.1. Bunch weight loss

Moisture loss of grape bunches in different multi-packaging combinations during cold storage are shown in Figure 10. The results indicated that although the moisture loss generally occurred in all packages, the differences between the multi-packaging combinations used were not significant ($P<0.05$). However, there were noticeable trends that suggested that the grape bunches in 5 kg punnet multi-packages tended to lose weight at a faster rate than those in 4.5 kg carry-bag multi-packages. These differences could be ascribed to the differences in the percentage relative humidity inside the package. Measured relative humidity inside the packages was 85.31±2.45%; 84.11±1.04% and 93.52±0.23% which resulted in different vapour pressure deficits (VPD) of 92.97 Pa; 100.71 Pa and 40.95 Pa between the open-top punnets; clamshell punnets and 4.5 kg carry-bag multi-packages,

respectively (Table 5). The differences would become more significant if the storage periods were longer than 35 days.

3.3.2. Stem dehydration and browning

The stem dehydration results are presented in Figure 11. According to the results, open-top punnet multi-packaging resulted in a higher level of stem dehydration with 5.6 % of the total stems reaching drying score 3 (i.e. all thinner stem were dry) after 28 days in storage, while the other multi-packaging treatments went up to drying level 2 (i.e. some of the thinner stems dry). After 35 days in cold storage, 83.33% of bunches had stems that reached drying level 2 and 16.67% of bunches still had fresh greener stems for the 4.5 kg carry-bag multi-packaging combination, while the clamshell punnets multi-packaging combination had 100% of bunch stems reaching level 2 drying after 35 days of cold storage. These results could also be ascribed to the VPD difference (Table 5). The stem drying results followed a similar trend as the weight loss results.

The stem browning results (Figure 12) did not show a similar trend as weight loss and stem dehydration results, as both the open-top punnet and 4.5 kg multi-packaging combinations reach browning scores of 3 after 28 days in cold storage. This observation could be ascribed to the fact that some of the stems were already showing some browning after 7 days in cold storage and this could clearly be attributed to pre-harvest sulphur sprays the affects of were, which was exacerbated in storage. The stem browning due to sulphur sprays is distinguishable as it tends to be localised on the outer surface of the stems, while the inner part of stems remain green.

2.1.1. SO_2 injury and decay incidence

During this study no incidences of SO_2 or decay were observed.

3. Conclusion

Results obtained from the three multi-scale packages used for table grapes showed that 5 kg punnet multi-package generally performs better in terms of cooling rates than the 4.5 kg bunch carry-bag multi-packaging combination, where the seven-eighths cooling times of the 4.5 kg multi-packaging were 30.30 % and 25.00 % (1 metre pallet orientation in airflow direction) and 46.14% and 12.69 % (1.2 metre pallet orientation in the airflow direction) longer than those of the open-top and clamshell punnet multi-packaging. However, there appears to be a trade-off between faster cooling rates and grape postharvest quality, given that the 4.5 kg box multi-package resulted in lower bunch moisture loss and stem dehydration rates than the 5 kg punnet multi-package. This trade-off could possibly be ascribed to the lower ability of 5 kg multi-packages to retain moisture (85.31±2.45 and 84.11±1.04% RH) and thus resulting in higher VDP of 92.97 Pa and 100.71 Pa, while the 4.5 kg multi-packaging maintained 93.52±0.23 % RH, which resulted in lower VDP of 40.95 Pa. Furthermore, the higher VPD inside the 5 kg punnet multi-package may have resulted from convective mass transfer due to higher air circulation inside the package.

The obtained results also suggested that the stacking of boxes influences the patterns of airflow within the stack as indicated by significant ($P<0.05$) differences in the cooling rates of individual boxes in a layer. The variation in cooling patterns within box stacks and layers may be ascribed to heterogeneous patterns of airflow due to poor alignment of vent-holes between boxes and further exacerbated by the presence of inner packaging. Future studies should focus at optimising the table grape multi-packages for improved cooling while ensuring that postharvest quality is not compromised.

References

Baird, C.D., and J.J. Gaffney. 1976. A Numerical Procedure for Calculating Heat Transfer in Bulk Loads of Fruits or Vegetables. *ASHRAE Transactions.* 82(2), 525-540.

Becker B.R., Misra A., Fricke B.A. 1995. Bulk refrigeration of fruits and vegetables, Part I: Theoretical considerations of heat and mass transfer. University of Missouri-Kansas City, USA

Brosnan T., Sun Da-Wen. 2001. Precooling techniques and applications for horticultural products - a review. Int. J. Refrig. 24, 154-170

Chau, K.V., Gaffney, J.J., Baird, C.D., Church, G.A., 1985. Resistance to air flow of oranges in bulk and in cartons. Trans. ASAE 28 (6), 2083–2088.

de Castro L.R., Vigneault C., and Cortez L.A.B. 2004. Container opening design for horticultural produce cooling efficiency. Food, Agric. Environ. 2 (1), 135-140.

Delele M.A., Tijskens E., Atalay Y.T., Ho Q.T., Ramon H., Nicolaï B.M., Verboven P. 2008. Combined discrete element and CFD modelling of airflow through random stacking of horticultural products in vented boxes. J. Food Eng. 89, 33-41

Delele M.A., Ngcobo M.E.K., Opara U.L., and Meyer C.J. 2012. Investigating the effects of table grape package components and stacking on airflow, heat and mass transfer using 3-D CFD modelling. Food Bioprocess Technol., DOI 10.1007/s11947-012-0895-5

Dincer, I. 1991a. Experimental and theoretical heat and mass transfer studies on the forced-air precooling of spherical food products, MSc thesis, Mech. Engng Dept, Yildiz University, Istanbul.

Dincer, I. 1992. Methodology to determine temperature distributions in cylindrical products exposed to hydrocooling. Int. Comm. Heat Mass Transfer. 19, 359-71.

Dincer, I., Akaryildiz, E., 1993. Transient temperature distributions within spherical products with internal heat generation and transpiration: experimental and analytical results. International Journal of Heat and Mass Transfer 36, 1998–2003.

Dincer I. 1995. Air flow precooling of individual grapes. J. Food Eng. 26, 243-249.

Ginsburg L., Combrink J.C. and Truter A.B. 1978. Long and short term storage of table grapes. Int. J. Refrig. 1 (3), 137-142.

Hardenburg RE, Watada AE, Wang CY. 1986. The Commercial Storage of Fruits, Vegetables, and Florist and Nursery Stocks. USDA Handbook, Government Printing Office: Washington, DC.

Neale M.A., Messer H.J.M. 1976. Resistance of Root and Bulb Vegetables to Airflow. J. Agric. Eng. Research. 21, 221-231

Neale M.A., Messer H.J.M. 1976. Resistance of Leafy Vegetables and Inflorescences to Airflow. J. Agric. Eng. Research. 23, 67-75

Neale, M.A., Messer, H.J.M., 1978. Resistance of leafy vegetables and inflorescences to airflow. Journal of Agricultural Engineering Research 23, 67–75.

Nelson K.E. 1978. Pre-cooling – its significance to the market quality of table grapes. *Int. J. Refrig.* 1, 207–215.

Ngcobo, M.E.K., Opara, U.L., Thiart, G.D. 2012a. Effects of packaging liners on cooling rate and quality attributes of table grape (cv. Regal seedless). Packag. Technol. Sci. 25 (2), 73-84.

Ngcobo M.E.K., Delele M.A., Opara U.L., Zietsman C.J., Meyer C.J. 2012b. Resistance to airflow and cooling patterns through multi-scale packaging of table grapes. Int. J. Refrig. 35, 445-452.

Smale, N.J. 2004. Mathematical modelling of airflow in the shipping systems: model development and testing. Ph.D. thesis, Massey University, Palmerston North, New Zealand.

Smale N.J., Moureh J., and Cortella G.2006. A review of numerical models of airflow in refrigerated food applications. Int. J. Refrig. 29, 911-930.

Thompson J.F., Mitchell F.G., Rumsey T.R., Kasmire R.F., Crisosto C.H. 1998. Commercial Cooling of Fruits, Vegetables, and Flowers. Publication 21567, Regents of the University of California: USA.

van der Sman, R.G.M., 2002. Prediction of airflow through a vented box by the Darcy-Forchheimer equation. J. Food Eng. 55, 49-57.

Vigneault C., Goyette B. 2002. Design of plastic container opening to optimize forced–air precooling of fruits and vegetables. *ASAE,* 18(1), 73–76.

Verboven P.; Hoang M.L.; Baelmans M.; Nicola B.M. 2004. Airflow through beds of apples and chicory roots. *Biosystems Eng.* 88 (1), 117–125

Zoffoli J.P., Latorre B.A., Naranjo P. 2008. Hairline, a postharvest cracking disorder in table grapes induced by sulfur dioxide. Postharvest Biol. Technol. 47, 90–97.

Zou, Q., Opara, L.U., McKibbin, R., 2006. A CFD modelling system for airflow and heat transfer in ventilated packaging for fresh foods: I. Initial analysis and development of mathematical models. J. Food Eng. 77, 1037-1047.

Table 1: Vent-hole ratio of the different table grape packaging components

Package component and its orientation to airflow direction	**Ratio of vent-hole to wall surface area of grape packages**		
	Wall area (m^2)	**Vent area (m^2)**	**Vent ratio (%)**
Punnet box 400 mm side	0.038	0.002	6.16
Punnet box 600 mm side	0.057	0.003	6.10
Punnet box bottom side	0.240	0.003	1.23
Punnet box top	0.240	0.204	85.00
Clamshell punnet long side	0.015	0.001	5.33
Clamshell punnet short side	0.009	0.000	6.51
Clamshell punnet bottom side	0.016	0.000	1.22
Clamp-shell punnet top side	0.018	0.001	5.32
Open top punnet long side	0.013	0.000	0.00
Open top punnet short side	0.008	0.000	0.00
Open top punnet bottom side	0.016	0.000	1.29
Open top punnet top side	0.018	0.018	100.00
114 x 4mm perforated punnet box liner	2.415	0.001	0.06
4.5 kg carton box 300 mm side	0.038	0.001	2.57
4.5 kg carton box 400 mm side	0.051	0.004	5.03
4.5 kg carton box bottom side	0.120	0.003	2.45

4.5 kg carton box top side	0.120	0.030	25.33
120 x 2 mm perforated liner bag	0.814	0.000	0.05

Table 2: The a and b coefficients derived from equation (5) for multi-scale packages and grapes with the maximum and minimum air velocity

Packaging combinations and fruits	**Equation (5) coefficients** $\nabla p = -aV^b$			**Measured Velocity (ms^{-1})**	
	a	b	**r^2**	**min**	**max**
Empty 4.5 kg box 300	9.00	1.90	0.999	0.081	0.441
Empty 4.5 kg box 400	8.92	1.99	0.999	0.087	0.430
4.5 kg box + Carry-bag + fruit (300 mm side perpendicular to airflow)	10.21	1.90	0.999	0.07	0.383
4.5 kg box + Carry-bag + fruit (400 side perpendicular to airflow)	10.83	2.06	0.999	0.069	0.339
4.5 kg box + liner film + Carry-bag + fruit (300 side perpendicular to airflow)	12.1	1.96	0.999	0.049	0.171
4.5 kg box + liner film + Carry-bag + fruit (400 side perpendicular to airflow)	14.17	2.10	0.999	0.086	0.455
Empty 5 kg punnet box (400 mm side perpendicular to airflow)	8.19	1.93	0.999	0.116	0.605
Empty 5 kg punnet box (600 mm side perpendicular to airflow)	8.2	1.92	1.000	0.115	0.61
5 kg box + empty clamshell punnet, (400 mm side perpendicular to airflow)	9.88	1.89	1.000	0.065	0.21
5 kg box + empty clamshell punnet, (600 mm side perpendicular to airflow)	9.71	1.99	1.000	0.097	0.489
5 kg box + clamshell punnets + fruit, (400 mm side perpendicular to airflow)	9.93	1.89	1.000	0.063	0.204
5 kg box + clamshell punnets + fruit, (600 mm side perpendicular to airflow)	9.82	1.96	0.999	0.092	0.278

5 kg box + liner film + clamshell punnets + fruit, (400 mm side perpendicular to airflow)	11.53	2.04	0.998	0.024	0.076
5 kg box + liner film + clamshell punnets + fruit, (600 mm side perpendicular to airflow)	12.76	2.34	0.999	0.014	0.063
5 kg box + empty open-top punnets,(400 mm side perpendicular to airflow)	9.57	1.93	0.999	0.078	0.404
5 kg box + empty open-top punnets,(600 mm side perpendicular to airflow)	9.46	2.01	0.999	0.11	0.54
5 kg box + open-top punnets + fruit, (400 mm side perpendicular to airflow)	9.46	1.79	0.991	0.072	0.383
5 kg box + open-top punnets + fruit, (600 mm side perpendicular to airflow)	9.35	1.92	0.999	0.104	0.496
5 kg box + liner film + open-top punnets + fruit, (400 mm side perpendicular to airflow)	12.96	2.6	0.997	0.037	0.175
5 kg box + liner film + open-top punnets + fruit, (600 mm side perpendicular to airflow)	9.95	1.92	1.000	0.039	0.118

Table 3: Rate of cooling (seven-eighths cooling time) of stacked table grapes multi-packages,

Pallet orientation in the airflow direction	7/8 cooling time of grape multi-packaging		
	Open-top punnets (5 kg boxes)	Clamp-shell punnets (5 kg boxes)	Carry-bags (4.5 kg boxes)
1 metre	576.67±7.88	620.50±42.50	827.40±25.73
1.2 metre	441.67±11.29	716.00±54.84	820.00±26.63
Significance level	**P=0.0006*	*P=0.3059*	*P=0.8573*

**P<0.05* means that the difference between cooling rates of pallets is significant when their orientation is changed with respect to airflow direction.

Table 4: Cooling rate (seven-eighths cooling time) pattern of individual table grapes boxes in the middle layer of a pallet stack

Carton position in a layer	1 metre in the airflow direction 7/8 cooling time			1.2 metre in the airflow direction 7/8 cooling time		
	Open-top punnets	Clamp-shell punnets	Carry-bags	Open-top punnets	Clamp-shell punnets	Carry-bags
A	640.56±37.91	593.22±29.83	971.86±41.02	645.33±37.62	593.22±29.84	969.42±24.14
B	557.11±30.21	508.00±11.88	973.18±45.14	557.11±30.21	508.00±11.88	1009.87±29.19
C	554.75±28.82	573.33±27.94	949.57±36.61	541.11±28.85	573.33±27.93	949.68±24.14
D	509.56±38.95	611.44±47.60	772.10±33.76	509.56±38.95	611.44±47.60	799.31±30.44
E	462.89±34.51	516.78±42.25	794.33±14.04	511.67±41.91	591.89±44.60	794.33±23.19
F			793.73±34.84			793.73±23.19
G			824.07±21.15			824.07±23.19
H			739.07±24.75			739.07±23.19
I			832.73±39.20			832.73±23.19
J			792.00±21.55			792.00±23.19
Significance level	**P=0.0000*	*P=0.0492*	*P=0.0000*	*P=0.0000*	*P=0.0000*	*P=0.0000*

**P<0.05* means that the cooling rates of boxed in different positions in a layer was significant

Table 5: Mean thermal and humidity conditions inside the grapes multi-packages during cold storage for quality measurements

Packaging treatment	Mean air temp inside boxes (^{0}C)	Mean RH (%)	VPD (Pa)
Open-top multi-package combination	0.48±0.32	85.31±2.45	92.97
Clamshell multi-package combination	0.50±0.30	84.11±1.04	100.71
4.5 kg carry-bag multi-package combination	0.46±0.34	93.52±0.23	40.95

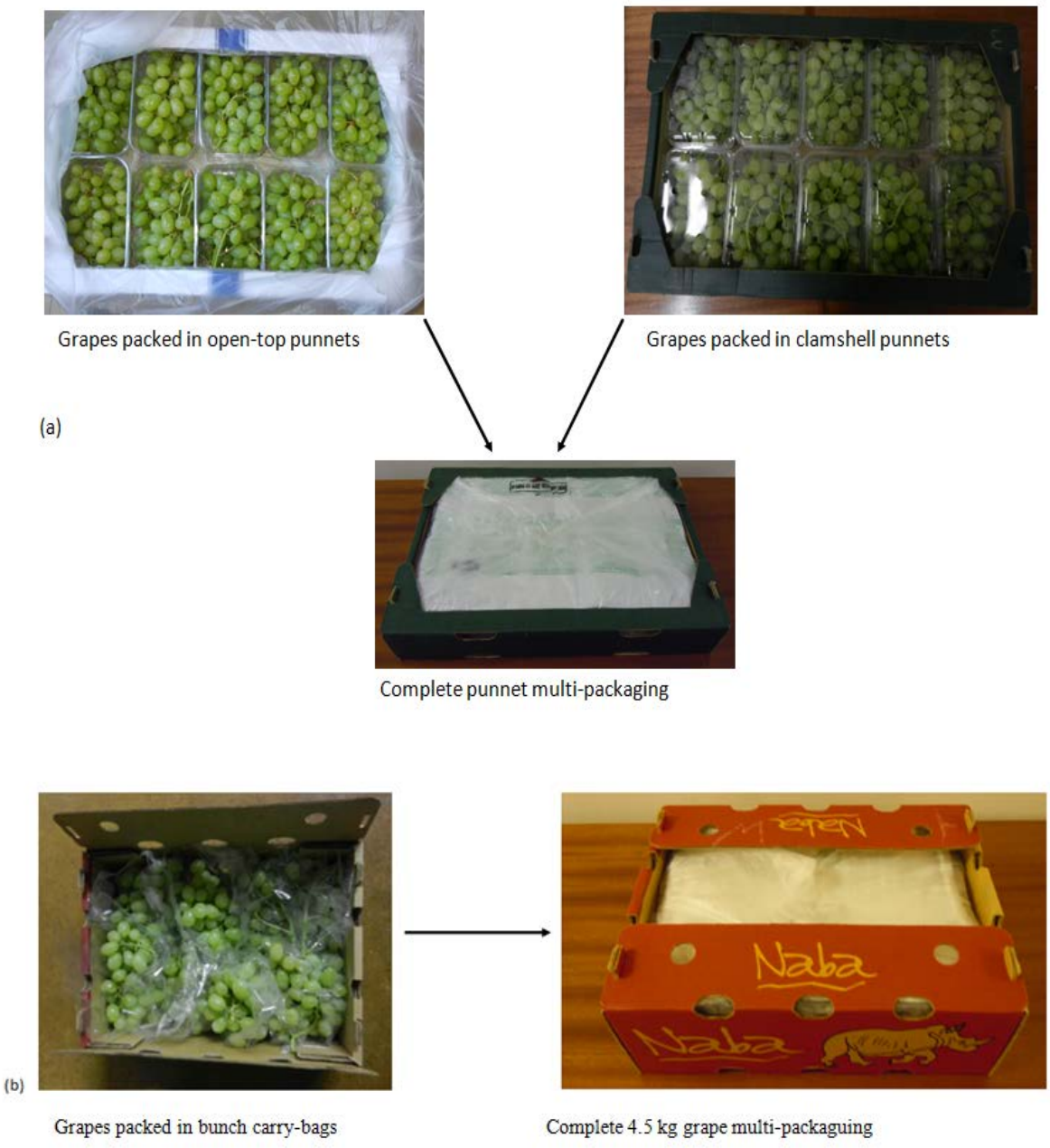

Figure 1: Table grape multi-packages combinations, (a) 5 kg punnet multi-packages and (b) 4.5 kg multi-package combination

Figure 2: Table grape box dimensions, (a) 4.5 kg grape box and; (b) 5 kg grape punnet box

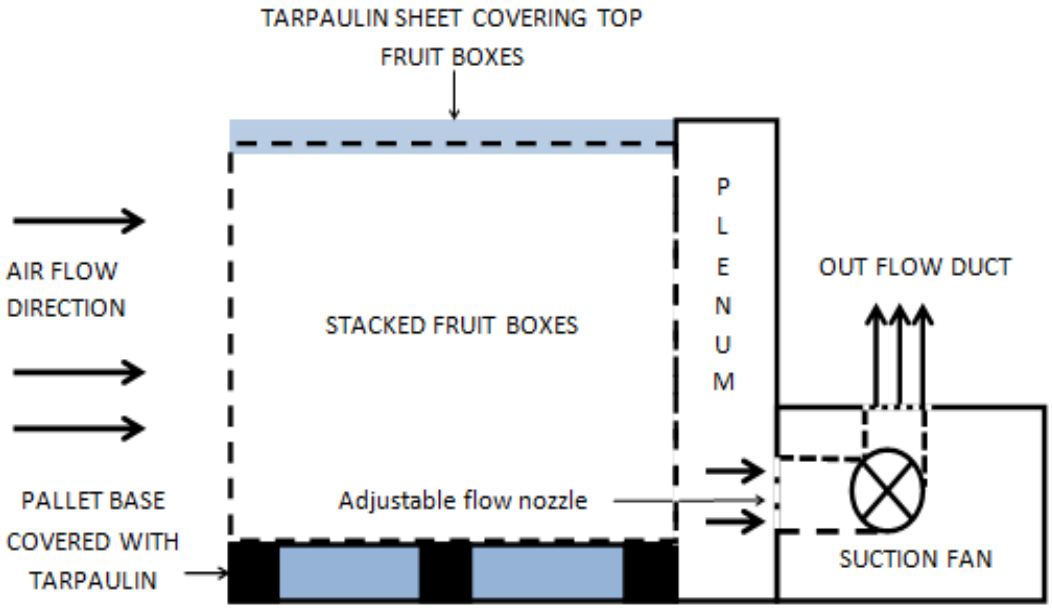

Figure 3: Experimental setup of a forced air cooler for measuring cooling rates of grapes inside stacked carton boxes of multi-scale grape packages.

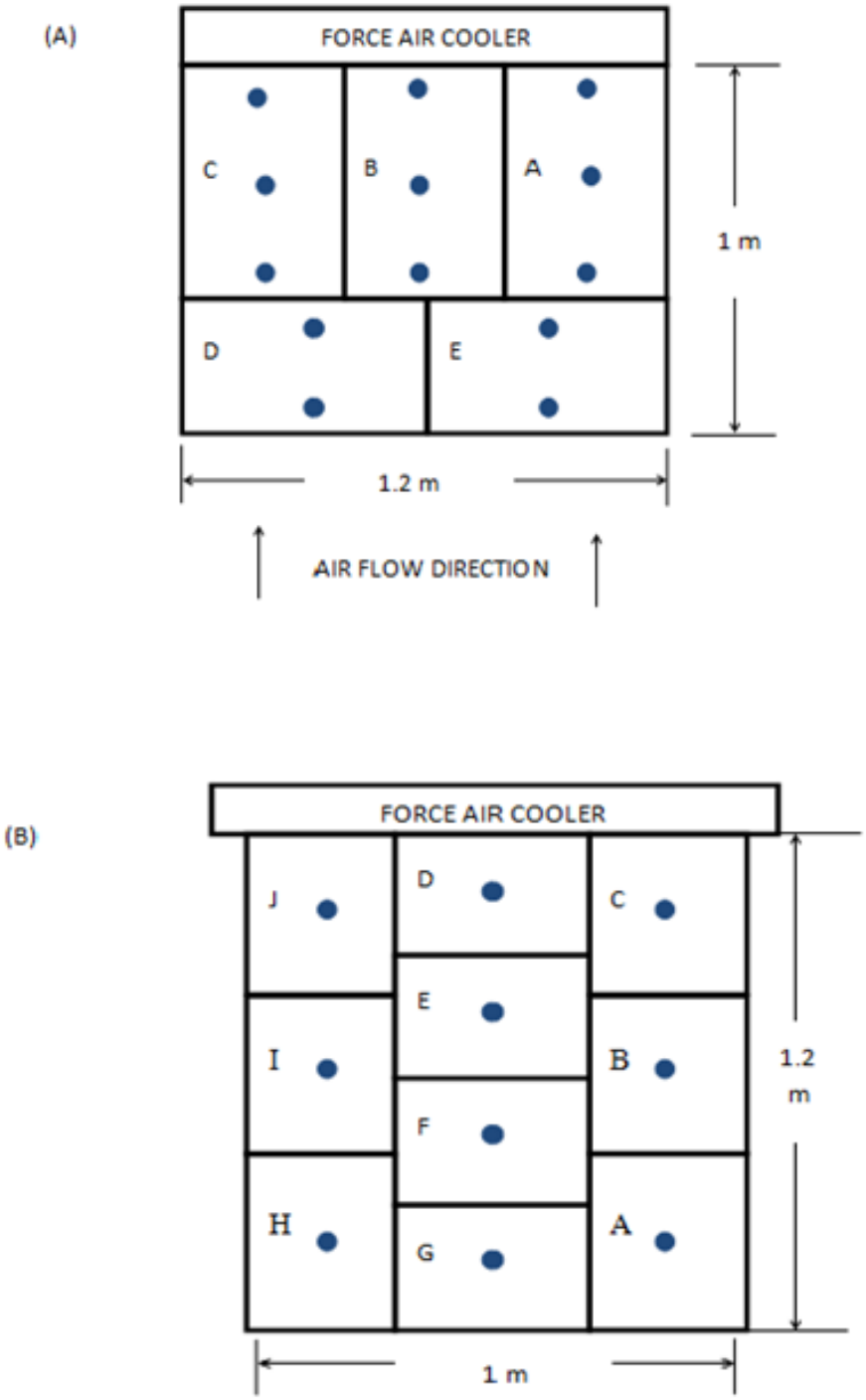

Figure 4: Top view of grape boxes stacking pattern and temperature sensor positions (●) in each layer of fruit pallet, (a) 5 kg grape punnet boxes and (b) 4.5 kg grape boxes

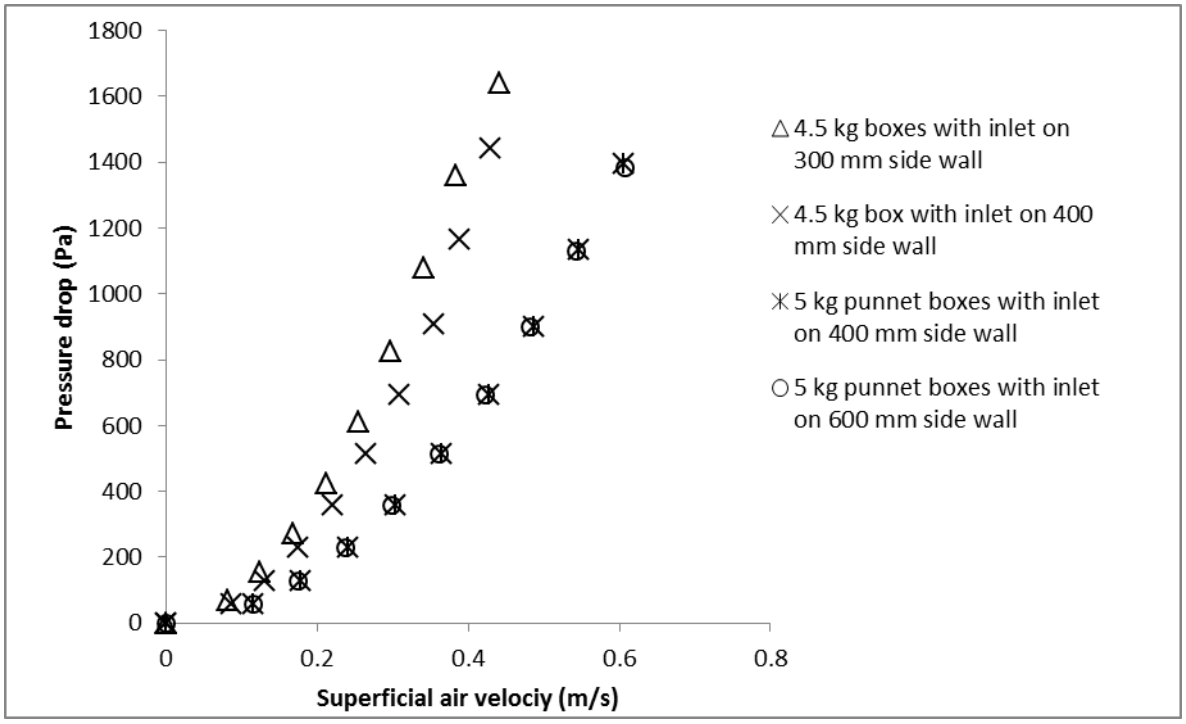

Figure 5: Pressure drop as a function of approach air velocity for the empty carton boxes.

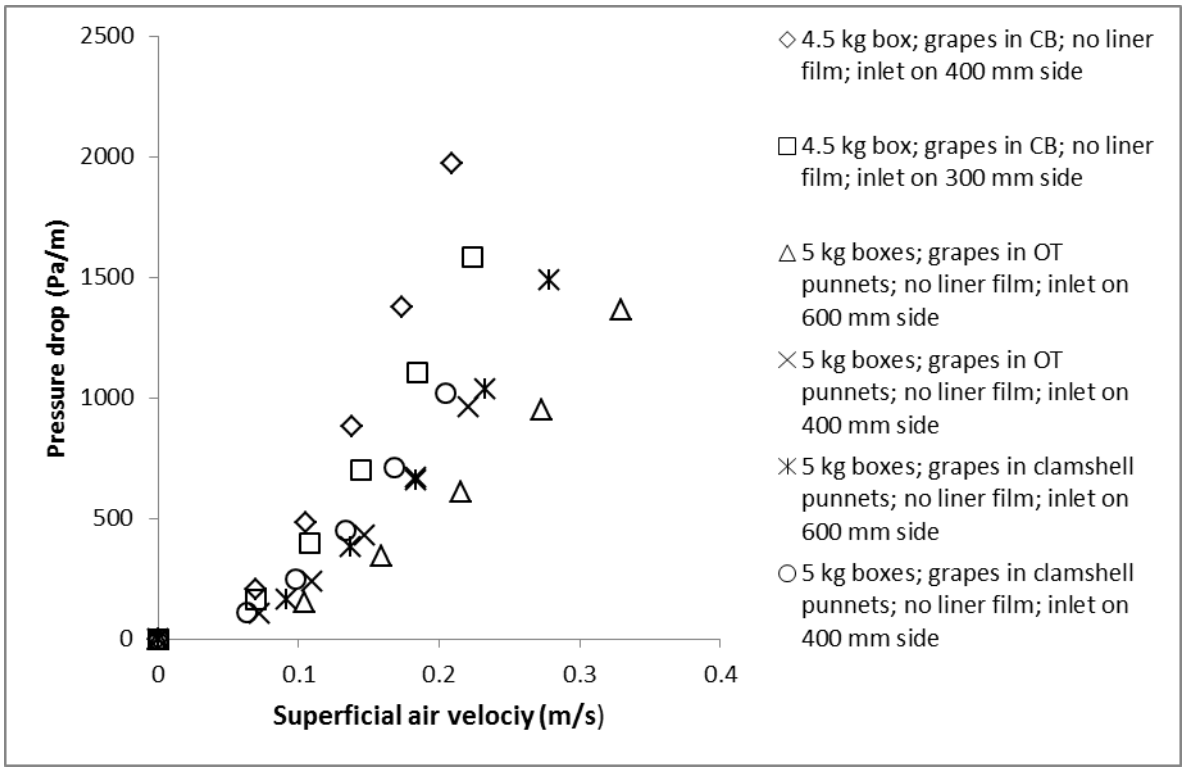

Figure 6: Pressure drop as a function of approach air velocity for the grapes in package combinations with no liner films. CB is the bunch carry-bag and OT is the open-top punnets

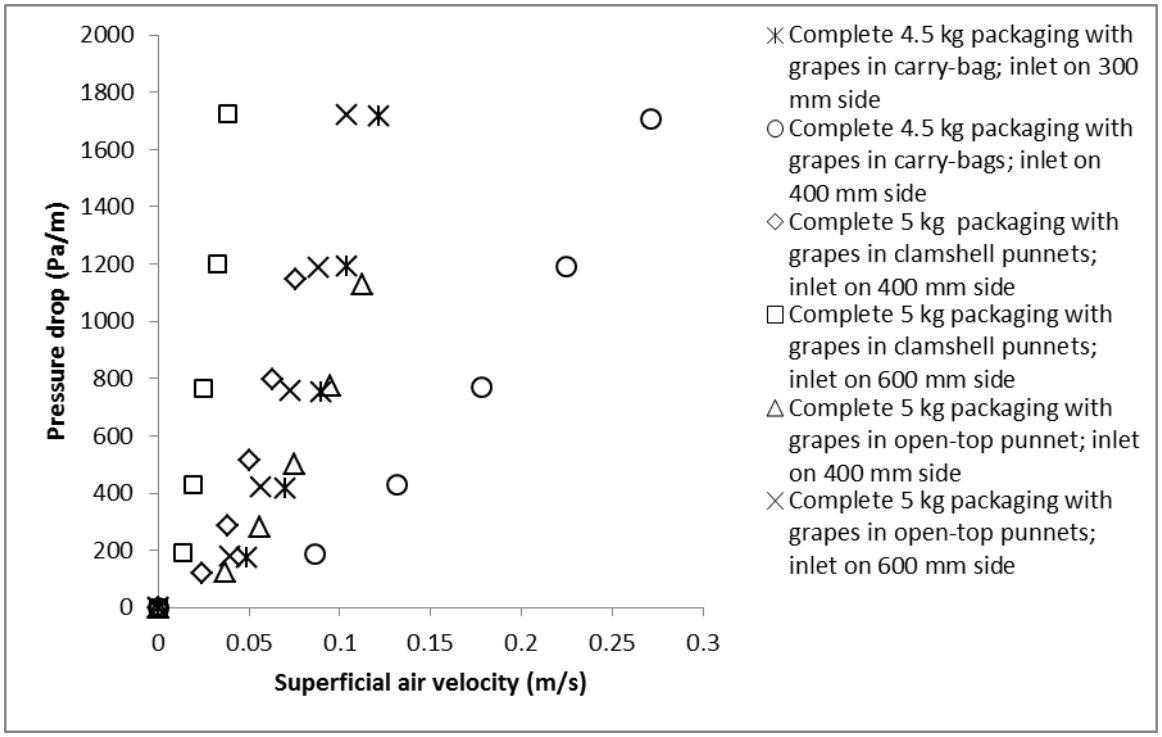

Figure 7: Total pressure drop as a function of approach air velocity for the different grape multi-packages.

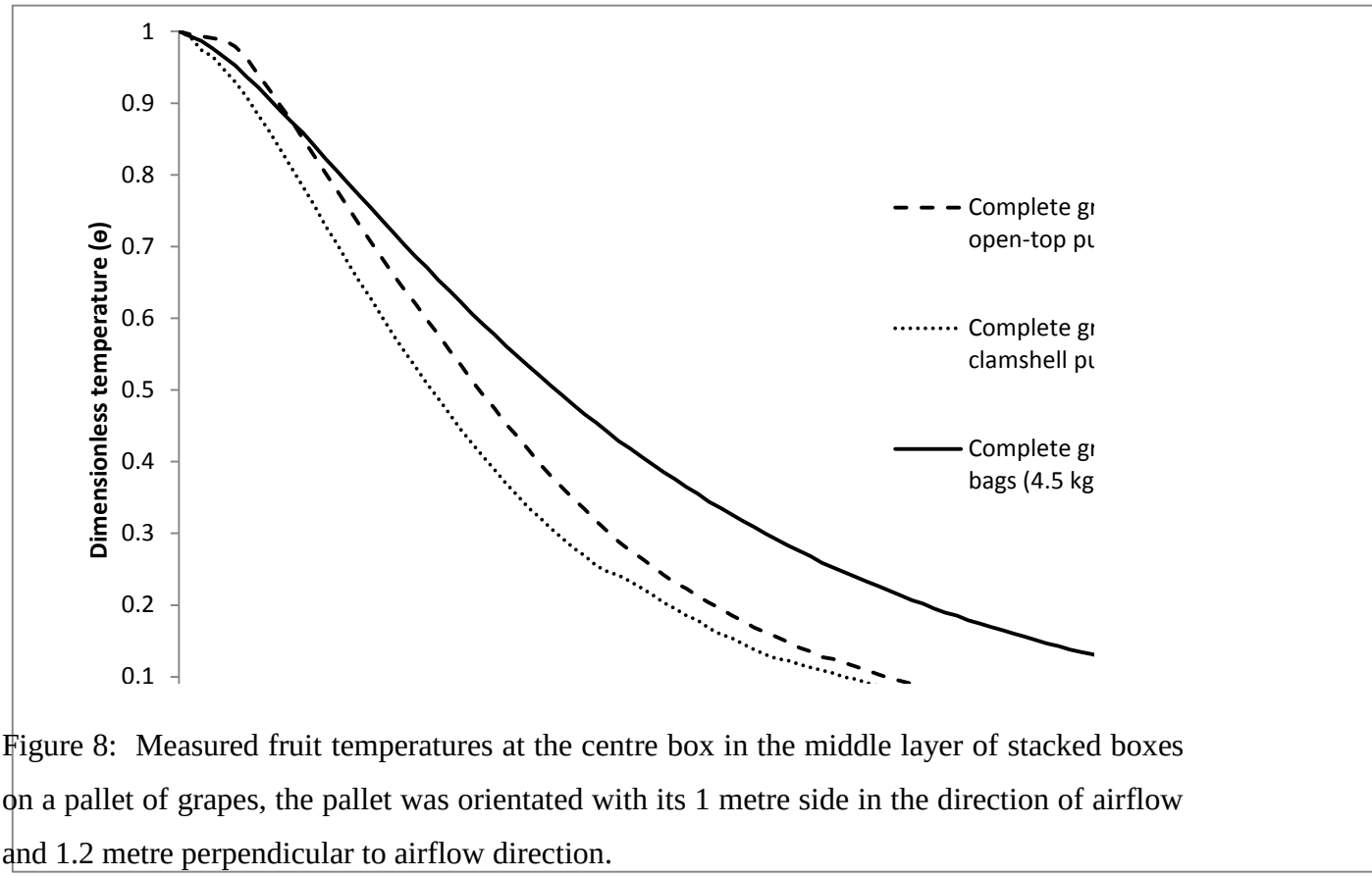

Figure 8: Measured fruit temperatures at the centre box in the middle layer of stacked boxes on a pallet of grapes, the pallet was orientated with its 1 metre side in the direction of airflow and 1.2 metre perpendicular to airflow direction.

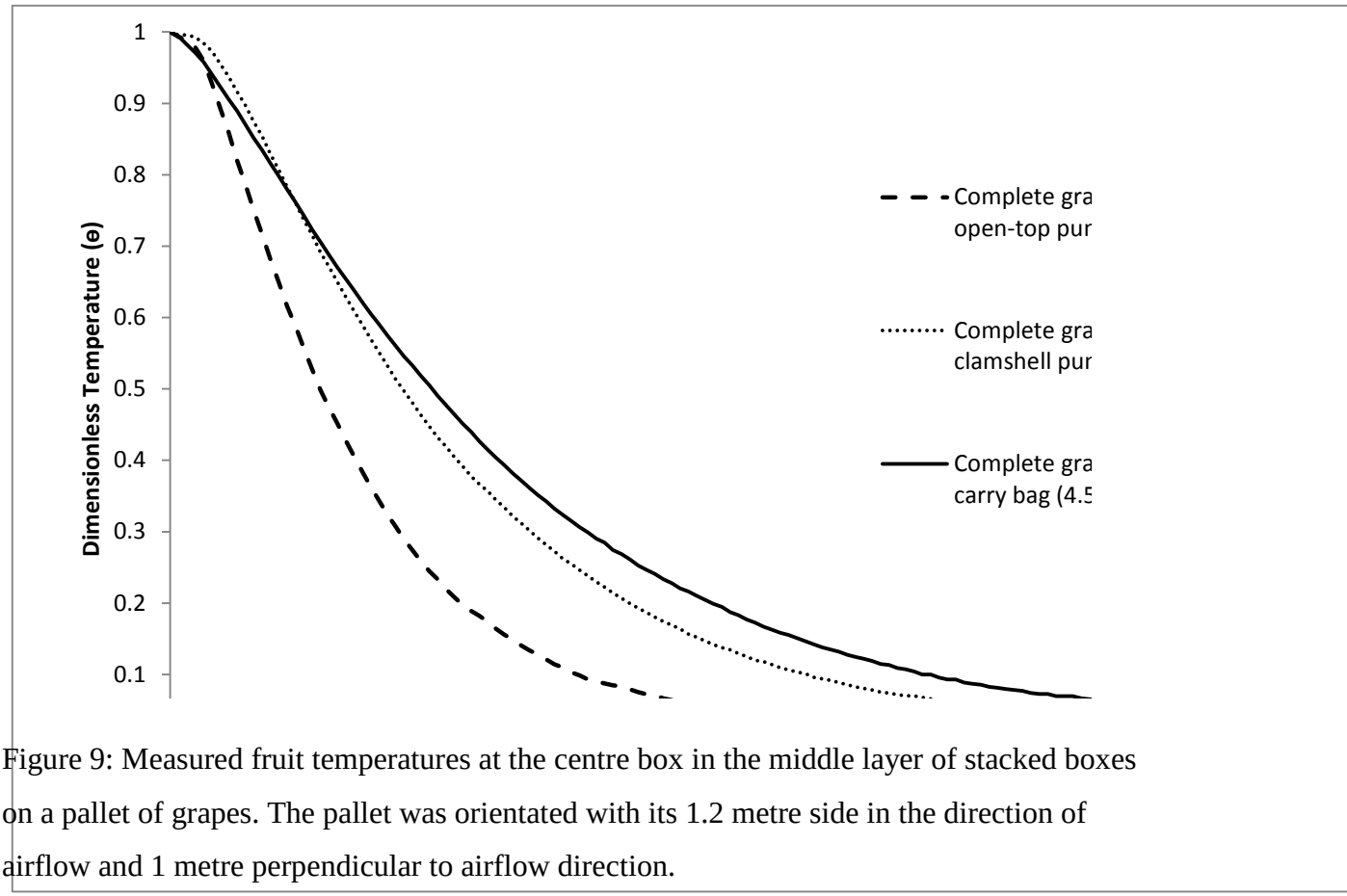

Figure 9: Measured fruit temperatures at the centre box in the middle layer of stacked boxes on a pallet of grapes. The pallet was orientated with its 1.2 metre side in the direction of airflow and 1 metre perpendicular to airflow direction.

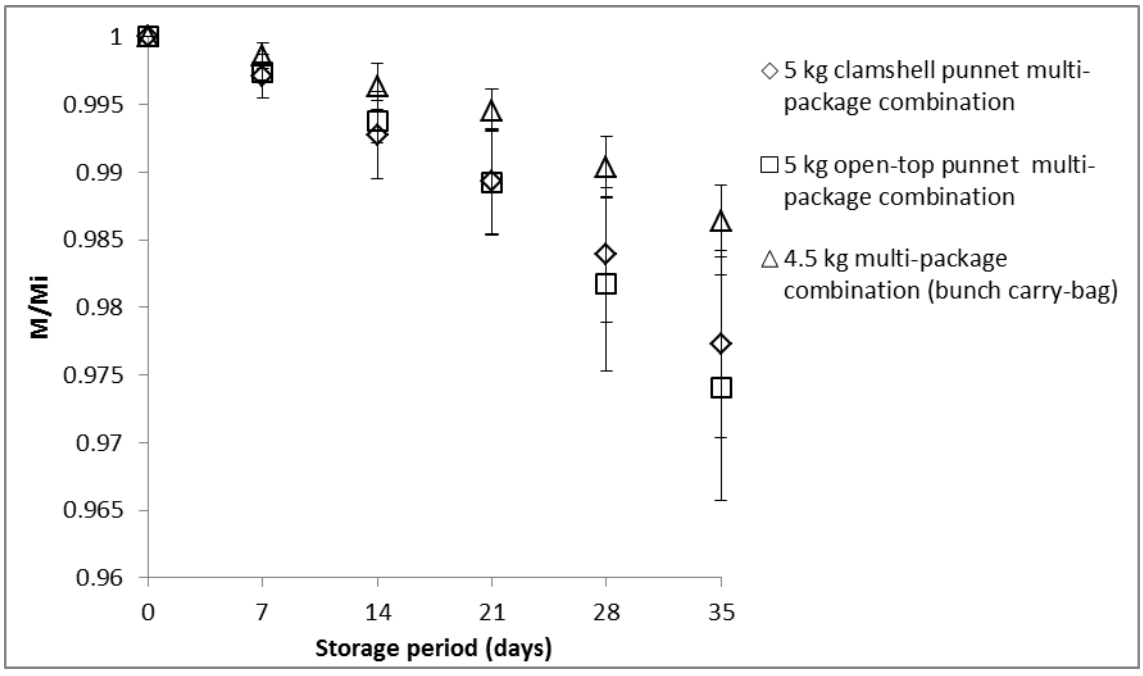

Figure 10: Changes in mass of grape bunches (M , g) over time in cold storage. The values were normalised with respect to the initial mass of grapes (M_i , g).

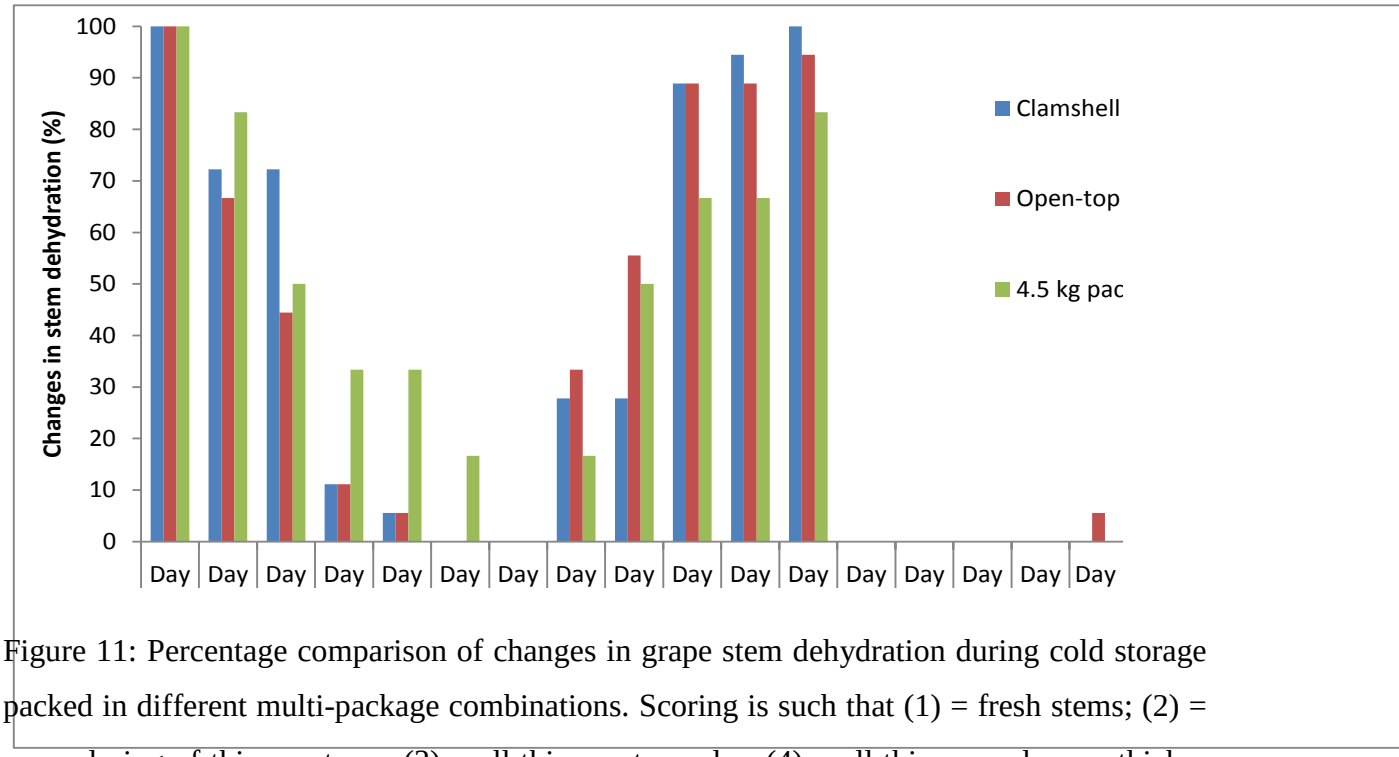

Figure 11: Percentage comparison of changes in grape stem dehydration during cold storage packed in different multi-package combinations. Scoring is such that (1) = fresh stems; (2) = some drying of thinner stems; (3) = all thinner stems dry; (4) = all thinner and some thicker stems dry and all stems dry = 5

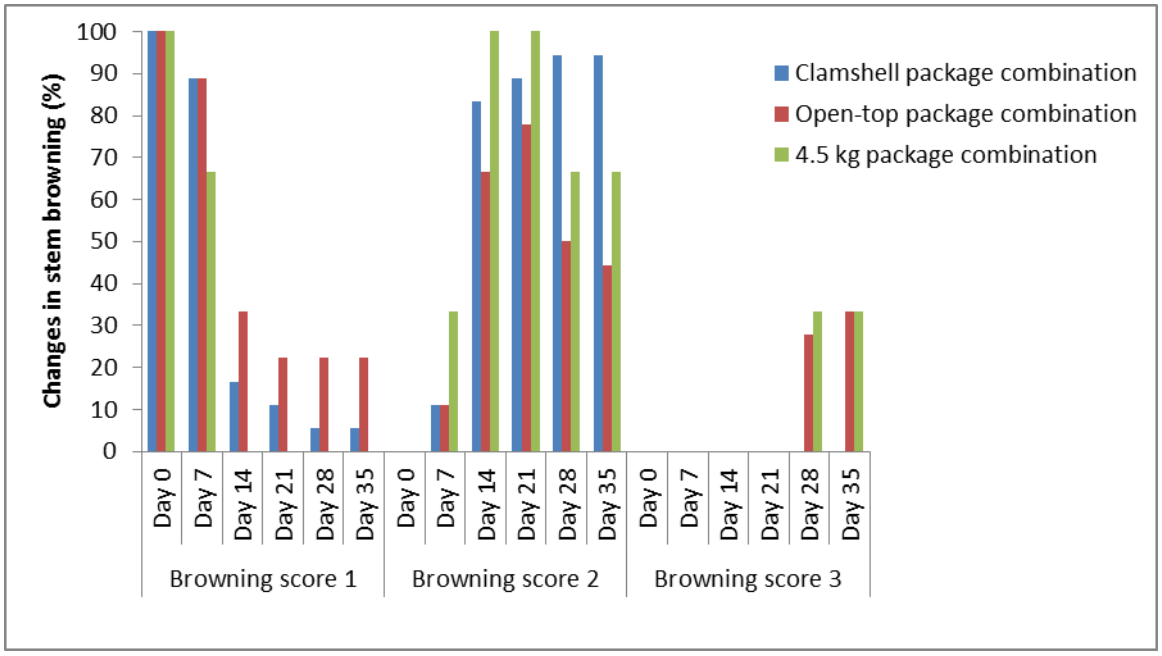

Figure 12: Percentage comparison of changes in grape stem browning during cold storage packed in different multi-package combinations. Scoring is such that (1) = fresh and green, (2) = some light browning, (3) = significant browning and (4) = severe browning.

PAPER 4

Moisture loss characteristics of fresh table grapes packed in different film liners during cold storage

Abstract

Moisture loss characteristics of grapes packed in different packaging liner films during cold storages (1.21±0.25 °C) were studied. The moisture loss rate from grapes packed in non-perforated liner films was significantly ($P<0.05$) lower compared to the moisture loss rate from grapes packed in perforated liner films (120 x 2 mm and 36 x 4 mm perforated liner films). After 72 days of cold storage, the maximum moisture loss of grape stems was significantly ($P<0.05$) higher (range from 49.24 ± 4.66 % for non-perforated liner films to 88.55 ± 0.61 for no packaging treatment) than moisture loss of grapes berries which was less than 10%. Transpiration coefficients of the different stem parts and grape berries, stored in a no packaging treatment decreased significantly ($P<0.05$) with storage period. The 36x4mm perforated liner film resulted in a significant ($P<0.05$) decrease of transpiration coefficients of the intermediate stem, large stem parts and berries. There were no significant differences between the transpiration coefficients of the bunch parts stored in the 120 x 2 mm and non-perforated liner films. The transpiration rates of stem parts were lowest in the non-perforated liner film compared to other packaging treatments, while the transpiration rates of grape berries showed no differences between the different packaging treatments (0.79 ± 0.51 g kg^{-1} d^{-1}, for the non-perforated liner film and 1.57 ± 0.58; 1.59 ± 0.75; 1.37 ± 1.00 g kg^{-1} d^{-1}, for the no packaging; 120 x 2mm and 36 x 4mm perforated liner films, respectively)

Keywords: Table grape; packaging; packaging liner; moisture loss; transpiration coefficient; vapour pressure.

Nomenclature

Transpiration rate per weight of product, g kg^{-1} d^{-1}

Transpiration coefficient of commodity on weight basis, g kg^{-1} d^{-1} Pa^{-1}

Water vapour pressure at evaporating surface, Pa

Ambient vapour pressure, Pa

Saturated vapour pressure, Pa

Vapour pressure deficit, Pa

1. Introduction

Table grapes are non-climacteric fruit with a low rate of biochemical activity after harvest, but they are subject to serious water losses during postharvest handling and storage (Crisosto et al., 2001). There are at least three symptoms of water loss from grapes: (i) first to appear are shriveled stems (also known as dry stems), which usually become brittle and break easily; (ii) browning of stems which occurs as stem dehydration becomes more severe; and (iii) berry softening, which is followed by wrinkle like formation that starts to appear radiating out from the pedicel (Nelson, 1978).

Dry and brittle stems often give rise to the detachment of berries from stems (often referred to as berry shatter or loose berries). Both the dry and brown stems detract seriously from the appearance of the grapes (Nelson 1978). Grape berries do not show symptoms of water loss until the damage is quite evident on the stems. At about 4-5% weight loss, berries feel soft and above 5% loss in weight the wrinkles start to appear (Nelson, 1978).

The moisture loss process in fresh produce involves diffusion of moisture from cells into the intercellular spaces until a level of saturation is reached in these intercellular spaces. Then the moisture diffuses from the intercellular spaces to the atmosphere through lenticels, stomates, scars, injured areas, or directly through the cuticle (Thompson et al., 1998; Veraverbeke et al., 2003).

The rate of loss of moisture from fresh fruit is largely dependent on the humidity and temperature of the surrounding air, as well as on the heat and mass transfer properties of the fruit such as thermal conductivity, thermal and moisture diffusivity, interface heat and mass transfer coefficients (Margaris and Ghiaus, 2007; Thompson *et al*., 1998). The rate of moisture loss is also influenced by the product surface area to volume ratio (Thompson et al., 1998). Produce with high surface area to volume ratios such as leafy vegetables lose moisture more rapidly than fruit, which has a lower ratio (Thompson et al., 1998).

Table grapes are mainly packed in multiple-scale packages and are cooled and stored at temperatures of -0.5°C to prolong fruit quality after harvest (Ngcobo et al., 2012). However, despite good temperature control during postharvest storage, table grapes continue to lose weight mainly due to the micro-climatic conditions that were created within the enclosed fruit packages. Ngcobo et al. (2012) reported that there were significant differences in weight loss of table grapes packed in different multi-packages, where the perforated liner films resulted in a higher weight loss than the non-perforated liner films during the cold storage period.

Intact table grape bunches have a very complex structure, comprising of branched stems (rachis) and grape berries. The stems act as ‘fruit handles’ for the consumers when they eat the fruit. The total weight loss model should, therefore, accommodate the different structures that make up the grape bunch. It is probable that the moisture loss characteristics of the whole table grape bunch could be different from the berries as well as the stalks. It is also obvious that for packed grapes the package components affect the rate of moisture loss. No work has been reported on the moisture loss characteristic of whole fresh table grape bunches in multi-scale packages during postharvest storage and handling.

The main objective of this work was to study the moisture loss characteristics of table grapes packed in different liner films during postharvest storage and handling.

2. Theory of transpiration

Estimation of the heat and mass transfer that occurs during postharvest refrigerated storage of fruit and vegetable products requires knowledge of various thermophysical properties of the commodities. Mass transfer calculations require the determination of the transpiration rate

which depends upon the air film mass transfer coefficient, the skin mass transfer coefficient and the vapour pressure lowering effect of the commodity (Becker et al., 1995).

Transpiration is the process exhibited by fresh fruits and vegetables that involve the transport of moisture through the skin of the commodity, the evaporation of this moisture from the commodity surface and the convective mass transport of the moisture to the surroundings (Becker et al., 1995). The factors affecting transpiration rates of freshly harvested fruits and vegetables are: water vapour pressure difference, air velocity, heat of respiration, size, shape, and surface area of the commodity, skin structure, maturity, endothermic effect of evaporation; solutes in the commodity and packaging (Sastry & Buffington, 1983; Sastry 1985). The driving force for transpiration is the vapour pressure difference between the fruit and its surrounding. Linear (Sastry & Buffington, 1983; Sastry, 1985; Nguyen et al., 2007; Delele et al., 2009), and nonlinear models (Sastry, 1983) have been developed over the years to predict transpiration rate. Linear models are expressed as per Eq. (1) below:

$$M = k_{ta}(p_s - p_\infty) \tag{1}$$

Where M is transpiration rate of the commodity per weight of the product (g kg^{-1} d^{-1}); k_{ta} is transpiration coefficient of the commodity on a weight basis (g kg^{-1} d^{-1} Pa^{-1}); p_s is the water vapour pressure at the evaporating surface (Pa) and p_∞ is ambient water vapour pressure (Pa). The transpiration coefficient of the commodity can be calculated by solving Eq. (1) above.

Linear models are the simplest and are applied primarily to storage situations, where steady state conditions prevail and the commodity is assumed to be in thermal equilibrium with the environment (Sastry & Buffington, 1983). The key assumption of this type of model is that the evaporating surface is at the same temperature as the environment, and the surface water vapour can be calculated accordingly.

Nonlinear modelling considers air velocity and skin structure in addition to vapour pressure difference (Sastry & Buffington, 1983). It was not considered in this work.

3. Materials and Methods

3.1. Plant material

The grapes were harvested, prepared and packed from a farm in the Worcester area of Cape Town, South Africa and were transported in an air-conditioned car to the Postharvest Technology Research Laboratory at Stellenbosch University. During preparation at the pack house, the grape bunches were ensured to contain uniform sized (diameter 21.04 ± 0.29 mm) berries. In the laboratory the grape bunches were considered as the composition of 3 kinds of cylinders (Garcia-Perez et al., 2006), 1 sphere and 1 ellipse structure. The 3 cylinders make up the stem part; the small sphere (stem: berry cap) is the cap like structure binding the stem and berries; and the berries were considered to be ellipse structures (Fig 1). The average diameter of each of the individual parts was measured: small spheres (2.55 ± 0.27 mm); small cylinders (1.53 ± 0.19 mm); intermediate cylinders (2.85 ± 0.70 mm); large cylinders (4.88 ± 1.03 mm) and berries (ellipse shaped) were minor diameter A: 21.04 ± 0.29 mm and major diameter B: 29.94 ± 2.49 mm (berry length).

3.2. Experimental procedure

An initial mass of small spheres; small cylinders; intermediate cylinders; large cylinders and berries (5.00 ± 0.00 g; 5.00 ± 0.00 g; 10.03 ± 0.02 g; 20.33 ± 0.37 g and 124.92 ± 4.41 g respectively), was prepared and replicated three times per packaging treatment (i.e. there were three of each packaging types containing similar grape bunch material inside the cold room). The packaging treatments included: no packaging (samples placed on open plastic trays); non-perforated liner film (LDPE); 36 x 4 mm perforated liner film (HDPE) and 120 x 2 mm perforated liner film (HDPE). All the samples were weighed using a scale (Mettler, Toledo, Switzerland, with an accuracy of 0.01 g) to get the initial mass and then stored at 1.21 ± 0.25 °C and 89.06 ± 2.63 % RH (Table 1) in an experimental cold room in the Postharvest Technology Research Laboratory. The weight of each sample was measured daily for the first 14 days, in order to capture detail moisture loss data from stem samples as they tend to dry out quickly and there after every seven days for the remainder of 80 days as moisture loss from grapes berries proved to be a relatively slow process. Due to the usual formation of condensation on the inside surface of packaging liners, the individual samples

were briefly removed from the liner films during measurement to avoid over estimation of weight due to water droplets.

Air temperature and relative humidity were measured inside the storage room and inside the liner films containing grapes (Table 1). Air temperature was measured with a LogTag air temperature recorder (LogTag Trix-8 Temperature Recorder, LogTag Recorder Limited, Auckland, New Zealand) and the air relative humidity (%RH) was measured with a SENSITECH TempTale 4 monitor (Temptale4 Humidity and Ambient Temperature 16000, SensiTech, Beverly, MA, USA).

3.3. Determination of vapour pressure deficit (Vpd)

The vapour pressure deficit ($Vpd = p_s - p_\infty$) (Eq. 1) was calculated from measured dry bulb temperature and relative humidity data. The corresponding vapour pressure (p_∞) of the surrounding air in the cold room and inside the liner films was determined by using apsychrometric chart. The determination of vapour pressure over the product surface (p_s) took into account vapour pressure lowering effect of the solutes:

$$p_s = VPL p_{sat} \tag{2}$$

Where p_{sat} is the saturated vapour pressure (Pa) at the produce surface temperature and VPL is the vapour pressure lowering effect of the produce. In the case of grapes, Becker *et al.* (1995) reported a value of 0.98, which was used in this study.

4. Results and Discussion

4.1. Moisture loss characteristics of fresh grape bunches

Figures 2**a-d**, show a comparison of moisture loss characteristics of the different parts of grape bunches in different packages during storage. The results indicated that moisture loss rate from the grapes stems (rachis) was significantly ($P<0.005$) higher (range from 49.24 ±

4.66 % for non-perforated liner films to 88.55 ± 0.61 % for no packaging treatment) than moisture loss from the grape berries (range between 3.62 ±0.21 % non-perforated liners to 8.68 ± 0.03 % for no packaging treatment) after 72 days of storage. This was true for all the package treatments. The reason for these results may be due largely to difference in skin tissue composition of berry skin and stem epidermal cells, where the berry skin's outer layer (cuticle) is covered by hydrophobic epicuticular waxes, and the lamellar zone underneath is made of cutin (Lecas and Brillouet, 1994). Significant ($P<0.005$) differences in moisture loss were also observed between the smallest (small stem cylinders and berry: stem attachment spheres) and the largest parts of the stems (large stem cylinders), where the smallest parts lost moisture at a faster rate than large stems. This could be attributed to the difference in surface areas of these stem parts, where the small-size parts with high surface area to volume ratios lose moisture rapidly compared to parts with small surface area to volume ratios (larger size stem parts).

4.2. Influence of packaging on moisture loss

Moisture loss from grape bunches in different packaging treatments during cold storage is shown in Fig. 3. The results showed that the rate of weight loss of bunches packed in non-perforated liner film was significantly ($P<0.05$) lower than that of bunches in perforated liner films and no packaging treatments. The maximum percentage moisture loss of bunches in non-perforated was 0.41 ±0.23 %; while bunches in 36 x 4 mm; 120 x 2 mm perforated liner films and no packaging treatment lost weight up to a maximum of 5.16 ± 2.31 %; 6.35 ± 0.47 % and 7.31 ± 0.70 %, respectively during the storage period (Fig. 4a). This means that the whole bunch moisture loss was less than 10% during the 75 days of cold storage. These results agree with results obtained by Ngcobo et al. (2012), where they showed that the weight loss of grapes packed in perforated liners was significantly higher than that of grapes packed in non-perforated liner films.

Figures 4b-g, show percentage moisture loss of individual parts of the stems and berries in different packages during cold storage. There was a similar trend in moisture loss from stem parts (i.e. berry: stem attachment spheres; small cylinders; intermediate cylinders and large cylinders) where the no package treatment resulted in significantly ($P<0.05$) higher rate and

percentage weight loss (86.87 ± 0.27 %; 87.84 ± 0.35 %; 89.95 ± 0.29 %; 89.11 ±0.70 % respectively), than the non-perforated liner film (50.71 ± 5.09 %; 49.82 ± 9.90%; 52.16 ± 10.74 % and 29.37 ± 5.31 %, respectively). The 36 x 4 mm and 120 x 2 mm perforated liner films resulted in intermediate values of weight loss (Fig 4b-e). The percentage moisture loss of whole stems and of grape berries packed in non-perforated liners was significantly lower (49.24 ± 4.67 % and 3.62 ± 0.21 % respectively) than that of the same material in other packaging treatments (with moisture loss in the no packaging treatment being 88.55 ± 0.61 % for whole stems and 8.68 ± 0.03 % for berries), while no significant differences were observed between no packaging, 36 x 4 mm and 120 x 2 mm perforated liner films (Figs. 4f and g). Figure 5 shows the visual appearance of whole grape stems after 80 days in cold storage and the appearance was in agreement with result presented in Fig. 4f.

4.3. Transpiration rates of grape bunches

Table 2 shows the mean transpiration rates of the different parts of the grape bunch packed in different liner films during cold storage. The mean transpiration rates were determined for each part from the experimental data on moisture loss and surface area (Eq.1). The results indicate that the non-perforated liner film resulted in the lowest transpiration rates for all the different parts of the bunch compared to the other packaging treatments. This may have been due to the lowest V_{pd} (52.99 Pa) in the non-perforated liner film compare to V_{pd} of no packaging; 120 x 2 mm perforated and 36 x 4 mm perforated liner films which were 72.96; 72.13 and 77.19 Pa, respectively. There were however, some arbitrary high variation (higher ±SD) which were observed in mean transpiration rates of from parts of the bunch that were stored in non-perforated liner film, and this could perhaps be attributed to pockets of condensation water droplets that tend to form on the inside surface of the liner film and the lack of air circulation inside non-perforated liner films. The transpiration rates of the different stem parts stored in no packaging treatment (i.e. direct exposure to air circulation) were the highest of the lot, and this may have been due to the convective effect of the circulating air inside the cold room, experienced by stem parts in a no packaging treatment. It is important to note that although the transpiration rate of grape berries was lowest when packed in non-perforated liner film (0.79 ±0.51 ≈ 1 g kg^{-1} d^{-1}), the rates were not significantly different between the different packaging treatments (berry transpiration rate was about 1.57 ± 0.58 g kg^{-1} d^{-1} for the no packaging; 1.59 ±0.75 g kg^{-1} d^{-1} for the 120 x 2 mm perforated liner film

and 1.37 ± 1.00 g kg^{-1} d^{-1} for the 36 x 4 mm perforated liner film) (Table 2). This shows that grape berries in storage are least affected by the influence of the V_{pd} of the different packaging treatments and by the convective effect of the cold air circulating in the cold room and this may be due to the lignification of the berry skins (Lecas and Brillouet, 1994). These results corresponded well with the percentage weight loss presented in Figs. 4 a – g.

4.4. Transpiration coefficient (k_{ta})

In literature (Sastry, 1985; Fockens and Meffert, 1972) there is discussion whether the transpiration coefficients of the same horticultural commodity are constant or vary with V_{pd}. In the current work, the transpiration coefficients were calculated at intervals of 3; 9 and 57 d of cold storage at a constant temperature and high relative humidity (Table 1), in order to investigate whether these coefficients vary or remain constant with packaging treatment (*Vpd*) and storage time. The results of transpiration coefficients are presented in Table 3. The results indicate that there was a decrease in transpiration coefficient with storage period in all the packaging treatments. However, the decrease in transpiration coefficients of all stem parts with storage time was only significant ($P<0.05$) for the no packaging treatment (i.e. direct exposure to circulating cold air), and the 36x4 mm perforation liner film treatment resulted in a significant ($P<0.05$) decrease of transpiration coefficients between the initial (after 3 d) and final (after 57 d) storage times for the intermediate and large stem parts only (Table 3). The no packaging treatment (i.e. direct exposure to cold air) and 36 x 4 mm perforation liner film also resulted in a significantly high ($P<0.05$) transpiration coefficients of grape berries over the storage period. There were no significant differences in transpiration coefficients over storage period of stem parts and berries stored inside 120x2 mm and non-perforation liner films. The decline in transpiration coefficients with cold storage time may be ascribed to the phenomenon described by Fockens and Meffert, (1972). Fockens and Meffert (1972) found that when the relative humidity of the air around the fruit is high, the skin cells of the fruit remain turgid (swollen) causing the intercellular spaces to be larger and resulting in low diffusion resistance; and when the relative humidity of the air is low, skin cells are flattened causing the intercellular spaces to become smaller and thus increasing the diffusion resistance. Applying this explanation to the results obtained in this study, the high transpiration coefficient of grape parts in the initial stages of storage observed in the no

packaging and 36x4 mm perforated liner film treatments may have been due to high initial diffusion rate from the cells to the surrounding air as a result of the convective effect of the circulating air in the cold room and vapour pressure differences. As these cells lost moisture to the surrounding air, they became flatter thereby increasing their diffusion resistance as the storage period progresses. Another possibility for the high transpiration coefficient of grape berries could be that, instead of a decreasing permeability, the permeability remained constant while the vapour pressure of the berry surface decreases because of the dehydration and corresponding increase in soluble solids.

The results (Table 3) also showed that the transpiration coefficients of the bunch parts stored in a non-perforated liner film treatment were lowest in comparison to the other treatments indicating that this treatment may be a good moisture barrier.

Conclusion

The moisture loss of the fresh grape bunches studied suggests that the stem part of the bunch loses moisture more rapidly compared to the berries. After 75 d of cold storage the maximum weight loss of berries was less than 10 %, while the maximum weight loss of stems was in the range of 49.24 ± 4.66 % (non-perforated liner films) to 88.55 ± 0.61 (with no packaging treatment). The smaller the size of the stem (i.e. the higher the surface area to volume ratio), the greater the rate of moisture loss became.

The use of non-perforated liner films significantly reduced the rate of moisture loss from the grape bunches and its parts compared to the perforated liner films and no packaging treatments during cold storage. This corresponded to the transpiration rate results, where the transpiration rates were lower in non-perforated liners than the other packaging treatments and this may have been due to the lower V_{pd} and no air circulation inside the non-perforated liner film.

The transpiration coefficients of the different stem parts and the berries stored in a no packaging treatment decreased significantly with storage period, while the 36 x 4 mm perforation resulted in significant decrease in transpiration coefficients over the storage period for the intermediate, large stem parts and berries. There were no significant decreases of transpiration coefficients for the parts stored in 120 x 2 mm and non-perforated liner films.

References

Becker B.R., Misra A., Fricke B.A. 1995. Bulk refrigeration of fruits and vegetables, Part I: Theoretical considerations of heat and mass transfer. University of Missouri-Kansas City, USA

Crisosto C. H., Smilanick J. L., Dokoozlian N.K. 2001. Table grapes suffer water loss, stem browning during cooling delays. California Agric. 55 (1), 39 – 42.

Delele MA, Schenk A, Tijskens E, Ramon H, Nicolaï BM & Verboven P (2009). Optimization of the humidification of cold stores by pressurized water atomizers based on a multiscale CFD model. J. Food Eng. 91(2), 228-239.

Fockens F.H., Meffert H.F.Th. 1972. Biophysical properties of horticultural products as related to loss of moisture during cooling down. J. Sci. Food Agric. 23, 285-298.

García-Perez J.V., Blasco M., Cárcel J.A., Clemente G., Mulet A. 2006. Drying kinetics of grapes stalk. Difect and Diffusion Forum. (258-260), 225-230.

Lecas M., Brillouet Jean-Marc. 1994. Cell wall composition of grape berry skins. Phytochem. 35 (5), 1241-1243.

Margaris D.P., Ghiaus A.G. 2007. Experimental study of hot air dehydration of Sultana grapes. J. Food Eng. 79, 1115-1121.

Nelson K.E. 1978. Pre-cooling – its significance to the market quality of table grapes. Int. J. Refrig. 1 (4), 207 – 215.

Ngcobo M.E.K, Opara U.L., Thiart G.D. 2012. Effects of packaging liners on cooling rate and quality attributes of table grape (cv. Regal seedless*).* Packag. Technol. Sci. 25(2), 73-84.

Nguyen TA, Verboven P, Schenk A & Nicolaï BM (2007). Prediction of water loss from pears (*Pyrus communis* cv. Conference) during controlled atmosphere storage as affected by relative humidity. J. Food Eng. 83, 149-155.

Sastry S.K., Buffington D.E. 1983. Transpiration rates of stored perishable commodities: a mathematical model and experiments on tomatoes. Int. J. Refrig. 6 (2), 84-96.

Sastry S.K. 1985. Moisture losses from perishable commodities: recent research and developments. Int. J. Refrig. 8, 343-346.

Thompson J.F., Mitchell F.G., Rumsey T.R., Kasmire R.F., Crisosto C.H. 1998. Commercial Cooling of Fruits, Vegetables, and Flowers. Regents of the University of California. USA.

Veraverbeke E.A., Verboven P., Scheerlinck N., Hoang M.L., Nicolaï B.M. 2003. Determination of the diffusion coefficient of tissue, cuticle, cutin and wax apple. J. Food Eng. 58, 285-294.

Table 1: Mean (± SD) temperature and RH profiles inside the cold room and packaging liner films

Packaging	Mean Temperatures (°C)	Mean Air RH (%)
No packaging	1.21 ± 0.25	89.06 ± 2.63
Non perforated liner film	1.79 ± 0.26	92.38 ± 4.81
120 x 2 mm perforated liner film	1.38 ± 0.28	89.32 ± 4.35
36 x4 mm perforated liner film	1.34 ± 0.24	88.54 ± 3.55

Table 2: Mean transpiration rate of grape bunch parts during postharvest storage in different packaging liner films

		Mean (±SD) transpiration rate of the different parts of the grape bunch, g kg^{-1} d^{-1}				
Packaging	Vapour pressure deficit (Pa)	Berries: stem attachment sphere	Small cylinders	Intermediate cylinders	Large cylinders	Berries
No packaging	72.957	89.08 ± 89.08	76.09 ± 93.65	87.70 ± 83.85	25.95 ± 26.88	1.57 ± 0.58
Non perforated liner film	52.994	35.37 ± 20.36	33.96 ± 15.57	12.76 ± 11.46	7.03 ± 5.70	0.79 ± 0.51
120x2 mm perforated liner film	72.129	65.78 ± 35.89	61.19 ± 28.28	21.79 ± 17.10	19.94 ± 1 4.43	1.59 ± 0.75
36x4mm perforated liner film	77.194	56.16 ± 24.49	52.57 ± 23.76	23.79 ± 18.84	13.19 ± 9 .66	1.37 ± 1.00

Table 3: Overall mean (±SD) transpiration coefficient (k_{ta}) of the grape bunch parts during postharvest storage in different packaging liner films

Packaging treatment	Days in storage	k_{ta}, (g kg^{-1} d^{-1} Pa^{-1})				
		Berries: stem attachment sphere	Small cylinders	Intermediate cylinders	Large cylinders	Berries
No packaging						
	3	2.42 ± 1.94	2.32 ± 1.13	1.37 ± 0.34	0.90 ± 0.37	0.03 ± 0.01
	9	0.02 ± 0.02	0.16 ± 0.13	0.52 ± 0.18	0.35 ± 0.12	0.02 ± 0.01
	57			0.06 ± 0.07	0.08 ± 0.08	0.02 ± 0.00
Non-perforated liner film						
	3	0.98 ± 0.47	0.84 ± 0.33	0.45 ± 0.32	0.24 ± 0.14	0.02 ± 0.01
	9	0.51 ± 0.24	0.51 ± 0.19	0.26 ± 0.17	0.16 ± 0.08	0.02 ± 0.01
	57			0.11 ± 0.03	0.05 ± 0.02	0.01 ± 0.00
120x2 mm perforation liner film						
	3	1.38 ± 0.36	1.04 ± 0.44	0.46 ± 0.22	0.36 ± 0.25	0.02 ± 0.01
	9	0.60 ± 0.27	0.72 ± 0.33	0.38 ± 0.28	0.39 ± 0.18	0.02 ± 0.01
	57			0.14 ± 0.09	0.13 ± 0.06	0.02 ± 0.00
36x4 mm perforated liner film						
	3	0.85 ± 0.33	0.86 ± 0.24	0.51 ± 0.19	0.32 ± 0.10	0.03 ± 0.01
	9	0.64 ± 0.31	0.56 ± 0.31	0.39 ± 0.27	0.22 ± 0.13	0.02 ± 0.02
	57			0.12 ± 0.08	0.14 ± 0.02	0.01 ± 0.00

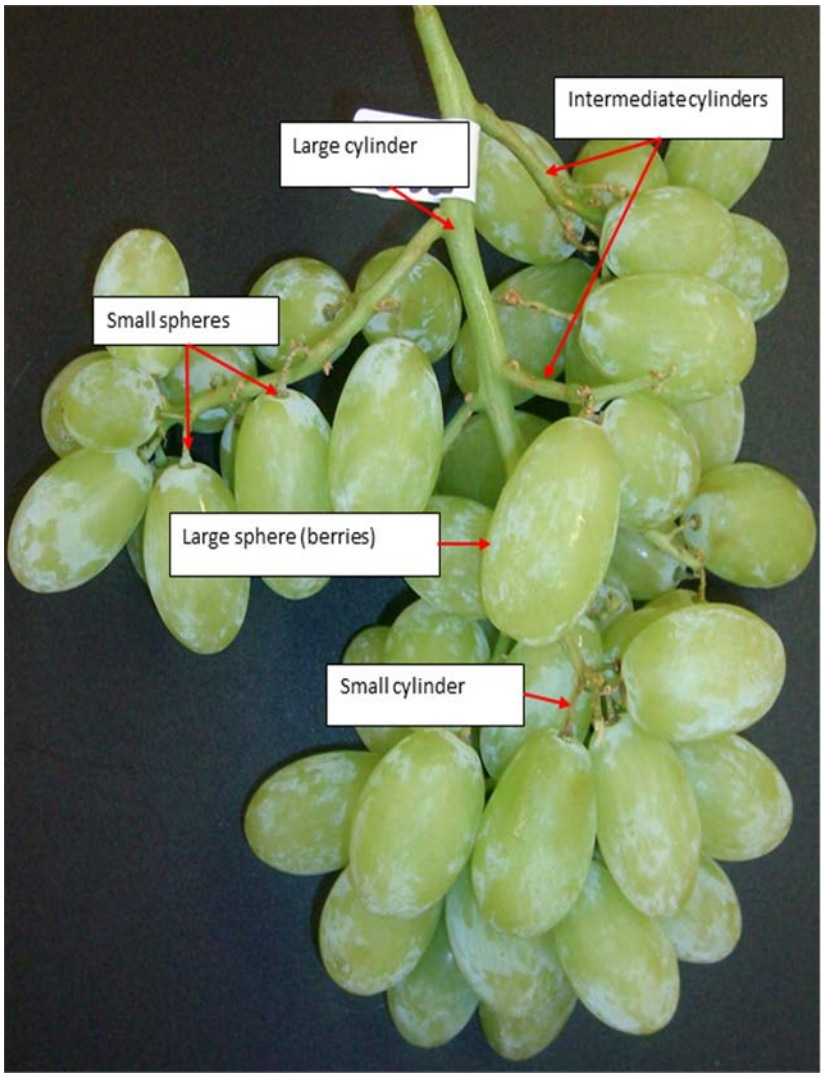

Figure 1: Parts of the bunch considered to study the mass transfer kinetics of grapes during postharvest storage.

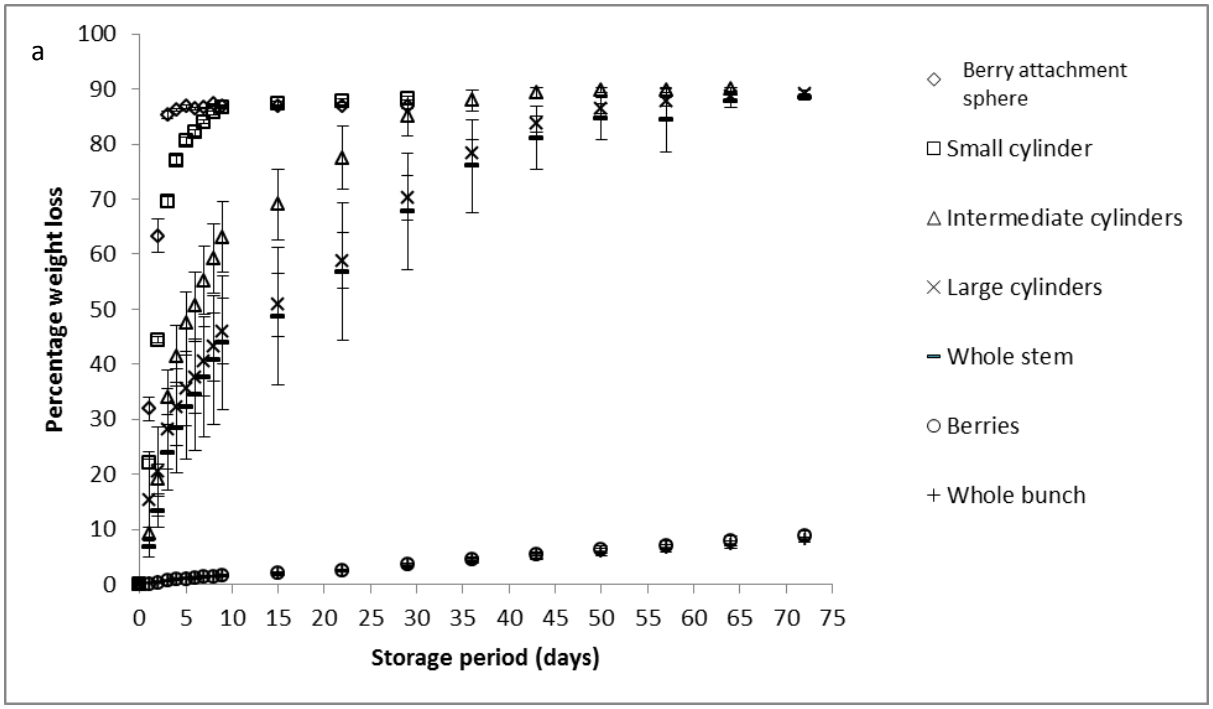

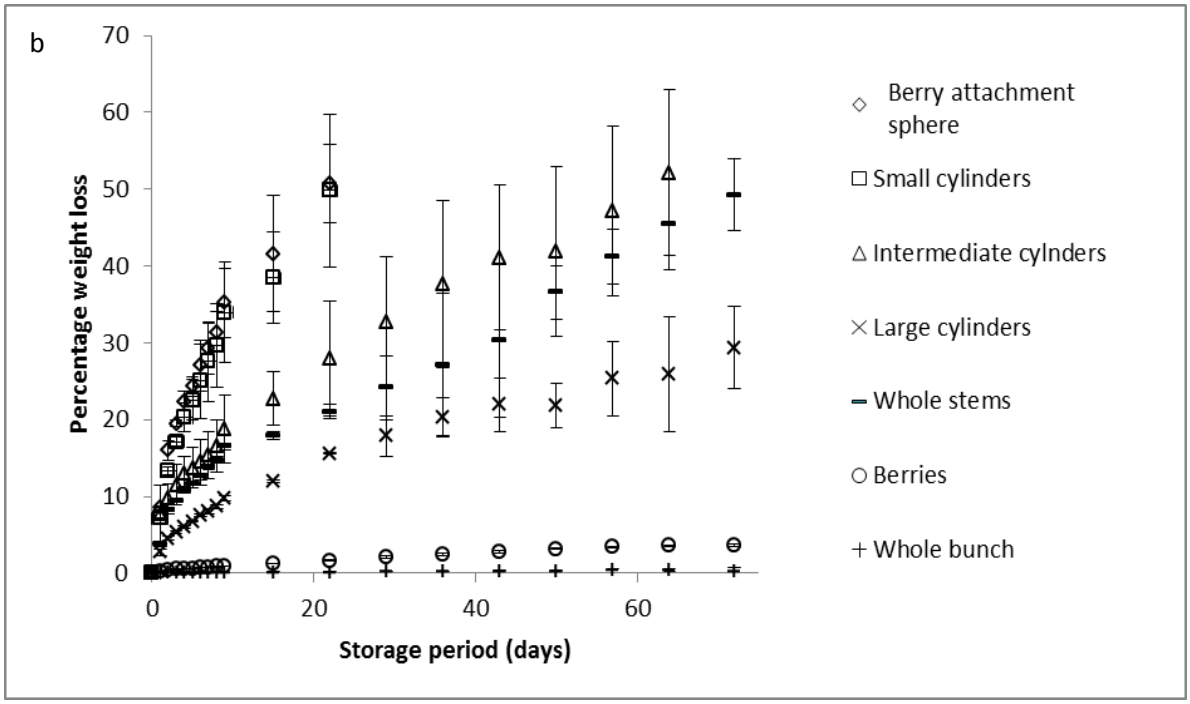

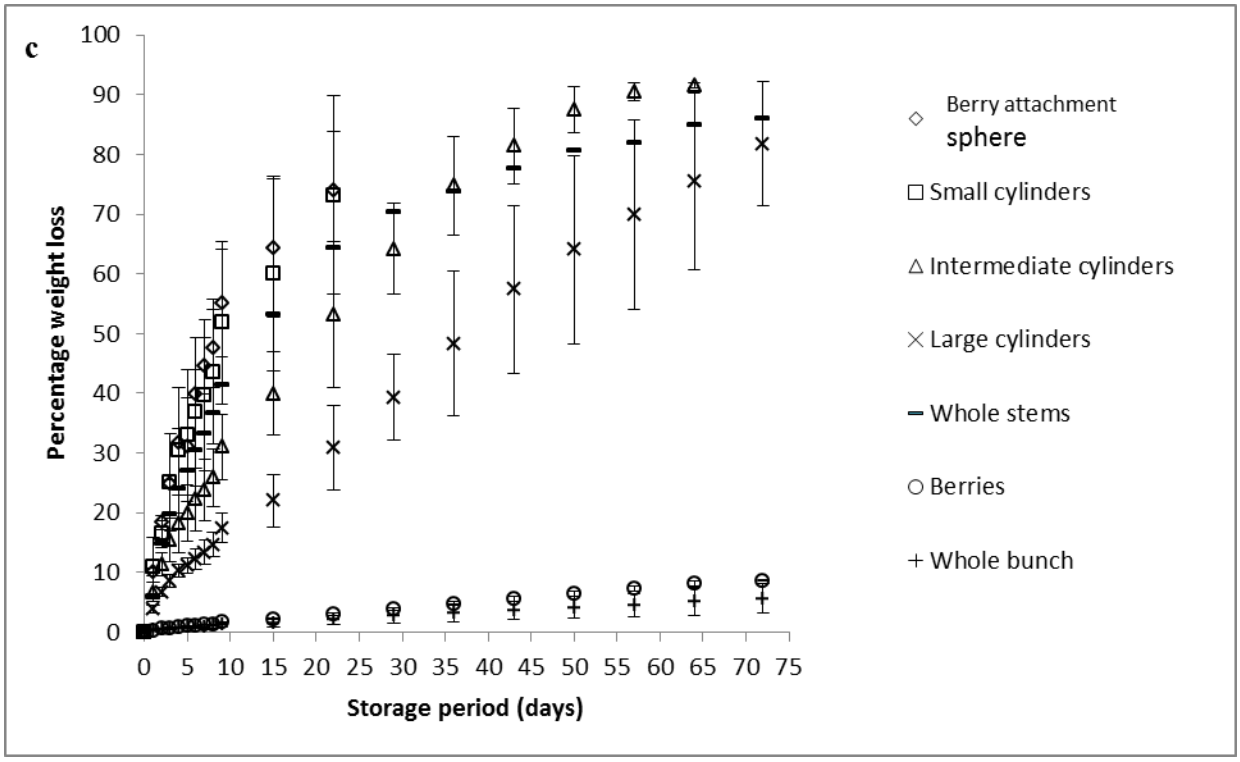

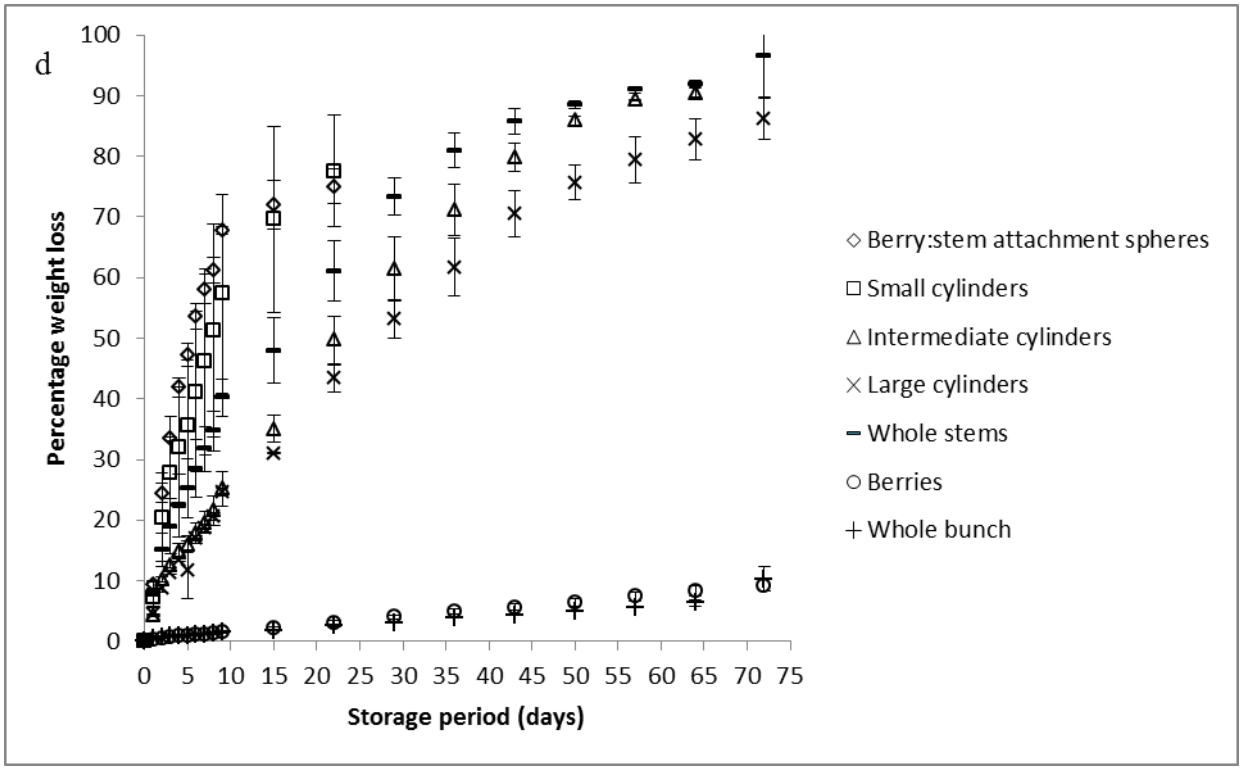

Figure 2: Moisture loss kinetics of grape bunches packed in different packaging treatments during the cold storage period. (a) no packaging; (b) non-perforated liner film; (c) 36x4 mm perforated liner film; (d) 120x2 mm perforated liner film. Error bars represent the standard deviation of the mean.

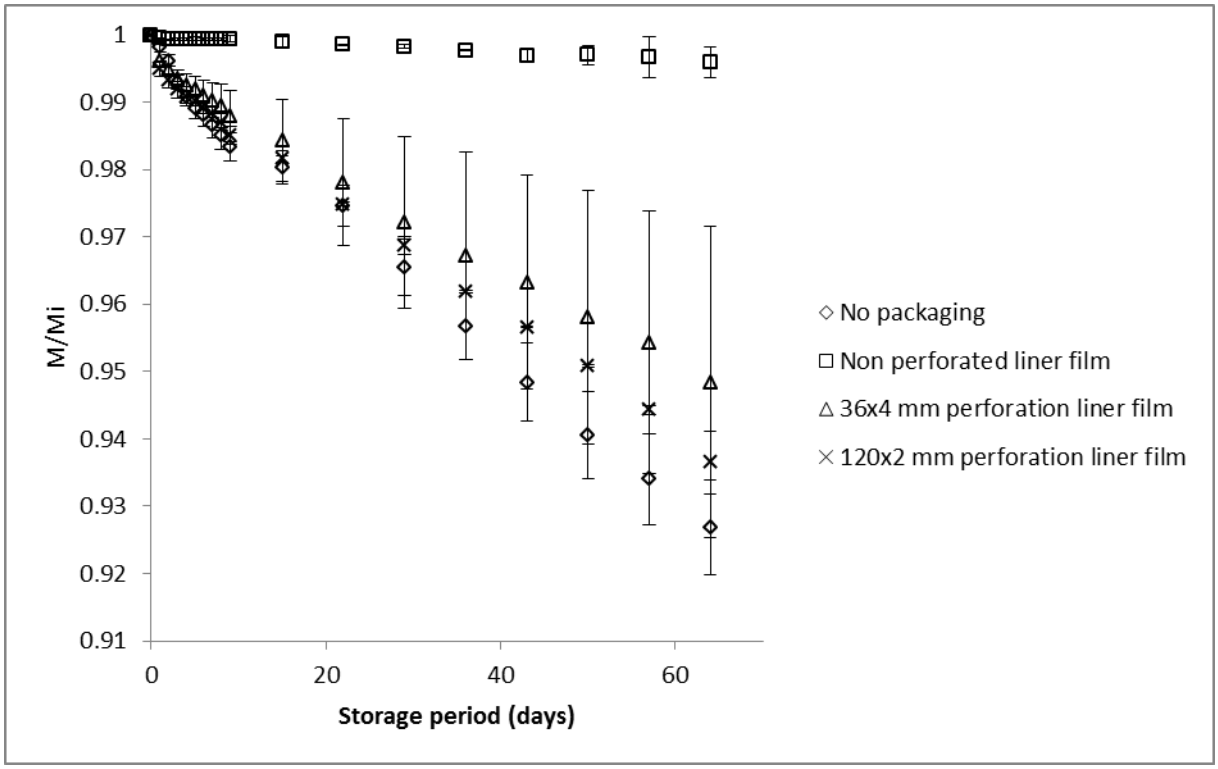

Figure 3: Changes in the mass of grape bunches (M, g) over time in cold storage. The values were normalised with respect to the initial mass of grapes (M_i, g). Error bars represent the standard deviation of the mean.

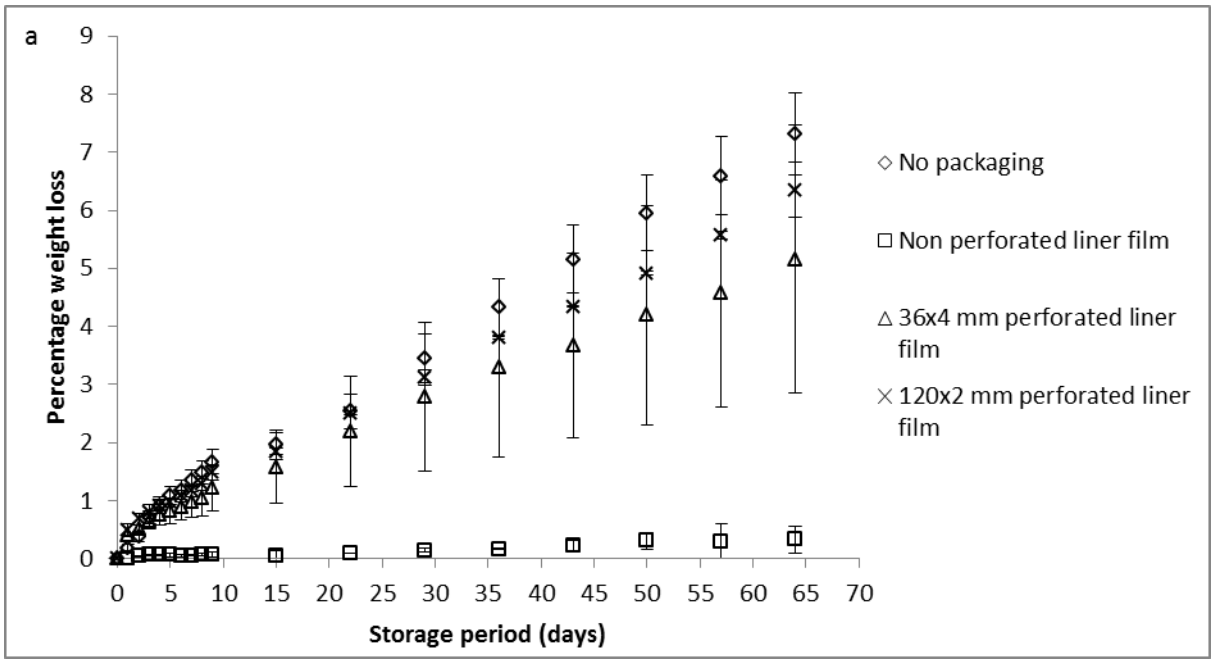

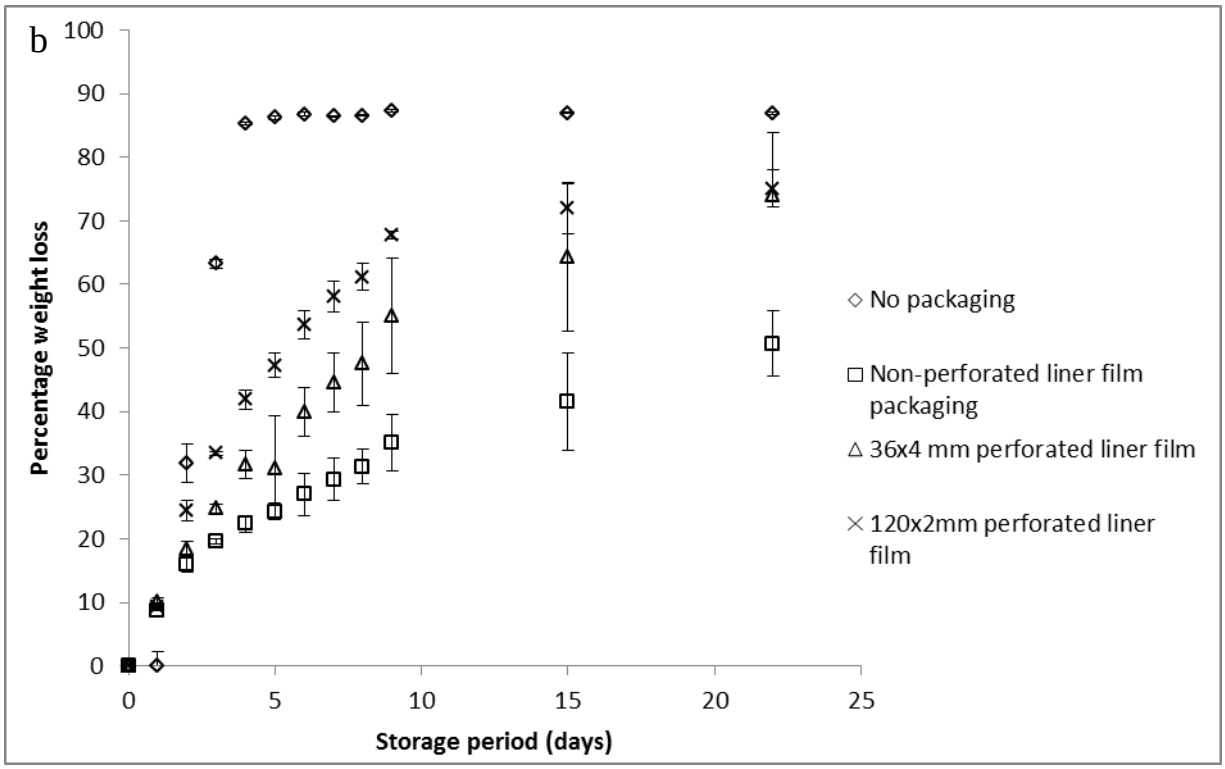

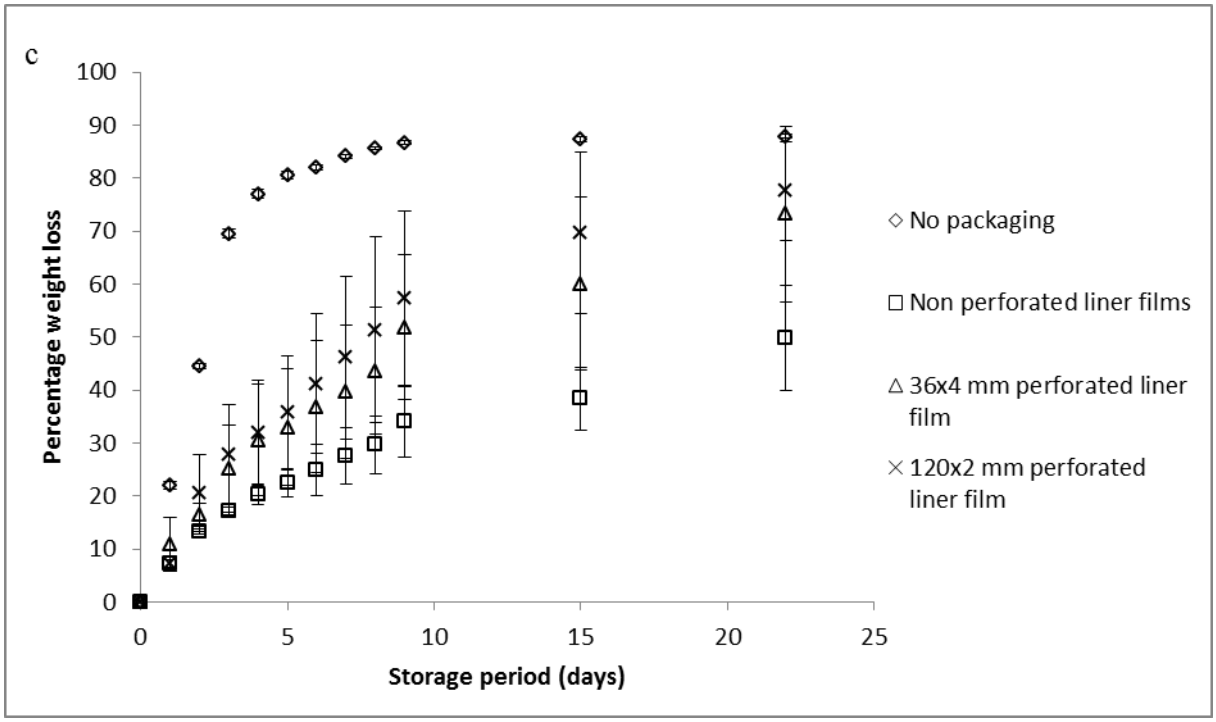

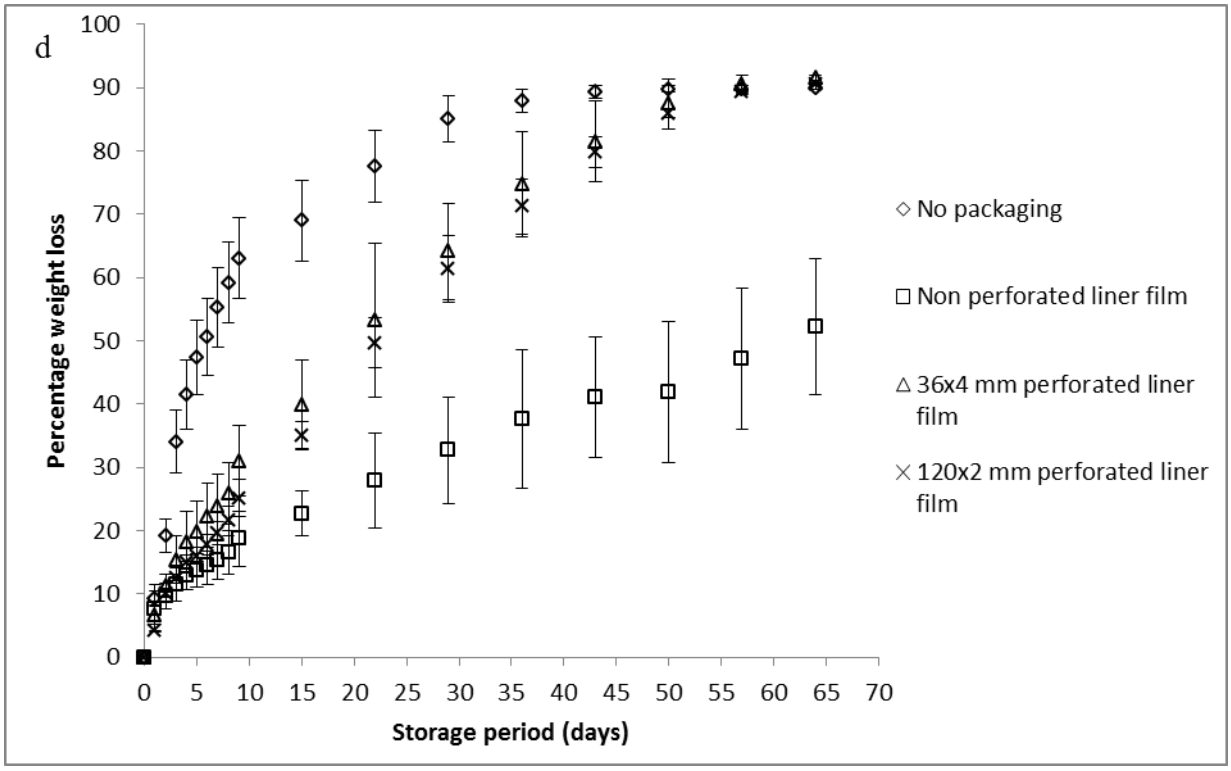

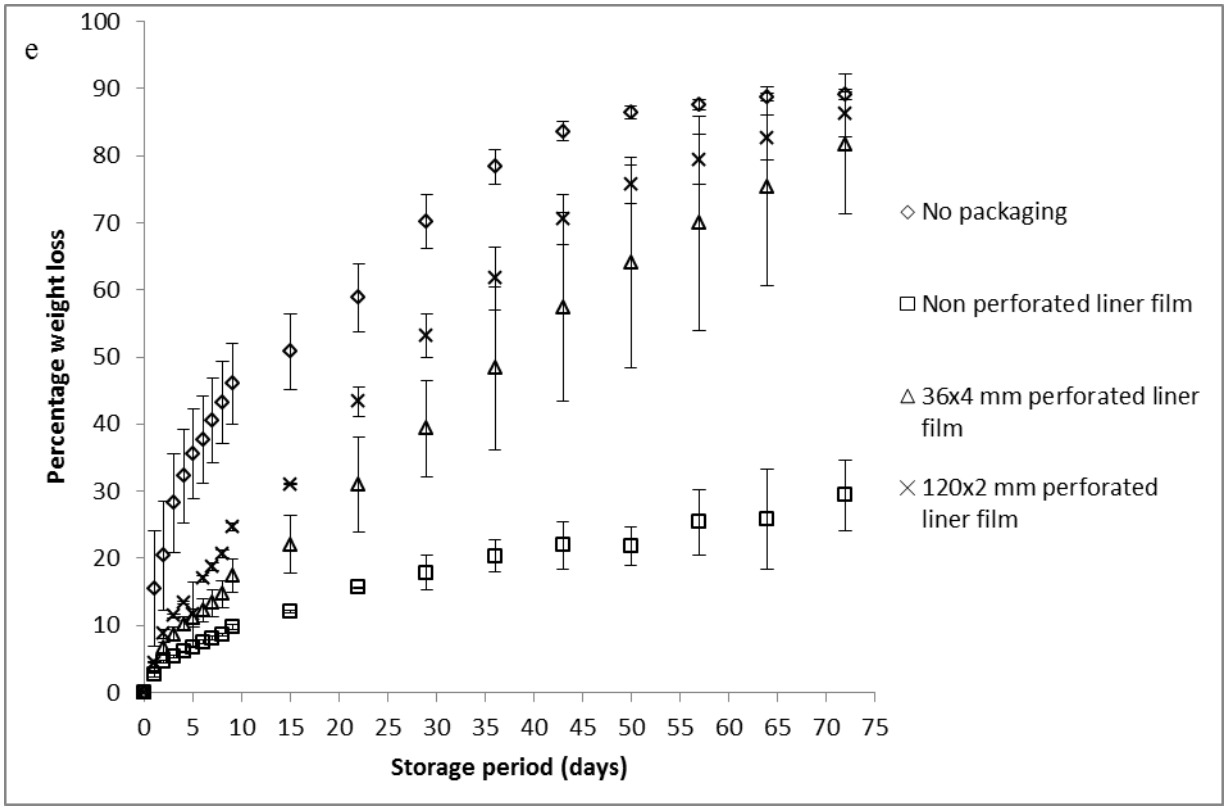

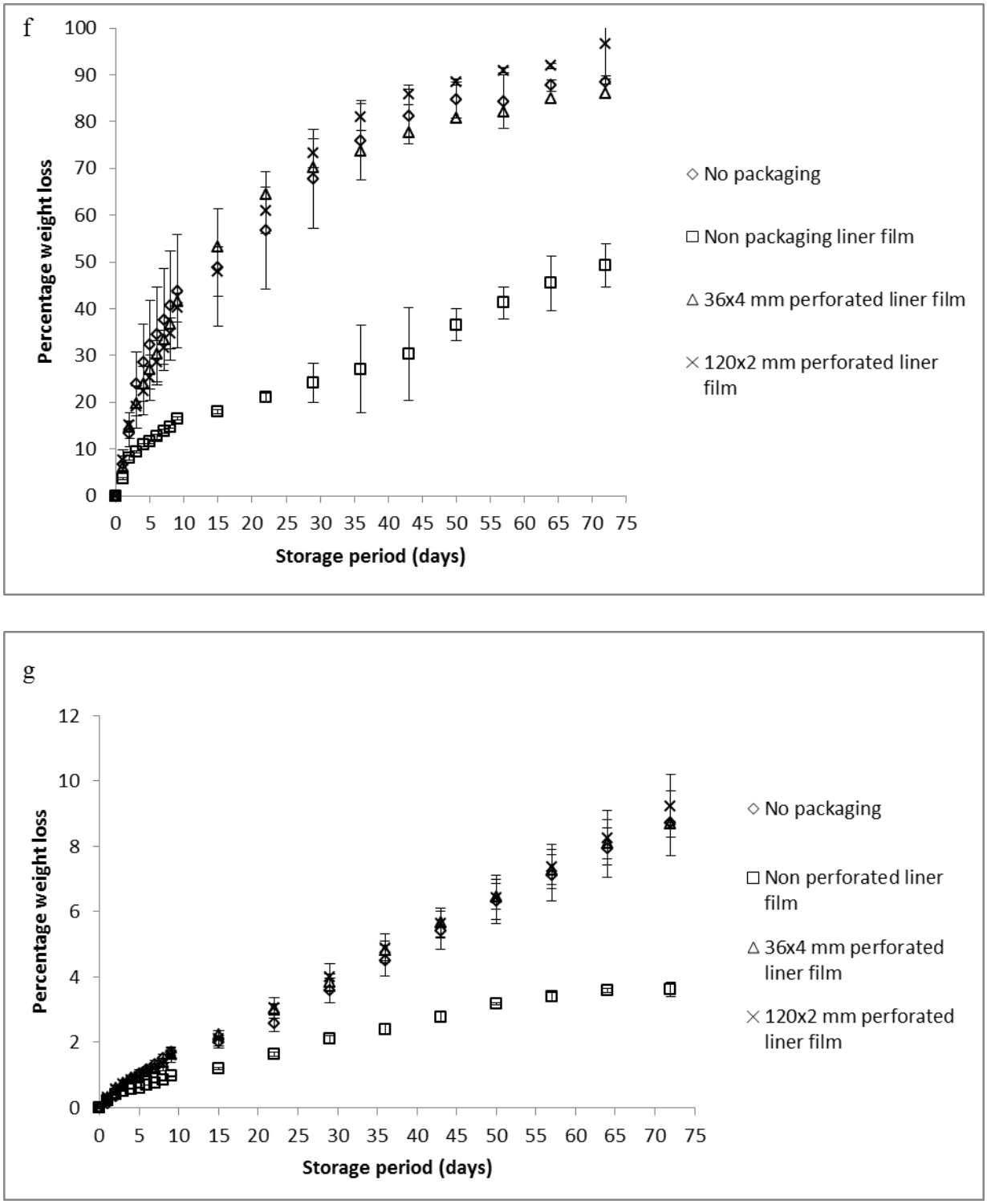

Figure 4: Percentage moisture loss from different parts of grape bunches in different packaging treatments during cold storage period (a) whole stem; (b) berry: stem attachment spheres; (c) small cylinders of the stems; (d) intermediate cylinders of the stems; (e) large cylinders of the stems; (f) whole stems; (g) grape berries. Error bars represent the standard deviation of the mean

Figure 5: Appearance of stems taken from the different packaging treatments after 80 days in cold storage.

PAPER 5

Moisture diffusivity of table grape stems during low temperature storage conditions

Abstract

Moisture diffusivity of grapes stems was studied under cold airflow storage conditions (1.21 ± 0.25 °C and 1.18 ± 0.23 ms^{-1}) during postharvest storage. The stems were stored without packaging liner films or with packaging liners (packed in non-perforated liner films) under low temperature conditions inside a cold room. Effective moisture diffusivity values for stem parts packed in non-perforated liner films were lower than the values obtained for stem parts stored without packaging liners, and varied from $5.06x10^{-14}$ – $1.05x10^{-13}$ m^2s^{-1}. Dehydration rate of stem parts directly exposed (without liners) to circulating cold air was significantly ($P<0.05$) higher than the dehydration rates of stem parts packed in non-perforated liner film. Empirical models were applied to describe the dehydration kinetics of the different parts of the stem.

Keywords: Grape stems; cold storage; non perforated liner film; dehydration; effective diffusivity; vapour pressure.

Nomenclature

a_0, a	a coefficient of drying models
$Deff$	effective moisture diffusivity, m^2s^{-1}
DR	drying rate, kg water/kg dry matter h^{-1}
e_s	standard error
k	drying coefficient
M	moisture content, kg water/kg dry matter

M_0	initial moisture content, kg water/kg dry matter
M_e	equilibrium moisture content, kg water/kg dry
MR	dimensionless moisture ratio
N	number of observations
n	exponential coefficient of Page's Eq.
R	radius of cylinder, m
r^2	coefficient of determination
t	time, s
λ	roots of Bessel function
χ^2	mean square of the deviation

1. Introduction

The stems of a grape bunch play a pivotal role in the overall appearance of a bunch, while acting as a handle for the consumer when they eat the fruit. However, during cooling and cold storage of fresh grapes, there is a simultaneous dehydration of stems, thus negatively affecting the postharvest quality of grapes (Ngcobo et al., 2012a, b). The water content in plants varies according to species, tissue and cell type and is also dependent on ambient and physiological conditions (Merva, 1995). The process of stem dehydration involves shriveling of the stem, which usually becomes brittle and break easily and this is followed by severe stages of dehydration where the stems start turning brown (Nelson, 1978). The dehydration of stems during long-term cold storage is an undesirable quality problem. However, there is a lack of information on the dehydration kinetics of fresh grape stems during prolonged storage periods and handling at low temperatures. The knowledge of the stem dehydration kinetics and its prediction models may assist in better managing postharvest quality of table grapes in the value chain.

Dehydration is characterised by complex moisture movements within the products and is largely dependent on surrounding conditions, as well as on heat and mass transfer properties of the product such as thermal conductivity, thermal and moisture diffusivity, interface heat and mass transfer coefficients (Margaris and Ghiaus; 2007; Thompson et al., 1998; Veraverbeke *et al.*, 2003). Effective moisture diffusivity describes all possible mechanisms of

moisture movement within the foods, such as liquid diffusion, vapour diffusion, surface diffusion, capillary flow and hydrodynamic flow (Pathare and Sharma, 2006, Kim & Blowmilk, 1995). A knowledge of effective moisture diffusivity is necessary for understanding and modelling mass transfer processes such as dehydration, adsorption and desorption of moisture during storage (Pathare and Sharma, 2006). Moisture transport in fruit has been modelled by means of Fick's second law of diffusion. Three mechanisms are often considered most dominant in foods in general: convection (Darcy flow), molecular diffusion and capillary diffusion (Datta & Zhang, 1999). The continuum approach to mass transfer is the simplest means to describe moisture diffusion in fruit tissue because it avoids the necessity of modelling the microscopic pore space. It constitutes a phenomenological approach as the mass transfer coefficients that appear in the macroscopic balances have to be determined experimentally. The macro-scale addresses the fruit as a whole and at this scale the fruit is considered as a continuum, and may consist of different connected tissues, all with homogeneous properties (Ho et al., 2006).

The stems of grapes are complex structures and therefore the dehydration kinetics of stems in cold storage should accommodate the different structures that make up the grape stem. No work has been reported on moisture diffusivity and dehydration of whole table grape stems in multi-scale packages during low temperature storage of table grapes. Several studies have reported on drying of grape berries (Azzouz et al., 2002; Cağlar et al., 2009; Cakmak and Yildiz, 2011; Doymaz, 2006; Fadhel et al., 2005; Margaris and Ghiaus, 2007; Ramos et al., 2010; Xiao et al., 2010) and stems (Garcia-Perez et al., 2006, Garcia-Perez et al., 2010). However, these studies were conducted under high temperature conditions. In literature, Lichter et al., (2011) studied the effects of water vapour pressure deficit under ambient conditions of 20°C or 10°C on the physical and visual properties of grape stems due to water loss. Given that table grapes suffer moisture loss and dehydration of stems during low temperature storage, even low (1 %) moisture loss manifests in significant quality losses of grapes (Nelson, 1978; Ngcobo et al., 2012a).

The objective of this study was therefore to investigate moisture diffusivity and dehydration characteristics of table grape stems during low temperature storage conditions. In addition, empirical models were applied to describe dehydration kinetics of the different parts of the stem.

2. Theory: Effective moisture diffusivity and dehydration

Fick's second law of diffusion was used to describe the transport of moisture from the stems (Crank, 1975). The moisture diffusivity is used to indicate the flow of moisture within a material. Moisture diffusivity is influenced mainly by moisture content and temperature of the material (Pathare and Sharma, 2006). To study the moisture diffusivity of stems, the complex structure was divided into 3 kinds of cylinders with different sizes and one sphere (berry and stem binding part), as per Garcia-Perez et al. (2006). The moisture diffusivity of an infinite sphere and cylinder were therefore calculated by the following equations 1 and 2 respectively (Crank; 1975) and taking the following assumptions into consideration (Garcia-Perez et al., 2006).

(i) The initial moisture and temperature are uniform inside the solid;
(ii) The surface is at equilibrium with the drying air;
(iii) Shrinkage is negligible
(iv) Solid symmetry
(v) There is only one material

$$M_R = \frac{M_t - M_e}{M_0 - M_e} = \frac{6}{\pi^2}\sum_{n=1}^{\infty}\frac{1}{n^2}\exp\left(-n^2\frac{\pi^2 D_{eff}\,t}{R^2}\right) \quad (1)$$

$$M_R = \frac{M_t - M_e}{M_0 - M_e} = \sum_{n=1}^{\infty}\frac{4}{\lambda_n^2}\exp\left(-\frac{\lambda_n^2 D_{eff}\,t}{R^2}\right) \quad (2)$$

Where D_{eff} is the effective moisture diffusivity in m^2s^{-1}; R is the radius of a cylinder and sphere in m. λ_n in (Eq. 2) are the roots of Bessel function (2.405, 5.520, 8.654,…) of zero order $J_0(r) = 0$. For $n > 1$, the second order and subsequent terms of the above equation become negligible (Sharma and Prasad, 2004). Thus, λ_1 is equal to 2.405 for Eq. (2).

The average moisture content for thin layer drying is presented by the following equation (3), (Jain and Pathare, 2007; Doymaz 2011):

$$M_R = \frac{M_t - M_e}{M_0 - M_e} \tag{3}$$

where M_e is the dynamic equilibrium moisture content in kg $[H_2O]kg^{-1}[DM]$; M_0 is the initial moisture content in $kg[H_2O]kg^{-1}$ [DM]; M_t is the initial moisture content in kg $[H_2O]kg^{-1}[DM]$ at time t in s and M_R is the dimensionless moisture ratio.

The equilibrium moisture content was determined using an indirect method described by Jain and Pathare (2004), where the rate of change of moisture content $\left(-dM/dt\right)$ was plotted against the average moisture content. The equilibrium moisture content was inferred from the intercept by extrapolating the plot to the point at which the rate of change of moisture content was zero.

Equations (1) and (2) can be further simplified to only the first term of the series, for long periods of dehydration. Eqs. (1) and (2) are written in a logarithmic form as follows:

$$\ln M_R = \ln\left(\frac{6}{\pi^2}\right) - \left(\frac{\pi^2 D_{eff} t}{R^2}\right) \tag{4}$$

$$\ln M_R = \ln\left(\frac{4}{\lambda_1^2}\right) - \left(\frac{\lambda_n^2 D_{eff} t}{R^2}\right) \tag{5}$$

The effective moisture diffusivity was calculated from a slope of a straight line by plotting data in terms of $\ln M_R$ *versus* drying time, which gives a straight line with a slope in which (Doymaz, 2006; 2011):

Sphere:

$$Slope_1 = \frac{\pi^2 D_{eff}}{R^2} \tag{6}$$

Cylinder:

$$Slope_2 = \frac{\lambda_1^2 D_{eff}}{R^2} \tag{7}$$

The moisture removal rate from grapes was expressed as the amount of evaporated moisture over time and was calculated using Eq. (8)

$$DR = \frac{M_{t1} - M_{t2}}{t_2 - t_1} \quad (8)$$

Where t_1 and t_2 are drying times (h); M_{t1} and M_{t2} are moisture content of samples (kg water/kg dry matter) at time t_1 and t_2 respectively (Doymaz; 2011). The moisture ratio data obtained were fitted to four thin-layer drying models detailed in Table 1. The best fitting model is determines by the coefficient of determination (R^2) and low standard error (e_s) is one of the primary criteria for selecting the best model to define the drying curves.

3. Materials and Methods

3.1. Plant material

The grapes were harvested, prepared and packed from a farm in the Worcester area of Cape Town, South Africa and were transported in an air-conditioned car to the Postharvest Technology Research Laboratory at Stellenbosch University. In the laboratory the stems were considered as the composition of 3 kinds of cylinders (Garcia-Perez et al., 2006) and one sphere (Fig. 1). The 3 cylinders make up the stem part and the sphere is the cap-like structure binding the stem and berries. The average diameter of each of the individual parts was measured: spheres (2.55 ± 0.27 mm); small cylinders (1.53 ± 0.20 mm); intermediate cylinders (2.85 ± 0.70 mm); and large cylinders (4.88 ± 1.03 mm).

3.2. Experimental procedure

Figure 2 shows a schematic representation of the experimental setup. An initial mass of spheres, small cylinders, intermediate cylinders and large cylinders (5 ± 0.00 g; 5 ± 0.00 g; 10.03 ± 0.02 g and 20.33 ± 0.37 g, respectively) was prepared and replicated three times per packaging treatment. The packaging treatments included: no packaging (samples stored without liner films and exposed to low temperature airflow conditions) and non-perforated (LDPE) liner film (0 airflow treatments). All the samples were weighed using a scale (Mettler, Toledo, Switzerland, with an accuracy of 0.01 g) to get the initial mass and then stored under low temperature conditions of 1.21 ± 0.25°C and 1.18 ± 0.23 ms^{-1} (airflow) in an

experimental cold room in the Postharvest Technology Research Laboratory. The weight of each sample was measured daily for the first 14 days (due to rapid dehydration of smaller size stem parts) and thereafter every seven days (due to a slow dehydration process of larger parts of the stems) for the remainder of storage period, in order to monitor weight loss rate during cold air storage. At the end of the storage period all the samples were dried at 75°C for 4 days in order to obtain the dry weight of individual parts for the calculation of the actual moisture content.

To calculate the moisture content of a sample, the dry weight was subtracted from the initial wet weight of each sample. The dimensionless moisture ratio was calculated as per equation (3) from the determined initial moisture content and average moisture content. Moisture removal (dehydration) rate was calculated as the difference in average moisture content between time intervals divided by the time difference between two measuring points.

Air temperature and relative humidity were measured inside the storage room and inside the liner film containing stems. Air temperature was measured with a LogTag air temperature recorder (LogTag Trix-8 Temperature Recorder, LogTag Recorder Limited, China) and the air relative humidity (%RH) was measured with a SENSITECH TempTale 4 monitor (Temptale4 Humidity and Ambient Temperature 16000, SensiTech, USA).

4. Results and Discussion

4.1. Effective moisture diffusivity

The results of effective diffusivity $\left(D_{eff}\right)$ of stem parts under the different storage conditions are summarized in Table 2. The effective moisture diffusivity values (1.66×10^{-13} $m^2 s^{-1}$; 5.06×10^{-14} $m^2 s^{-1}$; 1.05×10^{-13} $m^2 s^{-1}$; 3.09×10^{-13} $m^2 s^{-1}$) for stem parts (sphere; small cylinder; intermediate cylinder; large cylinder respectively) packed in non-perforated liner films were lower than the values (1.49×10^{-12} $m^2 s^{-1}$; 4.05×10^{-13} $m^2 s^{-1}$; 3.16×10^{-13} $m^2 s^{-1}$; 6.18×10^{-13}

$m^2 s^{-1}$ respectively) obtained from the cold air circulation treatment. This can be ascribed to the absence of the convective effect of airflow inside the liner films.

In comparison to the results obtained by García-Perez et al. (2006) under hot air drying, the diffusivity values of stem parts (sphere; small cylinder; intermediate cylinder; large cylinder) exposed to cold air circulating conditions were lower (1.49×10^{-12} $m^2 s^{-1}$; 4.05×10^{-1} $m^2 s^{-1}$ [3]; 3.16×10^{-13} $m^2 s^{-1}$; 6.18×10^{-13} $m^2 s^{-1}$ respectively) than the values they found on their hot-air drying studies (3.92×10^{-8} $m^2 s^{-1}$; 1.07×10^{-11} $m^2 s^{-1}$; 1.38×10^{-11} $m^2 s^{-1}$; 1.78×10^{-11} $m^2 s^{-1}$ respectively), (Table 4). However, all the diffusivity values obtained in the current study for the stem parts under cold air storage conditions were within the range of 10^{-15} -10^{-8} $m^2 s^{-1}$, reported in literature of similar studies (Veraverbeke et al., 2003 and Garcia-Perez et al., 2006). The observed difference of diffusivity value between the cold air storage conditions and hot-air conditions may have been due to the higher convective nature of the hot-air than that of cold air.

The results in this study follow similar trends as results reported in literature and were obtained using a macro-scale approach. The macro-scale considers the stem as a whole and at this scale the stem is considered as a continuum, and may consist of different connected tissues, all with homogeneous properties (Ho et al., 2006). However, an in-depth microstructural study would also be beneficial in order to comprehensively understand cellular changes associated with moisture diffusivity from stems (Vega-Gálvez et al., 2012; Ramírez et al., 2011).

4.2. Dehydration of stems during cold storage

The dehydration rate of the different parts of the stems under cold air storage conditions are shown in Figure 3a and b. The drying curves (Fig 3a and b) indicate that airflow plays a big role in stem dehydration under cold storage conditions as it significantly increased the dehydration rates of stems and its parts (Fig. 3a) compared to the lower dehydration rates of stems and its parts inside non perforated liner films (no airflow) (Fig. 3b). The rapid dehydration rate observed in Figure 3a may have been due to the convective nature of the

circulating air, while natural diffusion driven by vapour pressure difference in Figure 3b, may have resulted in a slow dehydration rate. Although stems and its parts were completely dehydrated under cold air storage conditions (1.21 ± 0.25 °C and 1.18 ± 0.23 ms^{-1}), it took a significantly longer time to dehydrate them, than it would normally take under hot air ambient conditions such as the 40° C and 2 ms^{-1} conditions that were used by Garcia-Perez et al. (2006). It took 3 days under cold air storage conditions to reach approximately the same moisture content that Garcia-Perez et al. (2006) achieved in 5.6 hours of drying time for the spheres. These results strongly emphasises the importance of low temperature storage conditions in reducing the rate of stem dehydration.

The results (Figure 3a and b) also indicated that the dehydration rate of the different parts of the stems is inversely proportional to the size (diameter) of the stem parts. These results are in agreement with the results obtained by Garcia-Perez et al. (2006), where they reported that the drying rate of stem parts increased as the cylinder gets smaller.

The moisture removal data obtained from the experiments were fitted by four thin-layer drying models mentioned in Table 1. All four models showed the high coefficient of determination $\left(r^2 > 0.980\right)$ and low standard errors, e_s (Table 3) indicating that they all fitted the moisture ratio data well. The small and intermediate cylinders showed the highest coefficient of determination ($r^2 > 0.99$) for all models whereas the large cylinder showed lower values ($r^2 < 0.99$), but still above 0.98. There was no single model that generally outperformed other 3 models in all cases in predicting drying of the different parts of the grape stem".

The four models were also tested for the prediction of whole stem drying under cold airflow and non-perforated liner film (no airflow) conditions. The results (Table 4) indicate that the Henderson and Pabis model appears to be the best fitted model in predicting dehydration of stems in different storage conditions (no packaging and non-perforated liner film). This was based on the fact that this model maintained high values for the coefficient of determination $\left(r^2\right)$ and low values of standard error $\left(e_s\right)$ in both drying conditions.

Conclusion

Moisture diffusivity and dehydration of stems under cold air storage conditions was studied. The effective moisture diffusivity values for stem parts packed in non-perforated liner films were lower than the values obtained from the no liner film cold storage condition.

Non-perforated liner film (no airflow) significantly reduced the dehydration rate of stems compared to no liner film treatment over the storage period, suggesting that air circulation was the main contributor to moisture diffusivity and dehydration of stem parts. The dehydration rate of the different parts of stems was inversely proportional to the size (diameter). The Newton, Page, Henderson and Pabis, and asymptotic models fitted the dehydration of the different stem parts of grape stems well, indicating that any of the tested models could be used to predict dehydration during cold storage of grapes. However, the Henderson and Pabis model was the best fitted model in predicting dehydration of grape whole stems under the different low temperature storage conditions (exposure to cold air flow and no airflow) studied.

The data obtained in this work and the tested models, could be applied and assist in predicting the quality of grape stems during the handling of fresh grapes in the cold chain.

References

Azzouz S., Guizani A., Jomaa W., Belghith A. 2002. Moisture diffusivity and drying kinetic equation of convective drying of grapes. J. Food Eng. 55, 323-330.

Cağlar A., Toğrul İ.T., Toğrul H. 2009. Moisture and thermal diffusivity of seedless grapes under infrared drying. Food and Bioprod. Process. 87, 292-300.

Cakmak G., Yildiz C. 2011. The drying kinetics of seeded grape in solar dryer with PCM-based solar intergrated collector. Food and Bioprod. Process. 89, 103-108.

Crank J. 1975. The Mathematics of Diffusion. Oxford University Press, Oxford, UK.

Crisosto C. H., Smilanick J. L., Dokoozlian N.K. 2001. Table grapes suffer water loss, stem browning during cooling delays. California Agric. 55 (1), 39 – 42.

Datta, A. K., & Zhang, J. (Eds.). 1999. Porous media approach to heat and mass transfer in solid foods. Department of Agricultural and Biological Engineering, Cornell University.

Deiana A.C., Silva H., Amaya A., Tencredi N. 2009. Use of grape stalk, a waste of the viticulture industry, to obtain activated carbon. J. Hazard. Mater. 172, 13-19.

Delele MA, Schenk A, Tijskens E, Ramon H, Nicolaï BM & Verboven P (2009). Optimization of the humidification of cold stores by pressurized water atomizers based on a multiscale CFD model. J. Food Eng. 91(2), 228-239.

Doymaz İ. 2006. Drying kinetics of black grapes treated with different solutions. J. Food Eng. 76, 212-217.

Doymaz İ. 2011. Drying of green bean and okra under solar energy. Association of the Chemical Engineering of Serbia AChE. DOI10.2298/CICEQ101217004D.

Fadhel A., Kooli S., Farhat A., Bellghith A. 2005. Study of the solar drying of grapes by three different processes. Desalin. 185, 535-541.

García-Perez J.V., García-Alvarado M.A., Carcel J.A., Mulet A. 2010. Extraction kinetics modeling of antioxidants from grape stalk (*Vitis vinifera* var. Bobal): Influence of drying conditions. J. Food Eng. 101, 49-58.

García-Perez J.V., Blasco M., Cárcel J.A., Clemente G., Mulet A. 2006. Drying kinetics of grapes stalk. Defect and Diffusion Forum. (258-260), 225-230.

García-Perez J.V., Carcel J.A., García-Alvarado M.A., Mulet A. 2009. Simulation of grape stalk deep-bed drying. J. Food Eng. 90, 308-314.

Henderson, S. M., Pabis, 1961. Grain drying theory—I, temperature effect on drying coefficient. J. Agric. Eng. Res. 6(3), 169–174.

Ho, Q. T., Verlinden, B. E., Verboven, P., Vandewalle, S., & Nicolai, B. M. (2006). A permeation-diffusion-reaction model of gas transport in cellular tissue of plant materials. J. Exp. Bot. 57(15), 4215-4224.

Jain D., Pathare P.B. 2004. Selection and evaluation of thin layer drying models for infrared radiative and convective drying of onion slices. Biosystems Eng. 89 (3), 289-296.

Jain D., Pathare P.B. 2007. Study the drying kinetics of open sun drying of fish. J. Food Eng. 78, 1315-1319.

Kilic A. 2009. Low temperature and high velocity (LTHV) application in drying: characteristics and effects on the fish quality. J. Food Eng. 91, 173-182.

Kingsly R.P., Goyal R.K., Manikantan M.R., Ilyas S.M. 2007. Effects of pretreatments and drying air temperature on drying behavior of peach slice. Int J Food Sci Technol. 42, 65–69.

Kim S.S., Blowmilk S.R. 1995. Effective moisture diffusivity of plain yoghurt undergoing microwave vacuum drying. J. Food Eng. 24, 137–148.

Lichter A., Kaplunov T., Zutahy Y., Daus A., Alchanatis V., Ostrovsky V., Lurie S. 2011.Physical and cisual properties of grape rachis as affected by water vapour pressure deficit. Postharvest Biol. Technol. 59, 25-33.

Margaris D.P., Ghiaus A.G. 2007. Experimental study of hot air dehydration of Sultana grapes. J. Food Eng. 79, 1115-1121.

Merva, G. E. (1995). Physical principles of the plant system. Michigan, USA: American Society of Agricultural Engineering.

Nelson K.E. 1978. Pre-cooling – its significance to the market quality of table grapes. Int. J. Refrig. 1 (4), 207 – 215.

Ngcobo M.E.K, Opara U.L., Thiart G.D. 2012a. Effects of packaging liners on cooling rate and quality attributes of table grape (cv. Regal seedless). Packaging Technol. Sci. 25 (2), 73-84.

Ngcobo M.E.K, Delele M.A., Opara U.L., Zietsman C.J., Meyer C.J. 2012b. Resistance to airflow and cooling patterns through multi-scale packaging of table grapes. Int. J. Refrig. 35(2), 445-452.

Nguyen TA, Verboven P, Schenk A & Nicolaï BM (2007). Prediction of water loss from pears (*Pyrus communis* cv. Conference) during controlled atmosphere storage as affected by relative humidity. J. Food Eng. 83, 149-155.

Page, G. E. 1949. Factors influencing the maximum rates of air drying shelled corn in thin layer. Master thesis, Purdue University, Lafayette, IN, USA.

Pathare P.B., Sharma G.P. 2006. Effective moisture diffusivity of onion slices undergoing infrared convective drying. Biosystems Eng. 93 (3), 285-291.

Ramírez C., Troncoso E., Muñoz J., Aguilera J.M. 2011. Microstructural analysis on pre-treated apple slices and its effect on water release during air drying. J. Food Eng. 106, 253-261.

Ramos I.N., Miranda J.M.R., Brandão T.R.S., Silva C.L.M. 2010. Estimation of water diffusivity parameters on grape dynamic drying. J. Food Eng. 97, 519-525.

Sastry S.K. 1985. Moisture losses from perishable commodities: recent research and developments. Int. J. Refrig. 8, 343-346.

Singh S., Raina C.S., Bawa A.S., Saxena D.C. 2006. Effect of pretreatments on drying and rehydration kinetics and color of sweet potato slices. Dry Technol. 24,1487–1494.Thompson J.F., Mitchell F.G., Rumsey T.R., Kasmire R.F., Crisosto C.H. Commercial Cooling of Fruits, Vegetables, and Flowers. Regents of the University of California. USA, 1998.

Vega-Gálvez A., Ah-Hen K., Chacana M., Vergara J., Martínez-Monzó J., García-Segovia P., Lemus-Mondaca R., Scala K.D. 2012. Effect of temperature and air velocity on drying kinetics, antioxidant capacity, total phenolic content, colour, texture and microstructure of apple (var. Granny Smith) slices. Food Chem. 132, 51-59.

Veraverbeke E.A., Verboven P., Scheerlinck N., Hoang M.L., Nicolaï B.M. 2003. Determination of the diffusion coefficient of tissue, cuticle, cutin and wax apple. Journal of Food Engineering. 58: 285-294.

Veraverbeke E.A., Verboven P., Van Oostveldt P., Nicolaï B.M. 2003. Prediction of moisture loss across the cuticle of apple (Malus sylvestris subsp. Mitis (Wallr.)) during storage Part 1. Model development and determination of diffusion coefficients. Postharvest Biol. Technol. 30, 75-88.

Wang C Y; Singh R P. 1978. A single layer drying equation for roughrice. ASAE Paper No. 78-3001. St Joseph, MI, USA

Xiao H.W., Pang C.L., Wang L.H., Bai J.W., Yang W.X., Gao Z.J. 2010. Drying kinetics and quality of Monukka seedless grapes dried in an air-impingement jet dryer. Biosystems Eng. 105, 233-240.

Table 1: Thin-layer drying models applied to the moisture dehydration data of grape stems

Model name	Model	Source
Newton	$\left(M_R = \exp\left(-kt\right)\right)$	Pathare and Sharma, (2006)
Page	$\left(M_R = \exp\left(-kt^n\right)\right)$	Singh et al. (2006)
Henderson and Pabis	$\left(M_R = a\exp\left(-kt\right)\right)$	Henderson and Pabis, (1961)
Asymptotic (logarithmic)	$\left(M_R = a_0 + a\exp\left(-kt\right)\right)$	Kingsly et al., (2007)

Table 2: Effective moisture diffusivity (m^2s^{-1}) of individual parts of grape stems under different cold air drying conditions and compared with results obtained under hot air drying by García-Perez et al., 2006.

Packaging	Stem : Berry attachment cap (sphere)	small size parts of stem (cylinder)	Intermediate size parts of stem (cylinder)	Large part of stem (cylinder)
No packaging	1.49×10^{-12}	4.05×10^{-13}	3.16×10^{-13}	6.18×10^{-13}
Non perforated liners	1.66×10^{-13}	5.06×10^{-14}	1.05×10^{-13}	3.09×10^{-13}
García-Perez et al., 2006: hot-air drying (40 °C and 2 ms^{-1})	3.92×10^{-8}	1.07×10^{-11}	1.38×10^{-11}	1.78×10^{-11}

Table 3: Coefficients of Newton's, Page's, Henderson and Pabis, and asymptotic's models for the dehydration of the different parts of grape stems under cold air circulation conditions.

	Model	Parameters	Value	Coefficient of determination (r^2)	Standard error (e_s)
Small sphere	Newton $(M_R = \exp(-kt))$	$k(h^{-1})$	0.0354	0.9830	0.03843
	Page $(M_R = \exp(-kt^n))$	$k(h^{-1})$	0.0148	0.9920	0.03589
		n	1.2423		
	Henderson and Pabis $(M_R = a\exp(-kt))$	a	0.8388	0.9849	0.01086
		$k(h^{-1})$	0.0309		
	Asymptotic (logarithmic) $(M_R = a_0 + a\exp(-kt))$	a_0	0.0095	0.9852	0.01024
		a	0.8307		
		$k(h^{-1})$	0.0319		
Small cylinder	Newton $(M_R = \exp(-kt))$	$k(h^{-1})$	0.0208	0.9906	0.0204
	Page $(M_R = \exp(-kt^n))$	$k(h^{-1})$	0.0211	0.9904	0.0204
		n	0.9969		
	Henderson and Pabis $(M_R = a\exp(-kt))$	a	0.9001	0.9905	0.0086
		$k(h^{-1})$	0.0188		
	Asymptotic (logarithmic)	a_0	0.0157	0.9910	0.0076
		a	0.8889		

	$\left(M_R = a_0 + a\exp\left(-kt\right)\right)$	$k\left(h^{-1}\right)$	0.0198		
Intermediate Cylinder	Newton $\left(M_R = \exp\left(-kt\right)\right)$	$k\left(h^{-1}\right)$	0.0060	0.9935	0.0272
	Page $\left(M_R = \exp\left(-kt^n\right)\right)$	$k\left(h^{-1}\right)$	0.0185	0.9956	0.0071
		n	0.7736		
	Henderson and Pabis $\left(M_R = a\exp\left(-kt\right)\right)$	a	0.9222	0.9918	0.0159
		$k\left(h^{-1}\right)$	0.0053		
	Asymptotic (logarithmic) $\left(M_R = a_0 + a\exp\left(-kt\right)\right)$	a_0	0.0564	0.9922	0.0143
		a	0.8934		
		$k\left(h^{-1}\right)$	0.0051		
Large cylinder	Newton $\left(M_R = \exp\left(-kt\right)\right)$	$k\left(h^{-1}\right)$	0.0033	0.9813	0.1119
	Page $\left(M_R = \exp\left(-kt^n\right)\right)$	$k\left(h^{-1}\right)$	0.0198	0.9880	0.0215
		n	0.6772		
	Henderson and Pabis $\left(M_R = a\exp\left(-kt\right)\right)$	a	0.8265	0.9881	0.0186
		$k\left(h^{-1}\right)$	0.0022		
	Asymptotic (logarithmic) $\left(M_R = a_0 + a\exp\left(-kt\right)\right)$	a_0	0.0255	0.9888	0.0171
		a	0.8109		
		$k\left(h^{-1}\right)$	0.0025		

Table 4: Coefficients of Newton's, Page's, Henderson and Pabis, and asymptotic's models for the dehydration of the whole stems under different cold air conditions.

Package type	Model	Parameters	Value	Coefficient of determination (r^2)	Standard error (e_s)
Exposure to cold air circulation	Newton $(M_R = \exp(-kt))$	$k(h^{-1})$	0.0022	0.9920	0.0148
	Page $(M_R = \exp(-kt^n))$	$k(h^{-1})$	0.0076	0.9949	0.0052
		n	0.8082		
	Henderson and Pabis $(M_R = a\exp(-kt))$	a	0.9252	0.9910	0.0078
		$k(h^{-1})$	0.0021		
	Asymptotic (logarithmic) $(M_R = a_0 + a\exp(-kt))$	a_0	0.0267	0.9921	0.0066
		a	0.9086		
		$k(h^{-1})$	0.0023		
Non perforated liner film	Newton $(M_R = \exp(-kt))$	$k(h^{-1})$	0.0008	0.9644	0.0210
	Page $(M_R = \exp(-kt^n))$	$k(h^{-1})$	0.0021	0.9607	0.0174
		n	0.8508		
	Henderson and Pabis $(M_R = a\exp(-kt))$	a	0.9380	0.9968	0.0136
		$k(h^{-1})$	0.0007		
	Asymptotic (logarithmic) $(M_R = a_0 + a\exp(-kt))$	a_0	-0.8405	0.9732	0.0109
		a	1.7541		
		$k(h^{-1})$	0.0003		

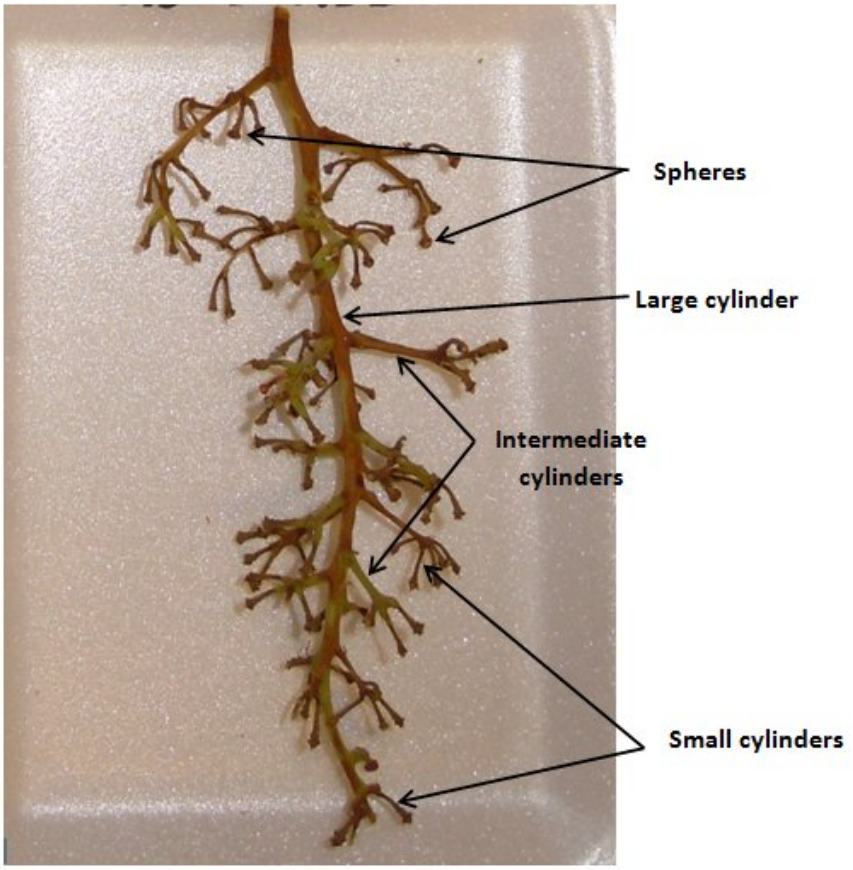

Figure 1: Different parts of the grape stem

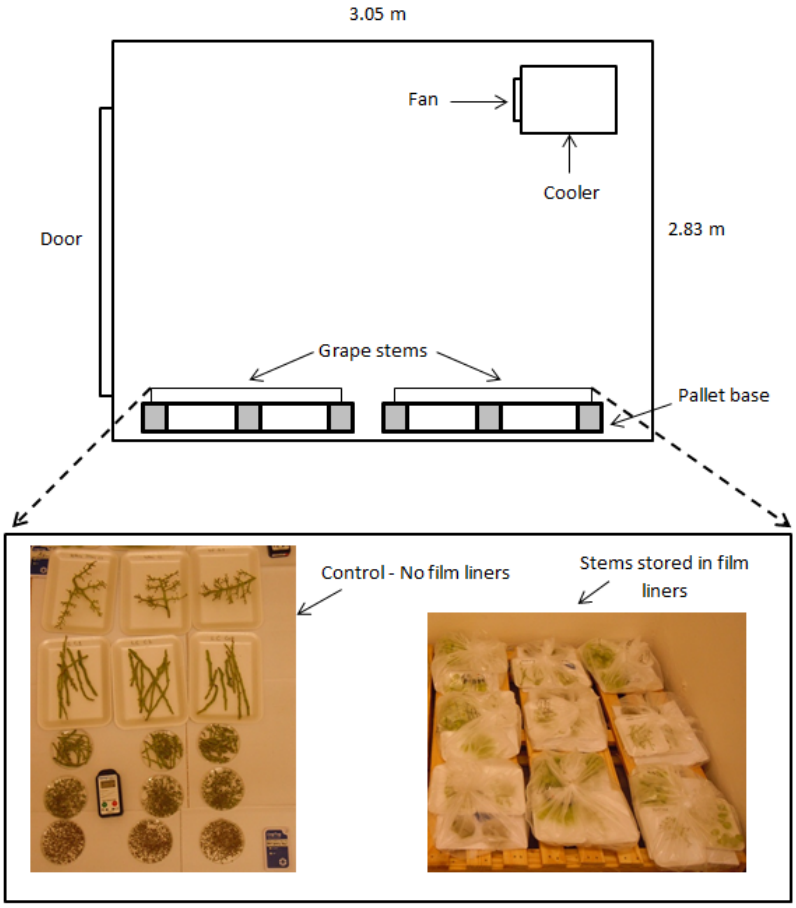

Figure 2: Stem dehydration experimental setup inside an experimental cold room

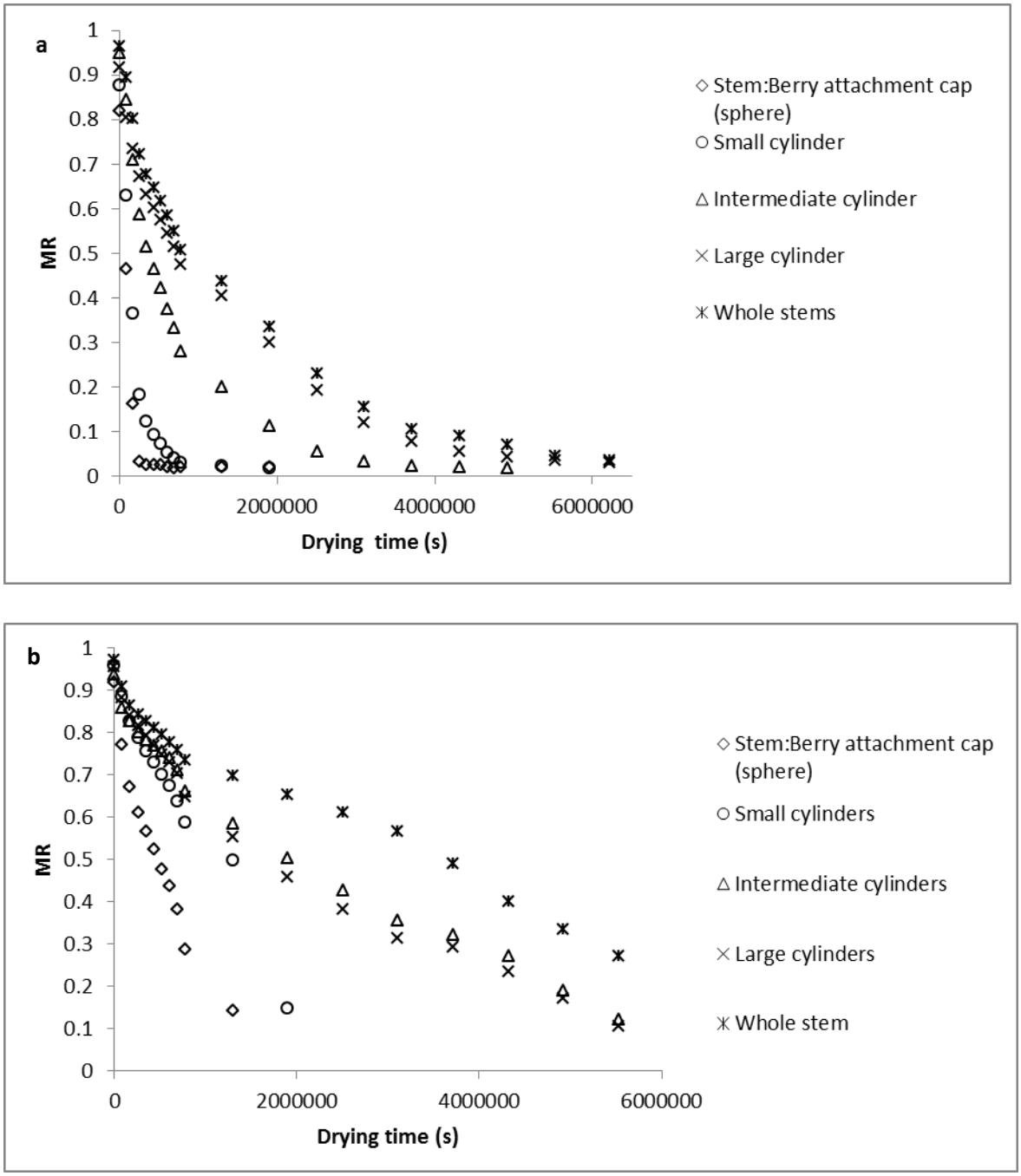

Figure 3: Dehydration kinetics of grape stems parts and whole stem. (a) Exposure to cold air circulation (no film) and (b) no airflow-low temperature (non-perforated LDPE liner film).

PAPER 6

Investigating the Potential of a Humidification System to Control Moisture Loss and Quality of Table Grapes (cv. 'Crimson Seedless') during Cold Storage

Abstract

The potential of humidifying cold storage rooms to control moisture loss and quality of table grapes in different package designs was studied. Fruit were cold stored with humidification (%RH) or no humidified (% RH) and assessed for weight loss and SO_2 injury at intervals during a 35 d period. After 21 d of cold storage under humidification, weight loss of grapes was significantly higher ($P<0.05$) in packages with open-top punnets than clamshell punnets and carry-bags. After 35 days in cold storage the grape weight loss was 1.45±0.32 %, 1.62±0.21 % and 2.01±0.57 % under non-humidified storage, and 0.97±0.34 %; 1.08±0.27 % and 2.00±0.57 % under humidification for the 4.5 kg carry-bag, 5 kg clamshell punnet and 5 kg open-top multi-packages, respectively. Cold storage humidification reduced the rate of stem dehydration and browning. However, humidification increased the SO_2 injury incidence in table grape bunches and caused wetting of the packages.

Keywords: Table grapes; Humidification; Cold storage; Multi-packaging; SO_2 injury; Moisture loss

1. Introduction

Rapid moisture loss is one of the main table grape postharvest quality problems and it is characterized by mass loss (Ngcobo et al., 2012b), shriveled stems which usually become brittle and break easily, and, at advanced stages, the dry stems become brown (Nelson, 1978; Ngcobo et al., 2012a; Lichter et al., 2011). The grape berries only show symptoms of

moisture loss at about 3% - 5% of bunch weight loss (Nelson, 1978), while the stems start to show signs of dehydration immediately after commencement of weight loss of as low as 1 % (Ngcobo et al., 2012a). High water vapour pressure deficit (WVPD) due to low relative humidity (RH) of the cooling air has been reported to be the main driving force for evaporation from fresh commodities stored under refrigerated storage conditions (Sastry, 1985; Paull, 1999; Thompson et al., 1998). High RH and low temperature storage environments play an important role in maintaining the quality of produce (Hung et al., 2011). In order to reduce moisture loss and preserve postharvest quality, table grapes are pre-cooled to sub-zero temperatures of -0.5°C (Ngcobo et al., 2012a). However, the moisture loss still remains a challenge inside refrigerated storage rooms.

In many cold storage rooms, temperature is controlled but the RH is not. In such cases the RH is dependent upon by the surface area of the refrigeration evaporator coil in the storage room and the temperature difference between the coil and the room air, along with air exchange rates, temperature distribution in the room, commodity and packaging material used (Paull, 1999). Humidification has been reported to reduce produce weight loss and maintain quality in cold stores (Hung et al., 2011; Delele et al., 2009) and on retail display cabinets (Brown et al., 2004; Moureh et al., 2009). Although humidification has proven to be successful in controlling weight loss and maintaining quality of produce, some drawbacks have been noted in literature. Some of the these drawbacks include the wetting of corrugated boards (packaging) under a high humidity environment, which causes weakening of cardboard strength, and this often leads to packaging collapse and ultimately to mechanical damage to produce (Marcondes, 1992; Hung et al., 2010). Mist fogging has also been reported to bring about conducive environments for microbial growth (Brown et al., 2004); and the wetting of surface of the produce causes the stomata to open, resulting in water loss (Hung et al., 2011). However, nano-mists have been reported to be able alleviate these drawbacks, whilst providing high humidification and its success lies in their droplets that evaporate easily and quickly before causing wetting of produce and packaging (Hung et al., 2010; Hung et al., 2011; Saenmuang et al., 2012).

The recommended RH for table grape storage is 95 % at -0.5°C (PPECB, 2012). Lichter et al. (2011) investigated the effects of WVPD on physical and visual properties of grape rachis

(stems) under ambient temperature conditions of 10°C and 20°C. Their results suggested that some cultivar differences may exist in terms of response to WVPD, where the rachis of 'Thompson Seedless' grapes remained green at high RH under both 10°C and 20°C, while the rachis of 'Superior Seedless' grapes suffered extensive browning at high RH under 20°C.

In this study the effects of humidification on table grape quality under cold storage at -0.5°C and in different multi-scale packaging was investigated.

2. Materials and Methods

2.1. Fruit and packaging

The grapes were harvested, prepared and packed from a farm in the Worcester area of Cape Town, South Africa and were transported in an air-conditioned car to the Postharvest Technology Research Laboratory at Stellenbosch University.

The grapes were packed in three different types of multi-scale packaging with vented 4.5 kg and 5 kg (punnet) carton boxes with dimensions of 0.4 m x 0.3 m x 0.13 m and 0.6 m x 0.4 m x 0.09 m respectively (Fig. 1). Depending on the size of the grape bunch, 6 to 8 bunches in carry bags were packed in 4.5 kg boxes, while 10 punnets were packed in each 5 kg box. The bunch carry bags and punnets were packed inside perforated liner films (120 x 2 mm and 114 x 4 mm perforated liner films for the 4.5 kg and 5 kg boxes, respectively) inside carton boxes. The moisture absorption and SO_2 pads were then placed over the carry bags and punnets, just before taping the liner films closed using an adhesive tape.

2.3. Cooling and Humidification system

The study was conducted in two experimental cold storage rooms 3.05 m in length, 2.4 m in width and 2.83 m in height (Fig. 2). Cooling of grapes boxes was achieved by means of room cooling. The room was equipped with three fans of diameter 30 cm that circulated the cooling air through the cooler and the room. The capacity of the fans was 1290 m^3/h each. The cooling unit was a finned tube heat exchanger with dimensions of 1.25 m long, 0.4 m wide and 0.36 m high.

The cold room was also equipped with an air-assisted Aqua Room-2 humidifier (Miatech Inc., Clackamas, US) with an air pressure capacity of 140 - 210 kPa; a liquid capacity of 2 L/h and a droplet size of 10 micron. The humidity was controlled with a digital hygrotransmitter 0-100% RH sensor device.

2.4. Temperature and RH measurements

Air temperature and relative humidity were measured the inside storage room and inside the multi-scale packages containing grapes. Air temperature was measured with a LogTag air temperature recorder (LogTag Trix-8 Temperature Recorder, LogTag Recorder Limited, China) and the air relative humidity (%RH) was measured with a SENSITECH TempTale 4 monitor (Temptale4 Humidity and Ambient Temperature 16000, SensiTech, USA).

2.5. Weight loss measurement

The weight of individual bunches was measured with a scale (Mettler, Toledo, Switzerland, with an accuracy of 0.01 g). Bunch weight loss was expressed as percentage loss of the initial weight.

2.5. Stem conditions evaluation

Stem dehydration was assessed using the following scoring system: without drying (fresh stems) = 1, some drying of thinner stems = 2, all thinner stems dry = 3, all thinner and some thicker stems dry = 4 and all stems dry = 5. Stem browning development was measured by using the following scoring system: (1) fresh and green, (2) some light browning, (3) significant browning and (4) severe browning.

2.6. SO_2 injury and decay incidence

SO2 injury was measured according to the following scoring system: (1) none (0%), (2) slight damage (<5%), (3) moderate damage (5–10%) and (4) severe damage (>10 %). Decay was scored as follows: (1) no decay, (2) slight (less than two infected berries per carton), (3) severe (two to five infected berries), and (4) extreme (more than five infected berries per carton).

2.7. Experimental set-up

Two identical cold rooms, one with humidification (-0.33±0.32 °C and 95.00±1.81 % RH) and one without humidification (-0.12±0.32 °C and 90.26±4.44 % RH) were used to cool and store the grapes (Table 1). Six boxes (2 per multi-packaging type) were placed on a pallet base at the central position in each cold room (Fig. 2). Six bunches from each box were labelled, evaluated for quality (stem condition; SO2 injury and decay incidence) and weight loss as per preceding sections 2.4 – 2.6 above, prior to the commencement of cooling. The same grape bunches were then evaluated at seven day intervals during cold storage for 35 days.

2.8. Statistical analysis

Twelve bunches were evaluated for quality attributes per multi-packaging type (treatment) and the data were subjected to the analyses of variance (ANOVA). The data were presented as Means±SD.

3. Results and Discussion

3.1. Weight loss

The percentage weight loss of grape bunches increased with storage period in all multi-packages (Fig. 3a and b). The results indicate that after 21 days of storage under humidification, the percentage weight loss of grapes in open-top punnets multi-packaging was significantly ($P<0.05$) higher than weight loss of grapes in clamshell punnet and carry-bag multi-packages (Fig. 3b). Under no-humidification storage the differences in weight loss of grapes in the different multi-packages were not significant. However the trend shows that the grapes in the open-top punnet multi-packaging had higher average weight loss than grapes in the other multi-packaging (Fig 3a). These results may have been due to a direct contact between grape bunches and the moisture absorption sheet that separates the SO_2 pad and the grapes in the open-top punnet multi-packaging. Also it could be that the open-top punnets allow for more contact of airflow with bunches and reduction of the water loss barrier.

Figure 4a-c shows comparative results of grape weight loss in individual multi-packaging when stored under humidification or no humidification. Although the results indicate that there were no statistically discernable differences in percentage weight loss (packed in the same packaging) of grapes stored under humidified cold storage and non-humidified cold storage, the trends indicate that humidification reduced the average grape weight loss in all tested multi-packaging (Fig. 4a-c). After 35 days in cold storage the grape weight loss was 1.45±0.32 %, 1.62±0.21 % and 2.01±0.57 % under no-humidification storage, and 0.97±0.34 %, 1.08±0.27 % and 2.00±0.57 % under humidification for 4.5 kg carry-bag, 5 kg clamshell punnet and 5 kg open-top multi-packages, respectively. The observed results are attributed to the low water vapour pressure difference (WVPD) which is achieved by increasing RH through humidification (Paull, 1999; Delele et al., 2009a).

The signs of stem dehydration became visible after 7 days of cold storage for both the humidified and non-humidified storage (Table 2). However, the results indicated that humidification reduced the rate of dehydration compared to no-humidification storage (Table 2). The stem dehydration rate of grapes packed in the 4.5 kg carry-bag multi-packaging under no humidification cold storage were 25 %; 50 %; 75%; 100% and 100 % (i.e. percentage of

grape bunches that reached drying score 4) after 7 d; 14 d; 21 d; 28 d and 35 d, respectively, while the dehydration rate of grapes in 4.5 kg multi-packaging under humidification was 25%; 50 % and 75 % after 21 d; 28 d and 35 d respectively. The dehydration rate of grapes packed in clamshell punnet multi-packaging under no humidification was 8 %; 75 % and 92 % after storage periods 7 d; 14 d and 21 d, respectively, and after 28 days all stems of bunches in this treatment were completely dehydrated (score 5), while for those stored under humidification were 25 %; 50 %; 50 %; and 100 % after storage days 14 d; 21 d; 28 d; and 35 d respectively. The visual differences in appearance of bunch stem dehydration in clamshell multi-packaging under humidification and non-humidification storage after 28 days is shown in Fig 5. The dehydration rate of grapes in open-top punnet multi-packaging under no humidification storage were 42 %; 83 %; 92 %; 100 %; 100 % after 7 d; 14 d; 21 d; 28 d; and 35 d of cold storage, respectively, while under humidification cold storage the rate were 25 %; 83 %; 84 % and 100 % after 14 d; 21 d; 28 d; and 35 d respectively.

The highest stem browning score recorded was score 3 (i.e. significant browning of stems), and thus is used as reference in the browning rate discussion. None of the grapes stored under humidification reached a stem browning score of 3, but most of the samples reached a browning score of 2 (i.e. some light browning of stems) (Table 2). Contrary to humidified cold storage, the percentage of bunches that reached the browning score of 3 under non-humidified storage in 4.5 kg was 25 % after 35 days; in clamshell punnet multi-packaging was 17 % after 28 days and in open-top punnet multi-packaging were 25 % and 33 % after 28 and 35 days, respectively. This may have been due to lower transpiration potential of the surrounding air as a result of humidification.

3.2. SO_2 injury and decay incidence

Figure 6 shows a bunch with SO_2 injury under humidified storage. The SO_2 injury occurred after 7 days of cold storage under humidification, for the 4.5 kg carry-bag multi-packaging, with 25 % of the bunches showing slight SO_2 injury (score 2) and after 28 days in storage the number of affected bunches increased to 50 % (Table 2). Under non-humidified storage in 4.5 kg multi-packaging the incidence of SO_2 injury appeared after 14 days with 25 % of bunches showing symptoms. This number of affected bunches only increased to 50 % after 35 days of storage. The grapes packed in clamshell multi-packaging under humidification showed 33 % of bunches affected after 28 days and after 35 days about 50 % of grapes

showed incidence of SO_2 injury, while under non-humidification storage 17 % of the bunches showed SO_2 injury and only 33 % bunches had SO_2 injury after 35 days. About 25 % of bunches in open-top multi-packaging showed the incidence of SO_2 injury after 35 days of storage under humidified storage and 59 % of grape bunches had SO_2 injury after 35 days under no-humidification storage. These results suggest that humidification could cause some incidence of SO_2 injury on grapes. This could be attributed to a possible acidic environment that tends to be created by high levels of humidity in the presence of the SO_2 sheet in the grape multi-packaging (Zoffoli et al., 2008; Ngcobo et al., 2012a). The water droplets were deposited on the package making the packaging soaked wet and this would have added in creating the acidic environment. This places emphasis on the optimization of humidifier to produce water droplets that would evaporated easily and not deposited on packaging such as nano-mists (Hung et al., 2010; Hung et al., 2011; Saenmuang et al., 2012).

4. Conclusion

The potential of humidification in controlling table grape quality disorders was investigated. The weight loss trends suggest that humidification can reduce the rate of moisture loss from grapes packed in different multi-packaging. Humidification also delayed the onset of and, in some, cases reduced the stem dehydration rate and browning development during postharvest storage. However, more SO_2 injury incidence was observed under the humidified storage due to high moisture and the presence of the SO_2 sheet creating an acidic environment. Humidification was also associated with packaging wetness due to high water droplet deposition on the packaging. This suggests that the humidification system needs to be optimized for successful postharvest storage in order to reduce the deposition of water droplets on the packaging structure. Also more work is warranted in optimizing table grape packaging where humidification applications are used in order to withstand the high humidity conditions.

References

Brown T., Corry J.E.L., James S.J. 2004. Humidification of chilled fruit and vegetables on retail display using an ultrasonic fogging system with water/air ozonation. Int. J. Refrig. 27, 862-868

Delele M.A., Schenk A., Ramon H., Nicolaï B.M., Verboven P. 2009. Evaluation of a chicory root cold store humidification system using computational fluid dynamics. J. Food Eng. 94, 110-121

Delele M.A., Schenk A., Tijskens E., Ramon H., Nicolaï B.M, Verboven P. 2009a. Optimization of the humidification of cold stores by pressurized water atomizers based on a multiscale CFD model. J. Food Eng. 91, 228-239

Hung D.V., Tong S., Tanaka F., Yasunaga E., Hamanaka D., Hiruma N., Uchino T. 2011. Controlling the weight loss of fresh produce during postharvest storage under a nano-size mist environment. J. Food Eng. 106, 325-330

Hung D.V., Yusuke N., Tanaka F., Hamanaka D., Uchino T. 2010. Preserving the strength of corrugated cardboard under high humidity condition using nano-sized mists. Compos. Sci. Technol. 70, 2123-2127

Lichter A., Kaplunov T., Zutahy Y., Daus A., Alchanatis V., Ostrovsky V., Lurie S. 2011. Physical and cisual properties of grape rachis as affected by water vapour pressure deficit. Postharvest Biol. Technol. 59, 25-33.

Marcondes J. 1992. Cushioning properties of corrugated fiberboard and the effects of moisture content. ASABE. 35 (6), 1949-1953

Moureh J., Letang G., Palvadeau B., Boisson H. 2009. Numerical and experimental investigations on the use of mist flow process in refrigerated display cabinets. Int. J. Refrig. 32, 203-219

Ngcobo M.E.K., Opara U.L., Thiart G.D. 2012a. Effects of packaging liners on cooling rate and quality attributes of table grape (cv Regal Seedless). Packag. Technol. Sci. 25 (2), 73-84

Ngcobo M.E.K., Delele M.A., Pathare P.B., Opara U.L., Meyer C.J. 2012b. Moisture loss characteristics of fresh table grapes packed in different film liners during cold storage. Biosystems Eng. 113 (4), 363-370.

Paull R.E. 1999. Effect of temperature and humidity on fresh commodity quality. Postharvest Biol. Technol.15, 263-277.

Saenmuang S., Al-Haq M.I., Makino Y., Kawagoe Y., Oshita S. 2012. Particle size distribution of nano-mist in a spinach-storage atmosphere and its effect on respiration and qualities. J. Food Eng. 112: 69-77

Sastry S.K. 1985. Moisture losses from perishable commodities: recent research and developments. Int. J. Refrig. 8, 343-346

Thompson J.F., Mitchell F.G., Rumsey T.R., Kasmire R.F., Crisosto C.H. 1998. Commercial cooling of fruits, vegetables, and flowers. Regents of the University of California. USA.

Zoffoli F.P., Latorre B.A., Naranjo P. 2008. Hairline, a postharvest cracking disorder in table grapes induced by sulfur dioxide. Postharvest Biol. Technol. 47, 90-97.

Table 1: Conditions inside experimental cold rooms during storage of table grapes

Room condition	Relative humidity (%)	Air Temperature (°C)
No humidification	90.26±4.44	-0.12 ± 0.32
Humidification	95.00±1.81	-0.33 ± 0.32

Table 2: Effect of humidification and packaging on stem condition and quality of table grapes during cold storage.

	Non-humidification cold storage (90.26±4.44 % RH)			Humidification cold storage (95.00±1.81 % RH)		
Packaging	Stem dehydration (1-5)[a]	Stem browning (1-5)[b]	SO_2 injury index[c]	Stem dehydration (1-5)[a]	Stem browning (1-5)[b]	SO_2 injury index[c]
Baseline data (0 days)						
4.5 kg bunch carry-bag multi-packaging	1.00±0.00	1.00±0.00	1.00±0.00	1.00±0.00	1.00±0.00	1.00±0.00
Clamshell punnet multi-packaging	1.00±0.00	1.00±0.00	1.00±0.00	1.00±0.00	1.00±0.00	1.00±0.00
Open-top punnet multi-packaging	1.00±0.00	1.00±0.00	1.00±0.00	1.00±0.00	1.00±0.00	1.00±0.00
After 7 days						
4.5 kg bunch carry-bag multi-packaging	2.25±1.26	1.00±0.00	1.00±0.00	2.00±0.00	1.00±0.00	1.25±0.50
Clamshell punnet multi-packaging	2.17±0.58	1.00±0.00	1.00±0.00	1.75±0.45	1.00±0.00	1.00±0.00
Open-top punnet multi-packaging	2.83±1.03	1.00±0.00	1.00±0.00	2.00±0.00	1.00±0.00	1.00±0.00
After 14 days						
4.5 kg bunch carry-bag multi-packaging	3.25±0.96	1.00±0.00	1.25±0.50	3.00±0.00	1.00±0.00	1.25±0.50
Clamshell punnet multi-packaging	3.50±0.90	1.00±0.00	1.00±0.00	2.50±0.90	1.00±0.00	1.00±0.00
Open-top punnet multi-packaging	3.67±0.78	1.00±0.00	1.08±0.29	2.92±0.79	1.00±0.00	1.00±0.00

After 21 days						
4.5 kg bunch carry-bag multi-packaging	3.75±0.50	1.75±0.50	1.25±0.50	3.75±0.50	1.00±0.00	1.25±0.50
Clamshell punnet multi-packaging	3.83±0.58	1.67±0.49	1.00±0.00	3.08±0.99	1.00±0.00	1.00±0.00
Open-top punnet multi-packaging	3.83±0.58	2.00±0.00	1.25±0.45	3.75±0.62	1.00±0.00	1.00±0.00
After 28 days						
4.5 kg bunch carry-bag multi-packaging	4.00±0.00	1.75±0.50	1.25±0.50	4.00±0.00	1.50±0.58	1.50±0.58
Clamshell punnet multi-packaging	5.00±0.00	1.83±0.49	1.17±0.39	3.08±0.99	1.58±0.51	1.33±0.49
Open-top punnet multi-packaging	5.00±0.00	2.25±0.45	1.50±0.52	3.83±0.39	2.00±0.00	1.25±0.45
After 35 days						
4.5 kg bunch carry-bag multi-packaging	4.00±0.00	2.25±0.50	1.50±0.58	4.00±0.00	2.00±0.00	1.50±0.58
Clamshell punnet multi-packaging	5.00±0.00	2.08±0.30	1.33±0.49	5.00±0.00	2.00±0.00	1.50±0.52
Open-top punnet multi-packaging	5.00±0.00	2.33±0.49	1.75±0.62	5.00±0.00	2.00±0.00	1.25±0.45

[a]Score: 1 = fresh stems, 2 = some drying of thinner stems, 3 = all thinner stems dry, 4 = all thinner and some thicker stems dry and 5 = all stems dry.

[b]Score: 1 = fresh and green stems, 2 = some light browning stems, 3 = significant browning of stems and 4 = severe browning of stems.

[c]SO2 injury score (1-4): 1 = no injury, 2 = slight injury (<5%), 3 = moderate injury (5-10%) and 4 = severe injury (>10%).

Figure 1: Grape multi-scale packaging. a) 5 kg punnet multi-packaging box and b) 4.5 kg bunch carry-bag multi-packaging box

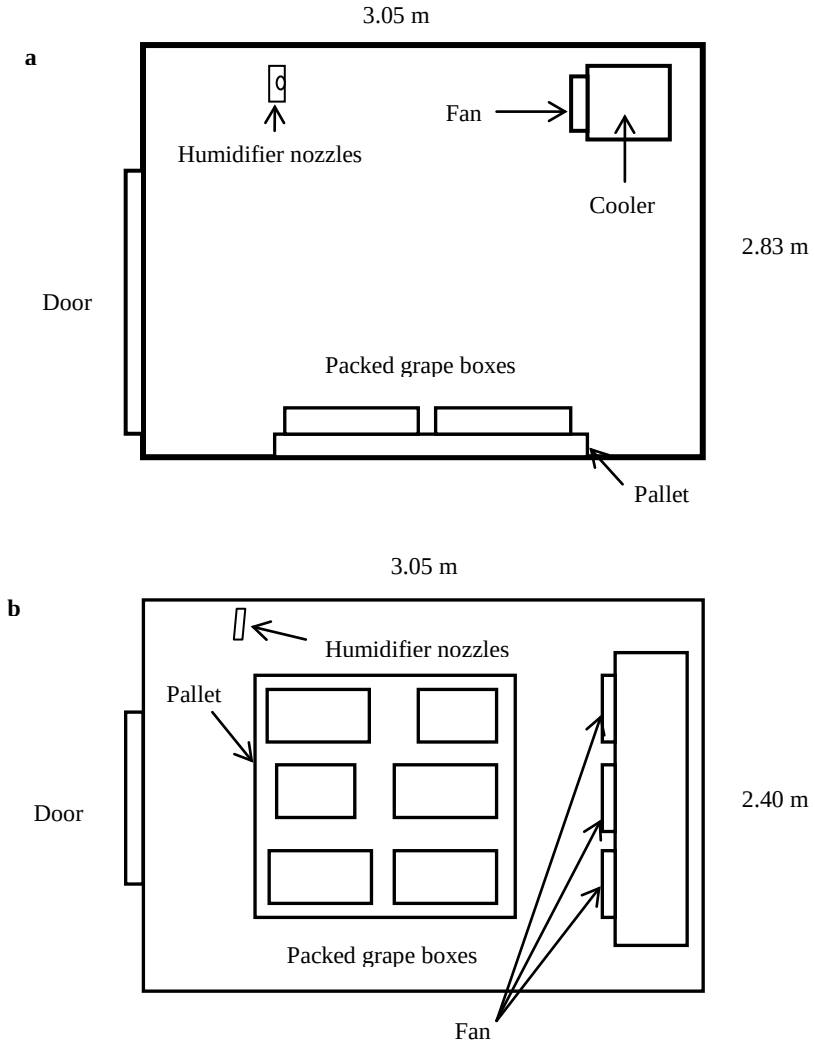

Figure 2: Experimental setup inside the cold storage room; a – side view and b – top view

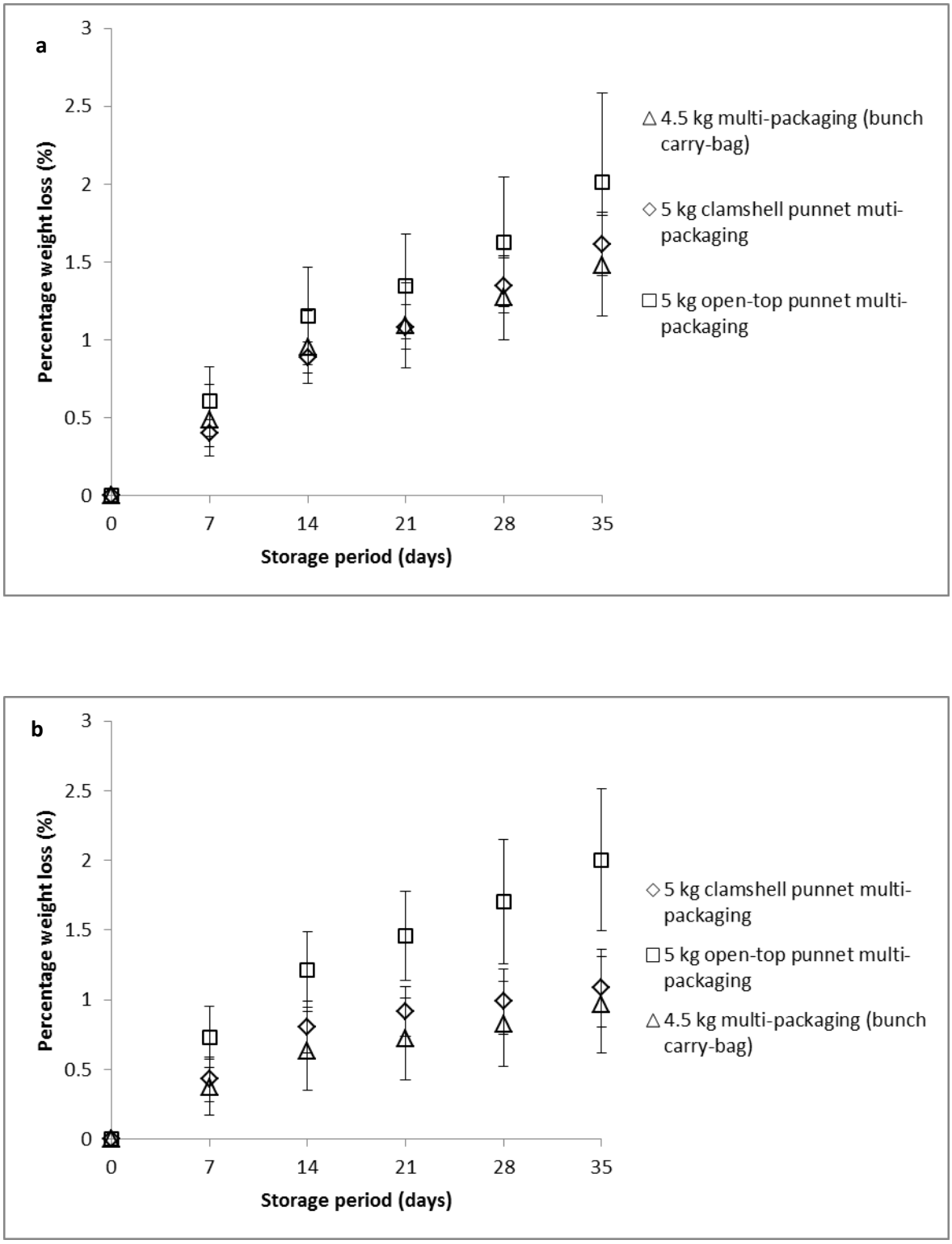

Figure 3: Percentage moisture loss of grape bunches in different multi-scale package combinations during cold storage. a) Non-humidification storage; and b) humidification storage

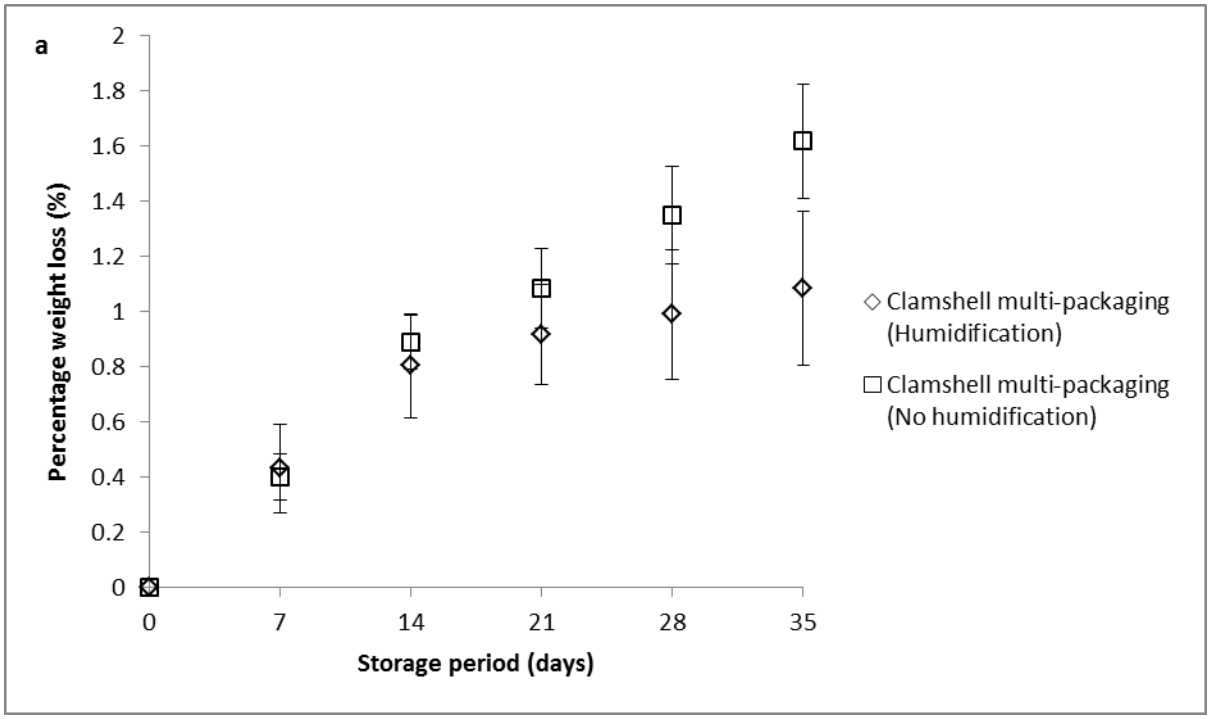

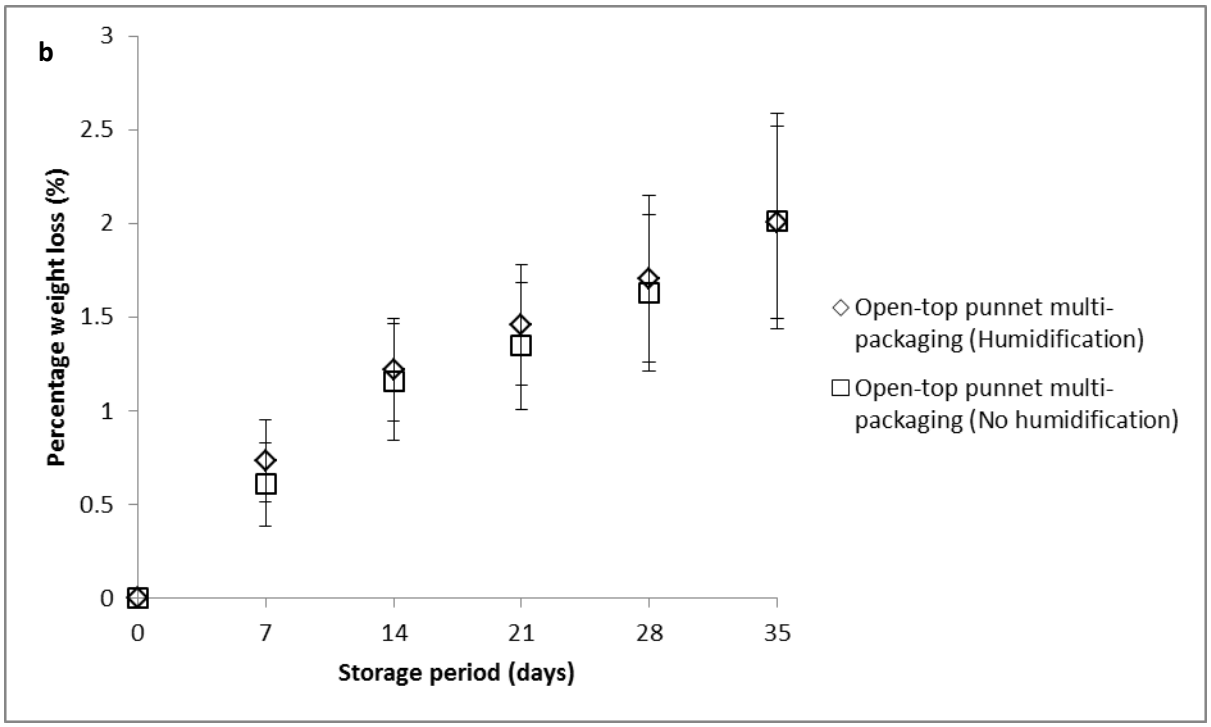

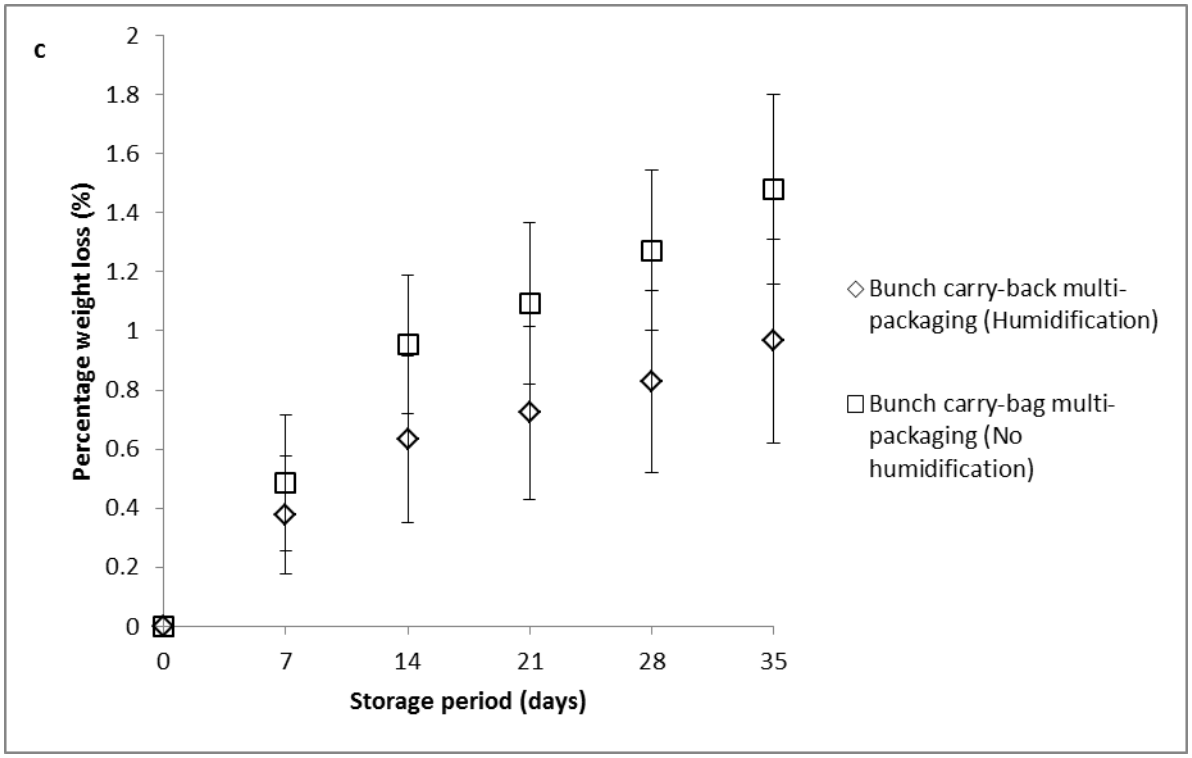

Figure 4: Percentage weight loss comparisons of grapes stored under humidified and non-humidified cold storage. a) Clamshell punnet multi-packaging; b) open-top punnet multi-packaging; and c) bunch carry-bag multi-packaging.

a

b

Figure 5: Visual appearance of grape bunches packed in clamshell punnet multi-packaging after 28 days of cold storage under (a) humidified and (b) non-humidified rooms.

Figure 6: SO_2 injury on grapes under humidified storage.

PAPER 7

Investigating the effects of table grape package components and stacking on airflow, heat and mass transfer using 3-D CFD modelling

Abstract

The flow phenomenon during cooling and handling of packed table grapes was studied using a computational fluid dynamic (CFD) model and validated using experimental results. The effects of the packaging components (bunch carry bag and plastic liners) and box stacking on airflow, and heat and mass transfer were analyzed. The carton box was explicitly modeled, the grape bunch with the carry bag was treated as a porous medium and perforated plastic liners were taken as a porous jump. Pressure loss coefficients of the grape bunch with the carry bag and perforated plastic liners were determined using wind tunnel experiments. Compared to the cooling of bulk grape bunches, the presence of the carry bag increased the half- and seven-eighth cooling time by 61.09 % and 97.34 %, respectively. The addition of plastic liners over the bunch carry bag increased the half- and seven-eighth cooling time by up to 168.90 % and 185.22 %, respectively. Non-perforated liners were most effective in preventing moisture loss but also generated the highest condensation of water vapor inside the package. For perforated plastic liners, cooling with a high relative humidity (RH) air minimized fruit moisture loss. Partial cooling of the grape bunch inside the carry bag before covering it with a non-perforated plastic liner maintained the required high RH inside the package without condensation. The stacking of packages on the pallet affected the airflow pattern, the cooling rate and moisture transfer. There was a good agreement between measured and predicted results. The result demonstrated clearly the applicability of CFD models to determine optimum table grape packaging and cooling procedures.

Keywords: Table grape; Packaging; CFD; Airflow; Heat and mass transfer; plastic liner.

Notation

A_c	cooler surface area, m^2
a_p	specific fruit area, m^{-1}
Bi	Biot number
C_p	Specific heat capacity, J kg^{-1} $^0C^{-1}$
D	diffusion coefficient, m^2 s^{-1}
D_c	collar diameter of heat exchanger tube, m
D_e	effective diffusivity, m^2 s^{-1}
D_P	fruit diameter, m
g	gravitational acceleration, m s^{-2}
h_h	heat transfer coefficient, W m^{-2} $°C^{-1}$
h_m	mass transfer coefficient, m s^{-1}
κ	Darcy permeability, m^2
k	turbulence kinetic energy, m^2 s^{-2}
L	latent heat, J kg^{-1}
p	pressure, Pa
Pr	Prandtl number
p_{sat}	saturated vapour pressure, Pa
p_v	vapour pressure, Pa
Re	Reynolds number
Sc	Schmidt number
S_e	heat source term, W m^{-3}

S_m	mass source term, kg m^{-3} s^{-1}
St	Stanton number
t	time, s
T	temperature, °C
T'	fluctuating temperature, °C
u_i, u_j	mean velocity components in X, Y, and Z directions, m s^{-1}
u_i', u_j'	fluctuating velocity components, m s^{-1}
V	volume, m^{-3}
x_i, x_j	Cartesian coordinates, m
X_v	moisture content, kg/kg
Y_v	vapour mass fraction
β	Forchheimer drag coefficient, m^{-1}
ε	dissipation rate of turbulence kinetic energy, m^2 s^{-3}
μ	dynamic viscosity, kg m^{-1} s^{-1}
λ	thermal conductivity, W m^{-1} $^0C^{-1}$
ω	specific dissipation rate, s^{-1}
ρ	density, kg m^{-3}
ϕ	Porosity
α	thermal expansion coefficient, $°C^{-1}$
Subscripts	
a	air phase

c	Cooler
o	reference condition
p	Product
t	Turbulence
i, j	Cartesian coordinate index

1. Introduction

Fresh table grapes are a major commodity in global food trade and South Africa is ranked third in the world export market, with the European market accounting for about 61 % of the total exports (Ngcobo et al., 2012). Packaging and refrigerated storage are critical technologies in maintaining quality of fresh and processed food products (de Paula et al., 2011; Opara, 2011; Caleb et al., 2011; Tsiraki & Savvaidis, 2011). For fresh table grape export, produce is typically packed in 4.5 kg vented cardboard boxes with multiple inner packaging materials that include plastic liner, SO_2 pad, moisture absorber and bunch carry bag (Fig. 1). The main functions of these package components are to maintain the quality of the grapes during postharvest handling and storage by providing a mechanical shield against injuries, minimizing product moisture loss and retarding microbial decay (Opara, 2011). Produce temperature is one of the most important parameters that control the rate of respiration, moisture loss and microbial growth. Cooling of table grapes as fast as possible retards quality deterioration associated with these phenomena. Table grapes are a non-climacteric fruit with a relatively low postharvest physiological activity. However, unless the appropriate measures are taken to maintain the cold chain, produce may be exposed to high levels of moisture loss and decay (Nelson, 1985; Lichter et al., 2008; Costa et al., 2011; Ngcobo et al., 2012). Moisture loss results in quality problems such as weight loss, stem drying, browning, softening and shattering of berries, which contribute to significant economic losses.

The cooling of packed table grapes is usually performed using a forced air cooling technique. Due to the high vapour pressure difference between the cooling air and the product surface, the initial cooling period of the produce from its field temperature to the desired storage temperature is usually associated with significant moisture loss (Nelson, 1978; Lichter et al., 2011). Crisosto et al. (2001) observed up to 1 % moisture loss during the cooling period of table grapes. Although this level of moisture loss is considered small, the authors noted that it caused stem browning. Lowering the vapour pressure difference as fast as possible either by decreasing the berry temperature or increasing the relative humidity (RH) of air can minimize moisture loss. Berry cooling rate depends on several factors including box vent area (Opara, 2011), cooling air properties (flow rate, temperature and RH), stacking pattern, liner properties and the presence of other components inside the package (such as moisture absorption pad and SO_2 pad). The properties of the liner include plastic type and vent size, number and distribution. Previous research has shown that the presence of packing materials and cooling duration significantly influence/alter the decay of grape berries (Nelson & Ahmedullah, 1976; Nelson, 1978). Therefore, fresh produce packaging must have enough vents to allow the delivery of the cooling medium (air) with minimum resistance and provide uniform airflow and cooling through the entire mass of the produce while providing suitable mechanical resistance (Vigneault & Goyette, 2002; Castro et al., 2004; Vigneault & Castro, 2005). Plastic liners are used in table grape packaging to minimize moisture loss from berries by maintaining high RH within the package. Recent experimental studies showed that non-perforated plastic liners maintained the RH of the package close to 100 % resulting in the highest stem quality (Ngcobo et al., 2012). However, the use of non-perforated plastic liners also produced the highest moisture condensation inside the package, SO_2 injury and berry drop while the use of perforated liners resulted in lower RH, higher stem dehydration and browning compared to the non-perforated liner. These findings highlight the need for optimization of plastic liner designs.

The airflow, and heat and mass transfer processes during postharvest handling of horticultural products have been studied using experimental and modelling techniques (Tassou & Xiang, 1998; Xu & Burfoot, 1999; Alvarez & Flick, 1999; van der Sman, 2002; Alvarez et al. 2003; Moureh & Flick, 2004; Nahor et al., 2005; Zou et al., 2006; Opara & Zou, 2006, 2007; Chourasia & Goswami, 2007; Delele et al., 2009a, 2009b; Ferrua & Singh, 2009; Tutar et al., 2009). Some researchers have studied the airflow, and heat and mass transfer processes

within the individual and packed grapes using experimental (Gentry & Nelson, 1964; Nelson, 1978; Frederick & Comunian, 1994) and modelling techniques (Dincer, 1995a, 1995b, Acevedo et al., 2007). However, none of the previous studies have developed a comprehensive 3-D CFD model which is capable of predicting the airflow, and heat and mass transfer within and around multiple package components such as that used for fresh table grapes (Fig. 1). These studies did not take into account the details of the packages and even the grape bunches. For better understanding of the flow behaviour in and around such complex packaging systems, the development of better modelling techniques is vital. Nowadays, the use of validated Computational Fluid Dynamics (CFD) modelling techniques has increasingly become an alternative approach to the difficult, time consuming and expensive experimental methods (Delele et al., 2009a; Tutar et al., 2009; Opara, 2011).

The aim of this study was to develop and experimentally validate a 3-D CFD model of a table grape cooling process that predicted the cooling air velocity, temperature, RH and product moisture loss, taking into account the detailed geometries of the packaging components (box, liner and pads). The validated model was used to evaluate the effect of different package components and cooling procedures on airflow, and heat and mass transfer processes.

2. Materials and Methods

2.1. Cold storage room and table grape packaging

The study was based on an experimental cold storage room with dimensions 3.05 x 2.40 x 2.83 m (Fig. 2). The room is equipped with three fans of 30-cm diameter that circulate the cooling air through the cooler and the room. The capacity of each fan is 1290 m^3/h and the cooling unit is comprised of a finned tube heat exchanger with dimensions of 1.25 x 0.40 x 0.36 m.

Grape bunches were packed using a vented carton box with dimensions of 0.4 m long, 0.3 m wide and 0.133 m high (Fig. 1). Every box contains about 4.5 kg of grape, equivalent to 6-8

bunches depending on the size of the grape bunch. The carry bags were well vented. During packing, each carry bag containing a bunch of berries is placed inside the plastic liner, the moisture absorption and SO_2 pads are placed over the carry bags and the liner is closed and sealed using a plastic adhesive tape. A corrugated paperboard sheet is placed in the bottom of the box to protect the berries against bruising. A more detailed description of the table grape packaging system can be found in Ngcobo et al. (2012).

2.2 CFD model formulation

The CFD code used for this work was ANSYS FLUENT 13.0 (ANSYS, Inc., Canonsburg, Pennsylvania, USA). The governing equations were solved using the Reynolds-averaged procedure. In Cartesian coordinates, for flow in a porous medium, the Reynolds-averaged fluid flow equations based on interstitial fluid velocity are as follows (Antohe & Lage, 1997; Nakayama & Kuwahara, 1999):

$$\frac{\partial(\rho_a)}{\partial t}+\frac{\partial(\rho_a u_i)}{\partial x_i}=S_m \tag{1}$$

$$\frac{\partial(\rho_a u_i)}{\partial t}+\frac{\partial(\rho_a u_i u_j)}{\partial x_j}=-\frac{\partial(p)}{\partial x_i}+\frac{\partial}{\partial x_j}\left[\mu_a\left(\frac{\partial u_i}{\partial x_j}+\frac{\partial u_j}{\partial x_i}\right)\right]-\frac{\partial}{\partial x_j}\left(\rho_a\overline{u_i'u_j'}\right) -\left[1-\alpha\left(T-T_o\right)\right]\rho_a g-\phi\frac{\mu_a}{\kappa}u_i-\phi^2\frac{1}{2}\beta\rho_a\left(u_j u_j\right)^{1/2}u_i \tag{2}$$

where ρ_a is the density (kg m^{-3}); u_i and u_j are mean air velocity components (m s^{-1}); t is the time (s); x_i and x_j are Cartesian coordinates (m); p is the pressure (Pa); μ_a is the dynamic viscosity (kg m^{-1} s^{-1}); u_i' and u_j' are fluctuating velocity components (m s^{-1}); T is the temperature (^{0}C); ϕ is the porosity; g is the gravitational acceleration (m s^{-2}); α is the thermal expansion coefficient (^{0}C^{-1}) and S_m is the mass source term (kg m^{-3} s^{-1}). The fourth term in the right side of equation (2) represents the buoyancy force, where the reference temperature (T_o) was taken as the storage room temperature. The last two terms in the right side of equation (2) represent the resistance of the porous medium to airflow and are expressed in the form of the Darcy- Forchheimer equation; where κ is the Darcy

permeability (m^2) and β is the Forchheimer drag coefficient (m^{-1}).

By assuming a local thermal equilibrium between the air and the porous solid matrix, the energy equation is:

$$\frac{\partial}{\partial t}\left(\phi\rho_a C_{pa}T+(1-\phi)\rho_p C_{pp}T\right)+\frac{\partial}{x_j}\left(\phi\rho_a C_{pa}u_j T\right)=\frac{\partial}{\partial x_j}\left[\lambda_e\left(\frac{\partial T}{\partial x_j}\right)\right] -\frac{\partial}{\partial x_j}\left(\phi\rho_a C_{pa}\overline{u_j'T'}\right)+S_e \quad (3)$$

Where C_P is the heat capacity (J kg^{-1} $^0C^{-1}$); λ_e is the effective thermal conductivity (W m^{-1} $^0C^{-1}$); T' is the fluctuating temperature (^0C) and S_e is the energy source term (W m^{-3}). The Effective thermal conductivity was estimated using: $\lambda_{eff}=\phi\lambda_a+(1-\phi)\lambda_p$ (Carson, 2006). The limitation of this thermal equilibrium assumption for porous systems with heat generation and transient problems, particularly for large products and low conductivity fluid has been discussed (Verboven et al., 2006; van der Sman, 2008; Laguerre et al., 2008). During such non-equilibrium cases, a two equation model is recommended. However, thermal equilibrium assumption has been used and reasonable model accuracy was reported in several heat and mass transfer studies related to agricultural product handling (Tassou & Xiang, 1998; Moureh & Flick, 2004; Chourasia & Goswami, 2007; Delele et al., 2009a, 2009b, 2012). Using scale analysis, van der Sman (2008) reported that this thermal equilibrium assumption is valid when the air Stanton number, $\mathrm{St}_a=\frac{L_x h_h a_p}{u_x\rho_a C_{pa}}\gg 1$, vapour Stanton number, $\mathrm{St}_v=\frac{L_x h_m a_p}{u_x}\approx 1$, Biot number, $\mathrm{Bi}=\frac{h_h D_p}{\lambda_p}\gg 1$ and the particle Reynolds number, $\mathrm{Re}_p=\frac{\rho_a u_x D_p}{\mu_a}<10^3$. The initial temperature of the grapes was 21 ^0C and the cooling air temperature was 0 ^0C. Density, specific heat and thermal conductivity of the grapes were 1077.9 kg m^{-3}, 3395 J kg^{-1} $^0C^{-1}$ and 0.551 W m^{-1} $^0C^{-1}$, respectively (Bingol et al., 2008). Corresponding values of the cooling air were 1.25 kg m^{-3}, 1005 J kg^{-1} $^0C^{-1}$ and 0.024 W m^{-1} $^0C^{-1}$. Length of the porous region (L_x) was 0.4 m, average diameter of the grapes (Dp) was 0.0201 m and calculated average air velocity inside the bulk grape region (u_x) was 0.059 m s^{-1}. Porosity of the grapes was determined by using a displacement method (Chau *et al.*, 1985) and it was 0.53. The specific grape area (a_p) was 158.21 m^{-1}. Correlations to determine the

heat transfer coefficient (h_h) in packed beds can be found in Wakao & Kaguei (1982) and van der Sman (2008). Using this correlation, the calculated value of h_h was 9.78 W m^{-2} ^{0}C^{-1}. The mass transfer coefficient (h_m) of table grapes takes into account convective mass transfer coefficient (h_{ma}) and skin mass transfer coefficient (h_{ms}), $\frac{1}{h_m}=\frac{1}{h_{ma}}+\frac{1}{h_{ms}}$. The convective mass transfer coefficient was determined from the heat transfer coefficient using Lewis analogy (Bird et al., 2002). Table grape skin mass transfer coefficient was taken from Becker et al. (1994). The calculated value of h_m was 8.23×10^{-4} m s^{-1}, and the calculated values of St_a, St_v, Bi and Re_p were 8.31, 0.87, 0.35 and 83.28, respectively. In this study, Bi value was close to 1. However, the agreement between measured and predicted results (see sections 3.1 and 3.2) shows the validity of the thermal equilibrium assumption.

The transport equation for vapour mass fraction is:

$$\frac{\partial(\phi\rho_a Y_v)}{\partial t}+\frac{\partial}{\partial x_j}\left(\phi\rho_a u_j Y_v\right)=\frac{\partial}{\partial x_j}\left[\rho_a D_e\left(\frac{\partial(Y_v)}{\partial x_j}\right)\right]-\frac{\partial}{\partial x_j}\left(\phi\rho_a\overline{u_j' Y_v'}\right)+S_m \qquad (4)$$

Where Y_v is the vapour mass fraction; Y_v' is the fluctuating vapour mass fraction and D_e is the effective diffusivity of the vapour (m^2 s^{-1}). The specific Reynolds stress term ($\overline{u_i' u_j'}$) in equation (2) and specific Reynolds flux terms $\overline{u_j' T'}$ and $\overline{u_j' Y_v'}$ in equations (3) and (4), respectively were approximated by (Versteeg & Malalasekera, 1995; Wilcox, 2000):

$$\overline{u_i' u_j'}=-\frac{\mu_t}{\rho_a}\left(\frac{\partial u_i}{\partial x_j}+\frac{\partial u_j}{\partial x_i}\right)+\frac{2}{3}k\delta_{ij} \qquad (5)$$

$$\overline{u_j' T'}=-\frac{\mu_t}{\rho_a \mathrm{Pr}_t}\left(\frac{\partial T}{\partial x_j}\right) \qquad (6)$$

$$\overline{u_j' Y_v'}=-\frac{\mu_t}{\rho_a \mathrm{Sc}_t}\left(\frac{\partial Y_v}{\partial x_j}\right) \qquad (7)$$

Appropriate turbulence models were used for closure of these equations. The Reynolds stress term (Eqn. 5) is commonly treated using Boussinesq hypothesis. This hypothesis relates the Reynolds stress term to the mean velocity gradient and assumes the turbulent viscosity to be

isotropic scalar quantity, which is not strictly true. The Boussinesq hypothesis is used in Spalart-Allmaras, k-ε, and k-ω turbulence models. The Reynolds stress turbulence model is an alternative approach that takes into account the anisotropy of the Reynolds stress term, but with additional computational cost. In most applications, models based on Boussinesq hypothesis perform very well (Wilcox, 2000; Ansys, 2010). Alvarez & Flick (1999) observed turbulence generation behind the stacked product and later Alvarez et al. (2003) proposed a semi-empirical model based on one equation for two-dimensional turbulence flow through porous medium that took into account this turbulence generation. Though the generation of turbulence behind the stacked product was reported (Alvarez & Flick, 1999; Alvarez et al., 2003), several previous studies on airflow, heat and mass transfer in loaded refrigerated systems used the porous medium approach and treated turbulence using conventional turbulence models that are employed in Reynolds-average approach (standard k-ε, RNG k-ε, SST-k-ω and Reynolds stress) (Hoang et al., 2000; Moureh & Flick, 2004; Nahor et al. 2005; Mirade & Picgirard, 2006; Delele et al., 2009a, 2009b). Generally, the accuracy of these models was reasonable. In this study, different two-equation eddy-viscosity turbulence models (standard k-ε, RNG k-ε, standard k-ω and SST-k-ω) were compared. For standard-k-ε, RNG-k-ε, standard-k-ω and SST-k-ω turbulence models, the overall average relative error of predicted product temperature relative to the measured values was 23.94 %, 20.34 %, 21.85 % and 17.13 % (see section 3.1), respectively. The SST-k-ω turbulence model was chosen and used in this study.

The grape bunches with the carry bags and the cooler were modelled as a porous medium with the corresponding mass, momentum and heat sources/sink. The porous medium model describes the flow behaviour within a matrix of solid structure that is usually characterized by its porosity. As a result of the low Reynolds number (Re = 83.28), the flow inside the liner (the grape bunches with the carry bags) was taken as a laminar flow. In all other regions the flow was turbulent. The source terms in equation (1) and equation (2) consisted of different contributions. S_m takes into account the moisture loss from the product surface (S_{mp}) and the condensation of water vapour on the cooling coils (S_{mc}). S_e represents the heat of respiration of the product (S_{ep}) and the heat exchange on the cooler (S_{ec}). Due to the relatively low temperature difference between the surfaces, the effect of radiation was neglected. The details about the calculations of these source terms are given in section 2.3. The model consisted of

the following four zones: solid box zone, product zone, cooler zone and free air zone. In all zones, in addition to the relevant source terms, the above equations were solved using the appropriate porosities. In the solid box zone, all source terms and porosity were zero and only the heat transfer equation (Eqn. 3) was solved. The product zone represented the region occupied by the grape bunches and the carry bags. In this zone, continuity, momentum, energy and vapour transport equations were solved. This zone included heat of respiration and product moisture loss as source terms and the porosity was taken as 0.53. The cooler zone represented the volume occupied by the cooler. The equations that were solved in the product zone were also solved here. Condensation of water vapour and heat exchange on the cooler were taken into account as source terms and the porosity was taken as 0.71. The free air zone consisted of the region that is not included in solid box, product and cooler zones. Similar to the product and cooler zones, equations 1-4 were solved. In this zone, the porosity and the sources terms were taken as 1 and zero, respectively.

2.3 Model parameters determination

Bulk grape bunches were treated as a porous medium and the vented plastic liner was modelled with porous jump boundary condition. Pressure loss coefficients were determined from experiments conducted in a wind tunnel (Fig. 3). The dimensions of the test section were 0.6 m in width (perpendicular to airflow), 0.4 m in height and 0.4 m in depth (in the airflow direction). The required airflow was attained using a suction fan. Independent pressure drop experiments were conducted for flow through bulk grape bunches which were not covered with carry bags (Fig. 3b), bulk grape bunches which were covered with carry bags (Fig. 3c) and vented plastic liner (Fig. 3d). To measure the pressure drop through the bulk grape bunches with and without carry bags, the load was contained in a wire mesh and placed inside the wind tunnel. The pressure drop through the wire mesh was measured using a pressure transducer device (PMD70-AAA7D22AAU, ENDRESS+HAUSER, Weil am Rhein, Germany) and was found to be close to zero. Measurements were done for fan frequency of 1 to 50 Hz, these frequencies corresponded to an air velocity of 0.064 m s^{-1} to 3.21 m s^{-1} for an empty wind tunnel.

For the porous bulk grape bunches, the measured pressure drop value was expressed as a function of air velocity and fitted to the Darcy-Forchheimer equation ($\frac{\Delta P}{L_b} = -\frac{\mu}{\kappa}u - \beta\frac{1}{2}\rho u^2$) with $r^2 \geq 0.993$ using Microsoft Excel solver. The solver determined the best fit by minimizing the deviation between measured and predicted values. From the fitted equations, the values of the Darcy permeability (κ) and Forchheimer drag coefficient (β) were determined. The first term in the right side of the equation is the Darcy term that accounts for the viscous drag which is dominant at low air velocities (laminar flow), while the second term is the Forchheimer term that accounts for the inertial drag which dominates the pressure drop at high air velocities (turbulent flow). Lb is the bulk length in the flow direction (0.4 m). In the case of bulk grapes without carry bags, the measured values of K and β were 3.62 × 106 m^{-2} and 80.19 m^{-1}, respectively. The presence of the carry bags increased the coefficients significantly and the corresponding values of the coefficients were 1.74 × 107 m^{-2} and 358.08 m^{-1}, respectively. These parameters were determined for a particle Reynolds number ($\mathrm{Re}_p = \frac{\rho u D_p}{\mu}$) range of 63-3347. This range corresponds to an intermediate to turbulent flow region. For flow through porous media, it is reported that $\mathrm{Re_p} < 10$, $10 \geq \mathrm{Re_p} \leq 300$ and $\mathrm{Re_p} > 300$ distinguish laminar, intermediate and turbulent flow regimes, respectively (Eisfeld & Schnitzlein, 2001). The flow in this experiment was in the range of intermediate to turbulent, but including the laminar flow region could improve the accuracy of parameter estimation.

Pressure loss coefficients of the porous jump boundary for vented plastic liners were also determined from measured data. The porous jump boundary condition is normally used to model a thin membrane with known pressure drop characteristics. For this boundary, the pressure drop is expressed as: $\Delta p = -\left(\frac{\mu}{\kappa}u + \beta\frac{1}{2}\rho u^2\right)t_l$, where t_l is the thickness of the liner. Pressure drop through the different vented plastic liners was measured by fixing the liner perpendicular to the airflow direction (Fig. 3d). Fan frequency range and pressure sensors used in this experiment were similar to the previous experiments on flow through bulk grape bunches and vented plastic liners. The Reynolds number of the flow based on the hydraulic diameter of the tunnel was in the range of 832-9280, the range covers laminar, intermediate and turbulent flow regions. The critical Reynolds number of channel flow is reported to be

around 1300 (Patel & Head, 1969; Högberg et al., 2003). The measured pressure drop data were fitted to the above equation and corresponding values of $\frac{1}{\kappa}$, β and liner thickness (t_l) for different vented plastic liners are given in Table 1 ($r^2 \geq 0.991$). The thickness of the liners was taken from Ngcobo et al. (2012).

The effect of the cooler on room airflow and humidity distribution was also included in the model. As the air passes through the finned tube heat exchanger, there is a significant pressure drop and condensation of water vapour over the cold heat exchanger surfaces. The cooler was also modelled as a porous medium. However, the Darcy term was neglected and the parameter β was calculated by taking into account losses due to wall friction, entrance and exit and acceleration/deceleration effects (Tso et al., 2006). The quadratic term dominates the pressure drop when the flow Reynolds number ($\mathrm{Re} = \frac{\rho_a u D_c}{\mu_a}$) is much greater than 1 (Zukauskas and Ulinskas, 1990; Tso et al., 2006; Verboven et al., 2006; Jacimovic et al., 2006). In this study the Re of the flow through the cooling unit was 3854.21 and corresponding value of β was 42.6 m^{-1}. The source due to the heat loss to the cooler (S_{ec}) was calculated using:

$$S_{ec} = \frac{Q_c}{V_c} = \frac{h_{hc} A_c (T_c - T_a)}{V_c} + L S_{mc} \tag{8}$$

To calculate the mass source due to the condensation of water vapour on the cooler (S_{mc}), where L is the latent heat of evaporation (J kg^{-1}), the following equation was used:

$$S_{mc} = \frac{m_c}{V_c} = \frac{h_{mc} A_c \rho_{da} (X_{vc} - X_{va})}{V_c} \tag{9}$$

The convective mass transfer coefficient (h_{mc}) was calculated according to Lewis correlation of heat and mass transfer ($h_{mc} = \frac{h_{hc}}{\rho C_p Le^{2/3}}$) (Tso et al., 2006), where Le is the Lewis number which was taken as 0.95 and 1 for frosting and non-frosting conditions, respectively.

The heat of respiration (S_{ep}) of the grapes was calculated using $S_{ep} = 4.599 e^{0.1134 T_p}$ (Becker et al., 1994). The product moisture loss was calculated using a lumped convection model,

neglecting the moisture diffusion inside the product:

$$S_{mp} = h_b a_p \left(P_{vp} - P_{va} \right) \tag{10}$$

where the P_{vp} and P_{va} are vapour pressures on the product surface and surrounding air, respectively. For thermodynamic equilibrium the surrounding air temperature approaches the product surface temperature and the vapour is assumed to follow the ideal gas law, $P_{vp} = a_w P_{sat}$ and $P_{va} = P_{sat}\left(\frac{RH}{100}\right)$. Details about the calculation of the bulk product mass transfer coefficient (h_b) can be found in section 2.2. The skin mass transfer coefficient and water activity (a_w) of the grapes were taken from Becker et al. (1994), with values of 4.02×10^{-10} kg m^{-2} s^{-1} Pa^{-1} and 0.98, respectively. Average specific area ($a_p = \frac{6\phi}{D_p}$) of the grape bulk was taken as 158.21 m^2 m^{-3} (Verboven et al., 2006). The model used user defined functions to include the heat and mass transfer source terms.

2.4 Boundary conditions and simulation procedure

The dimensions of the simulation domain were the same as the experimental cool room (Fig. 1). The fan was modelled as a fan boundary with a given pressure rise (32 Pa). This was a lumped parameter model that predicted the amount of flow through the fan, but did not take into account the detailed flow behaviour and the turbulence created through the fan blades. Detailed geometries of the vented carton box and pallet were explicitly modelled (Fig. 4). The product and cooler were treated as porous mediums; the determination of the relevant source terms is given in section 2.3. Vented liners were taken as porous jump boundaries with the corresponding loss coefficients (section 2.3), whereas the non-perforated plastic liner was treated as a wall boundary. Moisture absorption pad and corrugated riffle sheet were also taken as wall boundaries. Condensation of water vapour on these surfaces was modelled and it occurred when the vapour pressure of the air next to wall surfaces was higher than the saturated vapour pressure. The initial cool room temperature and RH were measured and found to be 0.13 ^{0}C and 90.77 %, respectively (Temptale4 Humidity and Ambient Temperature 16000, SENSITECH, Beverly, MA, USA).

The governing equations were numerically solved using the finite volume method. The computational domain was discretised using a tetrahedral hybrid mesh (Fig. 4). The selection of the optimum mesh size was based on the size and complexity of the zones. Mesh with a maximum edge length of 0.005 m and 0.01 m for box and product zones was used, respectively. The other regions were discretised using mesh with maximum edge length of 0.03 m. The mesh consisted of over 4.62×10^6 cells. This mesh size selection was made based on a mesh sensitivity study. Comparison of the calculated results (wall y^+ value, product temperature and RH) and central processing unit (CPU) time of calculation for different mesh sizes was made. Wall y^+ value is a dimensionless parameter defined by: $y^+ = \frac{\rho u_\tau y_p}{\mu}$, where u_τ is the friction velocity, y_p is the distance from point P to the wall, ρ is fluid density and μ is fluid viscosity at point P. There was no significant change in value of the results when the mesh was smaller than this size ($p < 0.05$). The calculated y^+ values were less than 5 and that fulfilled the requirement of enhanced wall function that was used in this model. The importance of such low y^+ values on wall surfaces was also discussed by Tutar et al. (2009).

The equations were discretised using a second order upwind scheme and pressure-velocity coupling was done using a SIMPLE (Semi-Implicit Method for Pressure-Linked Equations) algorithm. SIMPLE algorithm uses the relationship between velocity and pressure corrections to enforce mass conservation and to get the pressure field. SIMPLE calculation is initiated with a guessed pressure field and the discretised momentum equation is solved using the guessed pressure field. In the SIMPLE algorithm an iteration is used to improve upon the guessed pressure field. A time step of 120 s and 50 iterations per time step were used. The simulation was converged to a solution with a normalized scaled residual below 10^{-4} for all equations. In normalized scaled residual analysis, the residual shows the error in the conservation equations and it is scaled using the global value, finally normalized by dividing using the maximum residual value. The residual of the energy equation was converged below 10^{-7}. For most problems, normalized scaled residual values of 10^{-3} for all equations except energy and species transport equations and 10^{-6} for energy and species transport equations gives sufficient accuracy (Ansys, 2010). Sensitivity of the solution to different time steps (3600 s, 1800 s, 600 s, 120 s and 60 s) was assessed and no significant changes in the result

were found when the time step was lower than 120 s ($p<0.05$). The calculation was done using 64-bit, Intel® Core™2 i7 CPU, 2.93 GHz, 8 Gb RAM, Windows 7 computer and the CPU time of calculation was more than 22 h.

2.5 Model validation experiments

Validation experiments were conducted inside experimental cold storage room (Fig. 2). The inside fruit temperature and RH of the cooling air were measured using Logtag temperature probe (LogTag Recorder Limited, Northcote, Auckland, NewZealand) and SENSITECH TempTale 4 monitor (Temptale4 Humidity and Ambient Temperature 16000, SENSITECH, Beverly, MA, USA), respectively.

'Regal' seedless grapes were obtained from the HexRiver area of the Western Cape, South Africa. The size of the grapes used was extra-large and it was assumed to be spherical (diameter of 20.15±0.13mm). Cooling experiments were conducted for three packaging configurations. First, measurement was conducted with the grapes placed inside the vented carton box without the other package components (carry bag, plastic liner and SO_2 and moisture absorption pads). In the case of the second experiment, grapes were placed in carry bags and the carry bags with the grapes were packed inside the vented carton box. This experiment excluded plastic liner, SO_2 pad and moisture absorption pad. In the last case, the experiment was done with all the package components included as per the commercial requirement (Fig. 1). Different plastic liners were used, including non-perforated, 120 × 2 mm perforated, 54 × 2 mm perforated and 36 × 4 mm perforated. The numbers on the vented liners indicate the number and size of the holes. In all cases, the corrugated paper sheet was placed in the bottom of the vented carton box. The cooling experiments were conducted by placing two carton boxes with the same packaging configuration adjacent to each other on a pallet. Three temperature sensors and one RH sensor were included in every carton (Fig. 5). To evaluate the effect of stacking, 30 boxes of grapes were stacked on a pallet in three levels (10 boxes per level) according to the commercial guideline (Fig. 1a). The grapes were packed using 120 × 2 mm perforated liners. Each experiment was repeated three times.

3. Results and Discussion

3.1. Cooling airflow and temperature distribution

The predicted airflow and temperature profiles are shown in Fig. 6 and Fig. 7, respectively. High velocity cold air that was exited from the fan was channelled along the ceiling of the cold room, and down the door side wall of the room, cooled the product and circulated back to the cooler. A large portion of the cooling air was flowing over the surface of the packed product (Fig. 6). Only some portion of the cooling air was able to pass through the vent holes of the box. Due to the high flow resistance, the flow of cooling air through the plastic liner into the bulk of the grapes was very limited. The flow through the non-perforated liner was completely blocked, but in the case of perforated liner there was a very small amount of air that passed through it. The velocity of the air within the package was very low, and it was moving as a result of the buoyancy force. For instance, in the case of the non-perforated liner the average velocity inside the bulk grape after 12 h of cooling time was 0.0041 m s^{-1}.

The cooling process progressed from the surfaces that were exposed to the flowing cold air to the central region of the package (Fig. 7). Product temperature was expressed as a dimensionless temperature (θ) ($\theta = \frac{T - T_a}{T_i - T_a}$), where T_a and T_i are cooling air and initial product temperature, respectively (Dincer, 1995b). The half- and the seven-eighth cooling time correspond to a θ value of 0.5 and 0.125, respectively. Half- and seven-eighth cooling times of the side that was exposed to high velocity cold air (position 1 in Fig. 7) were 5.08 h and 17.42 h, compared to the 7.78 h and 23.67 h for centre region of the package (position 2 in Fig. 7), respectively. Gowda et al. (1997) reported an identical trend in a parametric study conducted on forced air pre-cooling of spherical food in bulk. The layer that was nearest to the entry of the cooling air, cooled earliest, whereas the layer that was farthest from the entry point had the highest temperature. The measured and predicted results were in agreement (Fig. 8). Inside the package, conduction was the dominant mode of heat transfer. This was due to relatively low flow of cooling air into the package. During cooling of the stack of

products with a low velocity air (≤ 0.20 m s $^{-1}$), conduction between products can be the same order of magnitude as convection (Amara et al., 2004). This result shows that for such packaging system a simple diffusion model combined with the appropriate boundary conditions may give reasonable accuracy with lower computational cost. However, in a complex flow system like room air cooling, determining the correct boundary conditions is challenging. Boundary conditions over the package are spatially highly variable and depend on several factors. For instance, in this study the heat transfer coefficients between front and back and top and bottom sides were different and there were also differences between different positions within the same side. The convective heat transfer coefficient over the surface of the package was in the range of 1.2 W m^{-2} $^0C^{-1}$ to 23.4 W m^{-2} $^0C^{-1}$. Boundary conditions for different design (box and liner) and operating conditions (airflow rate, stacking, etc) are different. Experimental determination of the boundary condition for each of the cases at high spatial resolution is time consuming, difficult and expensive. The cool room model that takes into account all the geometric, airflow, heat and mass transfer details is an alternative to predict the boundary conditions in a relatively easy and cheaper way. Such full scale refrigerated system models have been validated and used in a number of applications and found to be reasonably accurate (Hoang et al., 2000; Moureh & Flick, 2004; Moureh & Flick, 2004; Nahor et al., 2005; Mirade & Picgirard, 2006; Chourasia & Goswami, 2007; Delele et al., 2009a, 2009b;). The full scale model can be used to develop a database of boundary conditions for different design and operating parameters that can be incorporated in the development of a simplified diffusion model of the grape packaging system.

3.3. Effect of package components on heat and mass transfer during cooling and storage

The effects of bunch carry bags and plastic liners were analysed on heat and mass transfer. The bunch carry bags and plastic liners significantly affected the cooling time (Fig. 9). Placing the grape bunches in carry bags increased the half cooling time by 61.09 % from 1.8 h to 2.9 h, while the seven-eighth cooling time increased by 97.34 % from 3.7 h to 7.3 h. Nelson (1978) conducted an experimental study on the cooling of paper wrapped grape bunch clusters and reported a similar reduction in cooling rate as a result of the chimney wrap.

However, the addition of the carry bag did not affect the RH of the cooling air around the product which was 90.77 % on average. RH was calculated by taking the ratio of the partial pressure of water vapour actually present in the air-water vapour mixture to the saturation pressure of water vapour at the mixture temperature. ANSYS FLUENT calculates the saturation vapour pressure (p_{sat}) using: $\ln\left(\frac{p_{sat}}{p_c}\right)=\left(\frac{T_c}{T}-1\right)\times\sum_{i=1}^{8}F_i\left[\alpha\left(T-T_p\right)\right]^{i-1}$ (Ansys, 2010; Reynolds, 1979). Where $p_c = 22.089\,\text{MPa}$, $T_c = 647.283\,\text{K}$, $F_1 = -7.4192$, $F_2 = 2.9721$, $F_3 = -1.1553\times10^{-1}$, $F_4 = 8.6856\times10^{-3}$, $F_5 = 1.0941\times10^{-3}$, $F_6 = -4.3999\times10^{-3}$, $F_7 = 2.5207\times10^{-3}$, $F_8 = -5.2187\times10^{-4}$, $\alpha = 0.01$ $T_p = 338.15\,\text{K}$. Enclosing grape bunch loaded carry bags inside non-perforated liners increased the half cooling and the seven-eighth cooling time by 168.90 % and 185.22 %, respectively (Fig. 9). Nelson (1978, 1985) and Gentry & Nelson (1964) conducted an experimental study on the effect of plastic liners and observed a similar reduction in cooling rate. Covering with 120 × 2 mm perforated plastic liners increased half- and seven-eighth cooling time by 137.81 % and 175.70 %, respectively. Relative to the non-perforated liner, perforated liners decreased half- and seven-eighth cooling time by 11.46 % and 11.41 %, respectively. The improvement in cooling rate as a result of liner perforation was not that big. This could be due to suboptimal vent parameters (size, number and position) and blockage of the vents by the product and the box surfaces. This result shows that in order to get the required improvement in cooling rate, an optimal design and operation of perforated liners is necessary. The velocity of the air inside the perforated packaging was a little bit higher than when the non-perforated liner used. For instance, after 12 h of cooling time, the air velocity was 0.0059 m s^{-1} compared to 0.0041 m s^{-1} obtained when the non-perforated liner was used. The difference in cooling time between the different perforated plastic liners used in this study (120 × 2 mm, 36 × 4 mm and 54 × 2 mm) was not significant ($p < 0.05$).

The effect of the non-perforated liner on maintaining high RH inside the package was very vital (Fig. 10). Predicted total moisture loss from grapes that were packed with non-perforated liners and cooled from an initial temperature of 21 ^{0}C to a storage temperature of -0.5 ^{0}C and handled at this temperature for one month was only 0.18 %. After the cooling time of 8.2 h, the air inside the packed system was completely saturated (RH = 100 %) and resulted in a vapour condensation. This phenomenon was also reported by Ngcobo et al.

(2012) and Lichter et al. (2011). For perforated liners, the maximum RH that was attainable inside the package was the RH of the cooling air. In this case, after precooling and one month storage at -0.5 ^{0}C, the predicted total moisture was 1.23 %. These results show that the perforation of plastic liners mainly affect the moisture transfer. The non-perforated liner was able to minimize the moisture loss. The lower moisture loss could help to minimize weight loss, stem drying, browning, softening and shattering of berries, but the high degree of condensation inside the package could enhance microbial growth and SO_2 injury. Previous studies described the advantage of the plastic liner in minimizing grape moisture loss and in maintaining quality (Lichter et al., 2011, 2008; Nelson & Ahmedullah, 1976; Costa et al., 2011; Crisosto et al., 1994; Ngcobo et al., 2012). Crisosto et al. (1994) conducted a moisture loss study on Thompson Seedless grapes with and without a plastic liner. After 12 days of storage at 0-1 ^{0}C and 3 days of shelf life at 20 ^{0}C, the moisture loss of 0.4 % and 7.6 % was observed for the packages with and without plastic liners, respectively. In the same study, after 28 days of shipment at 0-1 ^{0}C and 3 days of shelf life at 20 ^{0}C, for the package with perforated liner, a moisture loss of 0.4 % was reported, whereas no moisture loss was observed for non-perforated liner. The experimental study conducted by Ngcobo et al. (2012) reported a moisture loss of 0.70 % and 1.80 % after 30 days of storage at 0.5 ^{0}C for table grapes packaged with non-perforated and perforated liner, respectively. The design of a liner film that is capable of minimizing grape moisture loss but that prevents the accumulation of the condensed water inside the package is very vital (Lichter et al., 2011).

Previous studies focused mainly on experimental evaluation of the effects of table grape liner vents on moisture loss and moisture condensation (Ngcobo et al., 2012). The vents in a plastic liner are expected to increase the cooling rate and to decrease the amount of condensation inside the package. Results obtained in the present study showed that vents only minimized condensation inside the package and increased moisture loss. However, the effect of liner vents on fruit cooling rate was relatively small. These results highlight the need to design liner vents that are capable of maximizing fruit cooling rate with minimum moisture loss. The developed CFD model can be used to optimize vent design of table grape liners, thereby reducing the cost of experimental studies.

3.4. Effect of product stacking on heat and mass transfer during cooling and storage

The airflow pattern and temperature distribution within and around the stack of grape packages is shown in Fig. 11. Only some portion of the cooling air appeared to penetrate the stack through the gaps between the boxes (Fig. 11a). The hottest region was located near the central region of the stack. The region that was located near the entry of the cooling air had a faster cooling rate than the interior region (Figs 11b and 11c). The half- and seven-eighth cooling time at the centre of the stack was 23.19 h and 63.92 h, respectively. These cooling times were 193.42 % and 204.09 % longer than the corresponding cooling time of the two boxes mentioned in section 3.2, respectively. Due to the perforated liner (120 × 2 mm) that was used in this study, the maximum RH attained inside the packed boxes was the same as the RH of the cooling air. To attain maximum RH at the hottest spot in the stack, a cooling time of 87.64 h was needed, which was an increase of 212.90 % relative to the case of the two boxes that was mentioned above. The predicted total moisture loss of the stack that was cooled from an initial temperature of 21 ^{0}C to a storage temperature of -0.5 ^{0}C and stored at this temperature for a period of one month was 1.88 %. This moisture loss was 34.6 % higher compared to the two boxes. This result indicated that stacking of the packages on the pallet during handling affected the heat and mass transfer characteristics of the package. Nelson (1978) conducted an experiment to study the precooling of grape packages and observed significant effects of number and arrangement of packages on the pallet. Due to the low penetration of the cooling air to the central region of the stack, the larger the pallet the more difficult to pre-cool.

3.5. Improving the grape packaging and cooling procedure

The validated model was applied to study alternative grape packaging and cooling procedures. First, bulk grape bunches were placed inside the vented box and cooled to the storage temperature. As soon as the storage temperature was attained grape bunches were placed inside the carry bag and plastic liner. In this method of cooling, the seven-eighth cooling time was reduced by 78.11 %, showing that this approach could help to reduce the

total energy consumption of the system. However, in this cooling procedure the RH inside the package was relatively low. During packing with perforated plastic liners the RH throughout the storage period was the same as the RH of the cooling air. However, in the case of non-perforated liners there was a slight increase of RH inside the package (2.12 %) during a one month storage period. Relative to the standard way of packaging and cooling, this method minimized the cooling energy and avoided the moisture condensation. The total energy consumption increases with precooling time (Thompson et al., 2010). However, the total moisture loss was relatively increased. After pre-cooling and one month storage at -0.5 ^{0}C, calculated total moisture loss of 0.57 % and 1.39 % was observed for non-perforated and perforated liners, respectively.

In the second case, grape bunches were covered with carry bags and placed inside vented boxes, followed by cooling to the storage temperature. When grapes reached the storage temperature they were covered by a plastic liner. In this case, the seven-eighth cooling time was reduced by 64.82 %. The behaviour of the RH inside the package was the same as the first case. In terms of energy saving, this method of cooling was worse than the first case. However, the degree of moisture loss and condensation was not significantly different from the first case ($p < 0.05$).

The third case studied the effect of cooling with high RH air. In this study the grapes were packed and cooled in a standard way but the cooling air had relatively high RH (96 %). The grapes were packed with perforated liners. With this cooling and storage method, it was possible to minimize the moisture loss by 71.16 %, but its effect on cooling rate was not significant ($p < 0.05$). It is known that high RH cooling air minimizes moisture loss by minimizing the vapour pressure deficit between the grape surface and the cooling air (Gentry & Nelson, 1964; Nelson, 1978; Lichter et al., 2011). This high level of RH can be attained by using an external humidifier. In addition to maintaining the required high RH, a humidifier that works with water misting can even increase the cooling rate by evaporative cooling effect (Delele et al., 2009a).

In the last case, the grape bunches were covered with carry bags and placed inside a vented

boxes and cooled to the half cooling time. After reaching the half cooling time the grapes inside the carry bags were then covered with a plastic liner and the cooling of the package was continued up to the storage temperature. In this scenario, the seventh-eight cooling time was reduced by 41.60 %. For the non-perforated plastic liner, it was possible to get high RH (97.15 %) inside the package with no condensation whereas, for perforated liners the RH inside the package was the same as the RH of the cooling air. The calculated total moisture loss after pre-cooling and one month storage at 0.5 ^{0}C was 0.34 % and 1.31 % for non-perforated and perforated liner, respectively.

4. Conclusion

Table grapes are normally packed in multilayer packages. For efficient postharvest handling and cooling of table grapes, optimal design, packing and operation of the package are very important. The airflow, heat and mass transfer characteristics in and around the table grape packaging system were studied using a computational fluid dynamic (CFD) model. The model was validated using experimental results.

The effects of different package components on airflow, and heat and mass transfer processes were studied. The validated model was applied to evaluate alternative packaging and cooling procedures. The presence of bunch carry bags and plastic liners affects the cooling rate of grapes. The contribution of plastic liners in reducing the cooling rate of packed grapes was higher than the other package components. Non-perforated liners produced the highest RH inside the package and gave the lowest moisture loss, but also the highest condensation. Pre cooling of table grape bunches with and without carry bags before covering it with a plastic liner reduced the cooling time significantly, up to 78.11 %. For perforated liners, the use of high RH (96 %) cooling air compared to 90.77 % reduced the moisture loss by 71.16 %. The cooling airflow pattern, cooling rate and moisture loss were also affected by the stacking of the product on the pallet. The result demonstrated the applicability of CFD models to determine the optimum table grape package design and handling that gives the maximum cooling rate with minimum water condensation and moisture loss. The approach followed in

this study can be applied in the optimization of other agricultural product packaging system design and handling. However, these models must include the appropriate system geometry, air supply properties and product physiochemical properties.

References

Acevedo C., Sánchez E., Young M.E. 2007. Heat and mass transfer coefficients for natural convection in fruit packages. J. Food Eng. 80, 655-661.

Alvarez G., Bournet P-E., Flick D. 2003. Two-dimensional simulation of turbulent flow and transfer through stacked spheres. Int. J. Heat and Mass Transfer. 46, 2459-2469.

Alvarez G., Flick D. 1999. Analysis of heterogeneous cooling of agricultural products inside bins. Part I: Aerodynamic study. J. Food Eng. 39(3), 227-237.

Amara S.B., Laguerre O., Flick D. 2004. Experimental study of convective heat transfer during cooling with low air velocity in a stack of objects. Int. J. Therm. Sci. 43, 1213-1221.

Ansys (2010) ANSYS FLUENT 13.0 users guide. ANSYS, Inc., Canonsburg, Pennsylvania, USA.

Antohe B.V., Lage J.L. 1997. A general two-equation macroscopic turbulence model for incompressible flow in porous medium. Int. J. Heat and Mass Transfer. 40(13), 3013-3024.

Becker B.R., Misra A., Fricke B.A. 1994. A computer algorithm for determining the moisture loss and latent heat load in the bulk storage of fruits and vegetables. Final report (project 777-RP), ASHRAE, Atlanta, USA.

Bingol G., Pan Z., Roberts J.S., Devres Y.O., Balaban M.O. 2008. Mathematical modelling of microwave-assisted convective heating and drying of grapes. Int. J. Agric. Biol. Eng. 1(2), 46-54.

Bird R, Stewart W., Lightfoot E. 2002. Transport Phenomena. John Wiley & Sons, New York, USA, 2nd Edition.

Caleb O.J., Opara U.L., Witthuhn C.R. 2011. Modified atmosphere packaging of pomegranate fruit and arils: A review. Food Bioprocess Technol. DOI: 10.1007/s11947-011-0525-7

Carson J.K. 2006. Review of effective thermal conductivity models for foods. Int. J. Refrig. 29, 958-967.

Castro (de) L.R., Vigneault C., Cortez L.A.B. 2004. Container opening design for horticultural produce cooling efficiency. J. Food Agric. Environ. 2(1), 135-140.

Chau K., Gaffney J., Baird C., Church G. 1985. Resistance to air flow of oranges in bulk and in cartons. Trans. ASAE. 28(6), 2083-2088.

Chourasia M.K., Goswami T.K. 2007. CFD simulation of effects of operating parameters and product on heat transfer and moisture loss in the stack of bagged potatoes. J. Food Eng. 80(3), 947-960.

Chyu M.K., Natarajan V. 1991. Local heat/mass distributions on the surface of wall-mounted cube. J. Heat Transfer. 113(4), 851-857.

Costa C., Lucera A., Conte A., Mastromatteo M., Speranza B., Antonacci A., Del Nobile M.A. 2011. Effects of passive and active modified atmosphere packaging conditions on ready-to eat table grape. J. Food Eng. 102, 115-121.

Crisosto C., Smilanick J., Dokoozlian N. 2001. Table grapes suffer water loss, stem browning during cooling delays. California Agric. 55, 39–42.

Crisosto C., Smilanick J., Dokoozlian N., Luvis D.A. 1994. Maintaining table grape post-harvest quality for long distant markets. International Symposium on Table Grape Production, June 28-29, 2004, California, USA, American Society for Enology and Viticulture, 195-199.

de Paula R., Colet R., de Oliveira D., Valduga E., Treichel H. 2011. Assessment of different packaging structures in the stability of frozen fresh Brazilian toscana sausage. Food Bioprocess Technol. 4(3), 481-485.

Delele M.A., Vorstermans B., Creemers P., Tsige A.A., Tijskens E., Schenk A., Opara U.L., Nicolaï B.M., Verboven P. 2012. Investigating the performance of thermonebulisation fungicide fogging system for loaded fruit storage room using CFD model. J. Food Eng. 109, 87-97.

Delele M.A., Schenk A., Tijskens E., Ramon H., Nicolaï B.M., Verboven P. 2009a. Optimization of the humidification of cold stores by pressurized water atomizers based on a multiscale CFD model. J. Food Eng. 91(2), 228-239.

Delele M.A., Schenk A., Ramon H., Nicolaï B.M., Verboven P. 2009b. Evaluation of a chicory root cold store humidification system using computational fluid dynamics. J. Food Eng. 94(1), 110-121.

Dincer I. 1995a. Determination of heat-transfer coefficients for cylindrical products exposed to forced-air cooling. Int. J. Energy Res. 19(5), 451-459.

Dincer I. 1995b. Air flow precooling of individual grapes. J. Food Eng. 26, 243-249.

Eisfeld B., Schnitzlein K. 2001. The influence of confining walls on pressure drop in packed beds. Chem. Eng. Sci. 56, 4321-4329.

Ferrua M.J., Singh R.P. 2009. Modeling the forced-air cooling process of fresh strawberry packages, Part III: Experimental validation of the energy model. Int. J. Refrig. 32(2), 359-368.

Frederick R.L., Comunian F. 1994. Air-cooling characteristics of simulated grape packages. Int. Commun. Heat Mass Transfer. 21(3), 447-458.

Gentry J.P., Nelson K.E. 1964. Conduction Cooling of Table Grapes. Am. J. Enol. Vitic. 15(1), 41-46.

Gowda B.S., Narasimham G.S.V.L., Murthy M.V.K. 1997. Forced-air precooling of spherical foods in bulk: A parametric study. Int. J. Heat Fluid Flow. 18, 613-624.

Hoang M.L., Verboven P., De Baerdemaeker J., Nicolaï B.M. 2000. Analysis of air flow in a cold store by means of computational fluid dynamics. Int. J. Refrig. 23, 127-140.

Högberg M., Bewley T.R., Henningson D.S. 2003. Linear feedback control and estimation of transition in plane channel flow. J. Fluid Mech. 481, 149-175.

Jacimovic B.M., Genic S.B., Latinovic B.R. 2006. Research on the air pressure drop in plate finned tube heat exchangers. Int. J. Refrig. 29, 1138-1143.

Lichter A., Kaplunov T., Zutahy Y., Daus A., Alchanatis V., Ostrovsky V., Lurie S. 2011. Physical and visual properties of grape rachis as affected by water vapour pressure deficit. Postharvest Biol. Technol. 59, 25-33.

Lichter A., Kaplunov T., Lurie S. 2008. Evaluation of table grape storage in boxes with sulfur dioxide-releasing pads with either an internal plastic liner or external wrap. Hort. Technol. 18, 206-214.

Mirade P-S., Picgirard L. 2006. Improvement of ventilation homogeneity in an industrial batch-type carcass chiller by CFD investigation. Food Res. Int. 39, 871-881.

Moureh J., Flick D. 2004. Airflow pattern and temperature distribution in a typical refrigeration truck configuration loaded with pallets. Int. J. Refrig. 27, 464-474.

Nakayama A., Kuwahara F. 1999. A macroscopic turbulence model for flow in a porous medium. J. Fluids Eng.- Trans. ASME, 121, 427-433.

Nahor H.B., Hoang M.L., Verboven P., Baelmans M., Nicolaï B.M. 2005. CFD model of the airflow, heat and mass transfer in cooling stores. Int. J. Refrig. 28, 368-380.

Nelson K.E. 1985. Harvesting and handling California table grapes for market. University of California Bulletin No 1913. DANR Publications, Oakland, CA, pp. 72.

Nelson K.E. 1978. Pre-cooling-its significance to the market quality of table grapes. Int. J. Refrig. 1(4), 207-215.

Nelson K.E., Ahmedullah M. 1976. Packaging and decay-control systems for storage and transit of table grapes for export. Am. J. Enol. Vitic. 27(2), 74-79.

Ngcobo M.E.K., Opara U.L., Thiart G.D. 2012. Effects of packaging liners on cooling rate and quality attributes of table grape (cv. Regal Seedless). Packaging Technol. Sci. 25 (2), 73-84.

Opara U.L. 2011. From hand holes to vent holes: What's next in innovative horticultural packaging? Inaugural Lecture delivered on 2 February, Stellenbosch University, 24 pages.

Opara L.U., Zou Q. 2007. Sensitivity Analysis of a CFD Modelling System for Airflow and Heat Transfer of Fresh Food Packaging: Inlet Air Flow Velocity and Inside-Package Configurations. Int. J. Food Eng. 3(5), article 16.

Opara L.U., Zou Q. 2006. Novel computational fluid dynamics simulation software for thermal design and evaluation of horticultural packaging. Int. J. Postharvest Technol. Innov. 1(2), 155-169.

Patel V.C., Head R. 1969. Some observations on skin friction and velocity profiles in fully developed pipe and channel flows. J. Fluid Mech. 38, 181–201.

Reynolds W.C. 1979. Thermodynamic properties in SI: Graphs, Tables, and Computational equations for 40 substances. Department of Mechanical Engineering, Stanford University.

Tassou S.A., Xiang W. 1998. Modelling the environment within a wet air-cooled vegetable store. J. Food Eng. 38, 169-187.

Thompson J.F., Mejia D.C., Singh R.P. 2010. Energy use of commercial forced-air cooler for fruit. Appl. Eng. Agric. 26(5), 919-924.

Tsiraki M.I., Savvaidis I.N. 2011. Effect of packaging and basil essential oil on the quality characteristics of whey cheese “Anthotyros”. Food and Bioprocess Technol. DOI: 10.1007/s11947-011-0676-6.

Tso C.P., Cheng Y.C., Lai A.C.K. 2006. An improved model for predicting performance of finned tube heat exchanger under frosting condition with frost thickness variation along fin. Appl. Therm. Eng. 26, 111-120.

Tutar M., Erdogdu F., Toka B. 2009. Computational modeling of airflow patterns and heat transfer prediction through stacked layers products in a vented box during cooling. Int. J. Refrig. 32, 295-306.

van der Sman R.G.M. 2008. Scale analysis and integral approximation applied to heat and mass transfer in packed beds. J. Food Eng. 85, 243–251.

van der Sman R.G.M. 2002. Prediction of air flow through a vented box by the Darcy–Forchheimer equation. J. Food Engin. 55(1), 49–57.

Verboven P., Flick D., Nicolaï B.M., Alvarez G. 2006. Modelling transport phenomena in refrigerated food bulks, packages and stacks: basics and advances. Int. J. Refrig. 29, 985-997.

Versteeg H.K., Malalasekera W. 1995. An introduction to Computational Fluid Dynamics-The Finite Volume Method. John Wiley and sons, New York, USA.

Vigneault C., de Castro L.R. 2005. Produce-simulator property evaluation for indirect airflow distribution measurement through horticultural crop package. J. Food Agric. Environ. 3(2), 67-72.

Vigneault C., Goyette B. 2002. Design of plastic container opening to optimize forced-air precooling of fruits and vegetables. Appl. Eng. Agric. 18(1), 73-76.

Wakao N & Kaguei S (1982) Heat and mass transfer in packed beds, pp. 243–295. Gordon & Breach, New York, USA.

Wilcox D.C. 2000. Turbulence Modeling for CFD. DCW Industries, Inc., La Canada, California, USA, 2nd edition.

Xu Y., Burfoot D. 1999. Simulating the bulk storage of food stuffs. J. Food Eng. 39, 23-29.

Zukauskas A., Ulinskas R. 1990. Banks of plain and finned tubes, In G. F. Hewitt, Handbook of heat exchanger design, pp. 2.2.4-1–2.2.4-17. Hemisphere, London, UK.

Zou Q., Opara L.U., McKibbin R. 2006. A CFD modeling system for airflow and heat transfer in ventilated packaging for fresh foods: II. Computational solution, software development, and model testing. J. Food Eng. 77(4), 1048-1058.

Table 1: Pressure loss coefficients of the different plastic liners

Liner type: number x size (mm)	Liner thickness: (μm)	1/K (m^{-2})	β (m^{-1})
0 × 0 (Non-perforated)	20	-	-
30 × 2	16	6.91×10^{7}	2.47×10^{4}
54 × 2	16	4.81×10^{7}	2.17×10^{4}
120 × 2	16	4.64×10^{7}	1.90×10^{4}
36 × 4	16	4.09×10^{7}	1.85×10^{4}

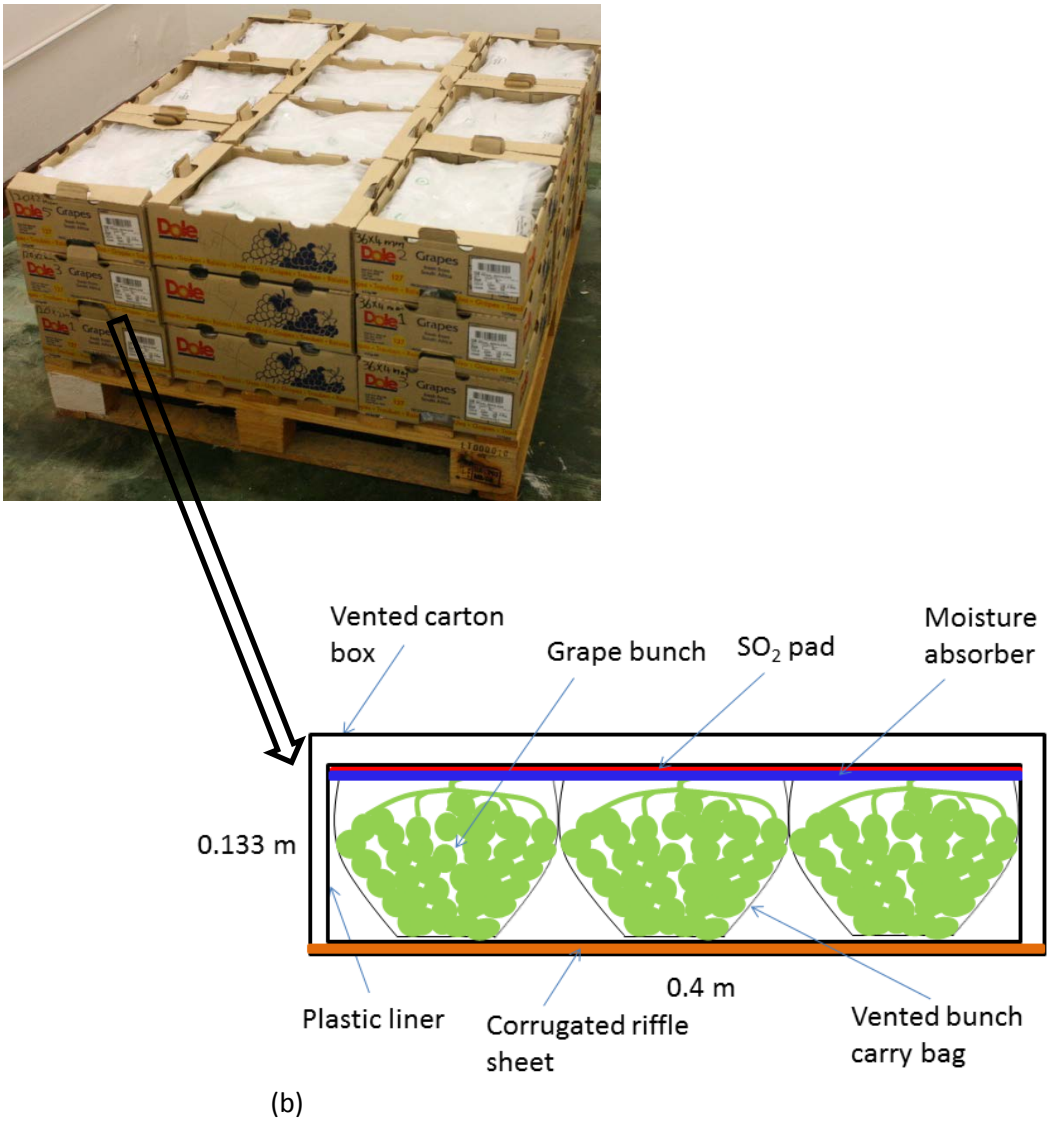

Figure 1: Table grape package: (a) Picture of packed table grape, (b) Diagram showing the details inside a packed box

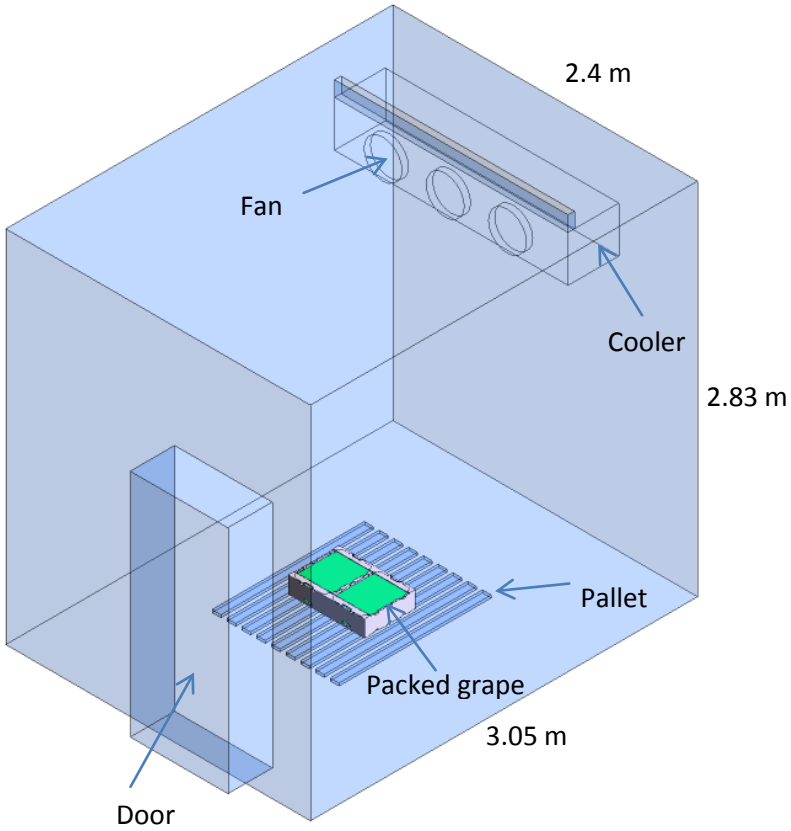

Figure 2. Details of the experimental cold storage room

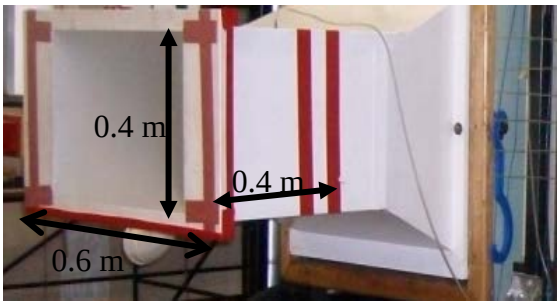

(a)

(b)

(c)

(d)

Figure 3: Wind tunnel experimental setup for airflow resistance measurement; (a) wind tunnel test section, (b) bulk of grape bunches without carry bags, (c) bulk of grape bunches with carry bags, (d) vented plastic liner

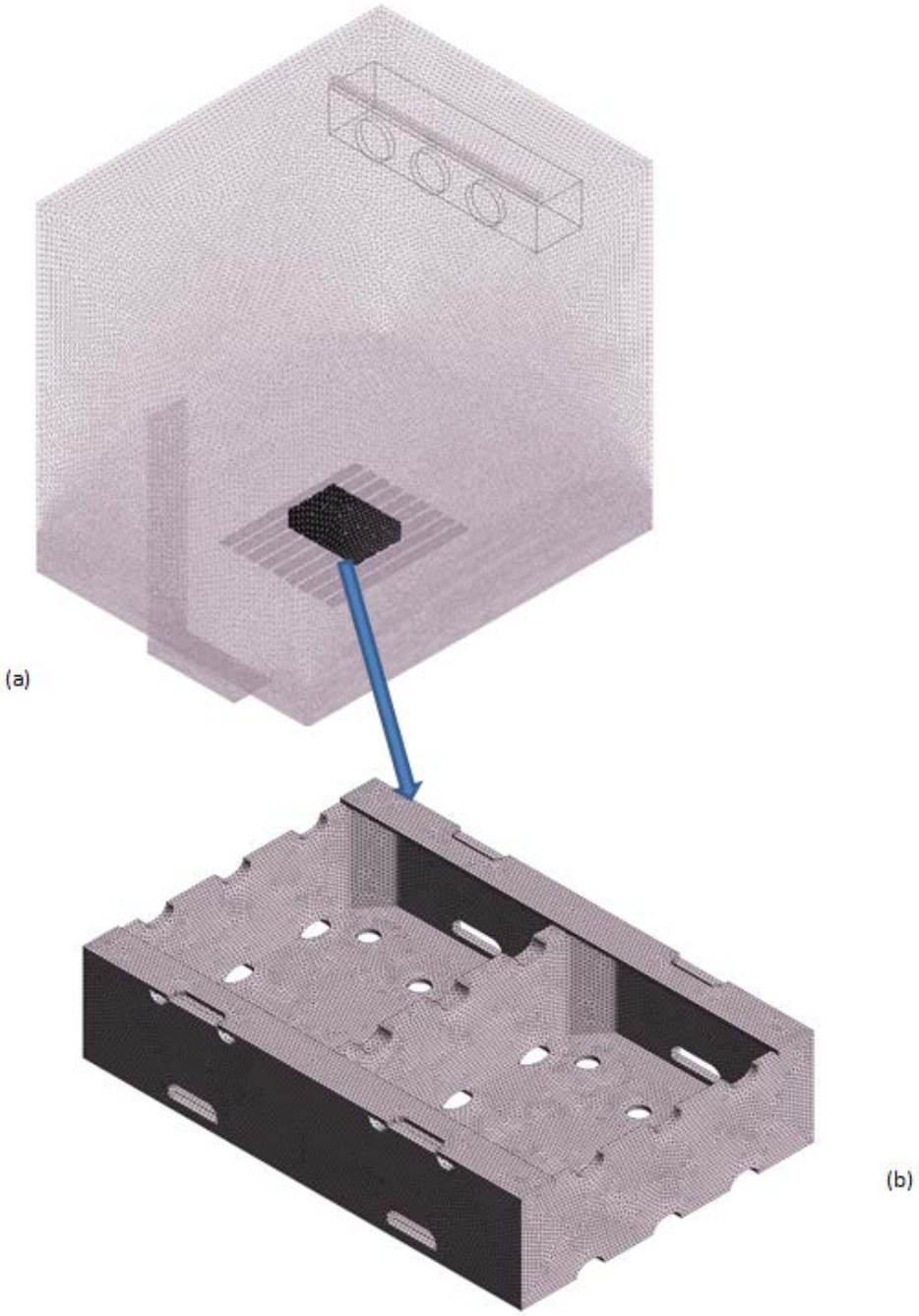

Figure 4: Details of the geometry and computational mesh used for the model simulation; (a) whole computational domain, (b) carton box

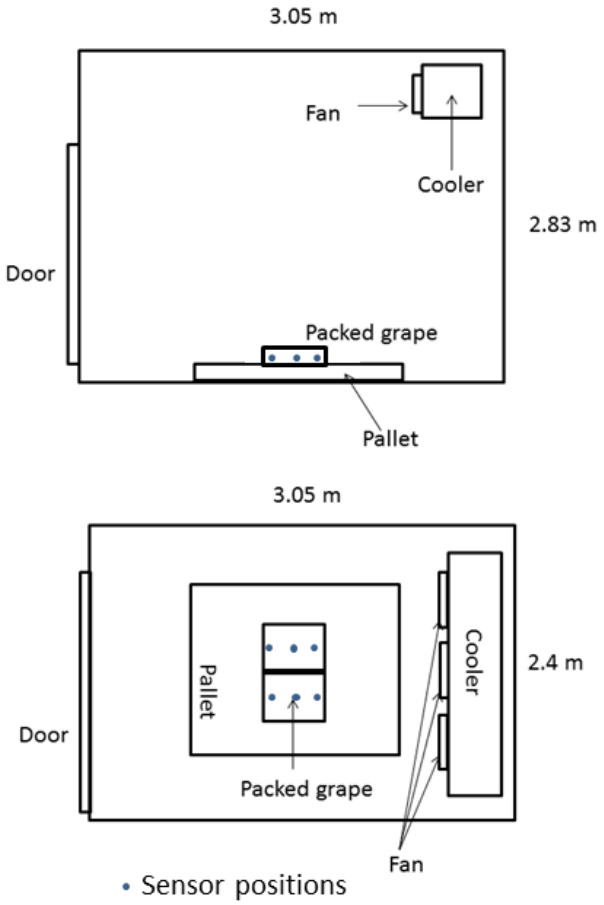

Figure 5: Experimental setup inside the cold storage room (● position of sensors)

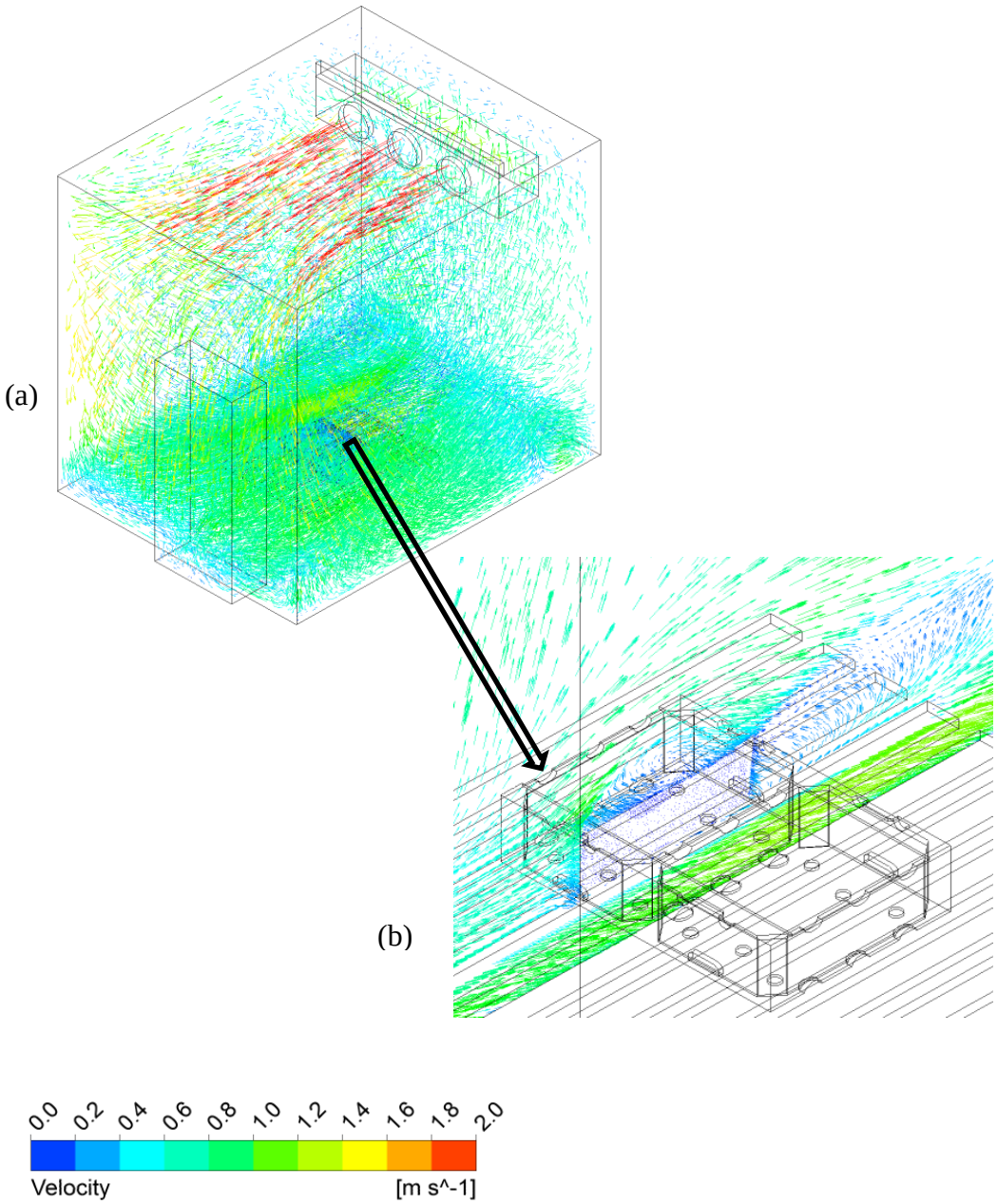

Figure 6: Predicted airflow profile inside the cold storage room loaded with a pallet with two grape boxes packed with non-perforated plastic liner; (a) air velocity vector throughout the room, (b) airflow contour on a plane that passes through the grape package

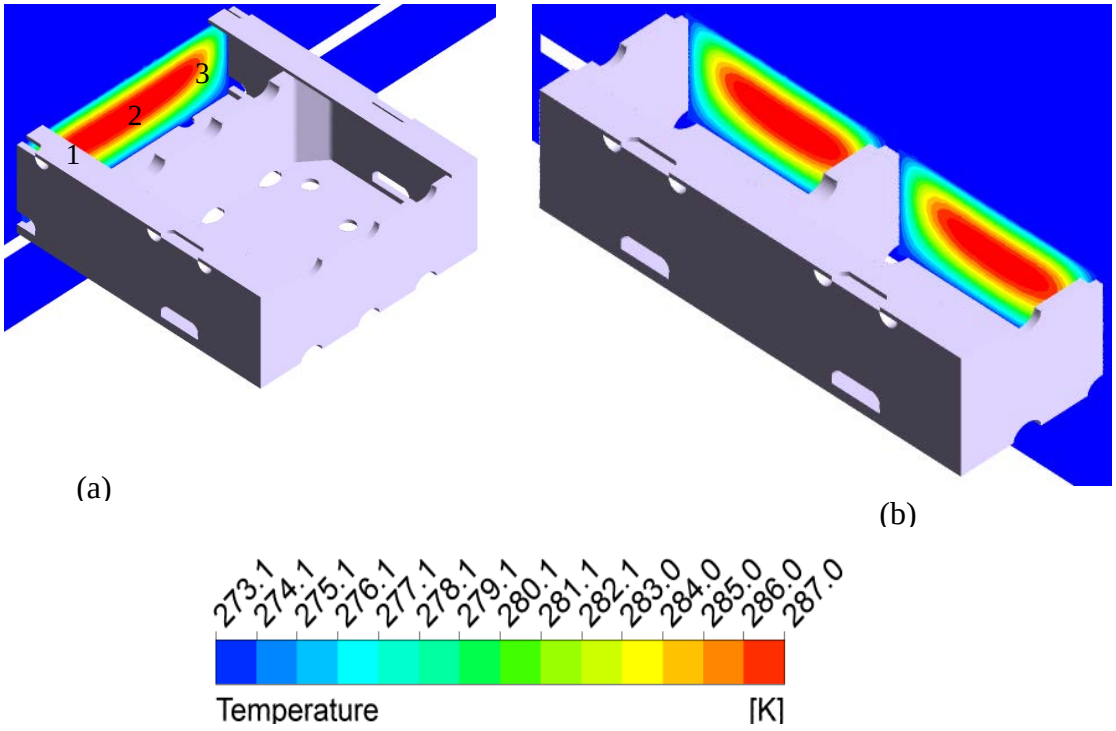

Figure 7: Predicted temperature distribution inside the grape package, packed with non-perforated plastic liner after 6 h of cooling from the initial temperature of 21 ^{O}C (294.15 K); (a) along the length of the box, (b) along the width of the box

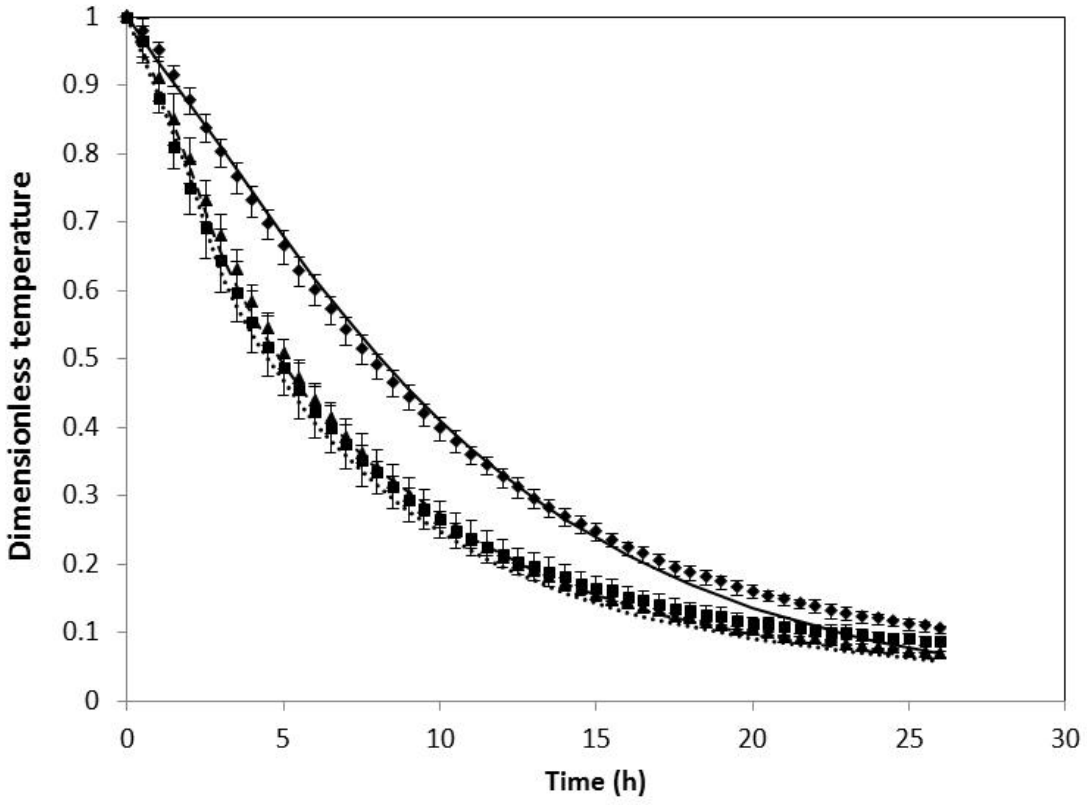

Figure 8: Measured and predicted product temperature during cooling at different positions within the grape package; position 1: measured (■), predicted (···); position 2: measured (◆), predicted (—); position 3, measured (▲) predicted (---); the positions are shown in Fig. 7

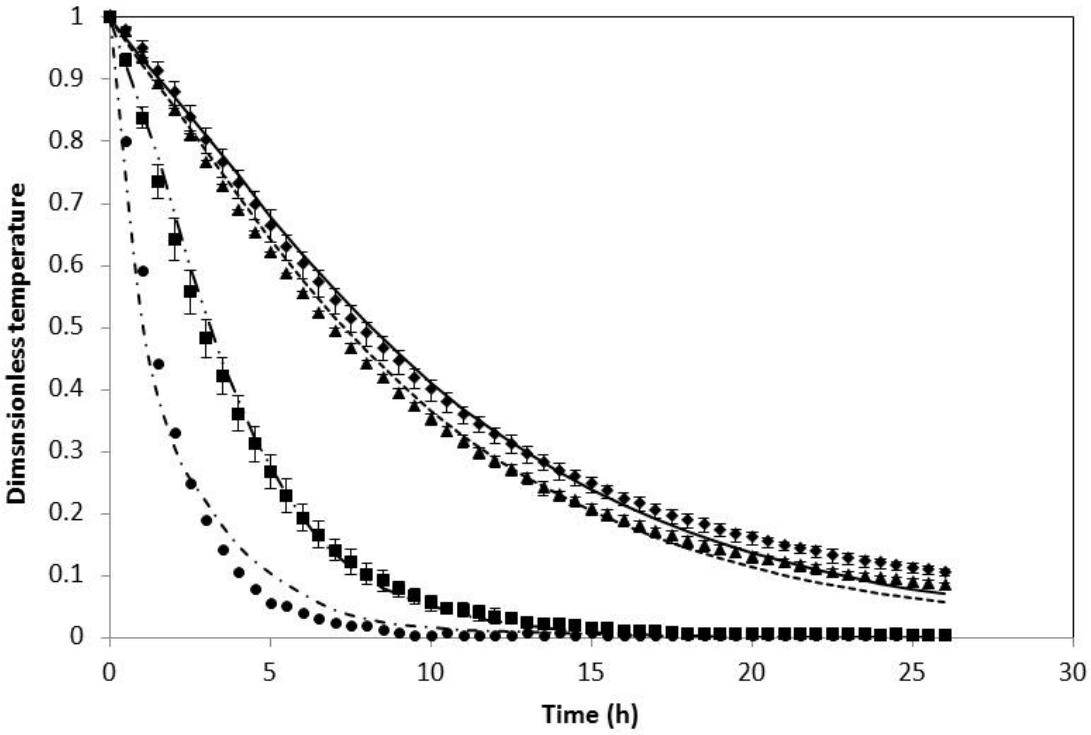

Figure 9: Measured and predicted temperatures at the centre of the grape package for different liner and packaging systems at the centre of the package (position 2 in Fig. 7); non-perforated liner: measured (◆), predicted (—); perforated liner (120 × 2 mm): predicted (---), measured (▲); no liner with carry bag, measured (■), predicted (-··-); grape bulk without carry bag and liner: measured (●), predicted (-·-)

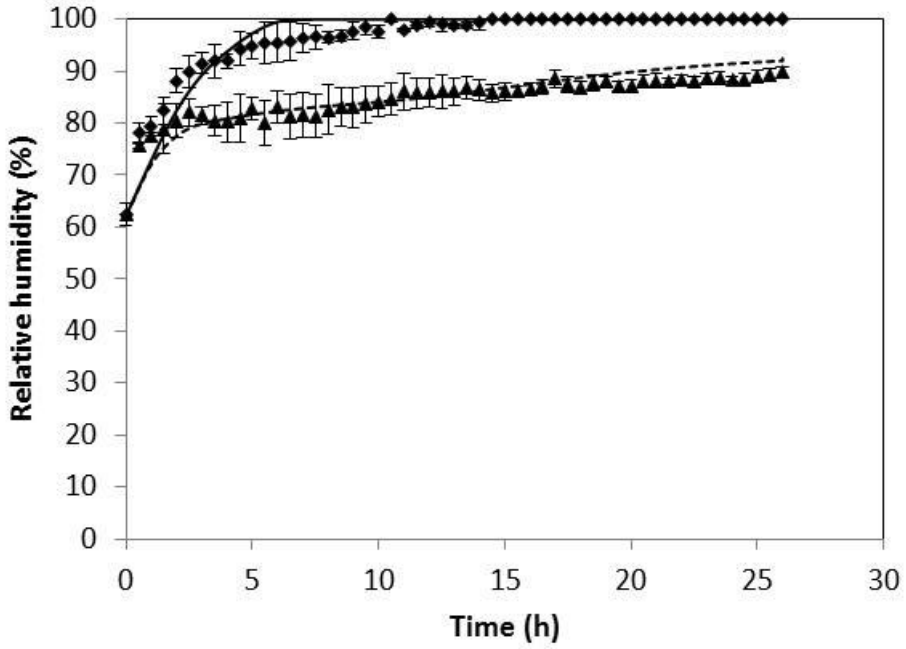

Figure 10: Measured and predicted relative humidity (RH) inside grape package packed using plastic liners; non-perforated: measured (◆), predicted (—), perforated liner (120 × 2 mm): predicted (---), measured (▲)

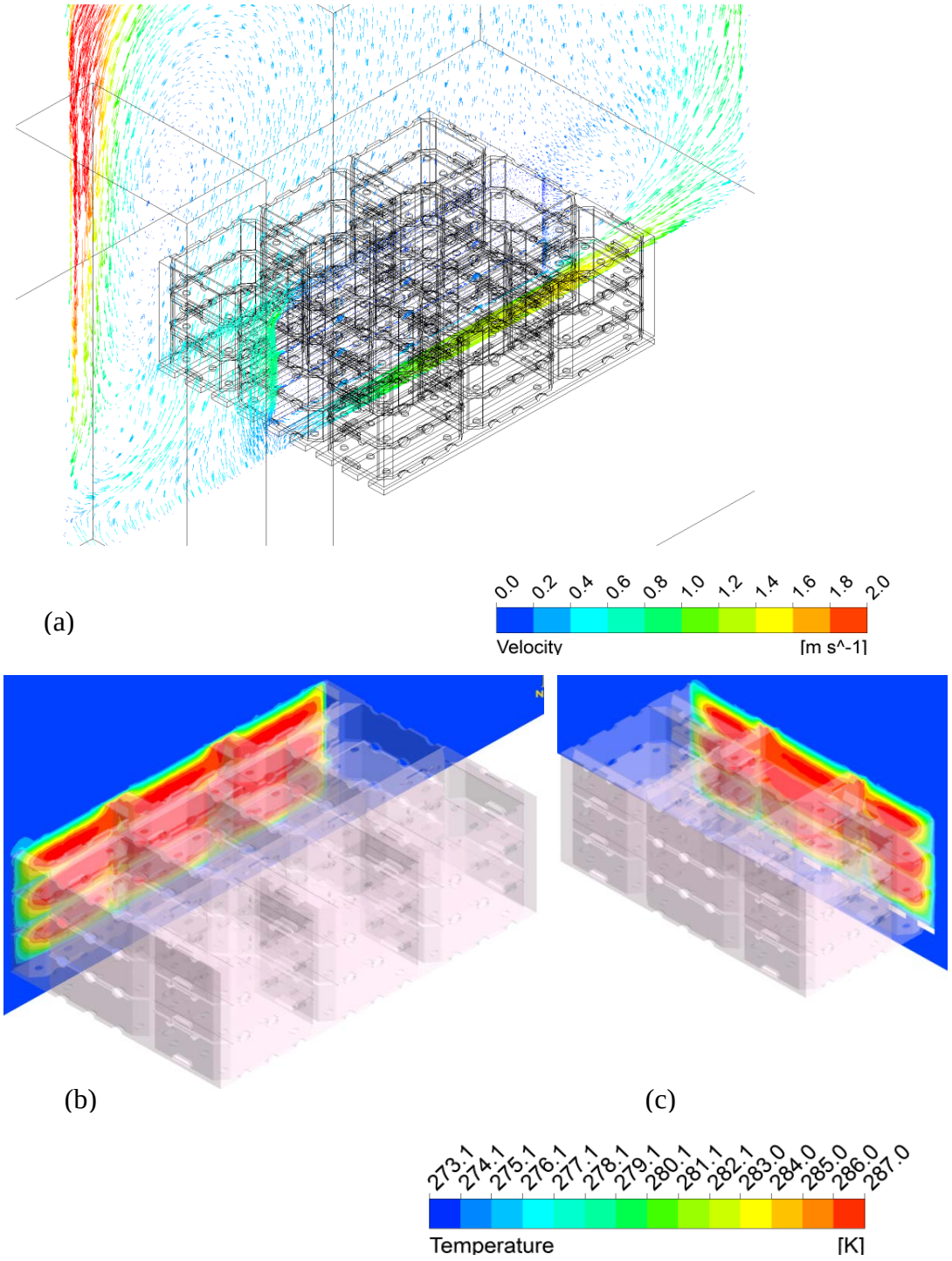

Figure 11: Predicted airflow and temperature profiles within and around the stack of grape packages, after 6 h of cooling from the initial temperature of 21 ^{O}C (294.15 K); (a) airflow vectors, (b) temperature along the length of the stack, (b) temperature along the width of the stack

General Discussion and Conclusion

Cooling is the most important and effective technique used to maintain table grape quality after harvest. During cooling, heat is transferred from grapes through forced air convection, where cold air is forced through individual fruit packages. Since cold air is the cooling medium, means that the magnitude of grape temperature and its homogeneity inside packages is largely governed by the patterns of airflow. Given that table grapes are packed inside multi-scale packages, it is likely that airflow patterns inside the multi-scale packages could become uneven resulting in heterogeneous grape temperatures. Poor temperature management in the cold chain often results in rapid deterioration of grape postharvest quality. The deterioration of quality in grapes is characterised by moisture loss, stem dehydration and browning, accelerated berry softening and decay. The main aim of this study was to investigate airflow resistance, cooling rates and patterns, and quality attributes of grapes during postharvest storage and handling using multi-scale packaging.

The effects of different multi-scale package components on airflow and heat transfer characteristics of table grapes were studied and reported in Paper 1. The results obtained from this study showed that liner films contributed the highest resistance to airflow of the package components. The contribution of liner films to total pressure drop for all the 4.5 kg packaging combinations ranged from 40.33±1.15% to 83.34±2.13 %, while grapes in bulk contributed the least at a range of 1.40±0.01 % to 9.41±1.23. The results also suggested that perforated liner films contributed less resistance to airflow when compared to non-perforated liner films. However, there were no clear trends that could be correlated to the size of perforation area of the liners, which suggested that airflow resistance did not necessarily decrease with an increase in perforation area of liners. This observation was attributed to the small size of perforation holes that could have been easily blocked by inner packages or berries. The blockage of liner perforations became more apparent as the resistance coefficients did not correlate to the vent:hole ratio of the liner films. It was therefore concluded that predicting airflow patterns through the liner films packed with grapes was difficult. The percentage

ventilation area on side walls of the 4.5 kg carton boxes was low (2.80% and 6.70%) compared to the 8 - 16% recommended in literature.

Table grapes are susceptible to quality defects during postharvest handling and marketing, and the combination of good cold chain management and postharvest packaging has been widely reported to play a crucial role in maintaining table grape quality. In Paper 2, the effects of different carton liner films on the cooling rate and quality attributes of 'Regal Seedless' table grapes were investigated. The results from this study showed that grape berries packaged and stored in perforated liners performed better in terms of faster cooling rate, low incidents of SO_2 damage and low berry drop, while non-perforated liners performed better in terms of maintaining higher RH (up to 100 %) and stem quality. There was SO_2 injury of berries observed in the non-perforated liners and this was attributed to SO_2 toxicity which may have been induced by the SO_2 generator pad releasing high rate under saturated atmospheres. This highlights the need to optimise the perforation area of liner bags in consideration of the SO_2 pad release rate. It is also important that quality attributes such as stem dehydration are considered during the optimization of liner films.

Further to investigating the effects of liner films, the performance of three table grape multi-package designs, namely the 4.5 kg box, 5 kg open-top punnet and 5 kg clamshell punnet were studied during cooling and cold storage of grapes (Paper 3). As part of this study, the effects of carton stacking and pallet orientation (i.e. 1 m or 1.2 m in the direction of airflow) on cooling rates were also investigated. The results obtained in this study indicated that grapes packed in the 4.5 kg multi-packaging cooled significantly slower than that of grapes packaged in 5 kg punnet multi-packaging. However, the 4.5 kg multi-packaging resulted in the lowest moisture loss (1.08%) of grapes, while the punnet multi-packages resulted in higher moisture loss (between 2.01-3.12 %) and stem dehydration. These moisture loss results were attributed to high vapour pressure deficits (VPD) experienced inside punnet multi-packages. These results suggest that there could be a possible trade-off between faster cooling rates of grapes and moisture loss, where high velocity of cooling air may result in rapid moisture loss of grapes. The results also suggested that stacking of boxes affected the patterns of airflow through the stack of boxes as indicated by significant spatial differences in the cooling rates of individual boxes of each layer. This variation in cooling patterns within stacked boxes and between layers may be ascribed to heterogeneous patterns of airflow due

to poor alignment of vent-holes between boxes and further exacerbated by the presence of inner packaging.

Moisture loss is one of the most urgent reasons why table grapes should be cooled promptly and maintained during postharvest. Even low levels of moisture loss (as low as 1 %) results in significant stem dehydration and browning which affects the grape quality negatively and tends to detracts consumers from buying. The symptoms of moisture loss do not show on grape berries until the loss is severe. In Paper 4, the characteristics of table grape moisture loss packaged in different liner films was studied. The results obtained indicated that the use of non-perforated liner films significantly reduced the rate of moisture loss from the grape bunches compared to the perforated liner films and the no packaging (zero packaging) treatments during cold storage. These results corresponded well with the transpiration rate results also obtained from the same study, where the transpiration rates were lower in non-perforated liners than the other packaging treatments, attributed to the lower vapour pressure deficit (VPD) and no air circulation inside the non-perforated liner film.

The moisture diffusivity of grape stems during storage was also studied under cold airflow conditions (1.21 ± 0.25 °C and 1.18 ± 0.23 ms^{-1}) (Paper 5). Effective moisture diffusivity values for stem parts packed in non-perforated liner films were lower than the values obtained from the no liner film cold storage condition. In agreement with results obtained in Paper 4, the non-perforated liner film (no airflow) significantly reduced the dehydration rate of stems compared to the no liner film treatment over the storage period, suggesting that air circulation was the main contributor to moisture diffusivity and dehydration of stem parts. The dehydration rate of the different parts of stems was inversely proportional to the size (diameter) of each stem part. The applicability of drying empirical models (Newton, Page, Henderson and Pabis, and asymptotic) to predict moisture loss from grape stems was also tested. Results obtained suggested that these models could potentially be used to predict moisture loss from stems, as indicated by the best fit to the dehydration data of the different stem parts. The data obtained in this work and the tested models, could be applied to assist in predicting the quality of grape stems during the handling of fresh grapes in the cold chain.

Following an in-depth study of moisture loss of grapes during postharvest storage and handling, the potential of humidifying cold storage rooms to control moisture loss and quality of grapes in different package designs was investigated (Paper 6). In this study, grapes were cold stored with or without supplementary and assessed for weight loss and SO_2 injury at intervals during a 35 d period. Results obtained showed that humidification reduced the rate of moisture loss and stem dehydration from table grapes. However, incidences of SO_2 injury were observed under the humidified storage condition and these defects were attributed to moist saturated air and the presence of an SO_2 sheet inside grape packages, creating some acidic environment. Humidification was also associated with packaging wetness due to high water droplet deposition on packaging. This suggests that although humidification has a potential to reduce moisture loss from grapes, the humidification systems needs to be optimized for successful postharvest storage in order to reduce the deposition of water droplets on packaging structure. Furthermore, further research work is warranted to optimize table grape packaging where humidification applications are used in order to withstand the high humidity conditions.

In Paper 7 a preliminary investigation of the flow phenomenon during cooling and handling of packed grapes was studied using a computational fluid dynamic (CFD) model which was validated using experimental results. During the study the package (carton box) was explicitly modeled, the grape bunch with the carry bag was treated as a porous medium and perforated plastic liners were taken as a porous jump. The good agreement between model and experimental results coupled with the advantage of visualising the predicted flow patterns demonstrated the applicability of CFD models to optimise table grape package design and handling to achieve optimum cooling rate with minimum moisture condensation on the package and reduction of moisture loss of grape berries. The approach followed in this study can be applied to investigate and optimize the design of other agricultural and horticultural product packaging system. However, the modelling necessary to optimise such packages must include the appropriate system geometry, air supply properties and product physiochemical properties.

Future studies

Future studies should focus at optimising specific table grape multi-packages for improved cooling while maintaining postharvest quality. More comprehensive study of the applicability of numerical modelling in the design and optimization of grape packaging is warranted.